UNIVERSIDADE DE SANTIAGO DE COMPOSTELA

Departamento de Física de Partículas

BPS SKYRME MODELS: EXACT METHODS IN HADRONIC AND NUCLEAR PHENOMENOLOGY

Ph.D. Thesis

Carlos Naya Rodríguez

Santiago de Compostela, maio 2015.

USC
UNIVERSIDADE
DE SANTIAGO
DE COMPOSTELA

UNIVERSIDADE DE SANTIAGO DE COMPOSTELA

Departamento de Física de Partículas

BPS SKYRME MODELS: EXACT METHODS IN HADRONIC AND NUCLEAR PHENOMENOLOGY

Tese presentada para optar ao Grao de Doutor en Física por:

Carlos Naya Rodríguez

Santiago de Compostela, maio 2015

Asdo: Carlos Naya Rodríguez

USC
UNIVERSIDADE
DE SANTIAGO
DE COMPOSTELA

Joaquín Sánchez Guillén,
Catedrático de Física Teórica da Universidade de Santiago de Compostela,

Christoph Adam,
Profesor Contratado Doutor da Universidade de Santiago de Compostela,

e

Andrzej Wereszczyński,
Doctor Habilitus da Universidade Iaguelónica de Cracovia,

CERTIFICAN:

que a memoria titulada *BPS Skyrme models: Exact methods in hadronic and nuclear phenomenology* foi realizada, baixo a nosa dirección, por Carlos Naya Rodríguez no departamento de Física de Partículas da Universidade Santiago de Compostela, e constitúe o traballo de Tese que presenta para optar ao grao de Doutor en Física.

Santiago de Compostela, maio 2015

Asdo: Joaquín Sánchez Guillén

Asdo: Christoph Adam

Asdo: Andrzej Wereszczyński

USC
UNIVERSIDADE
DE SANTIAGO
DE COMPOSTELA

To my family and friends

USC
UNIVERSIDADE
DE SANTIAGO
DE COMPOSTELA

Acknowledgments

There are many people to whom I am very gratful for all their help and support throughout all my life. These PhD years were no exception and I would like to thank to all of them.

To my supervisor, Joaquín Sánchez Guillén, and co-advisors, Christoph Adam and Andrzej Wereszczyński, for all their guidance, patience and trust. It was a pleasure to share all these years with them, working and learning a lot.

To my collaborators Ricardo Vazquez and Martin Speight. It was an excellent and fruitful experience to work with them.

To the Jagiellonian University in Krakow for its hospitality. Every year it has warmly welcomed and allowed me to discovered a great city besides interesting physical discussions. Especially to Kasia, who with Andrzej always made me feel like at home.

To CERN and Luis Álvarez-Gaumé for their hospitality and the opportunity to spend three exciting months of my PhD in such environment. It was a pleasure to be part of that great community which allowed me to learn a lot.

To all my friends I had the lovely opportunity to meet at the faculty not only during my PhD but also during my degree in Physics, with whom I enjoyed coffees, congresses and some parties too: Adrián, Alejandro, Álvaro, Antón, Carlota, Dani, Guille, Inés, Íñigo, Jorge, Liliana, Manoel Calvo, Manoel Moldes, Nacho, Pablo, Rosalía, Ruben y Xabi.

To my friends from Monte da Condesa, especially to Alba, Ana, Clara, Laura and Raquel.

To my friend Laura from Logroño, who is every day supporting me despite the distance.

To Aidé, Carla and Dani, my friends from school, that little family which is still providing me with good moments and support.

A very special thanks to Merche, who I met by chance and became an essential part of my life. Thank you so much for your unconditional support, understanding and patience, and for all the great moments too. You know all you mean to me, *mi niña*!

To all my family, in particular to my grandmother and brother, for all the hapinness and pride that they feel.

And, of course, a very special thanks to my parents, for providing me all the opportunities, support and courage to fulfil my dreams. Thank you for always being on my side!

Moitas grazas a todos! Thank you so much to everybody!

USC
UNIVERSIDADE
DE SANTIAGO
DE COMPOSTELA

Summary

It is well known that, up to now, QCD cannot give precise answers in its low-energy limit because here, the usual perturbative techniques are no longer useful. Instead, effective field theories are a common tool to achieve a description and understanding of the theory of strong interactions. Among these effective theories, a successful particular case corresponds to the so-called Skyrme model. This is a low-energy effective theory of strong interactions proposed by T. H. R. Skyrme in the 60's where the fundamental degrees of freedom are the pion mesons. His novel idea received further support when it was found that in the large number of colours limit of QCD (large N_C limit), an effective theory of mesons also appears.The original Lagrangian is made of two terms (we will call it standard Skyrme model), one term quadratic in first derivatives which corresponds to the non-linear sigma model (also known as Dirichlet term) and provides the kinetic energy of pions; and the other which is quartic in first derivatives and was explicitly introduced by Skyrme to circumvent the Derrick theorem of scale transformations so stable solutions can exist. Hadrons and nuclei emerge as collective excitations (topological solitons) of the effective degrees of freedom and are characterized by a topological property: the winding number or topological charge. Since this is a topological quantity it will be conserved, and identifying it with the baryon number we ensure its conservation.

Then, qualitative agreement between experimental data and observables derived from the Skyrme model are achieved, for instance, nuclear masses or charge radii. Although their quantitative values present a discrepancy of about $10 - 20\%$, one may improve this situation by generalizing the Skyrme model with further terms (remember this is an effective field theory so there are no reasons for not including more terms). The first contribution one can think of is a potential (if it is not stated otherwise, we will use the standard Skyrme potential with a quadratic approach to the vacuum). It has no derivatives and, in fact, has been widely considered before (especially to implement the pionic masses). For the next contribution, if a term at most quadratic in time derivatives is required, so a standard Hamiltonian formulation is possible, the only choice is a sextic (in first derivatives) term consisting in the topological (baryon) current squared. Two examples of these generalized models are the BPS (Bogomolny-Prasad-Sommefield) Skyrme model and the near-BPS Skyrme model.

In the present PhD thesis we will focus on the study of the BPS Skyrme model and its application to the thermodynamics of nuclear matter, the binding energies of nuclei and the description of neutron stars. It consists of only

two terms: a potential, and the sextic term. Its name comes from the BPS property which consists in a topological bound which is linear in the baryon number and with solutions saturating it. This implies that the corresponding nuclear mass is linearly related to the baryon number. Moreover, depending on how the potential approaches the vacuum, there exist compact solutions with a radius which grows with the third root of the baryon number. Hence, both behaviours agree with basic phenomenological facts of nuclear physics. Considering the symmetries, the BPS Skyrme model has the area preserving diffeomorphisms of the target space as symmetries (which implies an infinite number of solutions with different symmetries), and in addition, also the volume preserving diffeomorphisms on the base space. The latter are the symmetries of an incompressible ideal fluid which are related to the liquid drop model of nuclei.

However, we know this model is not complete because of, for instance, the absence of pion dynamics. In fact, some more evidence that an extension to the other mentioned generalized model (the near-BPS Skyrme model) is required, can also be found throughout this PhD thesis. In this case, the near-BPS model presents two well differentiated parts. On the one hand, a leading contribution consisting in the BPS model which we have just commented. On the other hand, the standard Skyrme model, to be introduced in a perturbative way by an overall small parameter ε. As a consequence, the BPS Skyrme model is responsible for the bulk properties even in this near-BPS setup, so as a first approximation, the study of the issues presented in this work using just the BPS Skyrme model is more than reasonable. Nevertheless, we must have in mind that for other subjects of nuclear physics like nuclear spectroscopy, the perturbative part is important.

After a brief comparison between the standard and the BPS Skyrme models, focused on the description of the Roper resonances, we start with the description of the BPS Skyrme thermodynamics at zero temperature with two important quantities: the compressibility and the baryon chemical potential. As a previous step, we introduce the pressure by calculating the corresponding energy-momentum tensor and imposing its conservation. Then, we find that the pressure has to be a constant and that this condition is, indeed, equivalent to the static field equations, where in the case of BPS solutions the constant is exactly zero. Furthermore, we arrive at expressions for the energy and volume as functions of the pressure which can be written in terms of integrals over the target space, so specific solutions are not needed to their calculation.

Concerning the compressibility or compression modulus (inversely related), we have found different behaviours which basically depend on the approach of the chosen potential to the vacuum. Summarizing the results, we have obtained a finite value of the compressibility when the vacuum approach is

lower than quadratic. However, these potentials are problematic from a physical point of view because their second variation around the vacuum is infinite. On the other hand, potentials with at least a quadratic approach are physically acceptable and present an infinite compressibility (zero compression modulus) which seems a rather generic result. Additionally, in this case, when the behaviour near the vacuum is less than sextic, the Skyrmions at zero pressure are compactons and a phase transition appears at the equilibrium volume (volume at zero temperature). The situation is as follows. At zero pressure and fixed baryon number we can have a larger volume than the one at equilibrium corresponding to an ideal gas of non-overlapping compactons. Nevertheless, we can lower this volume by reducing the empty space among them until the equilibrium volume is reached. Here, the volume can be further reduced by introducing the pressure and the system enters a liquid phase.

Considering another thermodynamical quantity, the baryon chemical potential, we present two different approaches. First, an exact field theoretical calculation where a linear relation between chemical potential and baryon density is found independently of the chosen potential. And second, a mean-field approach which is based on the average of some quantities, essentially the energy and volume. In this mean-field limit, the calculations are possible without knowing specific solutions and several potentials are analised. Here we find that only for a step-function potential we get exactly the same chemical potential (because both approaches are completely equivalent). Moreover, this baryon chemical potential allows to study the in-medium Skyrmions in Skyrmionic matter so the first steps within the BPS model are also taken.

Another important subject in this thesis is the calculation of the binding energies of nuclei. For this purpose, the BPS property of the model is of extreme importance. In fact, due to the linear energy bound in the baryon number, the binding energies are classically zero. However, the situation is improved because, for a proper description of nuclei, additional contributions to the energy are needed. Firstly, we need to proceed with a semi-classical quantization of spin and isospin, i.e., we introduce the time-dependent rotational and isorotational degrees of freedom around the static solutions and quantize in the usual way. As a consequence of the symmetry of our solution (we assume an axially symmetric ansatz), we obtain that, for baryon number greater than one, the resulting Hamiltonian consists of two copies of the symmetric top whereas a constraint for some quantum numbers also appears.

Secondly, we have to consider the Coulomb energy, which is given by the generalization for volume charge densities of the usual expression. Then, after calculating the charge density and quantizing it, we solve the integrals appearing by means of an expansion of the charge density into spherical harmonics and the multipole expansion of the Coulomb potential. These energy

contributions only depend on the baryon number and the third component of isospin.

Finally, since neutrons are heavier than protons, we also have to take into account a potential term breaking the isospin symmetry. The proper treatment, which would be the introduction into the Lagrangian of an isospin breaking potential with the corresponding semi-classical quantization, is too difficult at present. Therefore, we just considered the leading order given by a term proportional to the third component of isospin.

All in all, we obtain the binding energies coming from these contributions by fitting the three free parameters we have (corresponding to the two terms of the Lagrangian and the proportionality constant of the isospin-breaking) to three quantities, namely, the proton mass, the experimental mass difference between neutron and proton, and the mass of a nucleus with magic numbers. Then, we compare the values of our theory with experimental data finding a very good agreement for nuclei with high baryon number. Although the behaviour for small nuclei is not so good (the binding energies are overestimated), this was expected because the BPS Skyrme model is based on a collective description of the fundamental degrees of freedom and, for small nuclei, single-particle properties and propagating pionic degrees of freedom are important. Furthermore, the axial symmetry is not the right one. Thus, the BPS Skyrme model provides the leading contribution to the description of strong interactions but an extension to the near-BPS theory is required to improve this situation at low baryon number.

In addition, because of the nice properties of the BPS Skyrme model, our calculations give as a result an analytical expression for the binding energies depending on the baryon number, the atomic number and the spin quantum number. Therefore, we can establish a comparison between our formula and the semi-empirical mass formula (also known as Weizsäcker formula). Indeed, we obtain a direct correspondence with the volume and Coulomb terms from the semi-empirical mass formula. Moreover, in our model we get a term which is similar but slightly different from the asymmetry one in the Weizsäcker formula giving smaller contributions at large baryon number. Nevertheless, one may also expect this situation to improve when implementing the extension to the near-BPS version of the model.

To conclude with the binding energies, we further investigate the effect of different potentials. Then, besides the standard Skyrme potential considered up to now, we also study its square (with a quartic behaviour near the vacuum), and a family of step-like potentials with quadratic and quartic approach to the vacuum. The main result here is that, at least when talking about quadratic and quartic potential, the concrete shape of the potential has no dramatic effect and the main factor giving rise to differences is how it

approaches the vacuum.

The last main topic of this PhD thesis is the coupling of the BPS Skyrme model to gravity in order to describe neutron stars. Here, this BPS version seems to have some advantages with respect to the standard Skyrme model. The main reason is that the true structures minimizing the original Skyrmion action are Skyrmionic crystals whereas the core of neutron stars is more likely to be in a superfluid phase, and indeed, the energy-momentum tensor of the BPS Skyrme model is that of a perfect fluid. Then, we minimally couple the model to gravity assuming a static spherically symmetric metric. The minimization of the corresponding action is equivalent to solve the Einstein equations given in terms of the energy-momentum tensor and the Eistein tensor. After a lengthy calculation involving the Christoffel symbols, Ricci tensor and scalar curvature, we get the corresponding Eistein tensor and the Einstein equations are achieved. Concretely, because of the symmetry of the problem, there are only three independent Einstein equations so we are left with a system of ordinary differential equations consisting in two equations for a matter field and a metric (space-like) function plus an equation determining the other metric (time-like) function in terms of the other two fields.

We solve numerically this system by using a shooting from the centre with a Runge Kutta method and fitting the model parameters to some properties of nucleons (we need a different fit for each different potential). At this point, we do not follow the usual Tolman-Oppenheimer-Volkoff (TOV) approach assuming an algebraic equation of state of nuclear matter which closes the TOV equations. In contrast, we perform the exact and full field theory computations. An important feature of this calculation is the appearance of three different behaviours where the relevan parameter is now the baryon number. For small baryon number, there is only a unique solution. For larger values but below a certain baryon number two different solutions exist, although that with lower value of the energy density at the centre corresponds to the stable one. Finally, above the upper baryon number commented before, no physical solutions exist and Skyrmions are unstable and collapse to a black hole. Once we have the solution, the neutron star masses are easily obtained from the vacuum solution for the metric (space-like) function, whilst the neutron star radii correspond to the point where the matter field takes its vacuum value.

We perform these numerical full theory calculations for two different potentials, the standard Skyrme potential and the squared standard Skyrme potential. The main results we get are maximal neutron star masses before the collapse and their corresponding radii which are in concordance to the avaliable observational data, where neutron star masses of about two solar masses are well know and there is even evidence of masses up to about two and a half solar masses. Another important outcome is that in general, a uni-

versal and algebraic equation of state (realting pressure and energy density) is not possible without an approximation. Nevertheless, when a solution is found, we can numerically arrive at an on-shell equation of state from the corresponding expressions for the energy density and pressure as functions of the radial coordinate. However, the parameters appearing in the resulting equation of state depend on the baryon number instead of being constant.

Interestingly, this BPS Skyrme model also allows for the usual TOV approach which is followed when studying neutron stars, so both results can be fruitfully compared. To perform this TOV calculation we just have to recall the mean-field limit already presented in the description of the baryon chemical potential. Hence, we obtain the mean-field equation of state by means of an average procedure so this average equation is actually algebraic and no coordinate-dependent. We again numerically solve the TOV equations by a shooting from the centre with a Runge Kutta method with the same fit to some nucleon properties. In this case, besides the standard Skyrme potential and the squared standard Skyrme potential, we also consider the step-function potential where both the exact and the mean-field approaches are completely equivalent.

Comparing both calculations, we see that global quantities do not differ too much. In fact, the maximal values of neutron star masses are just slightly bigger in the mean-field limit than it the full field theory. However, when comparing local quantities, it is quite clear that the two approaches present important differences. For instance, the metric (space-like) function reaches its maximum value exactly at the surface of the neutron star in the mean-field calculation, whilst in the exact theory, the maximum of the metric function is inside the star. In addition, the difference between both approaches is the bigger the more the chosen potential differs from the step-function potential, i.e., the more it differs from a flat potential (which also corresponds to flat energy and particle densities). Therefore, one may expect that, concerning other theories beyond the BPS Skyrme model, the differences will be more relevant for those with more important inhomogeneities in the energy and particle densities.

At this point, although no precise quantitative predictions can be established (remember we would need the extension to the generalized near-BPS Skyrme model), we may compare our results with some constraints extracted from observational data, because bulk properties are mainly due to the BPS Skyrme model. For instance, this is the case of neutron star masses as functions of their radii. In our calculations we find that, except near the maximal mass, neutron star masses grow when increasing the radius, which is clearly at odds with the typical behaviour derived from a large class of equations of state used in nuclear physics. However, when considering some constraints

to the mass-radius relation coming from observational data, namely, from the estimated mass for a low-mass X-ray binary (LMXB), from quasi-periodic oscillations at high frequencies of another LMXB, and from the thermal radiation of an isolated pulsar; we find that our equation of state fulfils all the constraints in a very natural way. Moreover, we also obtain a reasonable agreement, especially for flatter potentials, when comparing to the relation between mass and baryon number derived from the lighter neutron star of a double pulsar (concretely, the double pulsar J0737-3039).

Finally, after the conclusions from this PhD thesis, we also present some relevant directions for a further investigation. The most obvious step forward to extend this BPS theory to the near-BPS Skyrme model which is necessary for a complete theory of strong interactions. As a consequence, this would improve the description of small nuclei and allow to obtain the right symmetry of nuclei (remember that due to the volume preserving diffeomorphisms the BPS model has an infinite number of solutions with different shapes) so a study of nuclear spectroscopy might be carried out. However, this implementation seems a quite difficult numerical task. Furthermore, one might continue to investigate different potentials and even use some observational data to constrain the possible allowed ones.

USC
UNIVERSIDADE
DE SANTIAGO
DE COMPOSTELA

Resumo

É ben coñecido que, até o de agora, QCD non pode dar respostas precisas no límite de baixas enerxías porque aquí, as técnicas perturbativas que se adoitan empregar xa non son útiles. No seu lugar, as teorías de campos efectivas son unha ferramenta común para acadar unha boa descrición e comprensión da teoría das interaccións fortes. De entre estas teorías efectivas, un caso particular, utilizado con éxito, correspóndese co chamado modelo Skyrme. Trátase dunha teoría efectiva a baixas enerxías das interaccións fortes proposta por T. H. R. Skyrme nos anos sesenta onde os graos de liberdade fundamentais veñen dados polos mesóns pións. Esta orixinal idea recibiu un pulo adicional cando se descubriu que, no límite dun número grande de cores de QCD (límite de N_C grande), tamén aparecía unha teoría efectiva de mesóns. O Lagranxiano orixinal consta de dous termos (nós o chamaremos modelo Skyrme estándar), un termo cuadrático en primeiras derivadas que se corresponde co modelo sigma non lineal (tamén coñecido coma termo de Dirichlet), e que proporciona a enerxía cinética dos pións; e outro que é quártico en primeiras derivadas e foi introducido explicitamente por Skyrme para evitar o teorema de transformacións de escala de Derrick, e que deste xeito, solucións estables poidan existir. Tanto hadróns como núcleos emerxen coma excitacións colectivas (solitóns topolóxicos) dos graos de liberdade efectivos e están caracterizados por unha propiedade topolóxica: o número de voltas ou carga topolóxica. Dado que se trata dunha cantidade topolóxica vai ser conservada, co que indentificándoa co número bariónico asegurámonos da súa conservación.

Así, atopamos unha concordancia cualitativa entre os datos experimentais e os observables derivados do modelo Skyrme, por exemplo, masas nucleares ou radios de carga. Aínda que os valores cuantitativos presentan unha discrepancia do $10-20\%$, pódese mellorar esta situación cunha xeneralización do modelo Skyrme por medio de termos adicionais (recórdese que se trata dunha teoría efectiva polo que non existen motivos para non incluir máis termos). A primeira contribución que se pode pensar é a dun potencial (se non se indica doutro xeito, utilizaremos o potential Skyrme estándar cunha aproximación cuadrática ao baleiro). Non ten derivadas e, de feito, tense empregado amplamente con antelación (especialmente para introducir as masas dos pións). Para a seguinte contribución, se como moito se quere un termo cuártico en primeiras derivadas, de xeito que unha fomulación Hamiltoniana estándar sexa posible, a única opción é un termo séxtico (en primeiras derivadas) que consiste no cadrado da corrente topolóxica (bariónica). Dous exemplos destes modelos xeneralizados son o modelo Skyrme BPS (Bogonolny-Prasad-Sommerfield) e o modelo Skyrme *near-BPS*.

Na presente tese de doutoramento ímonos centrar no estudo do modelo Skyrme BPS e as súas aplicacións á termodinámica da materia nuclear, as enerxías de enlace dos núcleos e a descrición das estrelas de neutróns. Este modelo consiste en dous únicos termos: un potential, e o termo séxtico. O seu nome vén da propiedade BPS que consiste nunha cota topolóxica lineal no número bariónico e con solucións que a saturan. Isto implica que a masa nuclear correspondente está linealmente relacionada co número bariónico. Ademais, dependendo de como se achega o potencial ao baleiro, existen solucións compactas cun radio que crece coa raíz cúbica do número bariónico. Polo tanto, ambos os dous comportamentos coinciden con feitos básicos fenomenolóxicos da física nuclear. Considerando as simetrías, o modelo Skyrme BPS presenta os difeomorfismos que preservan a área no espazo de chegada coma simetrías (o que implica un número infinito de solucións con diferentes simetrías), e ademais, tamén os difeomorfismos que preservan o volume no espazo base. Estes últimos corresponden ás simetrías dun fluído ideal incompresible e están relacionadas co modelo nuclear da gota líquida.

Non obstante, sabemos que este modelo non está completo porque, por exemplo, non recolle a dinámica dos pións. De feito, ao longo desta tese encontraremos algunhas evidencias máis de que unha extensión ao outro modelo xeneralizado anteriormente mencionado (o modelo Skyrme near-BPS) é precisa. Neste caso, o modelo near-BPS presenta dúas partes ben diferenciadas. Por un lado, unha contribución dominante que vén dada polo modelo BPS que acabamos de comentar. Doutra banda, o modelo Skyrme estándar, a ser introducido dunha maneira perturbativa por medio dun parámetro global ε. Como consecuencia, o modelo Skyrme BPS é responsable da meiranda parte das propiedades incluso nesta configuración near-BPS, polo que como primeira aproximación, o estudo dos temas presentados neste traballo usando tan só o modelo Skyrme BPS é máis que razoable. Así e todo, debemos ter en conta que para outras propiedades da física nuclear como a espectroscopía nuclear, a parte perturbativa si é importante.

Tras unha breve comparación entre o modelo Skyrme estándar e o BPS, centrado na descrición das resonancias Roper, comezamos co estudo da termodinámica de Skyrme BPS a temperatura cero con dúas cantidades importantes: a compresibilidade e o potencial químico bariónico. Como paso previo, introducimos a presión calculando o correspondente tensor de enerxía -momento e impoñendo a súa conservación. Así, atopamos que a presión ten que ser constante, e que precisamente esta condición é equivalente ás ecuacións estáticas dos campos, onde no caso de solucións BPS esta constante é exactamente nula. Ademais, chegamos a expresións para a enerxía e o volume en función da presión que poden ser escritas como integrais sobre o espazo de chegada, polo que non é preciso coñecer solucións específicas para calculalas.

No caso da compresibilidade ou módulo de compresión (inversamente relacionados), atopamos diferentes comportamentos que dependen, basicamente, de como se achega o potential considerado ao baleiro. Resumindo os resultados, obtivemos un valor finito da compresibilidade cando o comportamento do potencial é menor que cuadrático. Sen embargo, estes ponteciais son problemáticos dende un punto de vista físico porque a varación segunda en torno ao baleiro é infinita. Doutra banda, potenciais con polo menos unha aproximación cuadrática son fisicamente aceptables e presentan compresibilidade infinita (modulo de compresión cero), o que semella un resultado bastante xenérico. A maiores, neste caso, cando o comportamento preto do baleiro é menor ca séxtico, os Skyrmións a temperatura cero son compactóns e aparece unha transición de fase para valores do volume correspondente ao do equilibrio (ao volume a cero temperatura). A situación é como segue. A temperatura cero e número bariónico fixo podemos ter un volume maior que no equilibrio e que corresponde a un gas ideal de compactóns sen superpoñerse. Non obstante, podemos reducir este volume baleirando o espazo entre eles ata que o volume de equilibrio é acadado. Neste punto, o volume pódese reducir aínda máis introducindo a presión de xeito que o sistema entra nunha fase líquida.

No que atinxe á outra cantidade termodinámica, o potencial químico bariónico, presentamos dous tratamentos distintos. Primeiro, un cálculo teórico da teoría completa onde obtemos unha relación lineal entre o potencial químico e a densidade bariónica independente do potencial escollido. E segundo, unha aproximación de campo medio baseada no promedio dalgunhas cantidades, esencialmente a enerxía e o volume. Neste límite de campo medio, os cálculos son posibles sen coñecer solucións específicas e diversos potenciais son analizados. Así atopamos que só para o potencial escalón obtemos exactamente o mesmo potencial químico (porque os dous tratamentos son completamente equivalentes). Ademais, este potencial químico bariónico permítenos estudar as propiedades *in-medium* de Skyrmións en materia Skyrmiónica polo que os primeiros pasos no marco do modelo BPS son dados.

Outro tema importante desta tese é o cálculo das enerxías de enlace dos núcleos. Para isto, a propiedade BPS do modelo é de extrema importancia. De feito, debido á cota da enerxía, lineal no número bariónico, as enerxías de enlace clásicas son cero. Sen embargo, isto non é un problema xa que para unha descrición correcta dos núcleos, son necesarias contribucións adicionais á enerxía. Primeiramente, precisamos acometer unha cuantización semiclásica do espín e isospín, i.e., introducir graos de liberdade rotacionais e isorrotacionais que dependan do tempo en torno ás solucións estáticas, e cuantizalos no modo no que se adoita facer. Debido á simetría da nosa solución (supoñemos que é axial), obtemos que, para numero bariónico maior ca un, o Hamiltoniano resultante consiste en dúas copias do dun trompo simétrico á

vez que aparece unha restricción para algúns números cuánticos.

En segundo lugar, temos que considerar a enerxía de Coulomb, que vén dada pola xeneralización ás densidades de carga volumétricas da expresión usual. Así, tras calcular a densidade de carga e cuantizala, resolvemos as integrais que aparecen por medio dunha expansión da densidade de carga en harmónicos esféricos e a expansión multipolar do potencial de Coulomb. Estas contribucións á enerxía só dependen da terceira compoñente de isospín.

Finalmente, debido a que os neutróns son máis pesados que os protóns, tamén temos que ter en conta un potencial que rompa a simetría de isospín. O tratamendo adecuado, que sería a introducción no Lagranxiano dun potencial de rotura de isospín coa correspondente quantización semiclásica, é moi complicado a día de hoxe. Polo tanto, só consideramos a contribución principal que vén dada por un termo proporcional á terceira compoñente de isospín.

Con todo isto, obtivemos as enerxías de enlace procedentes destas contribucións axustando os tres parámetros libres dos que dispoñemos (correspondentes aos dous termos do Lagranxiano e a constante de proporcionalidade da rotura de isospín) a tres cantidades: a masa do protón, a diferencia experimental de mases entre o neutrón e o protón, e á masa dun núcleo con números máxicos. Desde xeito comparamos os valores da nosa teoría cos datos experimentais, atopando unha boa correspondencia para núcleos con número bariónico alto. Aínda que o comportamento para núcleos pequenos non é tan bo (as enerxías de enlace están sobreestimadas), era algo a esperar, porque o modelo Skyrme BPS baséase nunha descrición colectiva dos graos de liberdade fundamentais e, para núcleos pequenos, as propiedades dunha partícula e a propagación dos graos de liberdade piónicos son importantes. Ademais, a simetría axial non é a correcta. Polo tanto, o modelo Skyrme BPS proporciona a contribución principal para a descrición das interaccións fortes aínda que unha extensión á teoría near-BPS é precisa para unha mellora da situación a número bariónico baixo.

Debido ás boas propiedades do modelo Skyrme BPS, os nosos cálculos dan como resultado expresións analíticas para as enerxías de enlace que dependen do número bariónico, do número atómico e do número cuántico de isospín. Polo tanto, podemos establecer unha comparación entre a nosa fórmula e a fórmula semiempírica de masas (ou fórmula de Weizsäcker). De feito, obtemos unha relación directa cos termos de volume e de Coulomb da fórmula de Weizsäcker. Ademais, o noso modelo presenta un termo similar aínda que lixeiramente distinto do de asimetría, que dá contribucións máis pequenas a alto número bariónico. Non obstante, espérase que esta situación poida mellorar ao facer efectiva a extensión do modelo á súa versión near-BPS.

Para finalizar coas enerxías de enlace, tamén investigamos o efecto doutros potenciais. Así, ademais do potencial Skyrme estándar considerado até o de

agora, tamén estudamos o seu cadrado (cun comportamento quártico preto do baleiro), e unha familia de pontenciais tipo escalón con aproximacións cuadrática e cuártica ao baleiro. Aquí, o principal resultado é que, polo menos cando falamos dos potenciais cuadrático e cuártico, a forma concreta do potencial non ten un efecto determinante e o princial factor que dá lugar ás diferenzas é o xeito no que se achega ao baleiro.

O último tema a tratar nesta tese de doutoramento é o acoplo do modelo Skyrme BPS á gravidade para a descrición de estrelas de neutróns. Neste punto, a versión BPS parece ter certas vantaxes respecto to modelo Skyrme estándar. O principal motivo é que as verdadeiras estruturas que minimizan a acción do modelo Skyrme orixinal son cristais Skyrmiónicos, mentres que o máis probable é que o núcleo das estrelas de neutróns estea nunha fase de superfuído. Así, acoplamos o modelo á gravidade asumindo unha métrica esfericamente simétrica. A minimización da acción correspondente é equivalente á resolución das ecuacións de Einstein que veñen dadas en función do tensor de enerxía-momento e do tensor de Einstein. Tras un longo cálculo cos símbolos de Christoffel, o tensor de Ricci e a curvatura escalar; obtemos o tensor de Einstein e chegamos ás ecuacións do mesmo nome. Concretamente, debido á simetría do problema, só temos tres ecuacións de Einstein independentes, polo que temos un sistema de ecuacións diferenciais ordinarias que consiste en dúas ecuacións para o campo da materia e a función métrica (de tipo espacial) máis unha ecuación determinando a outra función métrica (de tipo temporal) en termos das outras dúas.

Para resolver numericamente este sistema, empregamos un *shooting* dende o centro cun método de Runge Kutta e axustamos os parámetros do modelo a algunhas propiedades dos nucleóns (precisamos un axuste distinto para cada potencial). Neste punto, non seguimos o tratamento de Tolman-Oppenheimer-Volkoff (TOV) que consiste en asumir unha ecuación nuclear de estado alxebraica que pecha es ecuacións de TOV. No seu lugar, realizamos o cálculo exacto da teoría de campos. Unha característica importante desde cálculo é a aparición de tres comportamentos distintos, onde agora o paramétro relevante é o número bariónico. Así, para valores pequenos só hai unha única solución. Para valores maiores pero por debaixo dun certo número bariónico existen dúas solucións, aínda que é aquela cun valor máis baixo da densidade de enerxía no centro a que se corresponde coa solución estable. Finalmente, por riba do número bariónico anteriormente comentado, non existen solucións físicas e os Skyrmións son inestables e colapsan nun burato negro. Unha vez que temos a solución, as masas das estrelas de neutróns obtéñense facilmente da solución no baleiro da función métrica (de tipo espacial), mentres que os radios corresponden ao punto onde o campo de materia faise nulo.

Estes cálculos numéricos exactos son feitos para dous potenciais distintos,

o potencial Skyrme estándar e o seu cadrado. Os principais resultados que obtemos son o valor máximo das masas das estrelas antes do colapso e os correspondentes radios, que están en consonancia cos datos observacionais á nosa disposición, onde as estrelas con masas ao redor de dúas masas solares son ben coñecidas e hai incluso evidencias de masas de até unhas dúas masas solares e media. Outro importante resultado é que, en xeral, unha ecuación de estado universal e alxebraica (relacionando a presión e a densidade de enerxía) non é posible sen unha aproximación. Non obstante, unha vez que temos a solución, podemos chegar numericamente a unha ecuación de estado *on-shell* a partir da presión e da densidade de enerxía como función da coordenada radial. Sen embargo, os parámetros que aparecen na ecuación de estado dependen do número bariónico no canto de seren constantes.

De xeito interesante, este modelo Skyrme BPS tamén permite o tratamento TOV habitual, polo que ambos resultados poden ser comparados de maneira frutífera. Para levar a cabo estes cálculos TOV, simplemente temos que recordar o límite de campo medio presentado na descrición do potencial químico bariónico. Así, obtemos unha ecuación de estado de campo medio a través dun proceso de promedio, polo que esta ecuación promedio é agora alxebraica e independente das coordenadas. Coma no caso anterior, resolvemos as ecuacións TOV numericamente cun shooting dende o centro cun método de Runge Kutta e co mesmo axuste a algunhas propiedades dos nucleóns. Neste caso, a maiores do potencial Skyrme estándar e o seu cadrado, tamén consideramos un potencial escalón onde os dous tratamentos, exacto e de campo medio, son completamente equivalentes.

Comparando ambas os dóus cálculos, vemos que as cantidades globais non presentan moita diferenza. De feito, os valores máximos das masas das estrelas de neutróns son lixeiramente maiores no límite de campo medio que no cálculo exacto. Sen embargo, ao comparar cantidades locais, ponse de manifesto que os dous tratamentos presentan importantes diferenzas. Por exemplo, a función métrica (de tipo espacial) alcanza o seu valor máximo exactamente na superficie da estrela no límite de campo medio, mentres que no cálculo exacto, o valor máximo atópase no seu interior. Ademais, a diferenza entre os dous tratamentos é maior canto máis se diferencia o potencial escollido do potencial escalón, i.e, canto máis se diferencia dun potencial constante (tamén corresponde a densidades de enerxía e de partículas constante). Polo tanto, esperamos que, para teorías alén do modelo Skyrme BPS, as diferenzas sexan máis notables para aquelas con inhomoxeneidades importantes nas densidades de enerxía e de partículas.

Neste punto, aínda que non se poden establecer predicións cuantitativas precisas (recordemos que se precisaría a extensión ao modelo Skyrme near-BPS), podemos comparar os nosos resultados con algunhas restriccións ex-

traídas de datos observacionais, dado que algunhas propiedades son debidas principalmente ao modelo Skyrme BPS. Por exemplo, é o caso das masas das estrelas de neutróns en función do radio. Nos nosos cálculos atopamos que, excepto preto do valor máximo da masa, as masas das estrelas crecen ao incrementar o radio, o que está en clara contradición co comportamento típico derivado dunha larga clase de ecuacións de estado usadas en física nuclear. Sen embargo, cando consideramos algunhas restriccións á relación masa-radio obtidas de datos observacionais, concretamente, da masa estimada para unha estrela binaria de raios X, das oscilacións quasiperiódicas a alta frecuencia doutra binaria de raios X, e da radiación térmica dun púlsar illado; atopámonos con que a nosa ecuación de estado cumple con todas as restriccións dun xeito moi natural. Ademais, tamén obtemos un acordo razoable, especialmente para potenciais máis planos, se comparamos coa relación entre masa e número bariónico derivada da estrela de neutróns máis lixeira dun púlsar dobre (concretamente, do púlsar dobre J0737-3039).

Finalmente, tras as conclusións desta tese de doutoramento, tamén presentamos algunhas direccións relevantes para proseguir coa investigación. O paso máis obvio é a extensión desta teoría BPS ao modelo Skyrme near-BPS, preciso para unha completa descrición da teoría das interaccións fortes. Como consecuencia, isto melloraría a descrición de núcleos pequenos e permitiría obter a simetría correcta dos núcleos (recórdese que debido aos difeomorfismos que preservan o volume, o modelo BPS ten un número infinito de solucións con formas diferentes), polo que se podería levar a cabo un estudo da espectroscopía nuclear. Non obstante, a súa execución parace tratarse dunha tarea numérica bastante difícil. Doutra banda, deberíase continuar tamén coa investigación de diferentes potenciais e incluso empregar algúns datos observacionais para restrinxir aqueles que poden ser permitidos dende un punto de vista físico.

USC
UNIVERSIDADE
DE SANTIAGO
DE COMPOSTELA

Contents

List of Figures

Abbreviations

BPS	Bogomolny-Prassad-Sommerfield
DBHF	Dirac-Brueckner-Hartree-Fock
e.g.	*exempli gratia*
Eq.	Equation
EoS	Equation of State
Fig.	Figure
i.e.	*id est*
LMXB	Low-Mass X-ray Binary
MF	Mean-Field
MF-EoS	Mean-Field Equation of State
QCD	Quantum Cromoynamics
QHD	Quantum Hadron Dynamics
SDiff	Special Diffeomorphisms
TOV	Tolman-Oppenheimer-Volkoff
VPD	Volume Preserving Diffeomorphism
vs	*versus*

USC
UNIVERSIDADE
DE SANTIAGO
DE COMPOSTELA

Chapter 1

Introduction

If asked nowadays about Quantum Chromodynamics (QCD), every physicist would agree on what it is: the theory of strong interactions describing forces between quarks and gluons. But if we look back in time for its origins, we find them in nuclear physics and the study of baryons and mesons and the ordinary matter they form. Paradoxically, like some kind of Nature's joke, it is in this regime of the theory where the nucleons live, that QCD still cannot give us precise answers.

Because of asymptotic freedom [1, 2] and the running of the coupling constant, we can use the perturbative regime of QCD when studying what happens at high energies. However, when looking at the realm of hadrons and nucleons, we arrive at the low energy limit of QCD, and here the fundamental interactions are so strong that perturbative techniques are no longer useful. One discipline which has reached considerable success here is *Lattice QCD*, based on the idea of discretizing the continuous space-time. Nevertheless, numerical problems make it difficult to use for the description of systems at high density and low temperature, i.e., nuclear matter and neutron stars. Besides this, numerical calculations corresponding to the lattice give us some kind of black box where we cannot completely either control or understand the physics behind these calculations.

But there is another attempt to understand the low-energy limit of strong interactions and the underlying physics, the one given by effective theories, and it is here where the theory we are interested in comes from: the *Skyrme Model*. This is a low-energy non-linear field theory of QCD proposed by the British physicist T. H. R. Skyrme in the 60's, where the fundamental degrees of freedom are mesons (and more concretely pions) [3, 4, 5]. Then, baryons and nuclei arise as collective excitations of these mesonic fields, and due to the non-trivial character of these solutions, a non-trivial topological charge appears which can be successfully identified with the baryon number. However, there were three different ideas in Skyrme's mind when proposing his theory [6] [1]:

1. **Unification:** Skyrme was not too convinced of fully understanding

[1] Reconstruction made by Dr. Ian Aitchison of a talk given by Skyrme at the workshop on "Skyrmions" held at Cosener's House, Abingdon, 17-18 November 1984.

fermions, so instead of having bosons and fermions as fundamental particles, he thought it would be better to have only one.

2. **Renormalisation problem:** He felt that renormalisation "is just a very good and useful way of enabling us to live with our ignorance of what really goes on at short distances".

3. **The fermion problem:** "Fundamental fermions are awkward to handle in the path integral formalism", so he liked "to think that the fermion concept was just a good way of talking about the behaviour of some semi-classical construction, and that it was no more fundamental than renormalisation".

Then, it seems that until the end of his days, Skyrme still had the hope that "the quarks or leptons introduced as sources in most theories" were "seen to be mathematical constructs helpful in its understanding, rather than fundamental constituents".

Despite his novel and brilliant ideas, Skyrme's model was forgotten for two decades, until G. t'Hooft [7], and especially E. Witten [8, 9], worked on the limit of a large number of colours of QCD, and showed that an effective theory of mesons arises. As a consequence, Skyrme's ideas received renewed attention and support. Then, a general acceptance of the Skyrme model emerged which was linked in most cases to the study of nuclear physics. In this sense, it was used for the description of protons and neutrons using a hedgehog ansatz [10, 11] or the deuteron by means of the axial symmetry [12, 13], as well as for some additional light nuclei [14, 15, 16]. Furthermore, an extension to SU(3) with some applications was developed, see, e.g., [17, 18, 19].

More recently, it was applied to higher baryon number nuclei and excitation spectra [20, 21], and some generalizations and submodels also appeared. Among them, there are some alternatives that probably deserve further attention, the models known as BPS models, like for instance [22] and [23, 24]. The main point here is the BPS property, which means the existence of a lower topological bound on the energy of the system and solutions saturating the bound [25, 26]. Then, solutions saturating or almost saturating this bound will allow for small nuclear binding energies, improving the results from the standard Skyrme model. Therefore, we will essentially use the second of these BPS models in the investigation presented here, since in addition to having solutions saturating the BPS bound for arbitrary baryon number, it also has some desired properties from the phenomenological point of view of nuclei such as the mass-baryon number relation or the volume preserving diffeomorphisms symmetry (related to the liquid drop model).

In addition, interesting research within the Skyrme model has been carried out in the last year too. For instance, a study of classically isospining Skyrmions [27] and Skyrmion-Skyrmion scattering [28] have been developed, besides an implementation of the structures and properties of the carbon-12 within the Skyrme model [29]. On the other hand, another variant of the model has been proposed [30], which is based in this case on some topological energy bounds [31, 32].

Thus, the aim of this PhD thesis is to provide a deeper insight in the BPS Skyrme model going from the properties and understanding of the model to the study of nuclear matter focusing on nuclei and neutron stars. With this purpose, the work is organized as follows: first, in Chapter 2, we will give some basic ideas about the Standard Skyrme model as well as presenting the BPS Skyrme model and its main properties, to further analyse its thermodynamics in Chapter 3. After this, we go directly into the nuclear world by the study of nuclei and, more precisely, their binding energies, with an excellent agreement with the experimental values for high nuclei. This is the main content of Chapter 4 where, as well as the classical energy, more contributions have to be taken into account, namely: the spin and isospin quantization, the Coulomb energy and the isospin breaking. As a final step, we couple the model to gravity in Chapter 5, allowing for a good description of neutron stars where the known values of masses and radii are supported. And just to conclude, conclusions and outlook are summarized in Chapter 6.

USC
UNIVERSIDADE
DE SANTIAGO
DE COMPOSTELA

Chapter 2

Exploring the Skyrme Models

In this chapter we will make our first contact with the low-energy effective theory of strong interactions known as the Skyrme model. The first Lagrangian proposed by Skyrme is presented [3, 4, 5], and its main features and results are reviewed. Then, the generalization of the model is introduced to finally arrive at the BSP Skyrme model [23, 24], which will be the basis of all the investigations presented here. We conclude by showing how this BPS model can help to improve the results given by the standard one focusing on the case of the Roper resonances [33].

2.1 The Standard Skyrme Model

As we have commented in the Introduction, the fundamental degrees of freedom of the Skyrme theory are mesonic fields. Thus, since this investigation will focus on nuclei and neutron stars, we will consider the simplest possible target space, SU(2), for the Skyrme field U because only two flavours are needed for the description of protons and neutrons. The static solutions are maps from the 3-dimensional Euclidean space, $\mathbb{R}$ into the SU(2) Lie group, so taking into account the compactification of the base space due to the finite energy boundary condition $U(\vec{x}) \to U_0 = \text{const.}$ as $\vec{x} \to \infty$, and that SU(2), as a manifold, is isomorphic to the 3-sphere, $\text{SU}(2) \cong \mathbb{S}^3$, we have

$$U: \quad \mathbb{R}^3 \cup \{\infty\} \cong \mathbb{S}^3 \ni \vec{x} \longrightarrow U(\vec{x}) \in \mathbb{S}^3. \tag{2.1}$$

Because of the topological character of the map (a map between two 3-spheres), it is characterized by a topological quantity depending on geometrical properties of the target space rather than on a specific solution of the theory. This is the winding number or topological charge, the one that Skyrme successfully identified with the baryon number, ensuring in this way its conservation. It is given by

$$B = \frac{1}{24\pi^2} \int d^3\, x \varepsilon^{ijk}\ \text{Tr}\ (L_i L_j L_k), \tag{2.2}$$

where $L_\mu = U^\dagger \partial_\mu U$ is the left-invariant Maurer-Cartan current.

Then, the model originally introduced by Skyrme (which we shall call the standard Skyrme model in the sequel) is the field theory defined by the following Lagrangian containing two terms [our Minkowski metric conventions are $\mathrm{diag}(g_{\mu\nu}) = (+---)$]:

$$\mathscr{L}_{Skr} = \mathscr{L}_2 + \mathscr{L}_4. \tag{2.3}$$

The first term, $\mathscr{L}_2$ is the non-linear sigma-model term

$$\mathscr{L}_2 = -\frac{f_\pi^2}{4}\,\mathrm{Tr}\,(L_\mu\, L^\mu), \tag{2.4}$$

which is quadratic in first derivatives and provides the kinetic energy of pions. And $\mathscr{L}_4$ is the Skyrme term, quartic in first derivatives:

$$\mathscr{L}_4 = \frac{1}{32e^2}\,\mathrm{Tr}\,([L_\mu, L_\nu]^2), \tag{2.5}$$

and sufficient to avoid Derrick's theorem [34] so stable solutions can exist. In fact, the static energy functional for the Lagrangian (2.3) can be written as $E = E_2 + E_4$, where

$$E_2 = \frac{f_\pi^2}{4}\int d^3x\,\mathrm{Tr}\,(L_i\, L^i), \qquad E_4 = \frac{1}{32e^2}\int d^3x\,\mathrm{Tr}\,([L_i, L_j]^2). \tag{2.6}$$

So regarding the scale transformation $\vec{x} \to \lambda\vec{x}$, which implies the field transformation $U(\vec{x}) \to U_\lambda = U(\lambda\vec{x})$, the energy functional scales like $E_\lambda = \lambda^{-1}E_2 + \lambda E_4$. Now, Derrick's theorem tells us that the first derivative of the energy functional with respect to the scaling (evaluated at $\lambda = 1$) has to be zero for stable solutions to exist. In our case it means:

$$\left.\frac{dE}{d\lambda}\right|_{\lambda=1} = -E_2 + E_4 = 0. \tag{2.7}$$

Therefore, we see from this theorem that stable solutions can exist and the E_4 term is crucial for their existence. In contrast, if we only had the E_2 contribution the value of the energy could always be lowered by a scale transformation corresponding to the case of a shrinking soliton, implying the need for the Skyrme term in the Lagrangian as stated above. Finally, it is worth noting that Derrick's theorem just tells us about the possibility of stable solutions to exist but not about their existence, so it can be used to conclude stable solutions do not exist but not the other way around.

Although (2.3) is the original Lagrangian proposed by Skyrme, a further term is usually added [11]. This new contribution is a potential term breaking chiral symmetry which is related to pion masses:

$$\mathscr{L}_0 = -\mu^2 \mathcal{U}. \tag{2.8}$$

When this potential is $\mathcal{U} = \mathcal{U}_\pi = \frac{1}{2}\ \mathrm{Tr}\ (1 - U)$, it is known as the standard Skyrme potential. Then, from now on, and if not stated otherwise, when referring to the standard Skyrme model we will mean the Lagrangian composed of the three terms presented so far, i.e.,

$$\mathscr{L}_{Skr} = \mathscr{L}_0 + \mathscr{L}_2 + \mathscr{L}_4. \tag{2.9}$$

Considering what we have presented above, the Skyrme model can be thought of as an effective field theory being a good starting point for the study of the low energy limit of QCD and which is also supported by the large N_C limit. However, it also presents some drawbacks:

- *Large binding energies.* In spite of the existence of a lower bound for the energy proportional to the baryon number (Skyrme-Faddeev bound [35, 36]), solutions do not saturate it. For instance, the simplest Skyrmion, corresponding to baryon number $B = 1$, presents an energy about 23% above the bound, whereas for higher solitons this excess is lowered to less than a 4%. This is translated into binding energies much higher than the experimental 1% of the mass, both for the massless [37, 38, 39] and massive Skyrme model [21, 40, 41].

- *Shell-like baryons.* The standard Skyrme model has no predilection for core or ball configurations. In the massless case [37, 38, 39], fullerene-like structures with empty regions inside are preferred, and the relation between radius and topological charge (baryon number) is not the desired one but $R \sim \sqrt{B}$. When including a pion mass term [21, 40, 41], we approach the phenomenological dependence $R \sim \sqrt[3]{B}$. Unfortunately, for reasonable physical parameter values, some shell-like structures still survive, particularly for small baryon number. Finally, it is worth commenting that in the limit of nuclear matter (large baryon number) the solution minimizing the energy is of crystal type.

- *Quantitative results.* Although there is an impressive qualitative agreement between experimental data and observables derived from the Skyrme model such as nuclear masses or charge radii, their quantitative values present a discrepancy of about $10 - 20\%$.

As a consequence of this, some modifications of the model have been proposed trying to improve the situation, and it is in this context where the BPS Skyrme model arises.

2.2 The BPS Skyrme Model

The Skyrme model is an effective theory; therefore, there are no reasons for not including more terms in the Lagrangian. For instance, we can think of this Lagrangian as a derivative expansion. With this idea in mind, and taking the original Lagrangian proposed by Skyrme, the first term we can think of is exactly the one presented in (2.8), a potential (it corresponds to no derivatives and in this case it is related to the pion mass). Going to higher derivatives, the next term will be a sextic one. If, in addition, we ask the Lagrangian to be no more than quadratic in time derivatives (so a standard Hamiltonian formulation is possible), the only term allowed is the square of the topological current:

$$\mathscr{L}_6 = -\lambda^2 \pi^4 \mathcal{B}_\mu^2, \tag{2.10}$$

where

$$\mathcal{B}^\mu = \frac{1}{24\pi^2} \mathrm{Tr}(\varepsilon^{\mu\nu\rho\sigma} U^\dagger \partial_\nu U U^\dagger \partial_\rho U U^\dagger \partial_\sigma U) \tag{2.11}$$

is the topological current with the integral of its zero component being just the topological charge defined by (2.2) and identified with the baryon number. This term has already been considered before, especially related to the vector meson exchange [42, 43, 44, 45]. Thus, the generalized Skyrme model is just the Lagrangian made of the four terms:

$$\mathscr{L} = \mathscr{L}_0 + \mathscr{L}_2 + \mathscr{L}_4 + \mathscr{L}_6, \tag{2.12}$$

respectively defined by equations (2.8), (2.4), (2.5) and (2.10).

One specific implementation of this idea is what we will call the near-BPS Skyrme model which is given by the Lagrangian

$$\mathscr{L} = \varepsilon \mathscr{L}_{Skr} + \mathscr{L}_{BPS}, \tag{2.13}$$

where ε is a small parameter and $\mathscr{L}_{BPS} = \mathscr{L}_0 + \mathscr{L}_6$. Thus, the near-BPS theory is a usual generalized Skyrme model with a special choice of the parameters. The original proposal here is the fact that the BPS part gives the leading contribution to the energy when ε is small. The importance of this BPS Skyrme model (limiting case when $\varepsilon \to 0$) is based on several important properties. First of all, the BPS property (see below) which will immediately give as a result classical zero binding energies. Obviously, if the full model has a small non-BPS part one then gets small classical binding energies, which can (and should) be also achieved in a semiclassical approach (see Chapter 4). On the other hand, it provides a good description of nuclear matter as a perfect

fluid. Indeed, it presents the energy-momentum tensor of a perfect fluid and SDiff symmetries, and even an Eulerian formulation of a perfect fluid (non-barotropic in general) is possible [46]; so we have an effective theory where the microscopic (field theory) and thermodynamical descriptions agree with each other. Finally, one more relevant property is the emergent omega meson within the BPS Skyrme model (see [46] for details). It is known that this is the main interaction channel in the high density/pressure limit so its inclusion is unavoidable. In this limit, its contribution is higher than that coming from other Skyrme terms which makes it important not only for dense matter (e.g. neutron stars) but also for the scattering. Therefore, all these properties are physically welcome since they constitute a well motivated idealization of nuclear matter and alleviate some shortcomings of the usual Skyrme model as the non-BPS part weakly modifies them. Moreover, there is one last point to take into account, the fact that the BPS limit gives a solvable model in contrast to the usual Skyrme model which appears as a complicated geometrical theory.

It is also important to note that the near-BPS Skyrme model (with a prominent role of the BPS part) allows us to separate the full model into two parts. On the one hand, we have a perturbative contribution, $\mathscr{L}_{Skr}$, which is resposible for the behaviour near the vacuum. It is directly related to kinetic and two-body interactions as well as to chiral dynamics (pions) and also encodes the long range attractive interaction. It is a surface term in the sense that it gives shape to the Skyrmions and therefore it is crucial in the proper rotational excitations. On the other hand, there is a non-perturbative part, $\mathscr{L}_{BPS}$, which has topological coherent degrees of freedom. In this case it is a bulk term since it gives the main contribution to the masses with the result of low binding energies. As commented above, this implies the behaviour of a liquid phase and determines the thermodynamics of the model.

As we know, not all properties are independent (or weakly dependent) on the perturbative part (like the scattering), but even for them, the BPS contribution may signifincatly improve the results. Summarizing, the motivation to study the pure BPS Skyrme model is that it provides a physically motivated idealization of nuclear matter and, besides solvability, it seems quite reasonable to assume that some properties of baryons, nuclei and even nuclear matter are governed by the BPS part. However, we should have in mind that the full theory is the near-BPS model, as we will also see throughout this work.

Then, as commented, the BPS Skyrme model [23, 24] appears in this generalized context as an extreme case where the quadratic and quartic terms are neglected:

$$\mathscr{L}_{06} = \mathscr{L}_0 + \mathscr{L}_6, \tag{2.14}$$

so it can be seen as a first approximation for a theory where the contributions from $\mathscr{L}_2$ and $\mathscr{L}_4$ are small, i.e., a first approximation to the near-BPS model. Here, similarly to what happens with the standard Skyrme model, the term $\mathscr{L}_6$ is not enough to avoid Derrick's theorem and a potential term is needed in order that stable static solutions can exist.

We have shown in section 2.1 that the Skyrme field U is a SU(2) field. Then we can use the standard parametrization

$$U = e^{i\xi\vec{n}\cdot\vec{\tau}} = \cos\xi + i\sin\xi\vec{n}\cdot\vec{\tau}, \tag{2.15}$$

where ξ is a real field called profile function, $\vec{\tau}$ are the Pauli matrices and $\vec{n}$ is a three-component unit vector field related to a complex field u by the stereographic projection

$$\vec{n} = \frac{1}{1+|u|^2}\left(u+\bar{u}, -i(u-\bar{u}), 1-|u|^2\right). \tag{2.16}$$

Furthermore, for the rest of the work the potential dependence

$$\mathcal{U} = \mathcal{U}(\mathrm{Tr}\, U) = \mathcal{U}(\xi) \tag{2.17}$$

will be assumed.

Thus, after the parametrization, the Lagrangian reads

$$\mathscr{L}_{06} = \frac{\lambda^2\sin^4\xi}{(1+|u|^2)^4}\left(\varepsilon^{\mu\nu\rho\sigma}\xi_\nu u_\rho\bar{u}_\sigma\right)^2 - \mu^2\mathcal{U}(\xi), \tag{2.18}$$

with the corresponding equations of motion:

$$\frac{\lambda^2\sin^2\xi}{(1+|u|^2)^4}\,\partial_\mu(\sin^2\xi\, H^\mu) + \mu^2\mathcal{U}_\xi = 0, \tag{2.19}$$

$$\partial_\mu\left(\frac{K^\mu}{(1+|u|^2)^2}\right) = 0, \tag{2.20}$$

where

$$H_\mu = \frac{\partial(\varepsilon^{\alpha\nu\rho\sigma}\,\xi_\nu\,u_\rho\,\bar{u}_\sigma)^2}{\partial\xi^\mu}, \qquad K_\mu = \frac{\partial(\varepsilon^{\alpha\nu\rho\sigma}\,\xi_\nu\,u_\rho\,\bar{u}_\sigma)^2}{\partial\bar{u}^\mu}. \tag{2.21}$$

2.2.1 Symmetries and integrability

Besides the standard Poincaré symmetries, the BPS model presents an infinite number of target space symmetries. Their base is the sextic term, $\mathscr{L}_6$, which is the square of the pullback of the volume form on the target space $\mathbb{S}^3$. This volume form is

$$d\Omega = -2i\frac{\sin^2\xi}{(1+|u|^2)^2}\,d\xi\,du\,d\bar{u}, \tag{2.22}$$

so all transformations leaving this form invariant, i.e., the volume preserving diffeomorphisms (VPDs) on the target space, are symmetries of the sextic term. However, the potential term breaks this symmetry in general, although there are some potentials which just break them partially. This is the case of our potentials, $\mathcal{U}(\xi)$, which restrict the symmetry to the subgroup of VPDs leaving the profile function ξ invariant:

$$\xi \to \xi\,, \quad u \to \tilde{u}(u,\bar{u},\xi)\,, \quad (1+|\tilde{u}|^2)^{-2}d\xi d\tilde{u}d\bar{\tilde{u}} = (1+|u|^2)^{-2}d\xi u d\bar{u}. \tag{2.23}$$

In fact, this subgroup corresponds to a one parameter family of the group of the area preserving diffeomorphisms on $\mathbb{S}^2$ (the 2-sphere being spanned by the fields u and $\bar{u}$) [47, 48]. These transformations are symmetries of the full action, i.e., Noether symmetries, which will not be the case for other symmetries considered.

In the BPS Skyrme model, the static energy functional presents, in addition, an infinite number of symmetry transformations. The corresponding static energy functional is given by

$$E = \int d^3x \left(-\frac{\lambda^2\sin^4\xi}{(1+|u|^2)^4}(\varepsilon^{mnl}\xi_m u_n \bar{u}_l)^2 + \mu^2\mathcal{U}(\xi)\right). \tag{2.24}$$

Here, both d^3x and $\varepsilon^{mnl}\xi_m u_n \bar{u}_l$ are invariant under coordinate transformations of the base space leaving the base space volume form, d^3x, invariant. Therefore, also the VPDs on the base space $\mathbb{S}^3$ are symmetries of the model considering the static energy functional. Furthermore, these are the symmetries of an incompressible ideal fluid, which seems to be a nice feature since they are related to the liquid drop model of nuclei [49].

Another interesting property of the model is that it is integrable in the sense of generalized integrability [50]. Thus, it presents infinitely many conservation laws. Then, if we define the currents

$$J^\mu = \frac{\delta G}{\delta\bar{u}}\bar{\mathcal{K}}^\mu - \frac{\delta G}{\delta u}\mathcal{K}^\mu, \tag{2.25}$$

where

$$\mathcal{K}^\mu = \frac{K^\mu}{(1+|u|^2)^2}, \tag{2.26}$$

K^μ is given by (2.21) and $G = G(u,\bar{u},\xi)$ is an arbitrary function of its arguments; it can be easily seen that they are conserved (see [24] for details):

$$\partial_\mu J^\mu = 0. \tag{2.27}$$

2.2.2 The BPS property

One of the main properties of the model (and where its name comes from) is its BPS nature. This implies the existence of a lower bound for the static energy which only depends on the topology of the system and not on a specific solution. To see this bound, we can take the static energy functional (2.24) and try to write it as a total square, arriving then at the inequality which gives rise to the bound:

$$\begin{aligned} E &= \int d^3x \left(\frac{\lambda^2 \sin^4 \xi}{(1+|u|^2)^4} (\varepsilon^{mnl} i \xi_m u_n \bar{u}_l)^2 + \mu^2 \mathcal{U}(\xi) \right) \\ &= \int d^3x \left(\frac{\lambda \sin^2 \xi}{(1+|u|^2)^2} \varepsilon^{mnl} i \xi_m u_n \bar{u}_l \pm \mu \sqrt{\mathcal{U}} \right)^2 \\ &\mp \int d^3x \frac{2\mu\lambda \sin^2 \xi \sqrt{\mathcal{U}}}{(1+|u|^2)^2} \varepsilon^{mnl} i \xi_m u_n \bar{u}_l \\ &\geq \mp \int d^3x \frac{2\mu\lambda \sin^2 \xi \sqrt{\mathcal{U}}}{(1+|u|^2)^2} \varepsilon^{mnl} i \xi_m u_n \bar{u}_l \\ &= 2\lambda\mu\pi^2 |B| \frac{1}{2\pi^2} \int_{S^3} d\Omega \sqrt{\mathcal{U}(\xi)} \equiv 2\lambda\mu\pi^2 \langle \sqrt{\mathcal{U}} \rangle_{S^3} |B|. \end{aligned} \tag{2.28}$$

Here, B is the baryon number and the upper (lower) sign corresponds to solitonic (anti-solitonic) solutions. As well, in the last line we have used that inside the integral we have the pullback of the volume form $d\Omega$ on the target space $\mathbb{S}^3$ [see Eq. (2.22)], so

$$\langle \sqrt{\mathcal{U}} \rangle_{S^3} \equiv \frac{1}{2\pi^2} \int_{\mathbb{S}^3} d\Omega \sqrt{\mathcal{U}}, \tag{2.29}$$

is the average value of $\sqrt{\mathcal{U}}$ on the target space. It is also clear from (2.28) that the static energy is linear with the baryon number. This is important to solve the problem of the large binding energies of the standard Skyrme model, as we will comment below.

One important question is if it is possible to fulfil this topological bound. The answer is given by (2.28): it will hold if the square in the second line is identically zero. This gives rise to the BPS equation

$$\frac{\lambda \sin^2 \xi}{(1+|u|^2)^2} \varepsilon^{mnl} i \xi_m u_n \bar{u}_l = \mp \mu \sqrt{\mathcal{U}}, \tag{2.30}$$

which is satisfied by solutions saturating the bound and implies to go from second order to first order equations. This is the case of the ansatz introduced in the next subsection and used in this work.

2.2.3 Exact Solutions: The Standard Skyrme Potential

One important feature of this BPS Skyrme model is that it allows to get analytical solutions. In order to achieve them, we should choose an ansatz. Since the static energy functional (2.24) has the VPDs on target space as symmetries, rather arbitrary shapes are possible, so for simplicity we will use the axially symmetric ansatz (hedgehog configuration when $B = 1$)

$$\xi = \xi(r), \qquad u(\theta, \phi) = g(\theta)e^{iB\phi}, \tag{2.31}$$

where $x \in [0, \pi]$ and u spans the whole complex plane in order to cover the target space $\mathbb{S}^3$ at least once so static topologically nontrivial solutions appear. Nevertheless, when considering the near-BPS model the situation will be different because the shape actually matters. The approach to follow here would be the one presented in [51], where a more suitable shape is given by those VPDs minimizing the Dirichlet energy (the energy corresponding to the $\mathscr{L}_2$ term in the Lagrangian).

Coming back to the axially symmetric ansatz, the corresponding equation of motion for u given by (2.20) reads

$$\frac{1}{sin\theta}\partial_\theta\left(\frac{g^2 g_\theta}{(1+g^2)^2\sin\theta}\right) - \frac{g g_\theta^2}{(1+g^2)^2\sin^2\theta} = 0, \tag{2.32}$$

which is satisfied when

$$g(\theta) = \tan\frac{\theta}{2} \tag{2.33}$$

independent of the value of B. Whereas for the profile function the equation (2.19) gives rise to

$$\frac{B^2\lambda^2\sin^2\xi}{2r^2}\partial_r\left(\frac{\sin^2\xi\,\xi_r}{r^2}\right) - \mu^2\mathcal{U}_\xi = 0. \tag{2.34}$$

If a new variable z is introduced,

$$z = \frac{\sqrt{2}\mu r^3}{3|B|\lambda}, \tag{2.35}$$

this equation can be simplified and integrated to

$$\frac{1}{2}\sin^4\xi\,\xi_z^2 = \mathcal{U}, \tag{2.36}$$

which is just the square of the BPS equation found in the previous subsection, (2.30), reading in the usual variable r

$$\frac{B^2\lambda^2}{4\mu^2 r^4}\sin^4\xi\,\xi_r^2 = \mathcal{U}. \tag{2.37}$$

We see that for this ansatz the BPS equation is obtained from the field equation of the profile function ξ, so solutions are always of the BPS type saturating the energy bound (2.28).

Finally, to arrive at a solution, a concrete potential must be specified. Although here the potential is not related to the pion masses as when it was introduced in (2.8) within the standard Skyrme model framework (in the BPS Skyrme model the kinetic term for pions, (2.4), is absent), we will also use the standard Skyrme potential just for simplicity, so unless stated otherwise, we will always assume through this work

$$\mathcal{U} = \mathcal{U}_\pi = \frac{1}{2}\mathrm{Tr}(1-U) \to \mathcal{U}(\xi) = 1-\cos\xi. \tag{2.38}$$

Then, from the BPS equation (2.36) with the right boundary conditions for the profile function, we arrive at the analytical compact solution

$$\xi = \begin{cases} 2\arccos\sqrt[3]{\frac{3z}{4}} & z \in \left[0, \frac{4}{3}\right] \\ 0 & z \geq \frac{4}{3} \end{cases} \tag{2.39}$$

with the total energy

$$E = \frac{64\sqrt{2}\pi}{15}\mu\lambda|B|. \tag{2.40}$$

Thus, we see that besides having a definite radius, the corresponding energy is linear with the baryon number, reproducing the phenomenological behaviour found for nuclei. Furthermore, if we introduce the rescaled radial coordinate $\tilde{r}$

$$\tilde{r} = \left(\frac{\sqrt{2}\mu}{4\lambda}\right)^{\frac{1}{3}} r \equiv \frac{r}{R_0}, \tag{2.41}$$

with R_0 the compacton radius, the energy density per unit volume (with the unit of length set by $\tilde{r}$) is

$$\mathcal{E} = \begin{cases} 8\sqrt{2}\mu\lambda(1-|B|^{-\frac{2}{3}}\tilde{r}^2), & 0 \leq \tilde{r} \leq |B|^{1/3} \\ 0, & \tilde{r} > |B|^{1/3}, \end{cases} \tag{2.42}$$

while for the baryon number density

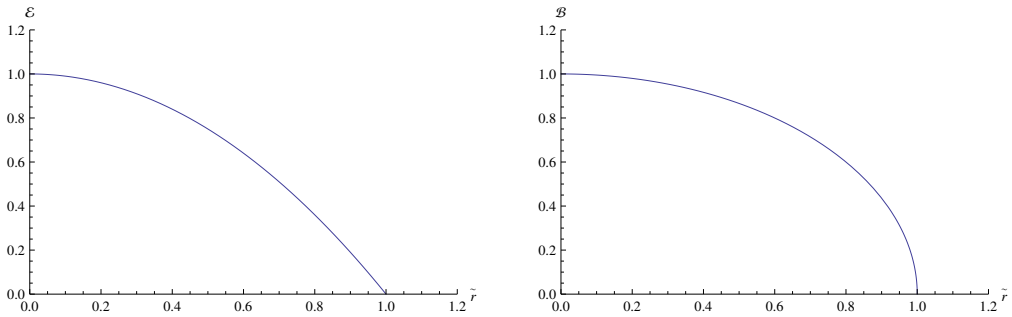

Figure 2.1: Normalized energy (left) and topological number (right) densities as functions of the renormalized radius $\tilde{r}$ for baryon number $|B| = 1$

$$\mathcal{B} = \begin{cases} \text{sign}(B)\frac{4}{\pi^2}(1 - |B|^{-\frac{2}{3}}\tilde{r}^2)^{1/2}, & 0 \leq \tilde{r} \leq |B|^{1/3} \\ 0, & \tilde{r} > |B|^{1/3}. \end{cases} \tag{2.43}$$

From these expressions not only the compact character of the solution is manifest again, but also the behaviour of the radius with the baryon number as $B^{1/3}$, which is a well known result for nuclei. Both densities are presented in Fig. 2.1 for baryon number one.

2.2.4 Main properties

If the most important features and results of the BPS Skyrme model are taken into account, it seems this can be a good starting point for an effective low-energy theory of QCD. In fact, it presents some of the very well established facts in nuclear physics, as can be seen from its fundamental properties (for a more detailed discussion see [23] or [24]):

- *Linear energy-charge relation.* As seen above, all the solutions of the model are BPS solutions so they fulfil the energy bound giving rise to a linear dependence of the topological charge (baryon number):

$$E = E_0|B|,$$

where $E_0 = 64\sqrt{2}\pi\mu\lambda/15$. This is the desired behaviour since it is a well known fact from nuclear physics. Furthermore, this relation leads to zero binding energies in contrast to the high values of the standard Skyrme model. Although the real values are not exactly zero, they do not exceed 1% of the mass, so a BPS theory seems a good starting point, with the inclusion of some small contributions (mainly the spin

and isospin quantization, the Coulomb energy and the isospin breaking, see Chapter 4).

- *Compact Solitons.* Since the solutions are analytical compactons there exists a well defined radius for nuclei given by

$$R_0 = R_0 \sqrt[3]{B}, \qquad R_0 = \left(\frac{2\sqrt{2}\lambda}{\mu} \right)^{1/3}.$$

We see that in this case also the experimental relation between nuclear radius and baryon number is achieved. As well, in contrast to the original Skyrme model where shell-like structures appear, here the energy density is spherically symmetric and monotonously decreasing from its maximum value at the centre, independently of the baryon number considered.

- *Liquid behaviour.* Because of the VPDs symmetry on the base space, deformations of the shape of nuclei will cost no energy when realized with fixed volume. Then, these deformations correspond to an ideal liquid so the model presents a liquid-drop behaviour for nuclear matter in contrast to the crystal-like structures appearing for the standard model when the baryon number is large. Although this is not the case for physical nuclei (it does cost energy), this symmetry is a good approximation for nature since deformations conserving the volume have much less cost in energy than volume-changing ones.

Taking into account these points, we see that the BPS Skyrme model solves some problems of the standard model from a qualitative point of view, giving a description which is closer to the phenomenological properties of nuclear matter. Finally, in the next section, we will see what happens in a quantitative way.

2.3 BPS vs Standard Skyrme Model: The Roper Resonances

In this last section we are going to quantitatively compare the BPS Skyrme model to the standard Skyrme theory by focusing on the study of the Roper resonances [33]. However, before going into the subject, we shall briefly see what happens between both models when considering the classical energy (mass) of the solutions.

B	$E_{\text{experiment}}$	E_{BPS}	$E_{\text{vec Skyrme}}$	E_{Skyrme}
1	939	931.75	996	1024
2	1876	1863.5	1999	1937
3	2809	2795.25	2913	2836
4	3727	3727	3727	3727
6	5601	5590.5	···	5520
8	7455	7454	···	7327
10	9327	9317.5	···	9113

Table 2.1: Classical energies in the BPS Skyrme model compared with experimental data and masses from the vector-Skyrme and the standard Skyrme model. All numbers are in MeV (Table taken from [24]).

As seen above, the static energy is given by $E = E_0|B|$, where E_0 is proportional to the product of the parameters μ and λ. Following [24], we can fix this product assuming $E_0 = 931.75$ MeV, which comes from asking the mass of He^4 to be equal to the mass of the solution corresponding to baryon number $B = 4$. This is the usual choice because the ground state of He^4 presents zero spin and isospin [41], so possible corrections do not have to be included. Results for some baryon numbers from 1 to 10 can be reproduced from [24] and are presented in Table 2.1, where a comparison between the BPS Skyrme model and experimental values and energies from the vector-Skyrme model [52] and the standard Skyrme model [40] has been realized.

Analysing the results we see there is an improvement in the value of the classical masses. The maximum discrepancy is of a 0.7% in the BPS theory instead of the 7% typical accuracy of the usual Skyrme models (obviously the experimental value is obtained for the mass of He^4 in every model). Moreover, although the BPS values are lower than the experimental ones, we should have in mind that more contributions to the energy are needed, for instance the inclusion of the spin and isospin. In [24] more observables like charge radii or magnetic moments are compared with the ones from [11].

2.3.1 Roper Resonance Masses

The study of the Roper resonances was already performed for the standard Skyrme model [53, 54, 55] and even its SU(3) version [56, 57]. It requires the calculation of the rotational-vibrational spectrum for baryon number $B = 1$, so the semiclassical quantization of the rotational and vibrational modes is needed in the BPS Skyrme model for the hedgehog solution (the detailed study of the quantization procedure will be discussed in Chapter 4).

In order to implement these transformations it will be useful to split the Lagrangian coming from (2.14) in the static and time dependent contributions:

$$\begin{aligned} L_{06} &= \int d^3x \left(-\frac{\lambda^2}{24^2}[\mathrm{Tr}(\varepsilon^{\mu\nu\rho\sigma} L_\nu L_\rho L_\sigma)]^2 - \mu^2 \mathcal{U} \right) \\ &= -E_{06} + \lambda^2 \pi^4 \int d^3x \mathcal{B}^i \mathcal{B}^i, \end{aligned} \tag{2.44}$$

where $\mathcal{B}^i$ are the spatial components of the topological current (2.11), and E_{06} is the static energy given by (2.24) which can be written using the Derrick scaling argument as

$$E_{06} = E_0 + E_6 = 2E_0, \tag{2.45}$$

with $E_0 = \mu^2 \int d^3x \mathcal{U}$ and $E_6 = \pi^4 \lambda^2 \int d^3x \, \mathcal{B}_0^2$.

Now, we have to consider both rotations and vibrations. The former is a symmetry of the action and is represented by a matrix $A \in \mathrm{SU}(2)$, whereas the latter corresponds to dilatation transformations which do change the action: $U(x) \to U(e^\Lambda x)$. Then, the idea of the semiclassical quantization is to let the corresponding parameters be time dependent and finally, promote them to quantum mechanical variables. Then, considering both transformations simultaneously and introducing this time dependence, we have for the Skyrme field

$$U(x) \to U'(x,t) = A(t) U_0(x e^{\Lambda(t)}) A^\dagger(t). \tag{2.46}$$

So we have to see how the Lagrangian behaves under this transformation. On the one hand, the static part changes only due to the scaling:

$$-E_{06} \to -(e^{-3\Lambda(t)} E_0 + e^{3\Lambda(t)} E_6). \tag{2.47}$$

On the other hand, $\mathcal{B}^i$ changes by both. Taking into account the time-like component of the Maurer-Cartan current we have

$$\begin{aligned} L_0(x) &\to L_0'(x') = A U_0^\dagger(x e^{\Lambda(t)}) A^\dagger \partial_0 (A U_0(x e^{\Lambda(t)}) A^\dagger) \\ &= A L_{m'} x'^m A^\dagger \dot{\Lambda} + A U_0^\dagger(x') A^\dagger \dot{A} U_0(x') A^\dagger - \dot{A} A^\dagger, \end{aligned} \tag{2.48}$$

where $x' = x e^{\Lambda(t)}$ and $L_{m'} = U_0^\dagger(x') \partial_{m'} U_0(x')$, while for the space-like components

$$\begin{aligned} L_j(x) &\to L_j'(x') = A U_0^\dagger(x e^{\Lambda(t)}) A^\dagger \partial_j (A U_0(x e^{\Lambda(t)}) A^\dagger) \\ &= A U_0^\dagger(x') \partial_{j'} U_0(x') A^\dagger e^\Lambda. \end{aligned} \tag{2.49}$$

Therefore, we arrive at the baryon current

$$\begin{aligned}\mathcal{B}^i(x) &\to \frac{3}{24\pi^2}\varepsilon^{i0jk}\mathrm{Tr}(L_0'(x')L_j'(x')L_k'(x')) \\ &= \frac{3}{24\pi^2}e^{2\Lambda(t)}\varepsilon^{i0jk}\Big(\mathrm{Tr}(L_{m'}x'^m L_{j'}L_{k'})\dot{\Lambda} + \mathrm{Tr}(U_0^\dagger(x')[A^\dagger\dot{A}, U_0(x')]L_{j'}L_{k'})\Big).\end{aligned} \tag{2.50}$$

The next step is to promote the parameters to quantum mechanical variables. The usual way of doing this is to introduce a rotation in the isospin space by $A^\dagger\dot{A} = \frac{i}{2}\vec{\Omega}\cdot\vec{\tau}$, where $\vec{\Omega}$ are the angular velocities and $\vec{\tau}$ the Pauli matrices, so we have

$$U_0^\dagger(x)[A^\dagger\dot{A}, U_0(x)] = \Omega_i T_i, \qquad \text{with} \quad T_i = \frac{i}{2}U_0^\dagger[\tau_i, U_0(x)]. \tag{2.51}$$

Then, using

$$\varepsilon^{i0jk}\mathrm{Tr}(L_m x^m L_j L_k) = -\mathrm{Tr}(L_1[L_2, L_3])x^i = \frac{24\pi^2}{3}\mathcal{B}_0 x^i, \tag{2.52}$$

we arrive, for the non-static part of L_{06}, at

$$\begin{aligned}\lambda^2\pi^4\int d^3x\mathcal{B}^i\mathcal{B}^i &\to \lambda^2\frac{3^2}{24^2}\int d^3x e^{\Lambda(t)}\left(\frac{24\pi^2}{3}\mathcal{B}_0 x^i\dot{\Lambda} + \varepsilon^{ijk}\Omega_a\mathrm{Tr}(T_aL_jL_k)\right)^2 \\ &= \lambda^2\pi^4 e^{\Lambda(t)}\dot{\Lambda}^2\int d^3x\mathcal{B}_0^2 r^2 \\ &+2\lambda^2\pi^2\frac{3}{24}e^{\Lambda(t)}\dot{\Lambda}\Omega_a\int d^3x\mathcal{B}_0\varepsilon^{ijk}x^i\mathrm{Tr}(T_aL_jL_k) \\ &+\lambda^2\frac{3^2}{24^2}e^{\Lambda(t)}\Omega_a\Omega_b\int d^3x\varepsilon^{ijk}\varepsilon^{irs}\mathrm{Tr}(T_aL_jL_k)\mathrm{Tr}(T_bL_rL_s).\end{aligned} \tag{2.53}$$

It can be seen that the second integral vanishes whereas the third one is related to the inertia tensor $\mathcal{I}_{ab}$ (see Chapter 4 for details):

$$\int d^3x\varepsilon^{ijk}\varepsilon^{irs}\mathrm{Tr}(T_aL_jL_k)\mathrm{Tr}(T_bL_rL_s) = \frac{1}{2}\frac{24^2}{3^2\lambda^2}\mathcal{I}_{ab}. \tag{2.54}$$

Thus,

$$\lambda^2\pi^4\int d^3x\mathcal{B}^i\mathcal{B}^i \to \lambda^2\pi^4 e^{\Lambda(t)}\dot{\Lambda}^2\int d^3x\mathcal{B}_0^2 r^2 + \frac{1}{2}e^{\Lambda(t)}\Omega_a\mathcal{I}_{ab}\Omega_b. \tag{2.55}$$

So finally, taking into account (2.47) and (2.55) we get the Lagrangian

$$L_{r+v} = e^{\Lambda(t)}\dot{\Lambda}^2 Q_6 - (e^{-3\Lambda(t)}E_0 + e^{3\Lambda(t)}E_6) + \frac{1}{2}e^{\Lambda(t)}\,\Omega_a\,\mathcal{I}_{ab}\,\Omega_b, \tag{2.56}$$

with $Q_6 = \lambda^2\pi^4 \int d^3\,x \mathcal{B}_0^2 r^2$.

Introducing the conjugated momentum of Λ,

$$p = \frac{\partial L_{r+v}}{\partial \dot{\Lambda}} = 2\dot{\Lambda}e^{\Lambda(t)}Q_6, \tag{2.57}$$

and the body-fixed angular momentum $\vec{L}$, $L_i = \partial L_{r+v}/\partial\Omega_i$, we can write the corresponding Hamiltonian

$$\mathcal{H}_{r+v} = e^{-\Lambda(t)}\frac{p^2}{4Q_6} + (e^{-3\Lambda(t)}E_0 + e^{3\Lambda(t)}E_6) + \frac{1}{2}e^{-\Lambda(t)}\left(\frac{L_1^2}{\mathcal{I}_{11}} + \frac{L_2^2}{\mathcal{I}_{22}} + \frac{L_3^2}{\mathcal{I}_{33}}\right). \tag{2.58}$$

Furthermore, we should consider the hedgehog configuration for $B = 1$ given by (2.31) and the standard Skyrme potential $\mathcal{U}_\pi$ (as commented in the previous subsection it is a quite arbitrary choice without the non-linear sigma-model term). Then, we get

$$Q_6 = 16\lambda^2 \int_0^{R_0} dr\, r^2 4\pi \frac{1}{R_0^6}\left(1 - \frac{r^2}{R_0^2}\right) r^2 = \frac{32}{35}4\pi\lambda^2 \left(\frac{\sqrt{2}}{4}\right)^{1/3} \left(\frac{\mu}{\lambda}\right)^{1/3}, \tag{2.59}$$

where R_0 is the compacton radius. Regarding the inertia tensor, the non-diagonal elements vanish because of the symmetry of the solution, whereas the diagonal ones are equal with the value

$$\mathcal{I} \equiv \mathcal{I}_{11} = \mathcal{I}_{22} = \mathcal{I}_{33} = \frac{2^8\sqrt{2}\pi}{15\cdot 7}\lambda\mu\left(\frac{\lambda}{\mu}\right)^{1/3}. \tag{2.60}$$

And, finally, the static energy is

$$E_{06} = \frac{64\sqrt{2}\pi}{15}\mu\lambda. \tag{2.61}$$

Therefore, having in mind that for the $B = 1$ hedgehog skyrmion spin and isospin take the same value, i.e., $\vec{L}^2 = \vec{J}^2$, the Hamiltonian expectation value is

$$H_{r+v} = e^{-\Lambda(t)}\frac{p^2}{4Q_6} + (e^{-3\Lambda(t)}E_0 + e^{3\Lambda(t)}E_6) + \frac{1}{2}\frac{e^{-\Lambda(t)}}{\mathcal{I}}j(j+1)\hbar^2. \tag{2.62}$$

Then, for a fixed value of j, the Λ corresponding to the ground state, $\Lambda_0(j)$, is given by the minimization of the mechanical potential

$$\mathcal{V} = e^{-3\Lambda(t)}E_0 + e^{3\Lambda(t)}E_6 + \frac{1}{2}\frac{e^{-\Lambda(t)}}{\mathcal{I}}j(j+1)\hbar^2, \tag{2.63}$$

that is, $\Lambda_0(j)$ is a solution of the equation $\partial\mathcal{V}(\Lambda)/\partial\Lambda = 0$:

$$-3e^{-3\Lambda_0(j)}E_0 + e^{3\Lambda_0(j)}E_6 - \frac{1}{2}\frac{e^{-\Lambda_0(j)}}{\mathcal{I}}j(j+1)\hbar^2 = 0. \tag{2.64}$$

Since the scaling transformation is not a symmetry of the action we will keep the quadratic terms in a perturbation around the vacuum value, $\Lambda = \Lambda_0 + \varepsilon$, which corresponds to the Hamiltonian of a harmonic oscillator:

$$\begin{aligned} H_{r+v} &= e^{-\Lambda_0(j)}\frac{p^2}{4Q_6} + \mathcal{V}\big|_{\Lambda_0(j)} + \varepsilon\left.\frac{\partial\mathcal{V}}{\partial\Lambda}\right|_{\Lambda_0(j)} + \frac{\varepsilon^2}{2}\left.\frac{\partial^2\mathcal{V}}{\partial\Lambda^2}\right|_{\Lambda_0(j)} \\ &= e^{-\Lambda_0(j)}\frac{p^2}{4Q_6} + 2E_0(-e^{-3\Lambda_0(j)} + 2e^{3\Lambda_0(j)}) + \varepsilon^2 3E_0(e^{-3\Lambda_0(j)} + 2e^{3\Lambda_0(j)}), \end{aligned} \tag{2.65}$$

where we have used $E_0 = E_6$ (see equation (2.45)). Hence, the energy spectrum will be that of a harmonic oscillator,

$$E = (n + 1/2)\omega\hbar + \mathcal{V}(\Lambda_0), \tag{2.66}$$

with $\omega^2 = \frac{1}{m}\partial^2\mathcal{V}/\partial\Lambda^2\big|_{\Lambda_0(j)}$ and $m = 2e^{\Lambda_0(j)}Q_6$, which reads

$$E_{n,j} = 2E_0(-e^{-3\Lambda_0(j)} + 2e^{3\Lambda_0(j)}) + \left(n + \frac{1}{2}\right)\left(\frac{3E_0(e^{-4\Lambda_0(j)} + 2e^{2\Lambda_0(j)})}{Q_6}\right)^{1/2}\hbar. \tag{2.67}$$

The last step is to fit the model parameters to the masses of the nucleon and Δ resonance:

$$E_{0,\frac{1}{2}} = M_N = 938.9 \text{ MeV}, \qquad E_{0,\frac{3}{2}} = M_\Delta = 1232 \text{ MeV}, \tag{2.68}$$

obtaining the values

$$\mu\lambda = 25.40 \text{ MeV}, \qquad \lambda^2\left(\frac{\mu}{\lambda}\right)^{1/3} = 17.78 \text{ MeV fm}^2. \tag{2.69}$$

The corresponding excitation energies of the Roper resonances are presented in Table 2.2 in comparison with experimental data [58] and standard Skyrme models [54, 55].

	BPS Skyrme	Skyrme [55]	Skyrme [54]	experiment
N(1440)	765	390	388	502 ± 20
Δ(1600)	773	290	292	368 ± 100

Table 2.2: Excitation energies of the nucleon and Δ Roper resonances with respect to the nucleon and Δ masses. All numbers are in MeV.

From the results, it is clear that whereas the standard Skyrme model gives excitation energies below the experimental data, the BPS Skyrme model overestimates them. This could be due to a higher compression modulus of the BPS version of the model with respect to the standard one (in the next Chapter we will see that, in some sense, this is the case). In addition, it seems that, combining both models, the situation could improve in order to obtain the real values of the resonances. Indeed, this supports the idea commented above of a BPS model as a leading order contribution from a more general theory where the terms corresponding to the original Skyrme model should also be taken into account as a small perturbation. This near BPS Skyrme model would take the form

$$\mathscr{L} = \mathscr{L}_0 + \mathscr{L}_6 + \varepsilon(\mathscr{L}_2 + \mathscr{L}_4), \tag{2.70}$$

where the main contribution coming from the BPS model is assumed because of the rather good description of some of the static properties of nuclear matter. More strong evidences of this near BPS Skyrme theory will be find through this thesis, leading to the hypothesis that it might be the correct low-energy effective field theory of nuclear matter.

Chapter 3

BPS Skyrme Thermodynamics

In the present chapter we will discuss the thermodynamics of the BPS Skyrme model at zero temperature ($T = 0$) and its equation of state (EoS) [59] as well as the baryon chemical potential [46]. It is worth noting that the excitation energies of the Roper resonances we have just seen at the end of Chapter 2 are related to the compression modulus since both deal with scaling transformations. In fact, where the standard Skyrme model gave low values for the Roper resonances, the study of the original Skyrme model (without the $\mathscr{L}_0$ term included) presents unacceptably big values for the compression modulus [60]. This behaviour seems to be due to the high stiffness of the theory which may be related to the crystal structure of Skyrme matter appearing when baryon number is large, i.e., $B \to \infty$ [61, 62, 63, 64, 65]. Considering the BPS version of the model, we have found higher excitation energies of the Roper resonances than the experimental ones, so higher value of the compression modulus might be expected. However, we know that this model has the symmetries of an ideal liquid (the VPDs on base space), where deformations which do not change the volume have no energy cost. Although this seems to imply that the Skyrmion will be quite incompressible under external pressure changing the volume, we will finally conclude that classically, the compression modulus vanishes. This does not mean that changing the volume cost no energy but that the infinitesimal pressure applied and the change in volume are not linearly related.

3.1 Compressibility and Equation of State

In thermodynamics, the compressibility at fixed temperature T and particle number B is defined by [66]

$$\kappa_{T,B} = -\frac{1}{V}\left(\frac{\partial V}{\partial P}\right)_{T,B}, \tag{3.1}$$

where V and P are the volume and the pressure respectively. As well, B is just the baryon number in our case. This quantity is important because it only depends on global variables and not on the position. Another useful quantity is the compression modulus. There exist several definitions [67, 68]

which are equivalent when the baryon density is constant as in the case of the Fermi gas. Then, taking again the definition depending on global variables we have

$$\mathcal{K} = \frac{9V^2}{B}\left(\frac{\partial^2 E}{\partial V^2}\right)_{T,B}. \tag{3.2}$$

Since the case of non-zero temperature is not an easy issue [69, 70], here we will only focus on the zero temperature case, $T = 0$. Therefore it seems we still have three thermodynamical variables: P, V and B. However, in this section (it will not be the case in the next section when studying the baryon chemical potential) we will treat the baryon number B as a constant taking integer values which depends on the boundary conditions of the Skyrme field instead of the thermodynamical state of the system. Then, the pressure and the volume are related by an equation of state $f(P, V) = 0$ (see below), so all thermodynamics functions depend on only one independent thermodynamical variable which will be P in our case. Thus, partial derivatives become ordinary ones and in this framework

$$\kappa = -\frac{1}{V}\frac{dV}{dP} \tag{3.3}$$

is the compressibility whereas for the compression modulus we have

$$\mathcal{K} = \frac{9V^2}{B}\frac{d^2E}{dV^2} = \frac{9V^2}{B}\left(\left(\frac{dV}{dP}\right)^{-2}\frac{d^2E}{dP^2} - \left(\frac{dV}{dP}\right)^{-3}\frac{d^2V}{dP^2}\frac{dE}{dP}\right), \tag{3.4}$$

where the second expression is useful when both volume, $V(P)$, and energy $E(P)$, are functions of the pressure, P.

Furthermore, as we will see in the next subsection, the compressibility and compression modulus are simply related for the free Fermi gas:

$$\mathcal{K} = \frac{9V}{B\kappa} \tag{3.5}$$

In addition, this relation also holds for our definition of $\mathcal{K}$ when our volume coincides with the thermodynamical volume, i.e., when the standard thermodynamical relation involving pressure and volume holds

$$P = -\frac{dE}{dV}. \tag{3.6}$$

Although this is not obvious, because our volume definition corresponds to the physical space occupied by the solution, both definitions agree in the frame of the BPS Skyrme model, as we will see below.

3.1.1 Free Fermi Gas and Derrick Scaling

Although the compression modulus can be defined in different ways [67, 68], the simplest and standard definition considers nuclear matter as a free Fermi gas at leading order. Then, the baryon density coinciding with the nuclear matter density is constant and given by

$$\rho = \frac{B}{V}, \tag{3.7}$$

which allow us to write the compressibility as [71]

$$\kappa = \frac{1}{\rho}\left(\frac{\partial \rho}{\partial P}\right)_{T=0,B}. \tag{3.8}$$

Thus, if we have a gas of N fermions in a volume V, the Fermi momentum is given by $p_F = \hbar(6\pi^2 N/(DV))^{1/3}$, where D is the degeneracy, i.e., the number of fermions which can occupy an energy state. Since in our case $N = B$ and $D = 4$ (2 nucleon species and 2 spin degrees of freedom), we have

$$p_F = \hbar\left(\frac{3}{2}\pi^2\rho\right)^{1/3}, \tag{3.9}$$

whereas the degeneracy energy (total kinetic energy due to the exclusion principle) is

$$E_T = \frac{3}{5}BE_F, \qquad E_F = \frac{p_F^2}{2m_N} = \frac{\hbar^2}{2m_N}\left(\frac{3}{2}\pi^2\rho\right)^{2/3}, \tag{3.10}$$

with E_F known as Fermi energy and m_N the nucleon mass. As well, the Fermi pressure is

$$P = \frac{2}{3}\frac{E_T}{V} = \frac{1}{5}\frac{\hbar^2}{m_N}\left(\frac{3}{2}\pi^2\right)^{2/3}\rho^{5/3}, \tag{3.11}$$

which results in the equation of state

$$P = c_{Fg}V^{-5/3}, \qquad c_{Fg} \equiv \frac{1}{5}\frac{\hbar^2}{m_N}\left(\frac{3}{2}\pi^2\right)^{2/3}B^{5/3}. \tag{3.12}$$

Then, the compression modulus of nuclear matter is defined as

$$\mathcal{K} = \frac{1}{p_F^2}\frac{\partial}{\partial p_F}\left(p_F^4\frac{\partial}{\partial p_F}\frac{E_T}{B}\right) = 9\frac{\partial}{\partial \rho}\left(\rho^2\frac{\partial}{\partial \rho}\frac{E_T}{B}\right), \tag{3.13}$$

where the second expression follows from equation (3.9). Moreover, as commented above, it can also be seen from here using (3.10) that the relation

(3.5) between the compressibility and compression modulus holds for the free Fermi gas.

Now, instead of the degeneracy energy we can use the Skyrme energy corresponding to the generalized model given by (2.12):

$$E = E_6 + E_4 + E_2 + E_0 \equiv E_N, \tag{3.14}$$

where E_N corresponds to the energy of the nucleon (for simplicity we will assume $B = 1$ in this discussion) without the small corrections coming from additional contributions like quantization of spin and isospin. Then, assuming again a constant baryon density, we can consider it is varied by a scale transformation as the one arising at the Derrick theorem, i.e.,

$$\vec{r} \to \Lambda\vec{r} \Rightarrow \rho = \Lambda^{-3}\rho_0, \tag{3.15}$$

with ρ_0 being the initial constant value. Considering that varying the baryon density corresponds to varying the scaling parameter Λ, we have

$$d\rho = -3\rho_0\Lambda^{-4}d\Lambda, \tag{3.16}$$

so the compression modulus can take the form

$$\mathcal{K} = \frac{9}{B}\partial_\rho(\rho^2\partial_\rho E) = \frac{1}{B}(\Lambda^2\partial_\Lambda^2 E - 2\Lambda\partial_\Lambda E), \tag{3.17}$$

and because of the Derrick stability argument at the equilibrium point $\rho = \rho_0$ (i.e., $\Lambda = 1$) which implies $\partial_\Lambda E|_{\Lambda=1} = 0$, we finally arrive at

$$\mathcal{K} = \frac{1}{B}(\Lambda^2\partial_\Lambda^2 E)_{\Lambda=1} = \frac{E^{(2)}}{B}, \tag{3.18}$$

where $E^{(2)} \equiv (d^2/d\Lambda)E(\Lambda)$ evaluated at the minimum ($\Lambda = 1$ in the case considered here). Hence, applying this scaling to the Skyrmionic field U, the energy (3.14) behaves like

$$E(\Lambda) \equiv E[U(\Lambda\vec{r})] = \Lambda^3 E_6 + \Lambda E_4 + \Lambda^{-1}E_2 + \Lambda^{-3}E_0, \tag{3.19}$$

whereas for the first derivative we have

$$E'(\Lambda) = 3\Lambda^2 E_6 + E_4 - \Lambda^{-2}E_2 - 3\Lambda^{-4}E_0, \tag{3.20}$$

with the Derrick condition

$$E'(1) = 3E_6 + E_4 - E_2 - 3E_0 \equiv 0. \tag{3.21}$$

Finally, for the second derivative we get

$$E''(\Lambda) = 6\Lambda E_6 + 2\Lambda^{-3}E_2 + 12\Lambda^{-5}E_0, \tag{3.22}$$

so the $E^{(2)}$ required for the compression modulus is just

$$E^{(2)} \equiv E''(1) = 6E_6 + 2E_2 + 12E_0 = E_N + 8(E_6 + E_0), \tag{3.23}$$

where we have used the Derrick condition (3.21).

Since for the study of Roper resonances a harmonic oscillator approximation is also required (see previous Chapter, section 2.3), this $E^{(2)}$ is the relevant quantity for both phenomena. From (3.23) we see that it is equal to the nucleon mass in the original Skyrme model with only the terms $\mathscr{L}_2$ and $\mathscr{L}_4$ in the Lagrangian, but it increases when either $\mathscr{L}_6$ or $\mathscr{L}_0$ are included. As a consequence, this is a good behaviour for the Roper resonances which require a higher value of $E^{(2)}$, but a complete disaster for the compression modulus. Considering that the nucleon mass is about $E_N \sim 940$ MeV, and the compression modulus $\mathcal{K} \sim 230$ MeV [72], additional contributions from $\mathscr{L}_6$ and $\mathscr{L}_0$ terms just make things worse. In the following we will see with detailed computations that there is a solution for this problem. The reason is that the scaling transformation $\vec{r} \to \Lambda\vec{r}$ is not a good approximation for the behaviour of the BPS nuclear matter under external pressure. Indeed, the baryon density, $\mathcal{B}_0$, for the BPS Skyrme model is not a constant function of the space coordinates in general, in contrast to the assumption made at the beginning of this subsection. However, when this is the case (constant baryon density), this simple calculation agrees with the general one (see the example of the Heaviside-like potential below).

3.1.2 Energy-Momentum Tensor and Pressure

As we will see in a moment, one of the important properties of this BPS Skyrme model is that its static solutions have identically zero pressure (for this reason sometimes BPS equations are called zero pressure conditions [73, 74]). It is this zero pressure which implies that BPS solutions do not react linearly to the external pressure producing a change of volume on it.

To include the pressure, the usual procedure is to calculate the energy-momentum tensor, $T_{\mu\nu}$, by introducing a general Lorentzian metric $g_{\mu\nu}$ in the Lagrangian and varying it with respect to this metric:

$$T^{\mu\nu} = -\frac{2}{\sqrt{|g|}}\frac{\delta}{\delta g_{\mu\nu}}\int d^4x\sqrt{|g|}\mathscr{L}_{06} = -2\frac{\delta\mathscr{L}_{06}}{\delta g_{\mu\nu}} - g^{\mu\nu}\mathscr{L}_{06}, \tag{3.24}$$

with $g = \det g_{\mu\nu}$, and the corresponding Lagrangian for a general metric given from (2.14) by

$$\mathscr{L}_{06} = -\lambda^2\pi^4|g|^{-1}g_{\mu\nu}\mathcal{B}^\mu\mathcal{B}^\nu - \mu^2\mathcal{U}. \tag{3.25}$$

Then, taking into account that $\delta(\sqrt{|g|}) = \frac{1}{2}\sqrt{|g|}g^{\mu\nu}\delta g_{\mu\nu} = -\frac{1}{2}\sqrt{|g|}g_{\mu\nu}\delta g^{\mu\nu}$, so

$$\delta\left(\frac{1}{|g|}\right) = -2\frac{1}{|g|\sqrt{|g|}}\delta(\sqrt{|g|}) = -\frac{1}{|g|}g^{\mu\nu}\delta g_{\mu\nu}, \tag{3.26}$$

the derivative of the Lagrangian density with respect to the metric is

$$\frac{\delta\mathscr{L}_{06}}{\delta g_{\mu\nu}} = -\lambda^2\pi^4\frac{1}{|g|}\mathcal{B}^\mu\mathcal{B}^\nu + \lambda^2\pi^4\frac{1}{|g|}g^{\mu\nu}g_{\alpha\beta}\mathcal{B}^\alpha\mathcal{B}^\beta, \tag{3.27}$$

and hence the energy-momentum tensor for the BPS Skyrme model is

$$T^{\mu\nu} = 2\lambda^2\pi^4\frac{1}{|g|}\mathcal{B}^\mu\mathcal{B}^\nu - g^{\mu\nu}\left(\lambda^2\pi^4\frac{1}{|g|}g_{\alpha\beta}\mathcal{B}^\alpha\mathcal{B}^\beta - \mu^2\mathcal{U}\right). \tag{3.28}$$

Thus, we see that in the case of static solutions only the time component of the topological current, $\mathcal{B}_0$, is not zero, so the components of the energy-momentum tensor are

$$T^{00} = \lambda^2\pi^4\mathcal{B}_0^2 + \mu^2\mathcal{U} \equiv \mathcal{E}, \tag{3.29}$$

$$T^{ij} = \delta^{ij}(\lambda^2\pi^4\mathcal{B}_0^2 - \mu^2\mathcal{U}) \equiv \delta^{ij}\mathcal{P}, \tag{3.30}$$

where $\mathcal{E}$ is the energy density corresponding to the BPS Skyrme model and $\mathcal{P}$ is the pressure. Then, from the conservation of the energy-momentum tensor, $\partial_\mu T^{\mu\nu} = 0$, we get that the pressure for static configurations has to be constant:

$$\mathcal{P} = P = \text{const.} \tag{3.31}$$

And since the BPS equation (2.30) can also be written as

$$\lambda^2\pi^2\mathcal{B}_0 = \pm\mu\sqrt{\mathcal{U}}, \tag{3.32}$$

from (3.30) we see that the value of this constant has to be identically zero for BPS solutions.

Finally, it can be proved that this constant pressure condition is a first integral of the static field equations, so (3.31) is equivalent to them and the only difference between the BPS and non-BPS configurations is the zero or non-zero value of the integration constant. In order to see it, we will introduce the parametrization (2.15) of the Skyrme field U where now, instead of the stereographic projection, we write the unit vector field $\vec{n}$ as

$$\vec{n} = (\sin\chi\cos\Phi, \sin\chi\sin\Phi, \cos\chi), \tag{3.33}$$

so the baryon density is

$$\mathcal{B}_0 = \frac{1}{2\pi^2}\sin^2\xi\sin\chi\varepsilon^{ijk}\xi_i\chi_j\Phi_k, \tag{3.34}$$

or introducing the notation $\xi^1 = \xi,\ \xi^2 = \chi,\ \xi^3 = \Phi$,

$$\mathcal{B}_0 = \frac{1}{2\pi^2}M(\xi^a)\varepsilon^{ijk}\xi^1_i\xi^2_j\xi^3_k, \tag{3.35}$$

where $M(\xi^a)$ is the volume element of the target space $\mathbb{S}^3$. Then, with the algebraic identity [75]

$$\left(\partial_j\frac{\partial}{\partial xi^a_j} - \frac{\partial}{\partial\xi^a}\right)\mathcal{B}_0 = 0, \tag{3.36}$$

we have for the Euler-Lagrange variation of the energy density (3.29)

$$\left(\partial_j\frac{\partial}{\partial xi^a_j} - \frac{\partial}{\partial\xi^a}\right)\mathcal{E} = 2\lambda^2\pi^4(\partial_j\mathcal{B}_0)\frac{\partial}{\partial\xi^a_j}\mathcal{B}_0 - \mu^2\frac{\partial}{\partial\xi^a}\mathcal{U} \equiv 0. \tag{3.37}$$

Multiplying by ξ^a_k, summing over a and using

$$\sum_a \xi^a_j\frac{\partial}{\partial\xi^a_j}\mathcal{B}_0 = \delta_{jk}\mathcal{B}_0, \tag{3.38}$$

we arrive at

$$2\lambda^2\pi^4(\partial_k\mathcal{B}_0)\mathcal{B}_0 - \mu^2\partial_k\mathcal{U} = 0. \tag{3.39}$$

Where noticing that $2(\partial_k\mathcal{B}_0)B_0 = \partial_k\mathcal{B}_0^2$, it integrates to

$$\lambda^2\pi^4\mathcal{B}_0^2 - \mu^2\mathcal{U} = \text{const.} \tag{3.40}$$

which is just the desired constant pressure condition (3.31).

The fact that fields of constant pressure fulfil the static field equations can be extended to a large class of models generalizing the BPS Skyrme model (see [59], *Proposition 1*).

3.1.3 The Equation of State

To calculate the equation of state (EoS) we need to solve the static field equations for non-zero pressure. As commented in Chapter 2, the potential $\mathcal{U}$ only depends on the profile function ξ, i.e., $\mathcal{U} = \mathcal{U}(\xi)$. Moreover, we will assume that these potentials approach the vacuum value $\xi = 0$ like

$$\lim_{\xi \to 0} \mathcal{U}(\xi) \sim \xi^{\alpha}, \qquad \alpha > 0. \tag{3.41}$$

This implies that in the BSP Skyrme model, compact solutions with a finite radius appear for $0 < \alpha < 6$, so the volume is well-defined. Then, we need to study how these compactons behave under external pressure. In this case, both the energy and baryon number density are not continuous at the compacton radius because of the external forces causing the pressure. Thus, plugging the axially symmetric ansatz (2.31) into the constant pressure equation (3.31) we arrive at

$$\frac{|B|\lambda}{2r^2} \sin^2 \xi \xi_r = -\mu \sqrt{\mathcal{U} + \tilde{P}}, \tag{3.42}$$

with $\tilde{P} = P/\mu^2$, and where the minus sign of the square root has been chosen in concordance with the boundary conditions for the profile function

$$\xi(r = 0) = \pi, \qquad \xi(r = \infty) = 0. \tag{3.43}$$

We can simplify this equation by introducing a new variable z (slightly different from the z of section 2.2)

$$z = \frac{2\mu}{3|B|\lambda} r^3, \tag{3.44}$$

so we get

$$\sin^2 \xi \xi_z = -\sqrt{\mathcal{U} + \tilde{P}}, \tag{3.45}$$

and with the new field

$$\eta = \frac{1}{2}\left(\xi - \frac{1}{2}\sin(2\xi)\right) \Rightarrow d\eta = \sin^2 \xi d\xi, \tag{3.46}$$

we finally arrive at the simple equation

$$\eta_z = -\sqrt{\mathcal{U} + \tilde{P}} \tag{3.47}$$

where the boundary conditions for η are

$$\eta(z = 0) = \frac{\pi}{2}, \qquad \eta(z = \infty) = 0. \tag{3.48}$$

Then, the behaviour of the η field near the vacuum corresponds to $\eta \sim \xi^3$, and the potential $\mathcal{U}(\eta) \sim \eta^\beta$ is equivalent to $\mathcal{U}(\xi) \sim \xi^{3\beta}$.

Once we have introduced the pressure into the field equations, we can get the corresponding volume from equation (3.45), which can be also written as

$$\frac{\sin^2 \xi}{\sqrt{\mathcal{U}+\tilde{P}}} d\xi = -dz. \tag{3.49}$$

Thus, integrating it

$$\int_0^\pi \frac{\sin^2 \xi d\xi}{\sqrt{\mathcal{U}+\tilde{P}}} = \int_0^Z dz, \tag{3.50}$$

and defining

$$\tilde{V}(\tilde{P}) \equiv Z(\tilde{P}) = \int_0^\pi \frac{\sin^2 \xi d\xi}{\sqrt{\mathcal{U}+\tilde{P}}} = \int_0^{\frac{\pi}{2}} \frac{d\eta}{\sqrt{\mathcal{U}+\tilde{P}}} \tag{3.51}$$

we get the volume as a function of the pressure:

$$V(P) = V(\mu^2 \tilde{P}) = 2\pi |B| \frac{\lambda}{\mu} \tilde{V}(\tilde{P}). \tag{3.52}$$

This is the general equation of state of our BPS Skyrme model. It can be seen from this EoS, that for positive pressure and arbitrary potentials $\mathcal{U}(\xi)$, the volume is always finite (as opposed to the case of zero pressure where compactons only exist for $0 < \alpha < 6$). As well, calculating the derivatives of $\tilde{V}(\tilde{P})$ with respect to $\tilde{P}$ we get

$$\frac{d\tilde{V}}{d\tilde{P}} = -\frac{1}{2} \int_0^\pi \frac{\sin^2 \xi d\xi}{(\mathcal{U}+\tilde{P})^{\frac{3}{2}}} = -\frac{1}{2} \int_0^{\frac{\pi}{2}} \frac{d\eta}{(\mathcal{U}+\tilde{P})^{\frac{3}{2}}}, \tag{3.53}$$

and

$$\frac{d^2\tilde{V}}{d\tilde{P}^2} = \frac{3}{4} \int_0^\pi \frac{\sin^2 \xi d\xi}{(\mathcal{U}+\tilde{P})^{\frac{5}{2}}} = \frac{3}{4} \int_0^{\frac{\pi}{2}} \frac{d\eta}{(\mathcal{U}+\tilde{P})^{\frac{5}{2}}}. \tag{3.54}$$

One important property of this BPS model is that, as trivially follows from (3.52), a specific solution does not have to be known in order to get the volume of the Skyrmion. We can see this also remains true for the energy. Regarding the constant pressure equation, the static energy can be written as

$$E = \int d^3x (\lambda^2 \pi^4 \mathcal{B}_0^2 + \mu^2 \mathcal{U}) = \int d^3x (2\mu^2 \mathcal{U} + P) = 4\pi\mu^2 \int dr r^2 (2\mathcal{U} + \tilde{P}), \tag{3.55}$$

and introducing the z variable

$$E(P) = E(\mu^2 \tilde{P}) = 2\pi\lambda\mu|B|\tilde{E}(\tilde{P}), \tag{3.56}$$

with

$$\tilde{E}(\tilde{P}) = \int_0^Z dz(2\mathcal{U} + \tilde{P}) = \int_0^\pi d\xi \sin^2\xi \frac{2\mathcal{U} + \tilde{P}}{\sqrt{\mathcal{U} + \tilde{P}}} = \int_0^{\frac{\pi}{2}} d\eta \frac{2\mathcal{U} + \tilde{P}}{\sqrt{\mathcal{U} + \tilde{P}}}. \tag{3.57}$$

Then, calculating the derivatives:

$$\frac{d\tilde{E}}{d\tilde{P}} = \frac{\tilde{P}}{2}\int_0^\pi \frac{d\xi \sin^2\xi}{(\mathcal{U} + \tilde{P})^{\frac{3}{2}}} = \frac{\tilde{P}}{2}\int_0^{\frac{\pi}{2}} \frac{d\eta}{(\mathcal{U} + \tilde{P})^{\frac{3}{2}}}, \tag{3.58}$$

and

$$\frac{d^2\tilde{E}}{d\tilde{P}^2} = \frac{1}{2}\int_0^\pi d\xi \sin^2\xi \frac{\mathcal{U} - \frac{1}{2}\tilde{P}}{(\mathcal{U} + \tilde{P})^{\frac{5}{2}}} = \frac{1}{2}\int_0^{\frac{\pi}{2}} d\eta \frac{\mathcal{U} - \frac{1}{2}\tilde{P}}{(\mathcal{U} + \tilde{P})^{\frac{5}{2}}}. \tag{3.59}$$

Thus, from the first derivatives of $\tilde{V}$ and $\tilde{E}$, the thermodynamical relation (3.6), $P = -(dE/dV)$, easily follows:

$$\frac{d\tilde{E}}{d\tilde{V}} = \frac{\frac{d\tilde{E}}{d\tilde{P}}}{\frac{d\tilde{V}}{d\tilde{P}}} = -\tilde{P}, \tag{3.60}$$

so with the relation between the tilde variables and V and E we get

$$\frac{dE}{dV} = \frac{\frac{dE}{d\tilde{P}}}{\frac{dV}{d\tilde{P}}} = \mu^2 \frac{\frac{d\tilde{E}}{d\tilde{P}}}{\frac{d\tilde{V}}{d\tilde{P}}} = -P. \tag{3.61}$$

It is striking that, although no thermodynamical definition has been introduced, the compacton volume saturates the thermodynamical relation between energy, volume and pressure. In fact, there are other possible definitions of the volume like $V_\gamma = (4\pi/3)\langle r\rangle_\gamma^3$, where

$$\langle r\rangle_\gamma = \left(\int d^3x r^{3\gamma}\mathcal{B}_0\right)^{\frac{1}{3\gamma}}, \tag{3.62}$$

which lead, however, to different results in general. Therefore, it is quite remarkable that the compacton volume is singled out as the correct volume definition from a thermodynamical point of view.

Finally, the compressibility at equilibrium ($\tilde{P} = 0$) can be approximately defined from equation (3.51) as

$$\kappa \sim -\frac{1}{Z}\frac{\partial Z}{\partial \tilde{P}}\bigg|_{\tilde{P}=0} = \frac{1}{2Z(0)}\int_0^\pi \mathcal{U}^{-\frac{3}{2}} \sin^2\xi d\xi. \tag{3.63}$$

As seen above, near the vacuum the potential behaves like $\mathcal{U} \sim \xi^{\alpha}$, so for the integrand of the right-hand side we have the behaviour $\xi^{2-\frac{3\alpha}{2}}$. Then, the integral is finite for $\alpha < 2$ but infinite for $\alpha \geq 2$, which is translated, because of the relation (3.5), to a zero compression modulus κ for $\alpha \geq 2$ as previously announced.

3.1.4 Examples: Some Potentials of Interest

Just for simplicity of the corresponding field equation (3.47), we will use the field variable η. Thus, we will study the problem of introducing pressure in the BPS Skyrme model by solving the equation for the simple potentials

$$\mathcal{U} = \eta^{\beta}, \tag{3.64}$$

where examples of different values of β are considered. The procedure for solving the field equations is always the same: to integrate the equation with the integration constant given by the condition $\eta(0) = \pi/2$ whereas the compacton boundary corresponds to impose $\eta(Z) = 0$. Remember that near the vacuum the correspondence between this variable η and the usual ξ is $\eta \sim \xi^3$, so $\mathcal{U}(\eta) \sim \eta^{\beta}$ is equivalent to $\mathcal{U}(\xi) \sim \xi^{3\beta}$.

i) $\boldsymbol{\beta = 1}$. This case corresponds to a potential with a cubic approach to the vacuum. The BPS equation for zero pressure is also given by (3.47) if the pressure is set to zero, i.e,

$$\eta_z = -\eta^{\frac{1}{2}}, \tag{3.65}$$

and integrating it we get the solution

$$\eta = \frac{1}{4}(z_0 - z)^2, \tag{3.66}$$

where the value of the integration constant z_0 follows from the condition $\eta(0) = \pi/2$ which implies $z_0 = \sqrt{\pi/8}$. On the other hand, the compacton boundary, i.e., the position Z where the field η takes its vacuum value is $Z = z_0 = \sqrt{\pi/8}$. Therefore, from this value of Z, and regarding that $r^3 = \frac{3|B|\lambda}{2\mu}$, the volume of the BPS solution for zero pressure is

$$V = \frac{4\pi}{3}R^3 = \frac{2\pi|B|\lambda}{\mu}Z = \frac{2\pi|B|\lambda}{\mu}\sqrt{\frac{\pi}{8}}. \tag{3.67}$$

For a non zero value of the pressure, the field equation is

$$\eta_z = -\sqrt{\eta + \tilde{P}}, \tag{3.68}$$

which has the solution

$$\eta = \frac{1}{4}(z_0 - z)^2 - \tilde{P}, \tag{3.69}$$

where now

$$z_0 = 2\sqrt{\frac{\pi}{2} + \tilde{P}}, \tag{3.70}$$

and the volume $\tilde{V}(\tilde{P})$ is

$$\tilde{V}(\tilde{P}) = Z = z_0 - 2\sqrt{\tilde{P}} = 2\left(\sqrt{\frac{\pi}{2} + \tilde{P}} - \sqrt{\tilde{P}}\right). \tag{3.71}$$

This allows us to obtain the equation of state by writing the pressure $\tilde{P}$ as a function of the volume $\tilde{V}$:

$$\tilde{P} = \frac{1}{16\tilde{V}^2}(2\pi - \tilde{V}^2)^2. \tag{3.72}$$

Furthermore, the compressibility can be easily calculated,

$$\kappa = -\left.\frac{1}{V}\frac{dV}{dP}\right|_{P=0} \sim -\left.\frac{1}{Z}\frac{dZ}{d\tilde{P}}\right|_{\tilde{P}=0} = \infty. \tag{3.73}$$

It is infinite (as previously announced) due to the second term in (3.71) proportional to the square root of $\tilde{P}$.

However, as commented before, we can think about a different definition of the volume like the one presented above related to the average baryon radius given by (3.62), which in the variables z and η reads

$$\langle V\rangle_\gamma \sim \langle z\rangle_\gamma \equiv \left|\int dz\eta_z z^\gamma\right|^{\frac{1}{\gamma}}. \tag{3.74}$$

Giving for instance the value $\gamma = 1$, we get

$$\langle z\rangle_1 = \left|\int_0^Z dz\eta_z z\right| = \frac{2}{3}\left(\left(\frac{\pi}{2} - 2\tilde{P}\right)\sqrt{\frac{\pi}{2} + \tilde{P}} + 2\tilde{P}\sqrt{\tilde{P}}\right). \tag{3.75}$$

So the value of the compressibility is finite when this alternative definition of the volume is chosen. However, although we get quite different results for κ, this is not a problem because we have to use the volume definition obeying the thermodynamical relation (3.6) which these alternative volumes do not satisfy.

ii) $\boldsymbol{\beta = 2/3}$. Here we have a potential which is quadratic near the vacuum, so it has the same behaviour as the usual standard Skyrme potential for the pion mass. The equation to be solved for a zero pressure is

$$\eta_z = -\eta^{\frac{1}{3}}, \tag{3.76}$$

which has the solution

$$\eta = \left(\frac{2}{3}(z_0 - z)\right)^{\frac{3}{2}}, \tag{3.77}$$

with the integration constant

$$z_0 = \frac{3}{2}\left(\frac{\pi}{2}\right)^{\frac{2}{3}}, \tag{3.78}$$

and the compacton radius $Z = z_0$. Then, introducing the pressure the resulting equation is

$$\eta_z = -\sqrt{\eta^{\frac{2}{3}} + \tilde{P}}, \tag{3.79}$$

with the implicit solution

$$\frac{3}{2}\left[\sqrt{\eta^{\frac{2}{3}} + \tilde{P}}\eta^{\frac{1}{3}} - \tilde{P}\ln\left(2\left(\sqrt{\eta^{\frac{2}{3}} + \tilde{P}} + \eta^{\frac{1}{3}}\right)\right)\right] = z_0 - z, \tag{3.80}$$

where the integration constant z_0 is given here by

$$z_0 = \frac{3}{2}\left[\sqrt{\left(\frac{\pi}{2}\right)^{\frac{2}{3}} + \tilde{P}}\left(\frac{\pi}{2}\right)^{\frac{1}{3}} - \tilde{P}\ln\left(2\left(\sqrt{\left(\frac{\pi}{2}\right)^{\frac{2}{3}} + \tilde{P}} + \left(\frac{\pi}{2}\right)^{\frac{1}{3}}\right)\right)\right]. \tag{3.81}$$

The position at which the vacuum value is reached corresponds to

$$Z = z_0 + \frac{3}{2}(\ln 2)\tilde{P} + \frac{3}{4}\tilde{P}\ln\tilde{P}, \tag{3.82}$$

so the volume, which is also the equation of state, reads

$$\tilde{V}(\tilde{P}) = \frac{3}{2}\left[\sqrt{\left(\frac{\pi}{2}\right)^{\frac{2}{3}} + \tilde{P}}\left(\frac{\pi}{2}\right)^{\frac{1}{3}} - \tilde{P}\ln\left(\sqrt{\left(\frac{\pi}{2}\right)^{\frac{2}{3}} + \tilde{P}} + \left(\frac{\pi}{2}\right)^{\frac{1}{3}}\right) + \frac{1}{2}\tilde{P}\ln\tilde{P}\right]. \tag{3.83}$$

Here, we again get an infinite compressibility as a consequence of the last term $\tilde{P}\ln\tilde{P}$. Since this is the softest possible divergence, we expect the compressibility will present finite values for $\beta < 2/3$, i.e., $\alpha < 2$, hypothesis which is confirmed by the general expression (3.63) at the end of the previous subsection.

iii) $\boldsymbol{\beta = 1/3}$. This potential presents a linear behaviour near the vacuum. For zero pressure, the field equation is

$$\eta_z = -\sqrt{\eta^{\frac{1}{3}} + \tilde{P}}, \tag{3.84}$$

which presents only the implicit solution

$$z_0 - z = \frac{2}{5}\sqrt{\eta^{\frac{1}{3}} + \tilde{P}}\left(8\tilde{P}^2 - 4\tilde{P}\eta^{\frac{1}{3}} + 3\eta^{\frac{2}{3}}\right). \tag{3.85}$$

The integration constant z_0 is

$$z_0 = \frac{2}{5}\sqrt{\left(\frac{\pi}{2}\right)^{\frac{1}{3}} + \tilde{P}}\left(8\tilde{P}^2 - 4\tilde{P}\left(\frac{\pi}{2}\right)^{\frac{1}{3}} + 3\left(\frac{\pi}{2}\right)^{\frac{2}{3}}\right), \tag{3.86}$$

whereas the value of Z is

$$Z = z_0 - \frac{2}{5}\tilde{P}^{\frac{5}{2}}. \tag{3.87}$$

which corresponds to the equation of state

$$\tilde{V}(\tilde{P}) = \frac{2}{5}\left(\sqrt{\left(\frac{\pi}{2}\right)^{\frac{1}{3}} + \tilde{P}}\left(8\tilde{P}^2 - 4\tilde{P}\left(\frac{\pi}{2}\right)^{\frac{1}{3}} + 3\left(\frac{\pi}{2}\right)^{\frac{2}{3}}\right) - \tilde{P}^{\frac{5}{2}}\right). \tag{3.88}$$

In this case the compressibility is finite since the last term $\frac{2}{5}\tilde{P}^{\frac{5}{2}}$ does not contribute at $\tilde{P}=0$, as can be seen from

$$\left.\frac{dZ}{d\tilde{P}}\right|_{\tilde{P}=0} = \left.\frac{dz_0}{d\tilde{P}}\right|_{\tilde{P}=0} = -\sqrt{\frac{\pi}{2}}. \tag{3.89}$$

iv) $\boldsymbol{\beta \to 0}$. This is a case of interest where the potential approaches the Heaviside function

$$\mathcal{U}(\eta) = \begin{cases} 1, & \eta \in [\pi/2, 0) \\ 0, & \eta = 0. \end{cases} \tag{3.90}$$

Thus, the non-zero pressure equation is

$$\eta_z = -\sqrt{1+\tilde{P}} = \text{const.} \tag{3.91}$$

which means that the baryon density is a constant, so we are in the case discussed in subsection 3.1.1 and the corresponding simple thermodynamical analysis applies. Indeed, the zero and non-zero pressure equations can be related by a scaling transformation $\vec{r}\,' \to \Lambda\vec{r}$:

$$\eta_{z'} = \Lambda^{-3}\eta_z = -\Lambda^{-3}\sqrt{1+\tilde{P}} = -1, \qquad \text{with} \quad \Lambda^3 = \sqrt{1+\tilde{P}}, \tag{3.92}$$

so both solutions are also related. The corresponding solution with the pressure included is given by

$$\eta(z) = \frac{\pi}{2} - z\sqrt{1+\tilde{P}} \tag{3.93}$$

with the compacton radius (in the z variable)

$$Z \equiv \tilde{V}(\tilde{P}) = \frac{\pi}{2\sqrt{1+\tilde{P}}}. \tag{3.94}$$

Therefore, the equation of state is just

$$\tilde{P} = \left(\frac{\pi}{2\tilde{V}}\right)^2 - 1. \tag{3.95}$$

Of course, the compressibility is not infinite and its value depends on the second derivative of the energy functional with respect to the scaling parameter as equation (3.18) indicates (remember that κ and $\mathcal{K}$ are inversely related in the BPS Skyrme model).

v) $\boldsymbol{\mathcal{U}(\eta) = 0}$. For this potential, if the pressure is set to zero, then due to Derrick's theorem only the trivial solution $\eta = 0$ is allowed. However, stable solutions can exist when the pressure is introduced. If this is done, the field equation is quite simple

$$\eta_z = -\sqrt{\tilde{P}} \tag{3.96}$$

and has the solution

$$\eta = \frac{\pi}{2} - z\sqrt{\tilde{P}}. \tag{3.97}$$

The corresponding volume is

$$\tilde{V}(\tilde{P}) \equiv Z = \frac{\pi}{2\sqrt{\tilde{P}}}, \tag{3.98}$$

which implies the equation of state

$$\tilde{P} = \left(\frac{\pi}{2\tilde{V}}\right)^2. \tag{3.99}$$

With no potential the compressibility is infinite due to the $1/\sqrt{\tilde{P}}$ of the volume $\tilde{V}$. This also agrees with the general discussion since $\mathcal{U} = 0$ can be seen like the limiting case of our potentials when $\beta \to \infty$.

vi) $\boldsymbol{\beta = 2}$. Finally, it is also of interest to consider a potential which for zero pressure has not compact solutions but solutions localized like e^{-z}. In this case, the equation for non-zero pressure is

$$\eta_z = -\sqrt{\eta^2 + \tilde{P}}, \tag{3.100}$$

and the solution is

$$\eta = \sqrt{\tilde{P}}\sinh(z_0 - z), \tag{3.101}$$

with the integration constant defined by

$$\sinh z_0 = \frac{\pi}{2\sqrt{\tilde{P}}.} \tag{3.102}$$

The compacton radius is $Z = z_0$, so we can write it like

$$Z \equiv \tilde{V}(\tilde{P}) = \sinh^{-1}\frac{\pi}{2\sqrt{\tilde{P}}} = \ln\left(\frac{\pi}{2\sqrt{\tilde{P}}} + \sqrt{\left(\frac{\pi}{2\sqrt{\tilde{P}}}\right)^2 + 1}\right). \quad (3.103)$$

It is clear from this expression that when the pressure approaches the value zero, then the radius tends to infinity. As well, we can get the equation of state

$$\tilde{P} = \left(\frac{\pi}{2\sinh\tilde{V}}\right)^2. \quad (3.104)$$

Computing the compressibility we see it is infinite as expected:

$$\begin{aligned} -\frac{1}{Z}\frac{dZ}{d\tilde{P}}\bigg|_{\tilde{P}=0} &= -\frac{1}{\sinh^{-1}\frac{\pi}{2\sqrt{\tilde{P}}}}\frac{1}{\sqrt{1+\left(\frac{\pi}{2\sqrt{\tilde{P}}}\right)^2}}\left(-\frac{\pi}{4}\right)\frac{1}{\tilde{P}^{3/2}}\bigg|_{\tilde{P}=0} \\ &= \frac{1}{2}\frac{1}{\sinh^{-1}\frac{\pi}{2\sqrt{\tilde{P}}}}\frac{1}{\tilde{P}}\bigg|_{\tilde{P}=0} = \infty. \end{aligned} \quad (3.105)$$

We have just seen how our BPS Skyrme model allows to make analytical calculations of important thermodynamical quantities such as the compressibility or the equation of state, besides getting solutions with external pressure also in an analytical way. Summarizing the results given by the former examples we see that for the case of $\beta \to 0$, the potential tends to the Heaviside function, taking a constant value and going suddenly to $\eta = 0$ at the vacuum. Then, the baryon density is constant and the standard thermodynamical discussion of subsection 3.1.1 applies, so the compression modulus κ takes a finite value. On the other hand, when $0 < \beta < 2/3$ (equivalent to $0 < \alpha < 2$ from $\mathcal{U} \sim \xi^\alpha$), the compressibility is still finite but higher than the case $\beta = 0$, i.e., we have more compressible Skyrmions. However, they are rather problematic since their second variation around the vacuum is infinite. And finally, for $2/3 \leq \beta < 2$, we have compactons with an infinite compressibility which means that the compression modulus is zero (for $\beta \geq 2$ the BPS Skyrmions for zero pressure are no longer compact). Therefore, as only potentials with $\alpha \geq 2$ (with at least a quadratic approach to the vacuum) are physically acceptable, the infinite value of the compressibility seems a quite generic result.

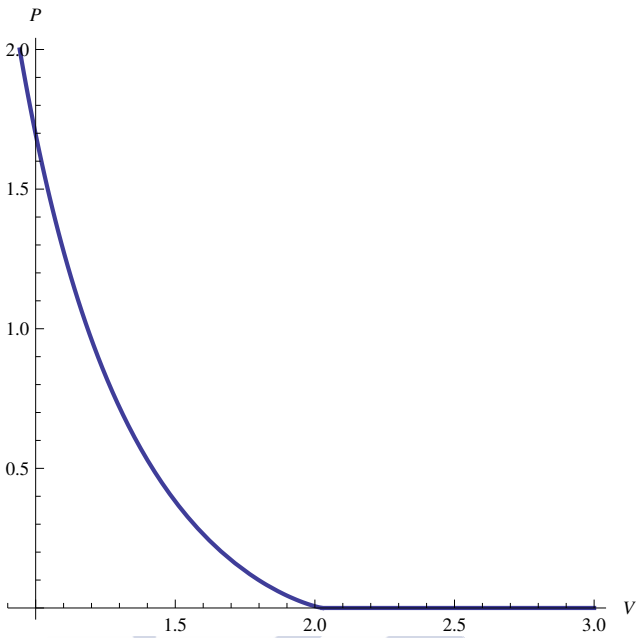

Figure 3.1: Equation of state for the quadratic potential $\mathcal{U} = \eta^{2/3}$.

It is interesting to further analyse the situation for potentials with $\alpha < 6$ at large baryon number B. In this case, a volume V greater than the equilibrium volume V_0 at zero pressure is possible. Since at volume V_0 our solution is a compacton, for $V > V_0$ we would have a collection of non-overlapping compactons where the additional space $\delta V = V - V_0$ would be made of empty space. Of course, the pressure of these configurations is zero. Therefore, a phase transition at the equilibrium volume V_0 arises. For $V > V_0$ we have an ideal gas of non-overlapping compactons, while when $V < V_0$ the system enters into a kind of liquid phase with a non-trivial equation of state. Then, this equilibrium volume V_0 corresponds to the point where all the empty space between compactons has disappeared. In Fig. 3.1 we plot the EoS for the potential $\mathcal{U} = \eta^{2/3}$, see Eq. (3.83). We have chosen this case because it behaves like the standard Skyrme potential $\mathcal{U}_\pi$ near the vacuum. Here it is easy to see both phases: the liquid phase for $0 \leq \tilde{V} \leq (3/2)(\pi/2)^{2/3}$, and the gaseous phase for $\tilde{V} > (3/2)(\pi/2)^{2/3}$, with the transition point at $\tilde{V}_0 = (3/2)(\pi/2)^{2/3} \simeq 2.2027$. A qualitatively similar EoS with this phase transition has been found for nuclear matter at zero temperature in some models based on the two- and three-body internuclear forces (see for instance Fig. 10 from [76]).

To conclude, it is worth commenting again on the problem of the too high compression modulus in the framework of the Skyrme models. It seems that the source of this problem may be related to assuming a uniform rescaling

under the action of external pressure, which leads to Skyrmions more incompressible than nuclear matter. However, this hypothesis only applies for a constant baryon density which clearly is not the case of the BPS Skyrme model in general. Indeed, from the constant pressure condition (3.31) it follows that $\mathcal{B}_0 \sim \sqrt{\mathcal{U} + \tilde{P}}$, so if the potential is not constant, neither is the baryon density $\mathcal{B}_0$. Then, for the physically acceptable potentials we have a zero value of the compression modulus, i.e., $\mathcal{K} = 0$. This does not mean it costs zero energy to squeeze a BPS Skyrmion under external pressure, but the pressure used to squeeze it and the resulting small change in volume are not linearly related. Of course, this value of the compression modulus is not the real value, but it also reinforces the vision of a BSP model as an approximation of a more general near-BPS theory where further small contributions from the $\mathscr{L}_2$ and $\mathscr{L}_4$ terms are required.

3.2 Baryon Chemical Potential and In-medium Skyrmions

There is one more thermodynamical quantity of extreme relevance, the baryon chemical potential, which is important for a reliable description of cold and dense nuclear matter since different coexisting phases and phase transitions depend on it. Furthermore, the baryon chemical potential allows to study BPS Skyrmions in a Skyrmionic medium, so a comparison with in-medium masses of baryons can be established. However, there is not too much information about it in the framework of Skyrme models (for more information about phase transitions and in-medium properties of hadrons in dense Skyrmionic matter see, e.g., [77, 78, 79, 80, 81, 82]). Here, we will study this baryon chemical potential not only in the full field theory but also in a mean-field (MF) approach.

It is necessary to comment that we will adopt the bold notation for the baryon chemical potential $\boldsymbol{\mu}$ to distinguish it from the μ parameter appearing in the $\mathscr{L}_0$ term of the Lagrangian.

3.2.1 Definition and General Properties of the Baryon Chemical Potential

Before presenting the definition of the baryon chemical potential we will introduce what we refer to as mean-field approach. The idea consists in going from the coordinate dependence appearing in the equation of state to an algebraic EoS by means of an average procedure. Thus, we define the average energy density $\bar{\varepsilon}$ as

$$\bar{\varepsilon} = \frac{E}{V}, \tag{3.106}$$

where E and V are the total energy and volume presented above as functions of the pressure. Moreover, by introducing the average of a function F on the target space, i.e.,

$$\langle F \rangle \equiv \frac{1}{2\pi^2} \int_{\mathbb{S}^3} d\Omega F, \tag{3.107}$$

the energy and volume read

$$E(P) = 2\pi\lambda\mu|B|\tilde{E}, \qquad V(P) = 2\pi|B|\frac{\lambda}{\mu}\tilde{V}, \tag{3.108}$$

with

$$\tilde{E} = \int_0^\pi d\xi \sin^2\xi \frac{2\mathcal{U}+\tilde{P}}{\sqrt{\mathcal{U}+\tilde{P}}} = \frac{\pi}{2}\left\langle \frac{2\mathcal{U}+\tilde{P}}{\sqrt{\mathcal{U}+\tilde{P}}} \right\rangle, \tag{3.109}$$

$$\tilde{V} = \int_0^\pi d\xi \sin^2\xi \frac{1}{\sqrt{\mathcal{U}+\tilde{P}}} = \frac{\pi}{2}\left\langle \frac{1}{\sqrt{\mathcal{U}+\tilde{P}}} \right\rangle. \tag{3.110}$$

A similar situation occurs for the baryon density $\rho_{\mathcal{B}} \equiv \mathcal{B}_0$ in the exact theory, which depends on coordinates although an algebraic equation exists relating three local quantities as pressure and energy density with the baryon density:

$$\varepsilon + P = 2\lambda^2\pi^4\rho_B^2. \tag{3.111}$$

Obviously, the MF definition of baryon density is just the baryon number B divided by the volume,

$$\bar{\rho}_B = \frac{B}{V}. \tag{3.112}$$

Let us study now the baryon chemical potential $\boldsymbol{\mu}$. The standard thermodynamical definition is given by its relation with the energy density ε and pressure P:

$$\varepsilon + P = \boldsymbol{\mu}\rho_B, \tag{3.113}$$

and comparing with the relation (3.111), we get

$$\boldsymbol{\mu} = 2\lambda^2\pi^4\rho_B. \tag{3.114}$$

Therefore, the baryon chemical potential is proportional to the baryon density, so a non-trivial dependence on spatial coordinates also appears. This is a general expression which does not depend on an explicit solution.

On the other hand, the MF definition of the average chemical potential is $\bar{\boldsymbol{\mu}} = \frac{\partial F}{\partial N}$, where F is the free energy and N the particle number. In our case at zero temperature $F \equiv E$ and $N \equiv B$, so the MF baryon chemical potential reads

$$\bar{\boldsymbol{\mu}} = \left(\frac{\partial E}{\partial B}\right)_V . \tag{3.115}$$

Of course, Eq. (3.113) has to hold for average quantities:

$$\bar{\varepsilon} + P = \bar{\boldsymbol{\mu}}\bar{\rho}_B. \tag{3.116}$$

The meaning of this definition is the following. We have a Skyrmionic solution in equilibrium (i.e., at $P = 0$) with baryon number B_0, in a volume V_0 and with E_0 energy. Then, we want to know how the energy changes by increasing the baryon number from B_0 to $B = B_0 + n$ but keeping a fixed volume. Obviously, this cannot be achieved in a smooth way since B is a conserved quantity by definition (it is a topological quantity). Thus, we have to introduce the pressure and find a solution of the pressure equation (**??**) for baryon number B but with the same volume V_0. As a consequence, the pressure depends on the increment n, $P = P(n)$, and two equations are obtained,

$$E(n) = 2\pi\lambda\mu(B_0 + n)\int_0^\pi d\xi \sin^2\xi \frac{2\mathcal{U} + \tilde{P}}{\sqrt{\mathcal{U} + \tilde{P}}} = \pi^2\lambda\mu(B_0 + n)\left\langle \frac{2\mathcal{U} + \tilde{P}}{\sqrt{\mathcal{U} + \tilde{P}}} \right\rangle, \tag{3.117}$$

$$V_0 = 2\pi(B_0 + n)\frac{\lambda}{\mu}\int_0^\pi d\xi \sin^2\xi \frac{1}{\sqrt{\mathcal{U} + \tilde{P}}} = \pi^2(B_0 + n)\frac{\lambda}{\mu}\left\langle \frac{1}{\sqrt{\mathcal{U} + \tilde{P}}} \right\rangle. \tag{3.118}$$

Remember the volume does not change so $V_0(n, P) = V_0(n = 0, P = 0)$.

From the definition of the MF chemical potential, Eq. (3.115), we can write

$$\bar{\boldsymbol{\mu}} = \left(\frac{\partial E}{\partial B}\right)_V = \frac{\partial E}{\partial B} + \frac{\partial E}{\partial \tilde{P}}\frac{\partial \tilde{P}}{\partial B}, \tag{3.119}$$

where the partial derivative $\frac{\partial \tilde{P}}{\partial B}$ can be found from the condition of a fixed volume, namely,

$$\frac{dV}{dB} = \frac{\partial V}{\partial B} + \frac{\partial V}{\partial \tilde{P}} \frac{\partial \tilde{P}}{\partial B} = 0, \tag{3.120}$$

so we arrive at the following expression for the MF baryon chemical potential

$$\bar{\boldsymbol{\mu}} = \pi^2 \lambda \mu \left[\left\langle \frac{2\mathcal{U} + \tilde{P}}{\sqrt{\mathcal{U} + \tilde{P}}} \right\rangle + \tilde{P} \left\langle \frac{1}{\sqrt{\mathcal{U} + \tilde{P}}} \right\rangle \right], \tag{3.121}$$

which can also be simplified to

$$\bar{\boldsymbol{\mu}} = 2\pi^2 \lambda \mu \left\langle \sqrt{\mathcal{U} + \frac{P}{\mu^2}} \right\rangle. \tag{3.122}$$

Furthermore, using equations (3.109) and (3.110) we can write

$$\bar{\boldsymbol{\mu}} = \frac{1}{B}(E + PV), \tag{3.123}$$

so as stated before, we easily recover the thermodynamical relation

$$P = \bar{\boldsymbol{\mu}} \bar{\rho}_B - \bar{\varepsilon}. \tag{3.124}$$

Therefore, our definition (3.115) is perfectly consistent with the standard thermodynamics.

An alternative definition for the MF baryon chemical potential can be given by integrating Eq. (3.111). Then,

$$PV + E = 2\pi^4 \lambda^2 \int d^3x \rho_B^2, \tag{3.125}$$

and by comparison between the last two relations we find

$$\bar{\boldsymbol{\mu}} = \frac{1}{B} 2\pi^4 \lambda^2 \int d^3x \rho_B^2 \equiv 2\pi^4 \lambda^2 \frac{\int d^3x \rho_B^2}{\int d^3x \rho_B}. \tag{3.126}$$

Here it is clear that $\bar{\boldsymbol{\mu}} \neq 2\lambda^2 \pi^4 \bar{\rho}_B$ except for the step-function potential where exact and average quantities are exactly the same.

On the other hand, we can also write the mean-field version of the baryon density,

$$\bar{\rho}_B = \frac{B}{V_0} = \frac{1}{\pi^2} \frac{\mu}{\lambda} \left\langle \frac{1}{\sqrt{\mathcal{U} + P/\mu^2}} \right\rangle^{-1}, \tag{3.127}$$

which by using Eq (3.124) allows us to write the average energy density $\bar{\varepsilon}$ in terms of the MF baryon chemical potential,

$$\bar{\varepsilon} = \bar{\boldsymbol{\mu}} \frac{1}{\pi^2} \frac{\mu}{\lambda} \left\langle \frac{1}{\sqrt{\mathcal{U} + P/\mu^2}} \right\rangle^{-1} - P. \tag{3.128}$$

Finally, with the expression for $\bar{\rho}_B$ and using Eq. (3.122), we arrive at the well-known relation

$$\left(\frac{\partial \bar{\boldsymbol{\mu}}}{\partial P} \right)_V = \frac{1}{\bar{\rho}_B}. \tag{3.129}$$

Although the explicit expressions of $\boldsymbol{\mu}$ and $\bar{\boldsymbol{\mu}}$ depend on the particular potential we choose, we find that at high pressure both tend to show the same behaviour corresponding to the step-function potential. In fact, for $P >> \mu^2$ at leading order we have for energy and volume

$$E = \pi^2 \lambda B \sqrt{P}, \qquad V = \pi^2 B \frac{\lambda}{\sqrt{P}}, \tag{3.130}$$

and then we get

$$\bar{\varepsilon} = P + B_\infty, \qquad \bar{\rho}_B = \frac{\sqrt{P}}{\pi^2 \lambda}, \tag{3.131}$$

where B_∞ is usually called bag constant at infinite pressure. If we proceed as we did when arriving at Eq. (3.121), we find $\frac{\partial P}{\partial B} = \frac{2P}{B}$, and the average chemical potential at high pressure tends to

$$\bar{\boldsymbol{\mu}} = 2\pi^4 \lambda^2 \bar{\rho}_B, \tag{3.132}$$

which is also the expression of the baryon chemical potential in the exact (non-average) full theory.

Considering the case of vanishing pressure, from Eq. (3.124) we see that the value of the MF chemical potential is

$$\bar{\boldsymbol{\mu}}_0 = \frac{E_0}{B}, \tag{3.133}$$

whilst the exact chemical potential is obviously the baryon density ρ_B at equilibrium up to a multiplicative constant, see Eq. (3.114).

3.2.2 Examples from Specific Potentials

As we have already shown, the expression of the baryon chemical potential in the exact theory is always the same, Eq. (3.114), although there is a dependence on spatial coordinates encoded in the baryon density, ρ_B, and its specific behaviour depends on the chosen potential. On the other hand,

considering the MF chemical potential, $\bar{\boldsymbol{\mu}}$, its concrete expression is totally different depending on the potential. Therefore, similarly to what we have done in section 3.1, we will study different examples coming from different potentials.

i) **Step-function potential.**

This is a special potential since it is the only case where the energy density and baryon charge density are constant in the BPS Skyrme model so the local quantities are exactly the same as their MF counterparts. Thus, for the step-function potential

$$\mathcal{U} = \Theta(\mathrm{Tr}(1-U)), \tag{3.134}$$

we found constant energy and volume for non-zero pressure given by

$$E(P) = 2\pi\lambda\mu|B|\tilde{E}(\tilde{P}), \qquad V(P) = 2\pi\frac{\lambda}{\mu}|B|\tilde{V}(\tilde{P}), \tag{3.135}$$

with

$$\tilde{E}(\tilde{P}) = \frac{\pi}{2}\frac{2+\tilde{P}}{\sqrt{1+\tilde{P}}}, \qquad \tilde{V}(\tilde{P}) = \frac{\pi}{2}\frac{1}{\sqrt{1+\tilde{P}}}. \tag{3.136}$$

Then, we will compute the MF baryon chemical potential from its definition Eq. (3.115). As commented above, we start from a configuration at equilibrium ($P = 0$) and increase the baryon number but with the volume fixed. Thus, at $P = 0$, the energy and volume read

$$E_0 = E(P=0) = 2\pi^2\lambda\mu|B_0|, \qquad V_0 = V(P=0) = \pi^2\frac{\lambda}{\mu}|B_0|, \tag{3.137}$$

whereas after going from the initial baryon number B_0 to $B = B_0 + n$ we get

$$V_0 = \pi^2\frac{\lambda}{\mu}B\frac{1}{\sqrt{1+\frac{P(B)}{\mu^2}}}, \tag{3.138}$$

$$E = \pi^2\lambda\mu B\frac{2+\frac{P(B)}{\mu^2}}{\sqrt{1+\frac{P(B)}{\mu^2}}}, \tag{3.139}$$

where this non-zero P is due to the higher baryon number than at equilibrium ($B > B_0$). Using Eq. (3.138) we can simplify the expression for the energy to

$$E(P) = \mu^2 V_0 \left(2 + \frac{P}{\mu^2}\right), \tag{3.140}$$

and since both E and P are functions of the non-equilibrium baryon number B, the derivative appearing in the definition of $\bar{\boldsymbol{\mu}}$ reads

$$\left(\frac{\partial E}{\partial B}\right)_V = V_0 \left(\frac{\partial P}{\partial B}\right)_V. \tag{3.141}$$

Writing from Eq. (3.138) the pressure as a function of the volume V_0 we have

$$P = \pi^4 \lambda^2 \frac{B^2}{V_0^2} - \mu^2 \Rightarrow \left(\frac{\partial P}{\partial B}\right)_V = \frac{2\pi^4 \lambda^2}{V_0^2} B, \tag{3.142}$$

so the chemical potential is

$$\boldsymbol{\mu} = 2\pi^4 \lambda^2 \frac{B}{V_0} = 2\pi^4 \lambda^2 \bar{\rho}_B, \tag{3.143}$$

where as announced, for the step-function potential exact and MF chemical potential agree.

Then, it is easy to write both the pressure and the average energy density in terms of $\boldsymbol{\mu}$ (see Fig. 3.2)

$$P = \pi^4 \lambda^2 \bar{\rho}_B^2 - \mu^2 = \frac{1}{4\pi^4 \lambda^2} \boldsymbol{\mu}^2 - \mu^2, \tag{3.144}$$

$$\bar{\varepsilon} = \pi^4 \lambda^2 \bar{\rho}_B^2 + \mu^2 = \frac{1}{4\pi^4 \lambda^2} \boldsymbol{\mu}^2 + \mu^2. \tag{3.145}$$

Adding both equations and with the help of Eq. (3.143), it is clear the following thermodynamical relation holds, i.e.,

$$P + \bar{\varepsilon} = \boldsymbol{\mu} \bar{\rho}_B. \tag{3.146}$$

Moreover, subtracting Eq. (3.144) to Eq. (3.145) the usual EoS is obtained:

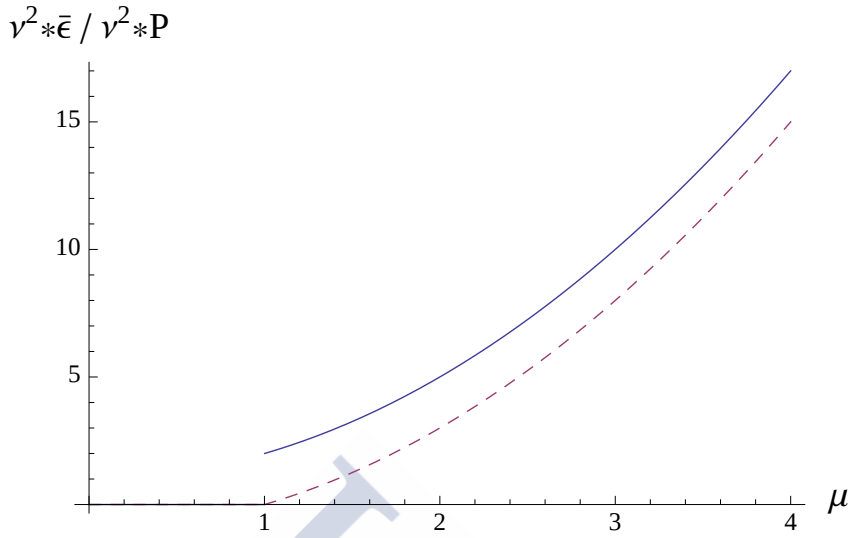

Figure 3.2: Average energy density (solid line) and pressure (dashed line) as functions of baryon chemical potential for the step-function potential.

$$\bar{\varepsilon} = P + 2\mu^2. \tag{3.147}$$

It is worth noting that for the step-function the chemical potential is always proportional to the baryon density and not only asymptotically as in the general case.

ii) **No potential.**

The next case we will study corresponds to having no potential, namely,

$$\mathcal{U} = 0. \tag{3.148}$$

As it was seen before, there is no solution for zero pressure although it does exist when P is introduced. In fact, for non-zero pressure, energy and volume read

$$E(B) = \pi^2 \lambda B \sqrt{P}, \qquad V = \pi^2 \lambda B \frac{1}{\sqrt{P}}, \tag{3.149}$$

and assuming we start with a non-zero pressure solution with baryon number B_0 and increase it to $B = B_0 + n$ keeping the volume fixed, we arrive at

$$E(B) = \pi^4\lambda^2\frac{B^2}{V} \Rightarrow \boldsymbol{\mu} = 2\pi^4\lambda^2\frac{B}{V}, \tag{3.150}$$

so we can write

$$\boldsymbol{\mu} = 2\pi^4\lambda^2\bar{\rho}_B. \tag{3.151}$$

Furthermore, from Eq. (3.149) we easily find $\bar{\varepsilon} = P$, so by means of Eq. (3.150),

$$P = \bar{\varepsilon} = \pi^4\lambda^2\bar{\rho}_B^2, \tag{3.152}$$

and from the expression for $\boldsymbol{\mu}$

$$P = \bar{\varepsilon} = \frac{1}{4\pi^4\lambda^2}\boldsymbol{\mu}^2. \tag{3.153}$$

Therefore, we see this case is quite similar to the step-function potential with the energy density and baryon density being constant. In fact, we can derive all quantities from the case above in the limit $\mu \to 0$.

iii) **Cubic potential.**

We will also consider one potential with a cubic approach to vacuum which belongs to the so-called BPS potentials. It was introduced before when calculating the compression modulus and can be easily written in terms of the η field defined by Eq. (3.46). This potential reads

$$\mathcal{U} = \eta = \frac{1}{2}(\xi - \frac{1}{2}\sin(2\xi)). \tag{3.154}$$

Then, volume and energy are proportional to the tilde quantities

$$\tilde{V} = 2\left(\sqrt{\frac{\pi}{2} + \tilde{P}} - \sqrt{\tilde{P}}\right), \tag{3.155}$$

$$\begin{aligned}\tilde{E} \quad &= \frac{1}{3}\left(2\pi\sqrt{\frac{\pi}{2} + \tilde{P}} - \tilde{P}\tilde{V}\right) \\ &= \frac{2}{3}\left(- \tilde{P}\left(\sqrt{\tilde{P} + \frac{\pi}{2}} - \sqrt{\tilde{P}}\right) + \pi\sqrt{\tilde{P} + \frac{\pi}{2}}\right),\end{aligned} \tag{3.156}$$

and thus, the average energy density is

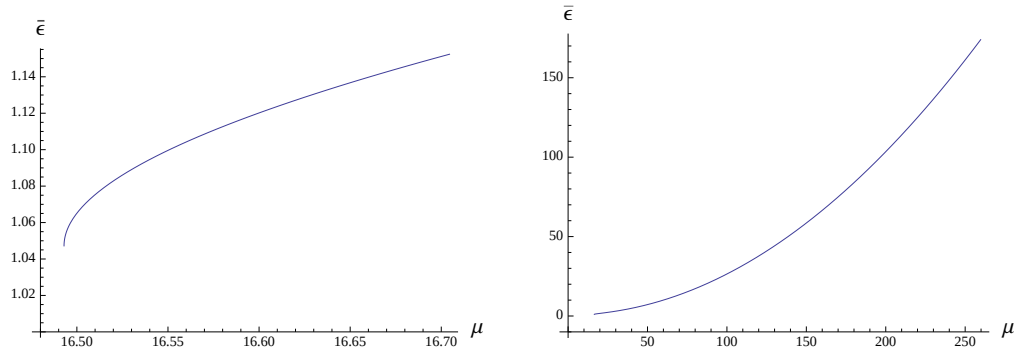

Figure 3.3: Left: Average energy density as a function of the MF baryon chemical potential for $\mathcal{U} = \eta$ with $\mu^2 = \lambda = 1$. Right: Zoom-in near the saturation density.

$$\bar{\varepsilon} = \frac{\mu^2}{3}\left(\pi\frac{\sqrt{\frac{\pi}{2}+\frac{P}{\mu^2}}}{\sqrt{\frac{\pi}{2}+\frac{P}{\mu^2}}-\sqrt{\frac{P}{\mu^2}}} - \frac{P}{\mu^2}\right). \tag{3.157}$$

Taking into account that the volume remains constant,

$$V_0 = 2\pi\frac{\lambda}{\mu}B_0\tilde{V}(P=0) = 2\pi\frac{\lambda}{\mu}B\tilde{V}(P), \tag{3.158}$$

we arrive at the following expression for the pressure

$$P = \mu^2\frac{\pi}{8}\frac{B^2}{B_0^2}\left(1-\frac{B_0^2}{B^2}\right)^2 = \mu^2\frac{\pi}{8}\frac{\bar{\rho}_B^2}{\bar{\rho}_{0,B}^2}\left(1-\frac{\bar{\rho}_{0,B}^2}{\bar{\rho}_B^2}\right)^2, \tag{3.159}$$

where $\bar{\rho}_{0,B}$ is the baryon density at $P=0$ and which allows to write the total energy like

$$E = \frac{2\pi^{5/2}}{3\sqrt{2}}B_0\lambda\mu\left(1+\frac{B^2}{B_0^2}-\frac{1}{4}\frac{B_0^2}{B^2}\left(1-\frac{B^2}{B_0^2}\right)^2\right). \tag{3.160}$$

From the definition of the MF chemical potential, Eq. (3.115), we easily get

$$\bar{\boldsymbol{\mu}} = \frac{\pi^{5/2}}{3\sqrt{2}}\lambda\mu\left(3\frac{B}{B_0}+\frac{B_0^3}{B^3}\right) = \frac{\pi^{5/2}}{3\sqrt{2}}\lambda\mu\left(3\frac{\bar{\rho}_B}{\bar{\rho}_{0,B}}+\frac{\bar{\rho}_{0,B}^3}{\bar{\rho}_B^3}\right), \tag{3.161}$$

and considering that $V_0 = (2\pi)^{3/2}B_0\frac{\lambda}{\mu}$,

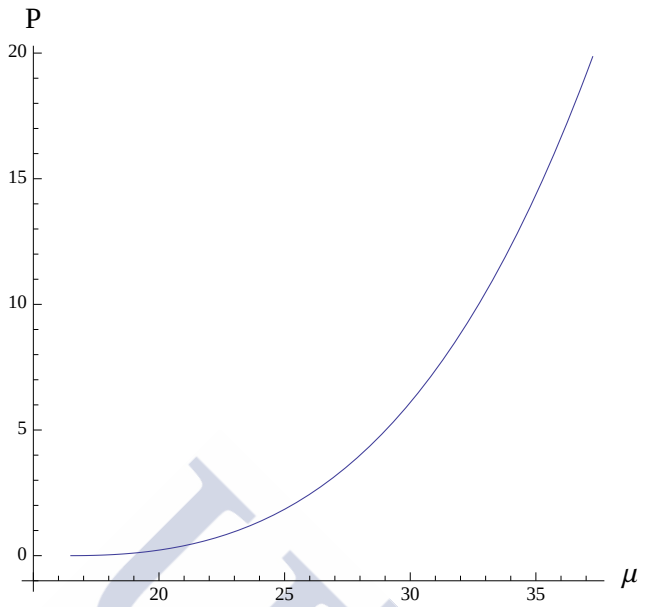

Figure 3.4: Pressure as a function of the MF baryon chemical potential for $\mathcal{U} = \eta$ with $\mu^2 = \lambda = 1$.

$$\begin{aligned}\bar{\varepsilon} &= \frac{\pi}{6}\mu^2\left(1+\frac{B^2}{B_0^2}-\frac{1}{4}\frac{B_0^2}{B^2}\left(1+\frac{B^2}{B_0^2}\right)^2\right)\\ &= \frac{\pi}{6}\mu^2\left(1+\frac{\bar{\rho}_B^2}{\bar{\rho}_{0,B}^2}-\frac{1}{4}\frac{\bar{\rho}_{0,B}^2}{\bar{\rho}_B^2}\left(1+\frac{\bar{\rho}_B^2}{\bar{\rho}_{0,B}^2}\right)^2\right).\end{aligned} \tag{3.162}$$

In Fig. 3.3 and Fig. 3.4 we can see the average energy density, $\bar{\varepsilon}$, and pressure, P, as function of the MF baryon chemical potential $\bar{\boldsymbol{\mu}}$, respectively.

In the case of high chemical potential, we have the asymptotical behaviour

$$\bar{\boldsymbol{\mu}} = \frac{\pi^{5/2}}{\sqrt{2}}\lambda\mu\frac{B}{B_0}, \tag{3.163}$$

whilst the pressure and energy are

$$P = \frac{\pi}{8}\left(\frac{B}{B_0}\right)^2\mu^2, \qquad \bar{\varepsilon} = \frac{\pi}{8}\left(\frac{B}{B_0}\right)^2\mu^2, \tag{3.164}$$

which can be written by means of Eq. (3.163) like

$$P = \frac{1}{4\pi^4\lambda^2}\bar{\boldsymbol{\mu}}^2, \qquad \bar{\varepsilon} = \frac{1}{4\pi^4\lambda^2}\bar{\boldsymbol{\mu}}^2. \tag{3.165}$$

Thus, we see that for high chemical potential we asymptotically get the EoS

$$P = \bar{\varepsilon}, \tag{3.166}$$

where the subleading constant B_∞ has been omitted.

iv) **Sextic potential.**

This is a potential we have already seen in section 3.1 and which is given by

$$\mathcal{U} = \eta^2 = \frac{1}{4}\left(\xi - \frac{1}{2}\sin(2\xi)\right)^2. \tag{3.167}$$

Here we have a sextic approach to the vacuum so compacton solutions do not exist for zero pressure and consequently, the average energy density is zero at equilibrium. Then, we have to proceed as in the case with no potential and start from a non-zero pressure solution since external pressure has the effect of constraining the Skyrmion in a finite volume. Hence, volume and energy read

$$V = 2\pi\frac{\lambda}{\mu}B\,\mathrm{arcsinh}\frac{\pi\mu}{2\sqrt{P}}, \qquad E = \pi^2\lambda\mu B\sqrt{\frac{P^2}{\mu} + \frac{\pi^2}{4}}, \tag{3.168}$$

where the volume allows us to write both the pressure and the energy like

$$P = \frac{\pi^2\mu^2}{4}\frac{1}{\sinh^2\left(\frac{\mu}{2\pi\lambda}\frac{V}{B}\right)}, \qquad E = \frac{\pi^3}{2}\lambda\mu B\coth\left(\frac{\mu}{2\pi\lambda}\frac{V}{B}\right), \tag{3.169}$$

or in terms of the average particle (baryon number) density

$$P = \frac{\pi^2\mu^2}{4}\frac{1}{\sinh^2\left(\frac{\mu}{2\pi\lambda\bar{\rho}_B}\right)}, \qquad E = \frac{\pi^3}{2}\lambda\mu B\coth\left(\frac{\mu}{2\pi\lambda\bar{\rho}_B}\right). \tag{3.170}$$

Thus, from the expression for the energy in Eq. (3.168) and using its definition, the MF chemical potential is given by

$$\bar{\boldsymbol{\mu}} = \frac{\pi^3}{2}\lambda\mu\left[\coth\left(\frac{\mu}{2\pi\lambda\bar{\rho}_B}\right) + \frac{\mu}{2\pi\lambda\bar{\rho}_B}\frac{1}{\sinh^2\left(\frac{\mu}{2\pi\lambda\bar{\rho}_B}\right)}\right]. \tag{3.171}$$

On the one hand, the behaviour of this $\bar{\boldsymbol{\mu}}$ at high MF baryon density is the usual linear relation

$$\bar{\boldsymbol{\mu}} = 2\pi^4\lambda^2\bar{\rho}_B, \quad \bar{\rho}_B \to \infty. \tag{3.172}$$

On the other hand, for vanishing particle density we find

$$\bar{\boldsymbol{\mu}} = \frac{\pi^3}{2}\lambda\mu + \pi^2\mu^2\frac{1}{\bar{\rho}_B}e^{-\frac{\mu}{\pi\lambda}\frac{1}{\bar{\rho}_B}}, \quad \bar{\rho}_B \to 0. \tag{3.173}$$

Thus, in the MF approach at $P = 0$ we do not have the picture of a bag type model because the average energy density vanishes (solutions correspond to infinitely extended solitons). As a result, the saturation density is just zero.

v) **Standard Skyrme potential.**

The last case we will study corresponds to the standard Skyrme potential which was already presented in Eq. (2.38):

$$\mathcal{U} = \mathcal{U}_\pi = \frac{1}{2}\mathrm{Tr}(1-U) = 2\sin^2\frac{\xi}{2}. \tag{3.174}$$

This is a potential with a quadratic behaviour near vacuum, which is related to the pionic masses in the standard Skyrme model.

Here the situation is slightly more complicated and the MF baryon chemical potential is related to the MF baryon density in an implicit way by the two following expressions

$$\begin{aligned}\bar{\boldsymbol{\mu}} \;=\; & 4\pi\lambda\mu\frac{4}{15\mu^4}\sqrt{2+\frac{P}{\mu^2}}\left((4\mu^4+2\mu^2P+P^2)E\left[\frac{2\mu^2}{2\mu^2+P}\right]\right.\\ & \left.-P(\mu^2+P)K\left[\frac{2\mu^2}{2\mu^2+P}\right]\right),\end{aligned} \tag{3.175}$$

$$\bar{\rho}_B = \frac{3\mu}{8\pi\lambda} \frac{\mu^2}{\sqrt{2+\frac{P}{\mu^2}}\left((\mu^2+P)E\left[\frac{2\mu^2}{2\mu^2+P}\right] - PK\left[\frac{2\mu^2}{2\mu^2+P}\right]\right)}, \tag{3.176}$$

where E and K are the complete elliptic integrals of the first and second kind, respectively.

To conclude, a comparison with other results would be really interesting. However, as stated above, there is not much information about the baryon chemical potential within the Skyrme model yet. The only possibility is to compare with the results obtained from the AdS/CFT correspondence in the framework of the Sakai-Sugimoto model [83] (a holographic version of a Skyrme-type model). In this case, their result is quite different from our behaviour, since for two flavours the baryon density asymptotically tends to the free fermion gas, that is to say, $\rho_B \propto \boldsymbol{\mu}^3$ [84]. Nevertheless, there actually exists one similarity between this approach and our exact calculations because in both cases, at finite chemical potential, the baryon density depends on the spatial coordinates. Moreover, it also tends to a homogeneous (constant) configuration in the limit of infinite baryon chemical potential in both models. Despite that, a linear relation between baryon density and chemical potential is possible in a holographic approach when a Maxwell action is considered instead of the Born-Infeld one [85], although the addition of more scalar fields can change it.

All in all, we think that a proper description of nuclear matter requires this exact chemical potential instead of the MF approximation. Indeed, local quantities will differ a lot in this MF limit, as will be clear in Chapter 5. It is also worth commenting that one more thermodynamical quantity is left for a complete description of the BPS Skyrme thermodynamics at $T = 0$, namely, the isospin chemical potential (some attempts have already been made in this issue, e.g., [86, 87, 88, 89]).

3.2.3 In-medium BPS Skyrmions

To finish this section we will analyse the subject of in-medium Skyrmions in Skymionic matter. Although strictly speaking this is not thermodynamics, the baryon chemical potential allows to study this problem. Moreover, this is an issue of high importance since it allows to obtain the masses of baryons (nucleons) immersed in nuclear matter. The energy of a Skyrmion with baryon number B_0 in Skyrmionic matter is given by the integral

$$E_{B_0}(n) = 2\pi\lambda\mu B_0 \int_0^\pi d\xi \sin^2\xi \frac{2\mathcal{U}+\tilde{P}}{\sqrt{\mathcal{U}+\tilde{P}}}. \tag{3.177}$$

Here, P is the external pressure coming from the medium with additional topological charge n, i.e., the Skyrmionic medium has baryon number B_0+n. Thus, this energy is quite similar to Eq. (3.117) with the only difference of the overall multiplicative factor B_0 instead of B_0+n. On the other hand, the external pressure P would be equivalent to go from baryon number B_0 to B_0+n keeping the volume V_0 fixed corresponding to the equilibrium solution at $P=0$, namely,

$$V_0 = 2\pi(B_0+n)\frac{\lambda}{\mu}\int_0^\pi d\xi \sin^2\xi \frac{1}{\sqrt{\mathcal{U}+\tilde{P}}}. \tag{3.178}$$

Obviously, this pressure is exactly the same both in the Skyrmionic medium and in the original Skyrmion which is now compressed, so Eq. (3.177) is the in-medium energy of a Skyrmion with baryon number B_0.

From this expression and the corresponding formula for the baryon chemical potential it is possible to write the in-medium energy as a function of the MF (average) chemical potential. For instance, we will consider the simplest case of the step-function potential. Then, from equations (3.177) and (3.178) we easily get

$$E_{B_0}(n) = \pi^2\lambda\mu B_0 \frac{2+\frac{P}{\mu^2}}{\sqrt{1+\frac{P}{\mu^2}}}, \tag{3.179}$$

$$V_0 = \pi^2\frac{\lambda}{\mu}(B_0+n)\frac{1}{\sqrt{1+\frac{P}{\mu^2}}}, \tag{3.180}$$

and writing from the last equation the pressure as a function of V_0 we arrive at

$$E_{B_0}(n) = \pi^2\lambda\mu(B_0+n)\left(1+\frac{B_0^2}{(B_0+n)^2}\right), \tag{3.181}$$

where we have also used that $V_0 = \pi^2\left(\frac{\lambda}{\mu}\right)^2 B_0$. Taking into account that for this potential $\boldsymbol{\mu} = \bar{\boldsymbol{\mu}}$ and that it can be written as [see Eq. (3.143)]

$$\boldsymbol{\mu} = 2\pi^4\lambda^2\frac{B_0+n}{V_0} = 2\pi^2\lambda\mu\frac{B_0+n}{B_0}, \tag{3.182}$$

we finally get the expression

$$E_{B_0}(\boldsymbol{\mu}) = \frac{B_0}{2}\boldsymbol{\mu}\left(1 + \frac{4\pi^4\lambda^2\mu^2}{\boldsymbol{\mu}^2}\right). \tag{3.183}$$

This formula corresponds to the case above equilibrium where $\boldsymbol{\mu} \geq \boldsymbol{\mu}_0$. For $\boldsymbol{\mu} = \boldsymbol{\mu}_0$, which is the value we get from vacuum up to the equilibrium, the in-medium masses of Skyrmions are always the same and equal to the equilibrium mass. To understand this we can think we have a collection of charge one Skyrmions with total baryon number B_0 occupying at equilibrium the volume V_0. Then, if we remove the Skyrmions one after the other, due to the contact form of the interaction and the BPS property of solutions, they still have the same mass. Therefore, we have a gas of BPS Skyrmions in the same fixed volume V_0 but with a lower density of the medium.

On the other hand, similarly to what was done at the beginning of the section, we can also study the asymptotical behaviour of this in-medium energy independently of the chosen potential. Then, we find

$$E_{B_0}(\boldsymbol{\mu}) = \frac{B_0}{2}\boldsymbol{\mu} \quad \text{at} \quad \boldsymbol{\mu} \to \infty. \tag{3.184}$$

Moreover, from Eq. (3.123) we can write a general expression for the in-medium energy of a Skyrmion with baryon number one [remember that the energy appearing in Eq. (3.123) is not the in-medium energy but the difference is only an overall factor]

$$E_{B=1} = \bar{\boldsymbol{\mu}} - \frac{PV_0}{1+n} = \bar{\boldsymbol{\mu}} - \frac{P}{\bar{\rho}_B}. \tag{3.185}$$

Here, the second part goes to zero at equilibrium ($P = 0$) whilst at large densities it asymptotically tends to $\frac{1}{2}\bar{\boldsymbol{\mu}}$ [see Eq. (3.184)].

In addition, we can also obtain the in-medium size of our BPS Skyrmions. We expect the volume V_0 occupied at equilibrium by a B_0 soliton to get reduced after increasing the medium density. In fact, from Eq. (3.178) we can easily find

$$V_{B_0} = \frac{B_0}{B_0+n}V_0 = \frac{B_0}{\bar{\rho}_B} \to \frac{2\pi^4\lambda^2}{\bar{\boldsymbol{\mu}}}B_0 \quad \text{at} \quad \bar{\boldsymbol{\mu}} \to \infty, \tag{3.186}$$

where the asymptotical behaviour is also shown. Hence, taking into account that the volume is given by $V_{B_0} = \frac{4}{3}\pi R_{B_0}^3$, the compacton radius reads

$$R_{B_0} = \left(\frac{3B_0}{4\pi\bar{\rho}_B}\right)^{1/3} \to \left(\frac{3\pi^3\lambda^2}{2}\right)^{1/3}\bar{\boldsymbol{\mu}}^{-1/3} \quad \text{at} \quad \bar{\boldsymbol{\mu}} \to \infty. \tag{3.187}$$

Now, the idea is to interpret these charge one Skyrmions as baryons so we can study the in-medium masses (energies) of nucleons. Indeed, we have

just seen that up to the saturation density this mass does not depend on the density, whereas when the medium density is above the saturation density the in-medium mass asymptotically grows like $M \sim \frac{\bar{\mu}}{2}$. This limit agrees with the behaviour found by means of a holographic approach [90], although here the in-medium masses decrease from their vacuum value until the saturation point where the nucleon masses start to grow. In general, this reduction of the in-medium masses between vacuum and saturation density is expected from a physical point of view. Although this is not the case of the BPS Skyrme model, the extension to a near-BPS Skyrme model with small contributions from other terms coming from the standard Skyrme model and/or semiclassical corrections to the static energy like spin and isospin quantization, Coulomb energy or isospin-breaking (see Chapter 4), would probably improve this behaviour.

There is also something important to note when comparing with other results from different approaches. It is clear from the definition that our in-medium nucleon masses are always the total static energies for in-medium Skyrmions per baryon number. However, this is not always the case. For instance in [91], [92] or [93], the in-medium nucleon mass is just induced by in-medium changes of some coupling constants, and a reduction of the in-medium mass for nucleons is even possible above the saturation density. Moreover, there exists additional contributions to the total energy coming from in-medium modified nucleon-nucleon interactions which may have a relevant effect on the total in-medium energies per baryon number. Thus, these total in-medium energies are the ones to which we have to compare our results.

On the other hand, it is worth commenting about another quite different approach consisting in an in-medium modified Skyrme Lagrangian [94, 95]. Here, in contrast to our present work, the in-medium properties of Skyrmions are achieved by introducing medium-dependent constants. Then, thinking about a medium modified BPS Skyrme Lagrangian, it would take the form

$$\tilde{\mathscr{L}}_{\text{BPS}} \equiv -\pi^4 \bar{\lambda}^2(\boldsymbol{\mu}, \vec{x}) \mathcal{B}_\sigma \mathcal{B}^\sigma - \bar{\mu}^2(\boldsymbol{\mu}, \vec{x}) \mathcal{U}. \tag{3.188}$$

Therefore, from our results we should try to write these coupling constants $\bar{\lambda}$ and $\bar{\mu}$ in terms of the medium chemical potential $\boldsymbol{\mu}$ and spatial coordinates $\vec{x}$, and then fit to the correct in-medium dependence. Interestingly, this would allow us to see how good this approximation is by comparison with other thermodynamical properties.

Here, as a first step, we will study the simple step-function potential. As seen before, we expect the in-medium coupling parameters to be spatially constant, so $\bar{\lambda} = \bar{\lambda}(\boldsymbol{\mu})$ and $\bar{\mu} = \bar{\mu}(\boldsymbol{\mu})$. Then, comparing the volume and energy at equilibrium, i.e.,

$$V_0 \equiv V_{B_0}(\boldsymbol{\mu}_0) = \pi^2 B_0 \frac{\lambda}{\mu}, \qquad E_0 \equiv E_{B_0}(\boldsymbol{\mu}_0) = 2\pi^2 \lambda\mu B_0 \equiv \boldsymbol{\mu}_0 B_0 \tag{3.189}$$

(where $\boldsymbol{\mu}_0 = 2\pi^4\lambda^2\frac{B_0}{V_0} = 2\pi^2\lambda\mu$), with their in-medium expressions given by equations (3.181) and (3.186), we arrive at

$$V_{B_0}(\boldsymbol{\mu}) = V_{B_0}(\boldsymbol{\mu}_0)\frac{\boldsymbol{\mu}_0}{\boldsymbol{\mu}}, \qquad E_{B_0}(\boldsymbol{\mu}) = E_{B_0}(\boldsymbol{\mu}_0)\frac{1}{2}\left(\frac{\boldsymbol{\mu}}{\boldsymbol{\mu}_0} + \frac{\boldsymbol{\mu}_0}{\boldsymbol{\mu}}\right). \tag{3.190}$$

Considering that $V_{B_0}(\boldsymbol{\mu}_0) \propto \frac{\lambda}{\mu}$ and $E_{B_0}(\boldsymbol{\mu}_0) \propto \lambda\mu$ we get,

$$\frac{\bar{\lambda}}{\bar{\mu}} = \frac{\lambda}{\mu}\frac{\boldsymbol{\mu}_0}{\boldsymbol{\mu}}, \qquad \bar{\lambda}\bar{\mu} = \lambda\mu\frac{1}{2}\left(\frac{\boldsymbol{\mu}}{\boldsymbol{\mu}_0} + \frac{\boldsymbol{\mu}_0}{\boldsymbol{\mu}}\right), \tag{3.191}$$

so the in-medium coupling constants read

$$\bar{\lambda}^2 = \lambda^2\frac{1}{2}\left(\frac{\boldsymbol{\mu}_0^2}{\boldsymbol{\mu}^2} + 1\right), \qquad \bar{\mu}^2 = \mu^2\frac{1}{2}\left(\frac{\boldsymbol{\mu}^2}{\boldsymbol{\mu}_0^2} + 1\right). \tag{3.192}$$

This is valid for the liquid phase corresponding to $\boldsymbol{\mu} \geq \boldsymbol{\mu}_0$. Remember that in the gaseous phase the baryon chemical potential always takes the same value $\boldsymbol{\mu}_0$ and the in-medium masses and volumes remain unaltered.

It is necessary to comment here that these medium modified Skyrme Lagrangians are usually associated to the study of nucleons in atomic nuclei or infinite nuclear matter both at equilibrium. Therefore, since the BPS Skyrme model does not distinguish between in-medium nucleons or vacuum solutions at equilibrium, further contributions from semiclassical corrections and/or from the near-BPS version of the model are needed in order to be able to make some predictions. Hence, we see again that a more precise description of the thermodynamics of nuclear matter requires the near-BPS Skyrme model although the leading contribution always comes from the BPS theory.

Chapter 4

Binding Energies in the BPS Skyrme Model

Once we have introduced more general and theoretical properties of the BPS Skyrme model, we will focus our efforts on a more phenomenological subject, the calculation of binding energies of nuclei [96, 97]. Here, the BPS model will fix (especially for high nuclei) one of the main problems of the standard Skyrme model, the high values of the binding energies. To calculate them, the classical energy presented in section 2.2 is not enough. For this purpose, we need to introduce the semi-classical quantization of rotations and iso-rotations, directly related to the spin and isospin of nuclei, E_{rot}. After quantizing the model, the electric charge density is also needed in order to calculate the corresponding Coulomb energy of nuclei, E_C. And finally, an isospin-breaking term proportional to the third component of isospin has to be included, E_I. Then, the total mass of a nucleus will be given by

$$E = E_0 + E_{\text{rot}} + E_{\text{C}} + E_{\text{I}}, \tag{4.1}$$

where E_0 is the classical energy Eq. (2.40) for the standard Skyrme potential $\mathcal{U}_\pi$:

$$E_0 = \frac{64\sqrt{2}\pi}{15}\mu\lambda|B|. \tag{4.2}$$

With all these contributions, a calculation of the binding energies is possible with very good results for nuclei with high baryon number, shedding light again on the convenience of a near-BPS Skyrme model where the original terms of the Lagrangian enter as small perturbations. Here we will only consider the BPS Skyrme model as usual, but some attempts have been already made to perturbatively include contributions from the $\mathscr{L}_2$ and $\mathscr{L}_4$ terms [98, 99] (we will comment further on this issue below).

4.1 Semi-classical Quantization: Spin and Isospin

Since spin and isospin are relevant quantum numbers for nuclei, a semi-classical quantization is needed. To proceed with this quantization of spin

and isospin, we introduce the time-dependent rotational and isorotational degrees of freedom around the static solitonic solution U_0:

$$U(t,\vec{x}) = \mathrm{A}(t)U_0(R_\mathrm{B}(t)\vec{x})\mathrm{A}^\dagger(t), \tag{4.3}$$

where $R_B = \frac{1}{2}\mathrm{Tr}(\tau_i B \tau_j B^\dagger) \in \mathrm{SO}(3)$, while A and B are SU(2) matrices parametrized as $A(t) = a_0(t) + ia_i(t)\tau_i$, with $a_0^2 + \vec{a}^2 = 1$, and equivalently for B. The next step is to insert this expression into the Lagrangian and transform the generalized velocities $\dot{a}_0$, $\dot{a}_i$, $\dot{b}_0$ and $\dot{b}_i$ into the canonical momenta, and the Lagrangian into the Hamiltonian. Then, we interpret the coordinates and canonical momenta as quantum mechanical variables and momenta with their corresponding commutator relations, whereas the quantum states will be the eigenstates of spin and isospin

$$|X\rangle = |i\, i_3\, k_3\rangle\, |j\, j_3\, l_3\rangle, \tag{4.4}$$

where X represents the nucleus, $\vec{J}$ ($\vec{L}$) is the space-fixed (body-fixed) angular momentum, $\vec{I}$ ($\vec{K}$) is the space-fixed (body-fixed) isospin angular momentum, and j, j_3, l, l_3 and i, i_3, k, k_3 are the corresponding eigenvalues. For a detailed discussion of the eigenstates and their explicit expressions see Appendix A.

The symmetries of the static Skyrmion U_0 must be taken into account because they imply that some combinations of A and B will act trivially on it. Here we can have two different situations. On the one hand, if they are continuous one-parameter symmetries, some combinations of collective coordinates will not appear in the quantum Hamiltonian as, for instance, it happens in the case of the $B = 1$ hedgehog solution. On the other hand, if we have discrete transformations instead, non-trivial constraints in the nuclear states $|X\rangle$ appear: the Finkelstein-Rubinstein constraints [100]. In general, this restricts physical nuclei to only some combinations of the product states given by (4.4). However, this will not be the case of the BPS Skyrme model with the axially symmetric ansatz we will study, where the allowed wave functions can always be written as a product state (for a detailed discussion of the Finkelstein-Rubistein constraints in the framework of the standard Skyrme model see [101, 102]).

As we have just commented, we will focus here on the axially symmetric ansatz given by (2.31). The quantization of spin and isospin with the corresponding moments of inertia has been already calculated in this case within the standard Skyrme model, either for the $B = 1$ hedgehog solution [10, 11], or for the axial Skyrmions with $B > 1$ [12, 13, 103, 104]. It is necessary to distinguish both cases because they have different symmetries. Therefore, if we consider the $B = 1$ hedgehog (it corresponds to a nucleon: proton or neutron), the solution presents spherical symmetry so an arbitrary rotation can

be undone by an isorotation and vice versa. This equivalence between spin and isospin means that only three of the initial six collective coordinates will remain, where for instance we are going to choose the ones corresponding to spin. As well, because of the symmetry, the moments of inertia tensor will be diagonal and proportional to the identity, i.e.,

$$\mathcal{J}_{ij} = \delta_{ij}\mathcal{J}, \tag{4.5}$$

with

$$\mathcal{J} = \frac{4\pi}{3}\lambda^2 \int dr \sin^4\xi\, \xi_r^2 = \frac{2^8\sqrt{2}\pi}{15\cdot 7}\lambda\mu\left(\frac{\lambda}{\mu}\right)^{\frac{2}{3}}. \tag{4.6}$$

And the Hamiltonian will be the one of a symmetric top:

$$\mathcal{H}_{\text{rot}} = \frac{1}{2\mathcal{J}}\vec{L}^2 = \frac{1}{2\mathcal{J}}\vec{J}^2, \tag{4.7}$$

where we have used that the squares of the body-fixed and space-fixed spins coincide. Then, the static energy as function of the total spin quantum number is

$$E_{\text{rot}} = \frac{1}{2\mathcal{J}}\hbar^2 j(j+1). \tag{4.8}$$

Thinking now about the $B > 1$ solutions (they correspond to nuclei), we know they present axial symmetry. Thus, a rotation by an arbitrary angle ϕ around the three-axis can be undone by a rotation in the isospin space by an angle $B\phi$ (where B is the baryon number). Therefore, because of this symmetry we expect the Hamiltonian to consist of two copies of the symmetric top (one copy for the spin and another one for isospin) which is characterized by the moments of inertia tensor

$$\mathcal{J}_{ij} = \mathcal{J}_i\delta_{ij}, \qquad \text{with} \quad \mathcal{J}_1 = \mathcal{J}_2 \neq \mathcal{J}_3, \tag{4.9}$$

and the Hamiltonian

$$\mathcal{H}_{\text{sym-top}} = \frac{L_1^2 + L_2^2}{2\mathcal{J}_1} + \frac{L_3^2}{2\mathcal{J}_3} = \frac{\vec{J}^2}{2\mathcal{J}_1} + \left(\frac{1}{2\mathcal{J}_3} - \frac{1}{2\mathcal{J}_1}\right)L_3^2. \tag{4.10}$$

Finally, taking into account the equivalence between rotations and isorotations, only one of the corresponding generators (L_3 or K_3) may appear, so choosing K_3 the expression for the energy reads

$$E_{\text{rot}} = \frac{\hbar^2}{2}\left(\frac{j(j+1)}{\mathcal{J}_1} + \frac{i(i+1)}{\mathcal{I}_1} + \left(\frac{1}{\mathcal{I}_3} - \frac{1}{\mathcal{I}_1} - \frac{B^2}{\mathcal{J}_1}\right)k_3^2\right), \tag{4.11}$$

where $\mathcal{I}_{ij} = \mathcal{I}_i \delta_{ij}$ ($\mathcal{I}_1 = \mathcal{I}_2 \neq \mathcal{I}_3$) is the isospin moments of inertia tensor with

$$\mathcal{I}_3 = \frac{4\pi}{3}\lambda^2 \int dr \sin^4 \xi \, \xi_r^2 = |B|^{-\frac{1}{3}} \mathcal{J}, \tag{4.12}$$

$$\mathcal{I}_1 = \frac{3B^2+1}{4}\mathcal{I}_3, \tag{4.13}$$

whereas $\mathcal{J}_{ij} = \mathcal{J}_i \delta_{ij}$, with $\mathcal{J}_1 = \mathcal{J}_2 = \mathcal{J}_3 = B^2 \mathcal{I}_3$ is the spin version. Of course, $\mathcal{J}$ is the same as defined by (4.6).

Up to now we did not calculate the Hamiltonian directly but just guessed how it should look like because of symmetry. Then, let us derive it from the Lagrangian to show that our assumption as well as the moments of inertia tensor expressions are correct. As commented above, the first step is to introduce the time-dependent rotations and isorotations given by (4.3). Since the Lagrangian can be split into a static part and the time-dependent one as shown in Chapter 2 with the Roper resonances, i.e.,

$$\mathscr{L}_{06} = -\mathcal{E}_0 + \lambda^2 \pi^4 \mathcal{B}^i \mathcal{B}^i = -\mathcal{E}_0 + \mathscr{L}_{\text{rot}}, \tag{4.14}$$

the additional terms, $\mathscr{L}_{\text{rot}}$, will only arise from the space-like components of the baryon density (remember that spin and isospin rotations are symmetries of the static energy functional):

$$\mathcal{B}^i = \frac{3}{24\pi^2}\text{Tr}(\varepsilon^{i0jk} L_0 L_j L_k). \tag{4.15}$$

Therefore, we have to study how the components of the Maurer-Cartan current change after introducing the collective coordinates. It is easy to see that for the spatial components we have (the R means they are functions of the rotated spatial coordinates)

$$L_j = U^\dagger \partial_j U = A L_j^R A^\dagger, \tag{4.16}$$

while for L_0 we arrive at

$$L_0 = A(U_R^\dagger [A^\dagger \dot{A}, U_R] + U_R^\dagger \partial_0 U_R) A^\dagger, \tag{4.17}$$

where we can forget about the overall A and $A^\dagger$ because they are inside the trace. We still have to introduce the angular velocities for both rotations and isorotations. In the case of the angular velocities in isospace, Ω_i, they are defined in the standard way as

$$A^\dagger \dot{A} = i\vec{\Omega} \cdot \frac{\vec{\tau}}{2}. \tag{4.18}$$

whereas for the rotation angular velocities, ω_i,

$$\dot{R}_{ik}R^{-1}_{kj} = -\varepsilon_{ijk}\omega_k. \tag{4.19}$$

so we can write

$$U_R^\dagger[A^\dagger \dot{A}, U_R] = U_R^\dagger[i\Omega_i \frac{\tau_i}{2}, U_R] = \Omega_i T_i, \tag{4.20}$$

$$U_R^\dagger \partial_0 U_R = L_i^R \dot{R}_{ik} R^{-1}_{kj} x_j^R = \varepsilon_{ijk} x_i^R L_j^R \omega_k. \tag{4.21}$$

And forgetting about the rotated coordinates (finally we will integrate over the whole space) we get

$$L_0 = T_i \Omega_i + \varepsilon_{ijk} x_i L_j \omega_k, \tag{4.22}$$

with $T_i = iU^\dagger[\frac{\tau_i}{2}, U]$. Thus, the trace appearing in (4.15) reads

$$\mathrm{Tr}(\varepsilon^{0ijk} L_0 L_j L_k) = \mathrm{Tr}(\varepsilon^{0ijk} T_p L_j L_k)\Omega_p + \varepsilon_{pqr} x_p \mathrm{Tr}(\varepsilon^{0ijk} L_q L_j L_r)\omega_r, \tag{4.23}$$

and after inserting it into $\mathscr{L}_{\mathrm{rot}}$ and integrating over the whole space we obtain

$$L_{rot} = \frac{1}{2}\Omega_i \mathcal{I}_{ij} \Omega_j - \Omega_i \mathcal{K}_{ij} \omega_j + \frac{1}{2}\omega_i \mathcal{J}_{ij} \omega_j, \tag{4.24}$$

where

$$\mathcal{I}_{ij} = \frac{18\lambda^2}{24^2} \int d^3x \mathrm{Tr}(\varepsilon^{pqr} T_i L_q L_r)\mathrm{Tr}(\varepsilon^{pst} T_j L_s L_t), \tag{4.25}$$

$$\mathcal{K}_{ij} = -\frac{18\lambda^2}{24^2}\varepsilon_{jkl} \int d^3x \; x_k \mathrm{Tr}(\varepsilon^{pqr} T_i L_q L_r)\mathrm{Tr}(\varepsilon^{pst} L_l L_s L_t), \tag{4.26}$$

$$\mathcal{J}_{ij} = \frac{18\lambda^2}{24^2}\varepsilon_{ikl}\varepsilon_{jmn} \int d^3x \; x_k x_m \mathrm{Tr}(\varepsilon^{pqr} L_l L_q L_r)\mathrm{Tr}(\varepsilon^{pst} L_n L_s L_t). \tag{4.27}$$

4.1.1 Moments of Inertia Tensors

To calculate the moments of inertia tensors we will use the standard parametrization of the U field, Eq. (2.15), together with the axially symmetric ansatz given by (2.31). Then, the main expressions we need are given by

$$T_i = -i \sin^2\xi \, \tau_i + i \sin^2\xi \, n_i \, n_k \, \tau_k - i \sin\xi \cos\xi \, \varepsilon_{ikl} \, n_k \, \tau_l, \tag{4.28}$$

$$L_q = i\,\xi_q\,n_k\,\tau_k + i\sin\xi\cos\xi\,\partial_q n_k\,\tau_k + i\sin^2\xi\,\varepsilon_{jkl}\,n_j\,\partial_q n_k\,\tau_l, \tag{4.29}$$

where n_k is the k-component of the unit vector $\vec{n}$, τ_k the k^{th} Pauli matrix, while ξ_q and $\partial_q n_k$ are the derivatives respect to the coordinate x_q of the profile function ξ and $\vec{n}$, respectively. Considering that the product $L_q L_s$ present inside the traces is always multiplied by ε^{pqs} and that $n_a\partial_q n_a = 0$, we can write

$$\begin{aligned} L_q L_s \;\approx\; & -2i\,\xi_q\,\sin\xi\cos\xi\,\varepsilon_{abc}\,n_a\partial_s n_b\,\tau_c + 2i\,\xi_q\,\sin^2\xi\,\partial_s n_a\,\tau_a \\ & -i\sin^2\xi\cos^2\xi\,\varepsilon_{abc}\,\partial_q n_a\,\partial_s n_b\,\tau_c - i\sin^4\xi\,\varepsilon_{abc}\,n_a\,\partial_q n_b\,\partial_s n_c\,n_d\,\tau_d, \end{aligned} \tag{4.30}$$

so the two traces we need to calculate the tensors are

$$\begin{aligned} \mathrm{Tr}(\varepsilon^{pqs}T_i L_q L_s) \;=\; & 2\varepsilon^{pqs}\big[2\xi_q\,\sin^2\xi\,\partial_s n_i + \sin^4\xi\cos^2\xi\,\varepsilon_{abc}\,n_i\,n_a\,\partial_q n_b\,\partial_s n_c \\ & -\sin^4\xi\cos^2\xi\,\varepsilon_{iab}\,\partial_q n_a\,\partial_s n_b\big], \end{aligned} \tag{4.31}$$

$$\begin{aligned} \mathrm{Tr}(\varepsilon^{pqs}L_l L_q L_s) \;=\; & 2\varepsilon^{pqs}\big[2\xi_q\,\sin^2\xi\,\varepsilon_{abc}\,n_a\,\partial_s n_b\,\partial_l n_c + \xi_l\,\sin^2\xi\,\varepsilon_{abc}\,n_a\,\partial_q n_b\,\partial_s n_c \\ & +\sin^3\xi\cos^3\xi\,\varepsilon_{abc}\,\partial_q n_a\,\partial_s n_b\,\partial_l n_c\big]. \end{aligned} \tag{4.32}$$

Thus, using also the relation

$$\varepsilon_{ijk}\varepsilon_{lmn} = \delta_{il}(\delta_{jm}\delta_{kn} - \delta_{jn}\delta_{km}) - \delta_{im}(\delta_{jl}\delta_{kn} - \delta_{jn}\delta_{kl}) + \delta_{in}(\delta_{jl}\delta_{km} - \delta_{jm}\delta_{kl}), \tag{4.33}$$

we have for the isospin moments of inertia tensor given by (4.25)

$$\begin{aligned} \mathcal{I}_{ij} \;=\; & \frac{\lambda^2}{2}\int d^3x\,\xi_r^2\,\sin^4\xi\,\partial_s n_i\,\partial_s n_j \\ & +\frac{\lambda^2}{2}\int d^3x\,\sin^8\xi\cos^4\xi\big[(\delta_{ij}-n_i n_j)(\partial_q n_b\,\partial_q n_b\,\partial_s n_c\,\partial_s n_c - \partial_q n_b\,\partial_s n_b\,\partial_s n_c\,\partial_q n_c) \\ & +2\partial_q n_i\,\partial_s n_j\,\partial_s n_b\,\partial_q n_b - 2\partial_q n_i\,\partial_q n_j\,\partial_s n_b\,\partial_s n_b\big]. \end{aligned} \tag{4.34}$$

Calculating the derivative $\partial_s n_b$ we arrive at

$$\partial_s n_b = \begin{pmatrix} \nabla_\theta n_1 & \nabla_\theta n_2 & \nabla_\theta n_3 \\ \\ \nabla_\phi n_1 & \nabla_\phi n_2 & \nabla_\phi n_3 \end{pmatrix} = \begin{pmatrix} \frac{1}{r}\cos\theta\sin(B\phi) & \frac{1}{r}\cos\theta\cos(B\phi) & \frac{1}{r}\sin\theta \\ \\ \frac{B}{r}\cos(B\phi) & -\frac{B}{r}\sin(B\phi) & 0 \end{pmatrix}, \tag{4.35}$$

so it can be seen that the second integral vanishes whereas in the first one only diagonal elements are non-zero because the resulting integrals over ϕ are

$$\int_0^{2\pi} d\phi \sin(B\phi)\cos(B\phi) = \int_0^{2\pi} d\phi \sin(B\phi) = \int_0^{2\pi} d\phi \cos(B\phi) = 0, \quad (4.36)$$

$$\int_0^{2\pi} d\phi \sin^2(B\phi) = \int_0^{2\pi} d\phi \cos^2(B\phi) = \pi. \quad (4.37)$$

Therefore, we get $\mathcal{I}_{ij} = \mathcal{I}_i \delta_{ij}$ with $\mathcal{I}_1 = \mathcal{I}_1 \neq \mathcal{I}_3$ as announced, and with the expressions as functions of ξ being

$$\mathcal{I}_1 = \mathcal{I}_2 = \frac{\pi}{3}\lambda^2(3B^2+1)\int dr\, \xi_r^2 \sin^4\xi, \quad (4.38)$$

$$\mathcal{I}_3 = \frac{4\pi}{3}\lambda^2 \int dr\, \xi_r^2 \sin^4\xi, \quad (4.39)$$

which obviously coincides with Eq. (4.12) and (4.13).

The next tensor we will calculate is the spin moments of inertia tensor, $\mathcal{J}_{ij}$, Eq. (4.27). Then, taking into account that $x_k\, \partial_k n_b = 0$, we can write

$$\mathcal{J}_{ij} = A + B + C, \quad (4.40)$$

where

$$\begin{aligned} A &= \frac{\lambda^2}{2}\int d^3x\, \xi_r^2 \sin^4\xi \big[(r^2\delta_{ij} - x_i x_j)(\partial_s n_b\, \partial_l n_c\, \partial_s n_b\, \partial_l n_c - \partial_s n_b\, \partial_l n_c\, \partial_s n_c\, \partial_l n_b) \\ &\quad -r^2(\partial_s n_b\, \partial_j n_c\, \partial_s n_b\, \partial_i n_c - \partial_s n_b\, \partial_j n_c\, \partial_s n_c\, \partial_i n_b)\big] \\ &= \frac{\lambda^2}{2}\int d^3x\, \xi_r^2 \sin^4\xi\, a_{ij}, \end{aligned} \quad (4.41)$$

$$\begin{aligned} B = \ & \frac{\lambda^2}{4}\int d^3x \sin^4\xi(\partial_q n_b\, \partial_s n_c\, \partial_q n_b\, \partial_s n_c - \partial_q n_b\, \partial_s n_c\, \partial_q n_c\, \partial_s n_b)\big[r^2\xi_l^2\delta_{ij} \\ & -(x_k\xi_k)^2\delta_{ij} - x_i x_j \xi_l^2 + x_i x_k \xi_k \xi_j + \xi_i x_j x_k \xi_k - \xi_i r^2 \xi_j\big], \end{aligned} \quad (4.42)$$

$$\begin{aligned} C &= \frac{\lambda^2}{4}\int d^3x \sin^6\xi\cos^6\xi\big[(r^2\delta_{ij} - x_i x_j)(\partial_q n_a\, \partial_s n_b\, \partial_l n_c\, \partial_q n_a\, \partial_s n_b\, \partial_l n_c \\ &\quad -\partial_q n_a\, \partial_s n_b\, \partial_l n_c\, \partial_q n_a\, \partial_s n_c\, \partial_l n_b - \partial_q n_a\, \partial_s n_b\, \partial_l n_c\, \partial_q n_b\, \partial_s n_a\, \partial_l n_c \\ &\quad +\partial_q n_a\, \partial_s n_b\, \partial_l n_c\, \partial_q n_c\, \partial_s n_a\, \partial_l n_b + \partial_q n_a\, \partial_s n_b\, \partial_l n_c\, \partial_q n_b\, \partial_s n_c\, \partial_l n_a \\ &\quad -\partial_q n_a\, \partial_s n_b\, \partial_l n_c\, \partial_q n_c\, \partial_s n_b\, \partial_l n_a) - r^2(\partial_q n_a\, \partial_s n_b\, \partial_j n_c\, \partial_q n_a\, \partial_s n_b\, \partial_i n_c \\ &\quad +\partial_q n_a\, \partial_s n_b\, \partial_j n_c\, \partial_q n_c\, \partial_s n_a\, \partial_i n_b + \partial_q n_a\, \partial_s n_b\, \partial_j n_c\, \partial_q n_b\, \partial_s n_c\, \partial_i n_a \\ &\quad -\partial_q n_a\, \partial_s n_b\, \partial_j n_c\, \partial_q n_c\, \partial_s n_b\, \partial_i n_a)\big] \end{aligned} \quad (4.43)$$

Furthermore, writing $\xi_l = \xi_r \frac{\partial_r}{\partial x_l} = \frac{x_l}{r}\xi_r$ and

$$\partial_k n_c = \partial_\theta n_c \frac{\partial \theta}{\partial x_k} + \partial_\phi n_c \frac{\partial \phi}{\partial x_k}, \tag{4.44}$$

it can be checked that both B and C vanish so the inertia tensor $\mathcal{J}_{ij}$ will be determined by a_{ij}, which after the calculation reads

$$a_{ij} = \begin{pmatrix} \frac{B^2}{4r^2}(3+\cos(2\theta)-2\cos(2\phi)\sin^2\theta) & -\frac{B^2}{r^2}\sin^2\theta\sin\phi\cos\phi & \cdots \\ -\frac{B^2}{r^2}\sin^2\theta\sin\phi\cos\phi & \frac{B^2}{4r^2}(3+\cos(2\theta)+2\cos(2\phi)\sin^2\theta) & \cdots \\ -\frac{B^2}{r^2}\sin\theta\cos\theta\cos\phi & -\frac{B^2}{r^2}\sin\theta\cos\theta\sin\phi & \end{pmatrix}$$

$$\begin{pmatrix} -\frac{B^2}{r^2}\sin\theta\cos\theta\cos\phi \\ -\frac{B^2}{r^2}\sin\theta\cos\theta\sin\phi \\ \frac{B^2}{r^2}\sin^2\theta \end{pmatrix}. \tag{4.45}$$

Therefore, due to the integrals (4.36) and (4.37), only the diagonal elements will survive ($\mathcal{J}_{ij} = \mathcal{J}_i \delta_{ij}$):

$$\mathcal{J}_1 = \mathcal{J}_2 = \mathcal{J}_3 = \frac{4\pi}{3}\lambda^2 B^2 \int dr\, \xi_r^2 \sin^4\xi. \tag{4.46}$$

Finally, the last moments of inertia tensor to be calculated is the mixed one, $\mathcal{K}_{ij}$. Inserting the traces (4.31) and (4.32) in its definition (4.26) we get

$$\begin{aligned} \mathcal{K}_{ij} = -\frac{18\lambda^2}{24^2}\varepsilon_{jkl}\int d^3x\, x_k \big[& 4\xi_r^2 \sin^4\xi\, \varepsilon_{def}\, \partial_s n_i\, n_d\, \partial_s n_e\, \partial_l n_f \\ & +2\xi_l \sin^6\xi\cos^2\xi\, \varepsilon_{abc}\,\varepsilon_{def}\, n_i\, n_a\, \partial_q n_b\, \partial_s n_c\, n_d\, \partial_q n_e\, \partial_s n_f \\ & -2\xi_l \sin^6\xi\cos^2\xi\, \varepsilon_{iab}\,\varepsilon_{def}\, \partial_q n_a\, \partial_s n_b\, n_d\, \partial_q n_e\, \partial_s n_f \\ & 2\sin^7\xi\cos^5\xi\, \varepsilon_{abc}\,\varepsilon_{def}\, n_i\, n_a\, \partial_q n_b\, \partial_s n_c\, \partial_q n_d\, \partial_s n_e\, \partial_l n_f \\ & -2\sin^7\xi\cos^5\xi\, \varepsilon_{iab}\,\varepsilon_{def}\, \partial_q n_a\, \partial_s n_b\, \partial_q n_d\, \partial_s n_e\, \partial_l n_f \big]. \end{aligned} \tag{4.47}$$

After a tedious calculation it can be seen that only the first line does not vanish before integrating. Consequently,

$$\begin{aligned} \mathcal{K}_{ij} &= -\frac{\lambda^2}{2}\varepsilon_{jkl}\int d^3x\, x_k \xi_r^2 \sin^4\xi\, \varepsilon_{def}\, \partial_s n_i\, n_d\, \partial_s n_e\, \partial_l n_f \\ &= -\frac{\lambda^2}{2}\int d^3x \xi_r^2 \sin^4\xi\, d_{ij}, \end{aligned} \tag{4.48}$$

with

$$d_{ij} = \begin{pmatrix} \frac{B}{r^2}(B\cos(B\phi)\sin\phi - \cos^2\theta\cos\phi\sin(B\phi)) & \cdots \\ -\frac{B}{r^2}(\cos^2\theta\cos\phi\cos(B\phi) + B\sin\phi\sin(B\phi)) & \cdots \\ -\frac{B}{r^2}\sin\theta\cos\theta\cos\phi & \end{pmatrix}$$

$$\begin{pmatrix} -\frac{B}{r^2}(B\cos\phi\cos(B\phi) + \cos^2\theta\sin\phi\sin(B\phi)) & \\ \frac{B}{r^2}(-\cos^2\theta\sin\phi\cos(B\phi) + B\cos\phi\sin(B\phi)) & \cdots \\ -\frac{B}{r^2}\sin\theta\cos\theta\sin\phi & \end{pmatrix}$$

$$\begin{pmatrix} \frac{B}{r^2}\sin\theta\cos\theta\sin(B\phi) & \\ \frac{B}{r^2}\sin\theta\cos\theta\cos(B\phi) & \cdots \\ \frac{B}{r^2}\sin^2\theta & \end{pmatrix}. \tag{4.49}$$

Because of the different behaviour of the integrals over ϕ, we have to distinguish two different situations: $B = 1$ and $B > 1$. Then, for the case $B = 1$, all integrals over ϕ vanish except those for $\mathcal{K}_{12}$, $\mathcal{K}_{21}$ and $\mathcal{K}_{33}$. Therefore,

$$\mathcal{K}_{12} = \mathcal{K}_{21} = \frac{4\pi}{3}\lambda^2 \int dr\, \xi_r^2 \sin^4\xi, \tag{4.50}$$

$$\mathcal{K}_{33} = -\frac{4\pi}{3}\lambda^2 \int dr\, \xi_r^2 \sin^4\xi, \tag{4.51}$$

so we can write the inertia tensor as $\mathcal{K}_{ij} = \int dr\, \xi_r^2 \sin^4\xi k_{ij}$, where

$$k_{ij} = \begin{pmatrix} 0 & \alpha & 0 \\ \alpha & 0 & 0 \\ 0 & 0 & -\alpha \end{pmatrix}, \qquad \alpha = \frac{4\pi}{3}\lambda^2. \tag{4.52}$$

Although we would like to have a diagonal tensor this expression is not a problem, because its shape suggest we have the space and isospace axes oriented in a different way. To solve this, we will do a rotation of the spatial ones. Thus, making a π rad rotation about the X axis, $R_x(\pi)$, first, and a $\frac{\pi}{2}$ rad rotation around the Z axis, $R_z(\pi/2)$, then, the global rotation is given by

$$R = R_z(\pi/2)R_x(\pi) = \begin{pmatrix} 0 & 1 & 0 \\ 1 & 0 & 0 \\ 0 & 0 & -1 \end{pmatrix}. \tag{4.53}$$

And finally, multiplying k_{ij} on the right by R, we get the new matrix in these rotated axes:

$$k_{ij} = \begin{pmatrix} \alpha & 0 & 0 \\ 0 & \alpha & 0 \\ 0 & 0 & \alpha \end{pmatrix}. \tag{4.54}$$

So the inertia tensor is again diagonal, $\mathcal{K}_{ij} = \mathcal{K}_i \delta_{ij}$, with the non-zero elements

$$\mathcal{K}_1 = \mathcal{K}_2 = \mathcal{K}_3 = \frac{4\pi}{3}\lambda^2 \int dr\, \xi_r^2 \sin^4 \xi. \tag{4.55}$$

The case $B > 1$ is easier. We can do the same rotation but now, the only non-zero element is $\mathcal{K}_3$:

$$\mathcal{K}_3 = \frac{4\pi}{3}\lambda^2 B \int dr\, \xi_r^2 \sin^4 \xi. \tag{4.56}$$

Therefore, summarizing we have:

i) Isospin moments of inertia tensor, $\mathcal{I}_{ij}$,

$$\mathcal{I}_1 = \mathcal{I}_2 = \frac{\pi}{3}\lambda^2(3B^2+1) \int dr\, \xi_r^2 \sin^4 \xi, \tag{4.57}$$

$$\mathcal{I}_3 = \frac{4\pi}{3}\lambda^2 \int dr\, \xi_r^2 \sin^4 \xi, \tag{4.58}$$

ii) Spin moments of inertia tensor, $\mathcal{J}_{ij}$,

$$\mathcal{J}_1 = \mathcal{J}_2 = \mathcal{J}_3 = \frac{4\pi}{3}\lambda^2 B^2 \int dr\, \xi_r^2 \sin^4 \xi. \tag{4.59}$$

iii) Mixed moments of inertia tensor ($B = 1$), $\mathcal{K}_{ij}$,

$$\mathcal{K}_3 = \frac{4\pi}{3}\lambda^2 B \int dr\, \xi_r^2 \sin^4 \xi. \tag{4.60}$$

In fact, we can see that $B^2\mathcal{I}_3 = B\mathcal{K}_3 = \mathcal{J}_3$.

4.1.2 Canonical Momenta and Energy

The canonical momenta are easily calculated from the $L_{\rm rot}$ given by Eq. (4.24), we just need to differentiate it with respect to the angular velocities Ω_i and ω_i. Thus, taking into account the symmetries of the moments of inertia tensors we obtain,

$$\begin{aligned} K_i &= \frac{\partial L_{\rm rot}}{\partial \Omega_i} = \mathcal{I}_{ij}\Omega_j - \mathcal{K}_{ij}\omega_j \\ &= (\mathcal{I}_1\Omega_1 - \mathcal{K}_1\omega_1, \mathcal{I}_1\Omega_2 - \mathcal{K}_1\omega_2, \mathcal{I}_3(\Omega_3 - B\omega_3)), \end{aligned} \tag{4.61}$$

$$\begin{aligned} L_i &= \frac{\partial L_{\rm rot}}{\partial \omega_i} = -\Omega_j\mathcal{K}_{ji} + \mathcal{J}_{ij}\omega_j \\ &= (\mathcal{J}_1\omega_1 - \mathcal{K}_1\Omega_1, \mathcal{J}_1\omega_2 - \mathcal{K}_1\Omega_2, -B\mathcal{I}_3(\Omega_3 - B\omega_3)), \end{aligned} \tag{4.62}$$

where $\vec{K}$ corresponds to the body-fixed isospin angular momentum, and $\vec{L}$ to the body-fixed spin angular momentum. Here we use the same sign conventions appearing for instance in [13], with the commutation relations

$$[K_i, K_j] = i\varepsilon_{ijk}K_k, \qquad [L_i, L_j] = i\varepsilon_{ijk}L_k, \tag{4.63}$$

and being related to the space-fixed variables by minus the corresponding rotation, i.e.,

$$I_i = -R_{ij}(A)K_j, \qquad J_i = -R_{ij}(B)^T L_j. \tag{4.64}$$

Then, we can write the Hamiltonian in the usual way,

$$\begin{aligned} \mathcal{H}_{\rm rot} &= K_i\Omega_i + L_i\omega_i - L_{\rm rot} = \frac{1}{2}\Omega_i\mathcal{I}_{ij}\Omega_j - \Omega_i\mathcal{K}_{ij}\omega_j + \frac{1}{2}\omega_i\mathcal{J}_{ij}\omega_j \\ &= \frac{1}{2}(\Omega_1^2 + \Omega_2^2)\mathcal{I}_1 + \frac{1}{2}(\omega_1^2 + \omega_2^2)\mathcal{J}_1 \\ &\quad + \frac{1}{2}(\Omega_3 - B\omega_3)^2\mathcal{I}_3 - (\Omega_1\omega_1 + \Omega_2\omega_2)\mathcal{K}_1, \end{aligned} \tag{4.65}$$

where we have also used the symmetries of the moments of inertia. We can go even further and, following [104], write it as a sum of complete squares,

$$\begin{aligned} \mathcal{H}_{\rm rot} = \frac{1}{2}\Big(\mathcal{J}_1 - \frac{\mathcal{K}_1^2}{\mathcal{I}_1}\Big)(\omega_1^2 + \omega_2^2) + \frac{1}{2}(\Omega_3 - B\omega_3)^2\mathcal{I}_3 \\ + \frac{1}{2}\Big[\big(\Omega_1 - \frac{\mathcal{K}_1}{\mathcal{I}_1}\,\omega_1\big)^2 + \big(\Omega_2 - \frac{\mathcal{K}_1}{\mathcal{I}_1}\,\omega_2\big)^2\Big]\mathcal{I}_1. \end{aligned} \tag{4.66}$$

And finally, writing the angular velocities as functions of the canonical momenta from expressions (4.61) and (4.62) we arrive at

$$\mathcal{H}_{\rm rot} = \frac{1}{2}\left[\frac{(L_1+\mathcal{K}_1\frac{K_1}{\mathcal{I}_1})^2}{\mathcal{J}_1-\frac{\mathcal{K}_1^2}{\mathcal{I}_1}}+\frac{(L_2+\mathcal{K}_1\frac{K_2}{\mathcal{I}_1})^2}{\mathcal{J}_1-\frac{\mathcal{K}_1^2}{\mathcal{I}_1}}+\frac{K_1^2}{\mathcal{I}_1}+\frac{K_2^2}{\mathcal{I}_1}+\frac{K_3^2}{\mathcal{I}_3}\right]. \tag{4.67}$$

This is the general expression, but we know it is simplified for nuclei where $B>1$ and $\mathcal{K}_1=\mathcal{K}_2=0$.

Before going from this Hamiltonian operator to the energy expression with the quantum numbers corresponding to the canonical momenta, it is necessary to come back again to the axial symmetry. As was commented above, a rotation by an angle ϕ around the three-axis can be undone by an isorotation of an angle $B\phi$ around the three-axis of isospin. This can be translated into the Hilbert space of nuclear states:

$$(L_3+BK_3)|X\rangle=0 \quad\Rightarrow\quad l_3+Bk_3=0, \tag{4.68}$$

we have found a relation between the third component of spin and isospin in the body-fixed system, $l_3=-Bk_3$. Nevertheless, this constraint has a deeper implication. Obviously $j\geq|l_3|$, so if $k_3\neq 0$ we will have unphysically large spin values for nuclei. To avoid this problem we have to assume that the only possible value for the third component of the body-fixed isospin angular momentum is $k_3=0$. However, (and here we differ from [98, 99]) this has a rather transcendental consequence and only nuclei with even baryon number can be described within the BPS Skyrme model when the axially symmetric ansatz is assumed (since the spin of odd nuclei is a half integer, the constraint $k_3=0$ cannot hold). It is important to remark that this does not mean odd nuclei cannot be studied with the BPS theory. We cannot use this specific axial ansatz but remember that the model has the VPDs on the base space as a symmetry, so an infinite number of different shapes are possible, some of them surely allowing for the description of odd baryon number. Moreover, we will fix $i=|i_3|$. The reason is that we will compare our results with the binding energies of the most abundant nuclei for the same values of B, j, and i_3. Usually, these nuclei correspond to the most tightly bound ones, so they should present the minimum excitation energies which are precisely achieved when $i=|i_3|$.

All in all, we can easily write the energy corresponding to this semi-classical quantization as a function of the quantum numbers j and $i=|i_3|$ from the Hamiltonian operator (4.67). Then, for $B>1$, regarding that in this case $\mathcal{K}_1=\mathcal{K}_2=0$, the Hamiltonian is simplified, and using the integral which defines $\mathcal{J}$, i.e., Eq. (4.6), it reads

$$E_{\text{rot}} = \frac{105}{512\sqrt{2}\pi}\frac{\hbar^2}{\lambda^2\left(\frac{\mu}{\lambda B}\right)^{1/3}}\left(\frac{j(j+1)}{B^2} + \frac{4|i_3|(|i_3|+1)}{3B^2+1}\right), \tag{4.69}$$

On the other hand, for nucleons ($B = 1$) spin and isospin take the same value, $j = i = \frac{1}{2}$, and the energy is exactly the same given by (4.8) as expected,

$$E_{\text{rot}} = \frac{105}{512\sqrt{2}\pi}\frac{3}{4}\frac{\hbar^2}{\lambda^2\left(\frac{\mu}{\lambda}\right)^{1/3}}. \tag{4.70}$$

4.2 Electric Charge Density and Coulomb Energy

The next obvious contribution we should add to the energy (mass) of nuclei in order to calculate the binding energies corresponds to the Coulomb energy. It will be just the generalization for volume charge densities of the usual expression, i.e.,

$$E_{\text{C}} = \frac{1}{2\varepsilon_0}\int d^3x d^3x' \frac{\rho(\vec{r})\rho(\vec{r}\,')}{4\pi|\vec{r}-\vec{r}\,'|}. \tag{4.71}$$

Therefore, for this purpose we need to calculate the electric charge density and quantize it before inserting it in the integral. Then, we will follow [98, 99] to perform the integration by introducing an expansion of ρ into spherical harmonics.

4.2.1 The Electric Charge Density

The ρ appearing in the expression of the Coulomb energy corresponds to the expectation value with respect to the nuclear states $|X\rangle$ of the electric charge density operator given by [105]

$$\hat{\rho} = \frac{1}{2}\mathcal{B}^0 + \mathbb{J}^0_3, \tag{4.72}$$

where $\mathcal{B}^0$ is the topological charge density (baryon number density), see (2.11), and $\mathbb{J}^0_3$ corresponds to the time component of the third isospin current density operator $\mathbb{J}^\mu_a$. According to [106], the isospin current density operator reads

$$\mathbb{J}^\mu_3 = -\frac{i\lambda^2\pi^2}{4}\varepsilon^{\mu\nu\alpha\beta}\mathcal{B}_\nu \text{Tr}\left[\frac{\tau_3}{2}(\partial_\alpha U U^\dagger \partial_\beta U U^\dagger - \partial_\alpha U^\dagger U \partial_\beta U^\dagger U)\right], \tag{4.73}$$

so the time component is just

$$\mathbb{J}_3^0 = -\frac{i\lambda^2\pi^2}{4}\varepsilon^{0imn}\mathcal{B}_i \mathrm{Tr}\left[\frac{\tau_3}{2}(\partial_m U U^\dagger \partial_n U U^\dagger - \partial_m U^\dagger U \partial_n U^\dagger U)\right] \tag{4.74}$$

where $\mathcal{B}_i$ represents the space-like component of the topological density, Eq. (4.15).

To calculate this electric charge density operator, we must proceed as in Section 4.1 introducing the semi-classical quantization of the collective coordinates by time-dependent rotations and isorotations, Eq. (4.3). In the case of $\mathcal{B}^0$, since it is invariant under rotations and isorotations and does not involve time derivatives, it will remain unchanged and proportional to the identity operator:

$$\mathcal{B}^0 = -\frac{B}{2\pi^2 r^2}\sin^2\xi\,\xi_r. \tag{4.75}$$

However, for the calculation of the operator $\mathbb{J}_3^0$ we will have an extra difficulty with respect to the quantization of the Hamiltonian above. Besides the angular velocities of rotation and isorotation, an explicit dependence on the isospin collective coordinates will appear, i.e., $\mathbb{J}_3^0 = \mathbb{J}_3^0(\vec{\Omega}, \vec{\omega}, a^n)$, and a Weyl ordering is required [106] (we also differ here from [98, 99]).

The first thing we need to see is how this $\mathcal{B}_i$ behaves, but this was exactly one of the time-dependent parts we used for the Lagrangian quantization. Then, using the expressions of Section 4.1 we easily find

$$\mathcal{B}_i = \frac{3}{24\pi^2}\varepsilon_i{}^{0jk}\mathrm{Tr}\left[(T_p^R\,\Omega_p + \varepsilon_{pqr}x_p^R\,L_q^R\,\omega_r)L_j^R\,L_k^R\right], \tag{4.76}$$

whereas for the trace appearing in the definition of $\mathbb{J}_3^0$ we have

$$\begin{aligned}&\mathrm{Tr}\left[\frac{\tau_3}{2}(\partial_m U U^\dagger \partial_n U U^\dagger - \partial_m U^\dagger U \partial_n U^\dagger U)\right]\\ &\quad = \frac{1}{2}\mathrm{Tr}\Big[A^\dagger\tau_3 A(\partial_m U_R U_R^\dagger \partial_n U_R U_R^\dagger - U_R^\dagger \partial_m U_R U_R^\dagger \partial_n U_R)\Big].\end{aligned} \tag{4.77}$$

Finally, we arrive at

$$\begin{aligned}\mathbb{J}_3^0 = \; & -\frac{i\lambda^2}{64}\varepsilon^{0imn}\varepsilon_i{}^{0jk}\big[\mathrm{Tr}(T_pL_jL_k)\mathrm{Tr}(A^\dagger\tau_3 A\partial_m U_0 U_0^\dagger \partial_n U_0 U_0^\dagger)\,\Omega_p\\ & -\mathrm{Tr}(T_pL_jL_k)\mathrm{Tr}(A^\dagger\tau_3 A L_m L_n)\,\Omega_p\\ & +\varepsilon_{pqr}x_p\mathrm{Tr}(L_qL_jL_k)\mathrm{Tr}(A^\dagger\tau_3 A\partial_m U_0 U_0^\dagger \partial_n U_0 U_0^\dagger)\,\omega_r\\ & -\varepsilon_{pqr}x_p\mathrm{Tr}(L_qL_jL_k)\mathrm{Tr}(A^\dagger\tau_3 A L_m L_n)\,\omega_r\big].\end{aligned} \tag{4.78}$$

The traces $\mathrm{Tr}(\varepsilon_i^{\ 0jk} T_p L_j L_k)$ and $\mathrm{Tr}(\varepsilon_i^{\ 0jk} L_q L_j L_k)$ have been already calculated in the previous section, Eq. (4.31) and (4.32), respectively. For the remaining ones we will take into account Eq. (4.30) and define

$$A^\dagger \tau_3 A = R_i \tau_i, \tag{4.79}$$

where

$$R_1 = 2(a_0 a_2 + a_1 a_3), \quad R_2 = 2(a_2 a_3 - a_0 a_1), \quad R_3 = a_0^2 - a_1^2 - a_2^2 + a_3^2. \tag{4.80}$$

It is worth noting that this $\vec{R}$ also corresponds to the third component of the rotation matrix from the body-fixed to the space-fixed coordinates, $R(A)$, i.e., $R_i \equiv R_{3i}(A)$, with

$$R_{jk}(A) = \frac{1}{2}\mathrm{Tr}(\tau_j A^\dagger \tau_k A), \tag{4.81}$$

which further implies

$$I_3 = -\sum_i R_i K_i. \tag{4.82}$$

Then, we can easily find,

$$\begin{aligned} \mathrm{Tr}(A^\dagger \tau_3 A L_m L_n) \;=\; & 2R_i(-2i\xi_m \sin\xi\, \cos\xi\, \varepsilon_{abi} n_a \partial_n n_b + 2i\xi_m \sin^2\xi\, \partial_n n_i \\ & -i \sin^2\xi\, \cos^2\xi\, \varepsilon_{abi} \partial_m n_a \partial_n n_b - i \sin^4\xi\, \varepsilon_{abc} n_a \partial_m n_b \partial_n n_c n_i). \end{aligned} \tag{4.83}$$

And for the last trace, taking into account that $\partial_m U_0 U_0^\dagger \partial_n U_0 U_0^\dagger = U_0 L_m L_n U_0^\dagger$, we get

$$\begin{aligned} \partial_m U_0 U_0^\dagger \partial_n U_0 U_0^\dagger \;=\; & -2i\xi_m \sin\xi\, \cos\xi\, \varepsilon_{abc} n_a \partial_n n_b \tau_c - 2i\xi_m \sin^2\xi\, \partial_n n_a \tau_a \\ & -i \sin^2\xi\, \cos^4\xi\, \varepsilon_{abc} \partial_m n_a \partial_n n_b \tau_c \\ & -i \sin^4\xi\, (1 + \cos^2\xi\,) \varepsilon_{abc} n_a \partial_m n_b \partial_n n_c n_d \tau_d. \end{aligned} \tag{4.84}$$

So it reads

$$\begin{aligned} \mathrm{Tr}(A^\dagger \tau_3 A \partial_m U_0 U_0^\dagger \partial_n U_0 U_0^\dagger) \;=\; & 2R_i(-2i\xi_m \sin\xi\, \cos\xi\, \varepsilon_{abi} n_a \partial_n n_b - 2i\xi_m \sin^2\xi\, \partial_n n_i \\ & -i \sin^2\xi\, \cos^4\xi\, \varepsilon_{abi} \partial_m n_a \partial_n n_b \\ & -i \sin^4\xi\, (1 + \cos^2\xi\,) \varepsilon_{abc} n_a \partial_m n_b \partial_n n_c n_i). \end{aligned} \tag{4.85}$$

Finally, as commented above, we need to introduce the Weyl ordering

$$R_i\Omega_p \to \frac{1}{2}(R_i\Omega_p + \Omega_p R_i),$$
$$R_i\omega_r \to \frac{1}{2}(R_i\omega_r + \omega_r R_i), \tag{4.86}$$

and after a lengthy calculation we arrive at

$$\begin{aligned}
\mathbb{J}_3^0 \;=\; & -\frac{\lambda^2}{4}(R_i\Omega_p + \Omega_p R_i)\xi_r^2 \sin^4\xi\, A_{ip} \\
& +\frac{\lambda^2}{16}(R_i\Omega_p + \Omega_p R_i)\sin^8\xi\, \cos^4\xi\, C_{ip}, \\
& -\frac{\lambda^2}{4}(R_i\omega_r + \omega_r R_i)\xi_r^2 \sin^4\xi\, B_{ir} \\
& +\frac{\lambda^2}{16}(R_i\omega_r + \omega_r R_i)\varepsilon_{pqr}x_p[\xi_q \sin^6\xi\, \cos^2\xi\, P_i + \sin^7\xi\, \cos^5\xi\, Q_{iq}],
\end{aligned} \tag{4.87}$$

where

$$A_{ip} = \partial_k n_p \partial_k n_i, \tag{4.88}$$

$$\begin{aligned}
C_{ip} \;=\; & \varepsilon_{abc}\varepsilon_{ide} n_p n_a \partial_j\, n_b \partial_j\, n_d \partial_k n_c \partial_k n_e \\
& +\varepsilon_{pab}\varepsilon_{def} n_i n_d \partial_j\, n_a \partial_j\, n_e \partial_k n_b \partial_k n_f \\
& -\varepsilon_{pab}\varepsilon_{ide} \partial_j\, n_a \partial_j\, n_d \partial_k n_b \partial_k n_e \\
& -\varepsilon_{abc}\varepsilon_{def} n_i n_p n_a n_d \partial_j\, n_b \partial_j\, n_e \partial_k n_c \partial_k n_f,
\end{aligned} \tag{4.89}$$

$$B_{ir} = x_p \varepsilon_{pqr}\varepsilon_{abc} n_a \partial_k n_b \partial_q n_c \partial_k n_i, \tag{4.90}$$

$$P_i = \varepsilon_{abc}\varepsilon_{ide} n_a \partial_j\, n_b \partial_k n_c \partial_j\, n_d \partial_k n_e - \varepsilon_{abc}\varepsilon_{def} n_i n_a n_d \partial_j\, n_b \partial_k n_c \partial_j\, n_e \partial_k n_f, \tag{4.91}$$

$$Q_{iq} = \varepsilon_{abc}\varepsilon_{ide} \partial_j\, n_a \partial_k n_b \partial_q n_c \partial_j\, n_d \partial_k n_e. \tag{4.92}$$

Then, using the expression (4.35), it can be seen that C_{ip}, P_i and Q_{iq} vanish. On the other hand, to calculate B_{ir} we have to follow the procedure presented in the calculation of the $\mathcal{K}_{ij}$ moments of inertia tensor: first, we introduce a rotation of π rad around the X axis, and then we make a rotation

of $\frac{\pi}{2}$ rad around the Z axis [the total rotation is implemented by the matrix (4.53), see above]. Therefore, the matrices A_{ip} and B_{ir} are

$$A_{ip} = \begin{pmatrix} \frac{1}{r^2}(B^2\cos^2(B\phi) + \cos^2\theta\sin^2(B\phi)) & \frac{1}{4r^2}(1 - 2B^2 + \cos(2\theta))\sin(2B\phi) & \cdots \\ \frac{1}{4r^2}(1 - 2B^2 + \cos(2\theta))\sin(2B\phi) & \frac{1}{r^2}(\cos^2\theta\cos^2(B\phi) + B^2\sin^2(B\phi)) & \cdots \\ \frac{1}{r^2}\cos\theta\sin\theta\sin(B\phi) & \frac{1}{r^2}\sin\theta\cos\theta\cos(B\phi) & \cdots \end{pmatrix}$$

$$\begin{pmatrix} \frac{1}{r^2}\sin\theta\cos\theta\sin(B\phi) \\ \frac{1}{r^2}\sin\theta\cos\theta\cos(B\phi) \\ \frac{1}{r^2}\sin^2\theta \end{pmatrix}, \tag{4.93}$$

$$B_{ir} = \begin{pmatrix} -\frac{B}{r^2}(B\cos\phi\cos(B\phi) + \cos^2\theta\sin\phi\sin(B\phi)) & \cdots \\ \frac{B}{r^2}(-\cos^2\theta\sin\phi\cos(B\phi) + B\cos\phi\sin(B\phi)) & \cdots \\ -\frac{B}{r^2}\sin\theta\cos\theta\sin\phi & \cdots \end{pmatrix}$$

$$\begin{pmatrix} \frac{B}{r^2}(B\cos(B\phi)\sin\phi - \cos^2\theta\cos\phi\sin(B\phi)) \\ -\frac{B}{r^2}(\cos^2\theta\cos\phi\cos(B\phi) + B\sin\phi\sin(B\phi)) \\ -\frac{B}{r^2}\sin\theta\cos\theta\cos\phi \end{pmatrix}$$

$$\begin{pmatrix} -\frac{B}{r^2}\sin\theta\cos\theta\sin(B\phi) \\ -\frac{B}{r^2}\sin\theta\cos\theta\cos(B\phi) \\ -\frac{B}{r^2}\sin^2\theta \end{pmatrix}. \tag{4.94}$$

Thus, summarizing, the electric charge density quantum operator reads $\hat{\rho} = \frac{1}{2}\mathcal{B}^0 + \mathbb{J}_3^0$, where $\mathcal{B}^0$ is given by Eq. (4.75) and for $\mathbb{J}_3^0$ we have just seen

$$\mathbb{J}_3^0 = -\frac{\lambda^2}{4}(R_i\Omega_p + \Omega_p R_i)\xi_r^2\sin^4\xi\, A_{ip} - \frac{\lambda^2}{4}(R_i\omega_r + \omega_r R_i)\xi_r^2\sin^4\xi\, B_{ir}. \tag{4.95}$$

The final step to obtain the required expectation value consists in evaluating the matrix elements in (4.95). In our case, the non-diagonal elements $\langle X|R_iK_j|X\rangle$ with $i \neq j$ vanish (see Appendix B), whereas for the diagonal case, $i = j$, we can forget about the Weyl ordering since the operators commute. It is also important to note that $\vec{L}$ and $\vec{R}$ act on different spaces so $\langle X|R_iL_1|X\rangle = \langle X|R_iL_2|X\rangle = 0$ because $\langle X|L_1|X\rangle = \langle X|L_2|X\rangle = 0$ (remember both L_1 and L_2 can be written as a combination of L_+ and L_-). All in all, we arrive at the following expression of the expectation value for the time component of the third isospin current density operator,

$$\langle X|\mathbb{J}^0_3|X\rangle = -\frac{\lambda^2}{2}\xi_r^2 \sin^4\xi \frac{1}{\mathcal{I}_3}\langle X|\left(\frac{4}{3B^2+1}(R_1K_1A_{11}+R_2K_2A_{22})+R_3K_3A_{33}\right)|X\rangle, \tag{4.96}$$

where we have replaced the angular velocities by the canonical momentum operators, Eq. (4.61) and (4.62), besides using $B_{33} = -BA_{33}$ and $\mathcal{I}_1 = \frac{3B^2+1}{4}\mathcal{I}_3$. Furthermore, because of the axial symmetry we have $\langle X|R_1K_1|X\rangle = \langle X|R_2K_2|X\rangle$ so we can replace each of these matrix elements by $\frac{1}{2}\langle X|R_1K_1 + R_2K_2|X\rangle$. Then

$$\begin{aligned}\langle X|\mathbb{J}^0_3|X\rangle &= -\frac{\lambda^2}{2r^2}\xi_r^2 \sin^4\xi \frac{1}{\mathcal{I}_3}\left[\frac{2}{3B^2+1}\langle X|R_1K_1+R_2K_2|X\rangle(B^2+\cos^2\theta)\right.\\ &\left.+\langle X|K_3R_3|X\rangle \sin^2\theta,\right], \end{aligned}\tag{4.97}$$

where we have used the fact that $A_{11}+A_{22} = B^2+\cos^2\theta$ and $A_{33} = \sin^2\theta$. Finally, adding and subtracting an additional R_3K_3 to complete the I_3 as shown by Eq. (4.82), and with the obvious value of the matrix element $\langle X|I_3|X\rangle = i_3$, we obtain

$$\begin{aligned}\langle X|\mathbb{J}^0_3|X\rangle &= \frac{\lambda^2}{2r^2}\xi_r^2 \sin^4\xi \frac{1}{\mathcal{I}_3}\left(\frac{2(B^2+\cos^2\theta)}{3B^2+1}i_3\right.\\ &\left.-\frac{(B^2+1)(1-3\cos^2\theta)}{3B^2+1}\langle X|R_3K_3|X\rangle\right). \end{aligned}\tag{4.98}$$

It is easy to check that, integrating and using the solution for the ξ function, the contribution to the electric charge is just i_3 (notice that here even when $k_3 \neq 0$ the factor going with $\langle X|R_3K_3|X\rangle$ integrates to zero). Of course this is expected, since the electric charge Z (we assume it is expressed in units of the electron charge so it is equal to the atomic number) is given by

$$Z = \int d^3x \left(\frac{1}{2}\mathcal{B}^0 + \langle X|\mathbb{J}_3^0|X\rangle \right) = \frac{1}{2}B + i_3, \tag{4.99}$$

with $\frac{1}{2}\int d^3x \mathcal{B}^0 = \frac{1}{2}B$ by definition.

To conclude, we can trivially write the electric charge density for $B > 1$ by means of expressions (4.75) and (4.98) remembering that for the nuclei we can describe with our ansatz $k_3 = 0$, so their nuclear states obey $K_3|X\rangle = 0$. Thus,

$$\rho = \frac{1}{2}\mathcal{B}^0 + \langle X|\mathbb{J}_3^0|X\rangle = -\frac{B}{4\pi^2 r^2}\sin^2\xi\,\xi_r + \frac{\lambda^2 i_3}{r^2\mathcal{I}_3}\sin^4\xi\,\xi_r^2\frac{B^2+\cos^2\theta}{3B^2+1}, \tag{4.100}$$

and using the BPS solution for the profile function, Eq. (2.39), which in the r coordinate reads

$$\xi = \begin{cases} 2\arccos\frac{r}{R_B} & r \in [0, R_B], \\ 0 & r \geq R_B \end{cases} \qquad R_B \equiv \left(\frac{2\sqrt{2}\lambda|B|}{\mu}\right)^{1/3}, \tag{4.101}$$

with R_B the compacton radius, and the component $\mathcal{I}_3$ of the isospin inertia tensor given by Eq. (4.58), we arrive at the useful expression

$$\rho(\vec{r}) = \frac{2B}{\pi^2 R_B^3}\sqrt{1-\frac{r^2}{R_B^2}} + \frac{105 i_3}{8\pi R_B^3}\frac{B^2+\cos^2\theta}{3B^2+1}\frac{r^2}{R_B^2}\left(1-\frac{r^2}{R_B^2}\right), \tag{4.102}$$

where we have also used

$$\sin^2\xi\,\xi_r = -8\frac{r^2}{R_B^3}\sqrt{1-\frac{r^2}{R_B^2}} \tag{4.103}$$

which is the BPS equation after inserting the solution (4.101) in it.

On the other hand, the electric charge density for the hedgehog solution $B = 1$ has been already calculated before in [23, 24], and we can easily reproduce it from Eq. (4.95), taking into account the equivalence between spin and isospin. The corresponding expression is

$$\rho(\vec{r}) = \frac{2}{\pi^2 R_1^3}\sqrt{1-\frac{r^2}{R_1^2}} \pm \frac{35}{16\pi R_1^3}\frac{r^2}{R_1^2}\left(1-\frac{r^2}{R_1^2}\right), \tag{4.104}$$

where the plus (minus) sign corresponds to the proton (neutron).

4.2.2 The Coulomb Energy

After studying the electric charge density, we are now ready to calculate the Coulomb energy (4.71). For this purpose we have to take into account the usual multipole expansion of the Coulomb potential [107]

$$\frac{1}{4\pi|\vec{r}-\vec{r}\,'|}=\sum_{l=0}^{\infty}\sum_{m=-l}^{l}\frac{1}{2l+1}\frac{r_<^l}{r_>^{l+1}}Y_{lm}^*(\theta',\phi')Y_{lm}(\theta,\phi), \tag{4.105}$$

with $r_< = \min(r, r')$ and $r_> = \max(r, r')$. Here, we will follow the method shown in [98, 99] .The first thing we have to do is to expand the electric charge density $\rho(\vec{r})$ into spherical harmonics, i.e.:

$$\rho(\vec{r})=\sum_{l,m}\rho_{lm}(r)Y_{lm}^*(\theta,\phi), \tag{4.106}$$

so we can define the quantities

$$Q_{lm}(r)=\int_0^r dr' r'^{l+2}\rho_{lm}(r'), \tag{4.107}$$

as well as

$$U_{lm}=\frac{1}{2\varepsilon_0}\int_0^{\infty}drr^{-2l-2}|Q_{lm}(r)|^2, \tag{4.108}$$

so the Coulomb energy (4.71) can be reduced to

$$E_{\mathrm{C}}=\sum_{l=0}^{\infty}\sum_{m=-l}^{l}U_{lm}. \tag{4.109}$$

Looking at the expression for the electric charge density with baryon number $B > 1$, Eq. (4.102), we realize only two different contributions appear

$$\rho(\vec{r})=\rho_{00}(r)Y_{00}+\rho_{20}(r)Y_{20}, \tag{4.110}$$

with

$$\rho_{00}(r)=\frac{4B}{\pi^{3/2}R_B^3}\sqrt{1-\frac{r^2}{R_B^2}}+\frac{35i_3}{4\sqrt{\pi}R_B^3}\frac{r^2}{R_B^2}\left(1-\frac{r^2}{R_B^2}\right), \tag{4.111}$$

$$\rho_{20}(r)=\frac{7\sqrt{5}}{2\sqrt{\pi}R_B^3}\frac{i_3}{3B^2+1}\frac{r^2}{R_B^2}\left(1-\frac{r^2}{R_B^2}\right). \tag{4.112}$$

The next step is to calculate the quantities Q_{lm}. To do this, we have to distinguish between the two regions for which the electric density is defined.

Having this in mind we will call $Q_{lm}^{<}(r)$ if $r < R_B$ and $Q_{lm}^{>}(r)$ for $r > R_B$. Then, starting with Q_{00} we have

$$\begin{aligned} Q_{00}^{<}(r) &= \int_0^r dr' r'^2 \rho_{00}(r') = -\frac{B}{2\pi^{3/2}} \frac{r}{R_B} \sqrt{1 - \frac{r^2}{R_B^2}} \left(1 - \frac{2r^2}{R_B^2}\right) \\ &+ \frac{i_3}{4\sqrt{\pi}} \frac{r^5}{R_B^5} \left(7 - \frac{5r^2}{R_B^2}\right) + \frac{B}{2\pi^{3/2}} \arcsin\left(\frac{r}{R_B}\right), \end{aligned} \tag{4.113}$$

$$Q_{00}^{>}(r) = \int_0^r dr' r'^2 \rho_{00}(r') = \int_0^{R_B} dr' r'^2 \rho_{00}(r') = \frac{B + 2i_3}{4\sqrt{\pi}}, \tag{4.114}$$

so we can easily find U_{00} by splitting the integral into the different regions mentioned, i.e.,

$$\begin{aligned} U_{00} &= \frac{1}{2\varepsilon_0} \int_0^\infty dr r^{-2} |Q_{00}(r)|^2 \\ &= \frac{1}{2\varepsilon_0} \int_0^{R_B} dr r^{-2} |Q_{00}^{<}(r)|^2 + \frac{1}{2\varepsilon_0} \int_{R_B}^\infty dr r^{-2} |Q_{00}^{>}(r)|^2 \\ &= \frac{128B^2}{315\pi^3 \varepsilon_0 R_B} + \frac{245B}{1536\pi\varepsilon_0 R_B} i_3 + \frac{805}{5148\pi\varepsilon_0 R_B} i_3^2. \end{aligned} \tag{4.115}$$

In a similar way, using ρ_{20} we arrive at the corresponding expressions for Q_{20}:

$$Q_{20}^{<}(r) = \int_0^r dr' r'^4 \rho_{20}(r') = \frac{\sqrt{5}}{18\sqrt{\pi}} \frac{i_3}{1 + 3B^2} \frac{r^7}{R_B^5} \left(9 - \frac{7r^2}{R_B^2}\right), \tag{4.116}$$

$$Q_{20}^{>}(r) = \int_0^r dr' r'^4 \rho_{20}(r') = \int_0^{R_B} dr' r'^4 \rho_{20}(r') = \frac{\sqrt{5}}{9\sqrt{\pi}} \frac{i_3}{1 + 3B^2} R_B^2, \tag{4.117}$$

which when inserted into Eq. (4.108) give as a result

$$\begin{aligned} U_{20} &= \frac{1}{2\varepsilon_0} \int_0^\infty dr r^{-6} |Q_{20}(r)|^2 \\ &= \frac{1}{2\varepsilon_0} \int_0^{R_B} dr r^{-6} |Q_{20}^{<}(r)|^2 + \frac{1}{2\varepsilon_0} \int_{R_B}^\infty dr r^{-6} |Q_{20}^{>}(r)|^2 \\ &= \frac{7}{429\pi\varepsilon_0 R_B} \frac{i_3^2}{(1 + 3B^2)^2}. \end{aligned} \tag{4.118}$$

Finally, we trivially get the Coulomb energy from (4.109): $E_{\rm C} = U_{00} + U_{20}$. Thus, taking into account that $R_B = \sqrt{2}\left(\frac{\lambda B}{\mu}\right)^{1/3}$, the Coulomb energy for nuclei (i.e., baryon number $B > 1$) is

$$E_{\rm C} = \frac{1}{\sqrt{2}\pi\varepsilon_0}\left(\frac{\mu}{\lambda B}\right)^{1/3}\left(\frac{128}{315\pi^2}B^2 + \frac{245}{1536}Bi_3 + \frac{805}{5148}i_3^2 + \frac{7}{429}\frac{i_3^2}{(1+3B^2)^2}\right). \tag{4.119}$$

The last step will be the calculation of the Coulomb energy for proton and neutron. In this case, as we can see from the corresponding electric charge density (4.104), only one term remains in the spherical harmonic expansion due to the different symmetry of the hedgehog solution $B = 1$. Indeed, since the symmetry is now spherical we will just have ρ_{00} as a contribution,

$$\rho_{00} = \frac{4}{\pi^{3/2}R_1^3}\sqrt{1-\frac{r^2}{R_1^2}} + \frac{35i_3}{4\sqrt{\pi}R_1^3}\frac{r^2}{R_1^2}\left(1-\frac{r^2}{R_1^2}\right), \tag{4.120}$$

where $i_3 = \pm\frac{1}{2}$ with the plus (minus) sign for the proton (neutron). Comparing it with Eq. (4.111) for a general nucleus we see both are exactly the same. Therefore, $Q_{00}^{<}(r)$ and $Q_{00}^{>}(r)$ are given as above and since we only have one term in the expansion, the Coulomb energy is directly $E_{\rm C} = U_{00}$. Consequently, using that $R_1 = \sqrt{2}\left(\frac{\lambda}{\mu}\right)^{1/3}$ the resulting energies are

$$E_{\rm C}^{\rm p} = \frac{1}{\sqrt{2}\pi\varepsilon_0}\left(\frac{\mu}{\lambda}\right)^{1/3}\left(\frac{128}{315\pi^2} + \frac{156625}{1317888}\right), \tag{4.121}$$

$$E_{\rm C}^{\rm n} = \frac{1}{\sqrt{2}\pi\varepsilon_0}\left(\frac{\mu}{\lambda}\right)^{1/3}\left(\frac{128}{315\pi^2} - \frac{53585}{1317888}\right), \tag{4.122}$$

where $E_{\rm C}^{\rm p}$ and $E_{\rm C}^{\rm n}$ refers to the proton and neutron respectively.

4.3 Isospin-breaking Contribution

The Coulomb energies for proton and neutron we have just calculated at the end of the previous section, Eq. (4.121) and (4.122), will result in a proton heavier than a neutron. Of course we know this situation is not correct since nature tells us the opposite, with a mass difference given by

$$\Delta M = M_{\rm n} - M_{\rm p} = 1.29333\ \text{MeV}. \tag{4.123}$$

At a microscopical level, this fact comes from a down quark which is more massive than the up quark, so within the Skyrme framework it is translated

into charged pions heavier than neutral ones. This means that isospin is not an exact symmetry of strong interactions.

As the Skyrme model is an effective field theory, a proper treatment of this issue would require the introduction into the Lagrangian of an isospin breaking potential [108, 109, 110] with the corresponding semi-classical quantization of the collective coordinates. However, this is a difficult task so here we will just take into account the effect at leading order which is obviously given by the Hamiltonian

$$\mathcal{H}_{\rm I} = a_{\rm I} I_3, \tag{4.124}$$

which trivially commutes with the quantum number I_3 and where $a_{\rm I} < 0$ in order to get a slightly higher neutron mass. Thus, the corresponding energy contribution is

$$E_{\rm I} = a_{\rm I} i_3, \tag{4.125}$$

and comparing it with the proton-neutron mass difference, we can get a rough bound on this $a_{\rm I}$ parameter, $|a_{\rm I}| > 1.29333$ MeV.

4.4 Results: Binding Energies

At this point, we are ready to achieve the main purpose of this chapter, the calculation of binding energies per nucleon within the BPS Skyrme model. Thus, considering the classical (solitonic) energy we have already found in Chapter 2 and all the contributions presented above, the energy (mass), E_X, of an arbitrary nucleus X will be given by

$$E_X = E_0 + E_{\rm rot} + E_{\rm C} + E_{\rm I}. \tag{4.126}$$

To be able to calculate these masses and therefore the binding energies, the first step will be to determine the value of the model parameters. Here, it is worth noting the simplicity of our model with only three parameters, namely, λ, μ and $a_{\rm I}$. Then, we will fit expression (4.126) to the proton mass,

$$M_{\rm p} = 938.272 \text{ MeV}, \tag{4.127}$$

the experimental mass difference between neutron and proton, Eq. (4.123), and the mass of the nucleus with magic numbers ${}^{138}_{56}$Ba (among all nuclei with magic numbers we chose the one which gives the best fit to data),

$$M({}^{138}_{56}\text{Ba}) = 137.894\ u, \tag{4.128}$$

where $u = 931.494$ MeV is the unified atomic mass unit (since this corresponds to the atomic mass we must subtract the electron masses, $m_e = 0.511$ MeV). Moreover, we have to take into account the numerical value of the universal constants appearing in the different energy contributions like the Planck constant or the vacuum permittivity, i.e.,

$$\hbar = 197.327 \text{ MeV fm}, \tag{4.129}$$

$$\varepsilon_0 = \frac{1}{e} 8.8542 \cdot 10^{-21} \frac{1}{\text{MeV fm}}, \tag{4.130}$$

$$e = 1.60218 \cdot 10^{-19}. \tag{4.131}$$

All in all, we get the following parameter values from the fit:

$$\lambda\mu = 48.9902 \text{ MeV}, \quad \left(\frac{\mu}{\lambda}\right)^{1/3} = 0.604327 \text{ fm}^{-1}, \quad a_{\text{I}} = -1.68593 \text{ MeV}. \tag{4.132}$$

Once we have obtained these values, we can calculate the mass of an arbitrary nucleus (with even number baryon) within the BPS Skyrme model using Eq. (4.126), and then determine the corresponding nuclear binding energy, $E_{\text{B},X}$ given by

$$E_{\text{B},X} = ZE_{\text{p}} + NE_{\text{n}} - E_X, \tag{4.133}$$

with Z and N the number of protons and neutrons inside the nucleus X. It is clear from this expression that the parameter a_{I} and the isospin-breaking energy does not enter explicitly into the binding energy, but it actually does in an indirect way through the fit of the parameters.

As we have found analytical expressions for each energy contribution (the possibility of doing calculations analytically is one of the main features of the BPS Skyrme model), we can also write a general expression for the binding energies of nuclei, although we have to remember that because of the axial symmetry of our ansatz only nuclei with even baryon number are allowed. Then, changing the notation to the commonly used variables in nuclear physics,

$$i_3 = \frac{1}{2}(Z - N), \qquad B \equiv A = Z + N, \tag{4.134}$$

with A the atomic weight number, we finally arrive at an analytical binding energy depending only on this atomic weight number A, the number of protons, Z, and the spin quantum number j:

$$
\begin{aligned}
E_{\mathrm{B},X}(A,Z,j) &= a_1 A + a_2 Z - a_3 A^{5/3} - a_4 A^{2/3} Z - a_5 A^{-1/3} Z^2 \\
&\quad - a_6 \frac{A^{1/3}}{1+3A^2}(A-2Z) - a_7 \frac{A^{1/3}}{1+3A^2}(A-2Z)^2 \\
&\quad - a_8 \frac{A^{-1/3}}{(1+3A^2)^2}(A-2Z)^2 - a_9 A^{-5/3} j(j+1), \qquad (4.135)
\end{aligned}
$$

where these a_i coefficients are given by

$$
\begin{aligned}
a_1 &= \frac{315}{2048\sqrt{2}\pi}\frac{\hbar^2}{\lambda^2\left(\frac{\mu}{\lambda}\right)^{1/3}} + \frac{1}{46126080\sqrt{2}\pi^3\varepsilon_0}(18743296 - 1875475\pi^2)\left(\frac{\mu}{\lambda}\right)^{1/3} \\
&= 10.0503 \text{ MeV}, \\
a_2 &= \frac{53585}{329472\sqrt{2}\pi\varepsilon_0}\left(\frac{\mu}{\lambda}\right)^{1/3} = 0.400307 \text{ MeV}, \\
a_3 &= \frac{1}{46126080\sqrt{2}\pi^3\varepsilon_0}(18743296 - 1875475\pi^2)\left(\frac{\mu}{\lambda}\right)^{1/3} = 1.26027 \cdot 10^{-3} \text{ MeV}, \\
a_4 &= \frac{53585}{1317888\sqrt{2}\pi\varepsilon_0}\left(\frac{\mu}{\lambda}\right)^{1/3} = 0.100077 \text{ MeV}, \\
a_5 &= \frac{805}{5148\sqrt{2}\pi\varepsilon_0}\left(\frac{\mu}{\lambda}\right)^{173} = 0.384881 \text{ MeV}, \qquad (4.136) \\
a_6 &= \frac{105}{256\sqrt{2}\pi}\frac{\hbar^2}{\lambda^2\left(\frac{\mu}{\lambda}\right)^{1/3}} = 26.7974 \text{ MeV}, \\
a_7 &= \frac{105}{512\sqrt{2}\pi}\frac{\hbar^2}{\lambda^2\left(\frac{\mu}{\lambda}\right)^{1/3}} = 13.3987 \text{ MeV}, \\
a_8 &= \frac{7}{1716\sqrt{2}\pi\varepsilon_0}\left(\frac{\mu}{\lambda}\right)^{1/3} = 0.0100404 \text{ MeV}, \\
a_9 &= \frac{105}{512\sqrt{2}\pi}\frac{\hbar^2}{\lambda^2\left(\frac{\mu}{\lambda}\right)^{1/3}} = 13.3987 \text{ MeV}.
\end{aligned}
$$

In analysing these coefficients we can see that a_1 comes from the classical solitonic energy of the nucleus as well as from the proton and neutron masses. On the other hand, a_2 is non-zero because we have different Coulomb energies for proton and neutron, whilst $a_3 - a_5$ and a_8 stem from the Coulomb energy of nuclei. Finally, a_6 and a_7 are originated by the isospin quantization whereas a_9 corresponds to the spin excitation.

To compare now our theory with the experimental values we will follow the strategy used in [98, 99]: for each value of the atomic weight number A we choose the values of Z and j corresponding to the most abundant nucleus. The

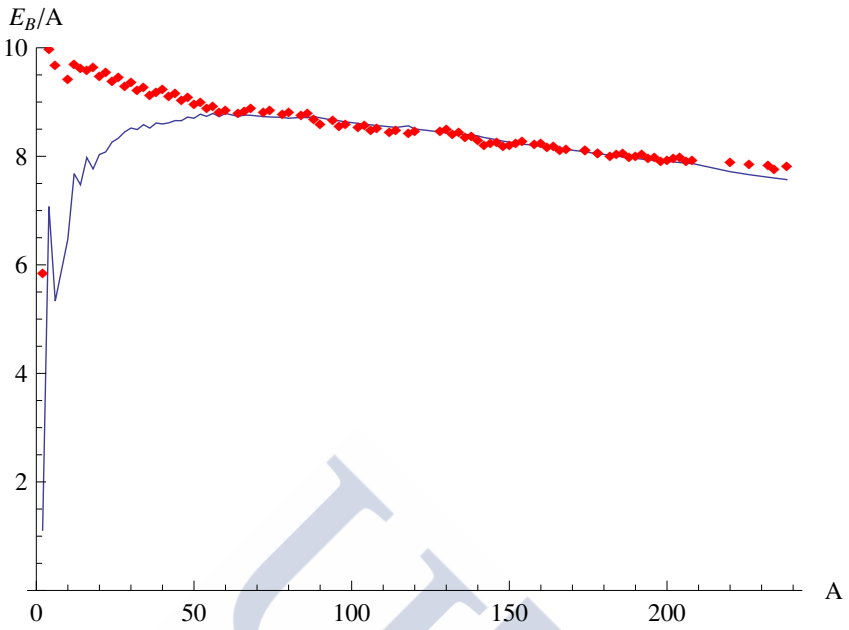

Figure 4.1: Binding energies per nucleon in MeV. The experimental values are described by the (blue) solid line whereas our model results are represented by the (red) diamonds.

result is presented in Fig. 4.1 where we have plotted the binding energy per nucleon given by our Eq. (4.135), $E_{\rm B}/A$, in comparison with its experimental value [111].

We see that the BPS Skyrme model gives excellent results for sufficiently high weight number A, but it overestimates the binding energies of the small nuclei. Nevertheless, this is a behaviour we could expect from our theory. The BPS Skyrme model is based on a collective description of the fundamental degrees of freedom favoured by the terms appearing in the Lagrangian. Besides, it has the symmetries of an incompressible ideal liquid as in the liquid drop model, which is again related to a collective description of nuclei. Therefore, this seems suitable for large nuclei, but for low baryon (atomic weight) number, single-particle properties and propagating pionic degrees are needed. Then, an extension of the model is required with the inclusion of small contributions into the Lagrangian, as for instance the $\mathscr{L}_2$ term or even the $\mathscr{L}_4$. Thus, we arrive again at the same idea, the BPS Skyrme model is a good description of strong interactions at leading order, but it must be improved with a generalization to a near-BPS Skyrme model, Eq. (2.70).

In addition, it would be interesting to also compare our results within the BPS Skyrme model with the semi-empirical mass formula (Weizsäcker

formula) [112]

$$E_{\mathrm{B}}^{\mathrm{W}}(A,Z) = a_{\mathrm{V}}A - a_{\mathrm{S}}A^{2/3} - a_{\mathrm{C}}Z(Z-1)A^{-1/3} - a_{\mathrm{A}}\frac{(A-2Z)^2}{A} + \delta(A,Z), \tag{4.137}$$

where

$$\delta(A,Z) = \begin{cases} a_{\mathrm{P}}A^{-3/4} & N \text{ and } Z \text{ even}, \\ 0 & A \text{ odd}, \\ -a_{\mathrm{P}}A^{-3/4} & N \text{ and } Z \text{ odd}, \end{cases} \tag{4.138}$$

with the values

$$a_{\mathrm{V}} = 15.5 \text{ MeV}, \qquad a_{\mathrm{S}} = 16.8 \text{ MeV}, \qquad a_{\mathrm{C}} = 0.72 \text{ MeV},$$

$$a_{\mathrm{A}} = 23 \text{ MeV}, \qquad a_{\mathrm{P}} = 34 \text{ MeV}. \tag{4.139}$$

All these parameters are empirical and, as in our case, they come from a fit to the binding energies. The first two constants, a_{V} and a_{S}, are related to the liquid drop model of nuclei so they also arise from a collective description of the system; a_{V} is the volume term and accounts for the leading linear contribution on A to the binding energy (specially for large nuclei), whilst a_{S} corresponds to the surface term and takes into account that nucleons on the surface are less tightly bound than those on the bulk. Moreover, the Coulomb energy is represented here by the a_{C} term, but unlike our model, neutrons do not contribute, just protons. The asymmetry term, a_{A} is due to the Pauli principle which requires higher energy for additional fermions of the same species because the lower states are already occupied. Finally, there is the pairing term, a_{P}, which encodes the idea that nucleons of the same kind tend to couple in pairs to obtain a more stable configuration.

In comparing this Weizsäcker formula (4.137) with our expression for the binding energies, Eq. (4.135), we find two terms which are in direct correspondence: the volume term, $a_{\mathrm{V}} \sim a_1$, and the Coulomb one, $a_{\mathrm{C}} \sim a_5$. As well, the term a_7 in the BPS Skyrme binding energy is similar to the asymmetry term in the semi-empirical mass formula, both are proportional to $(A-2Z)^2$, i.e., proportional to the third component of isospin i_3. However, since a_7 comes from the isospin moment of inertia $\mathcal{I}_1 \sim (3A^2+1)^2/A^{1/3}$, its contribution is much smaller for large atomic weight number because our term behaves like $\sim A^{-5/3}(A-2Z)^2$ whereas the asymmetry one is $\sim A^{-1}(A-2Z)^2$. The situation can be improved if another ansatz different from the axially symmetric one is used since the moments of inertia tensors would be distinct (remember this is not a problem due to the VPD symmetry). This relation between the

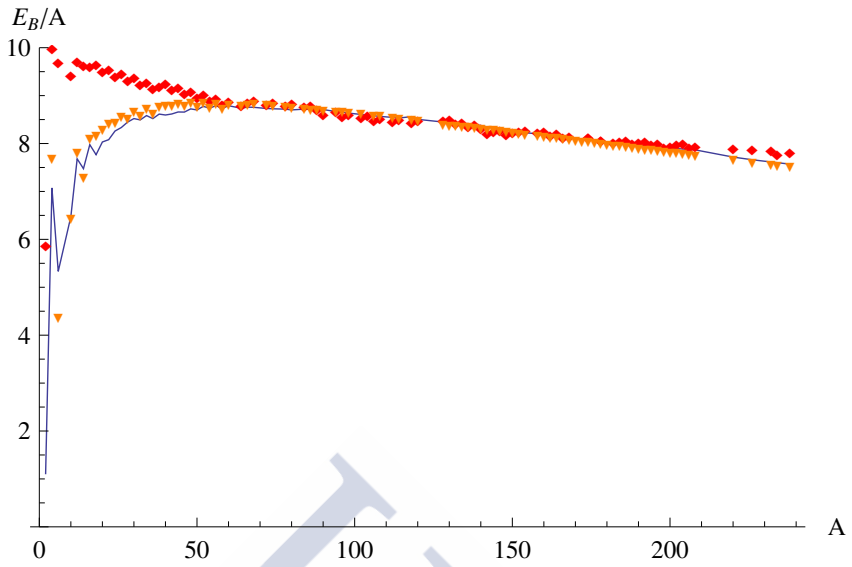

Figure 4.2: Binding energies per nucleon in MeV from the BPS Skyrme model (red diamonds) and Weizsäcker's formula (orange triangles) compared to the experimental values (solid blue line).

isospin quantum corrections and the Weizsäcker asymmetry term has been already investigated before in the framework of Skyrme models for atomic weight number up to $A \sim 30$ (see [45]). On the contrary, the other terms present in our binding energy expression seem to have no direct correspondence with the semi-empirical mass formula terms.

In Fig. 4.2, both formulae, (4.135) and (4.137), are compared to the experimental data. Although they agree at large baryon number, the Weizsäcker formula also describes very well the binding energies of small nuclei, precisely where the BPS Skyrme model has some problems. This is due to the surface term said before, which in the case of the semi-empirical mass formula contributes to the binding energy per nucleon like $\sim -a_S A^{-1/3}$ with the significant value of the constant $a_S \sim 17$ MeV. Then, the binding energy per nucleon is appreciable reduced for small values of the atomic weight A.

On the other hand, in Fig. 4.3 we can see in more detail how they behave for large nuclei, with some wiggles appearing for the BPS model, i.e., the binding energy per nucleon suddenly jumps between nearby nuclei. This effect comes from the Coulomb energy and has a simple explanation. To understand it we need to think about what happens when adding a neutron. First, since the neutron has a non-zero but small electric charge density, the Coulomb energy tends to a higher value, but at the same time, the nuclear radius increases which leads to a decreasing of the Coulomb energy. This last effect

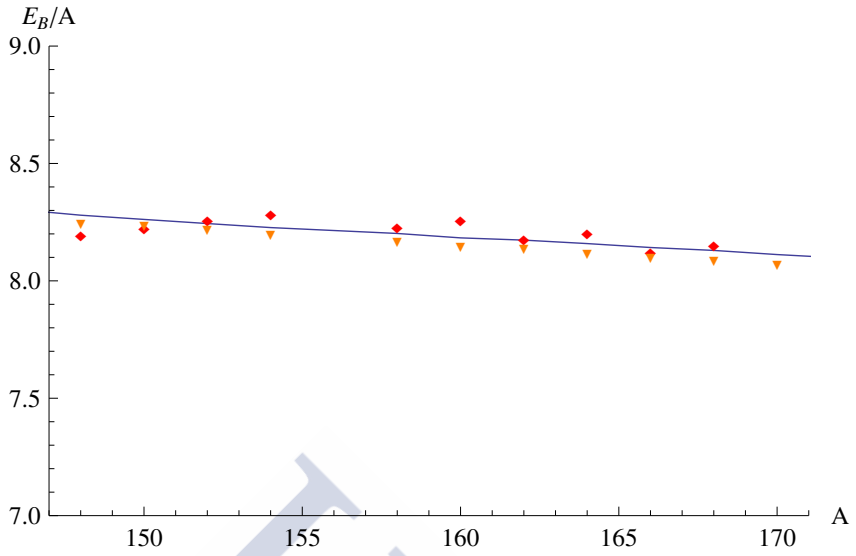

Figure 4.3: Zoom on Fig 4.2 for baryon numbers from 148 to 170.

is the dominant one so finally, when adding a neutron, the Coulomb energy goes down which means that the binding energy increases. Thus, if we move from a nucleus with atomic weight number A to another with $A+2$, we have two different possibilities. If we go from A to $A+2$ by adding two neutrons, the binding energy goes up as we have just seen. However, if we add a neutron and a proton the binding energy will decrease. It is worth noting that this effect does not happen in the semi-empirical mass formula even when there is no contribution to the Coulomb energy for neutrons. The reason is that the Weizsäcker formula compensates this more marked decreasing in the Coulomb energy when adding a neutron by the strong asymmetry term.

4.5 Extending Frontiers: The Quartic Potential

As stated in Chapter 2, since there is no kinetic term in the Lagrangian related to pions, the standard Skyrme potential $\mathcal{U}_\pi$, Eq. (2.38), is not mandatory so other different potentials may and should be further studied. For instance, we can think about a quartic potential (quartic approach to the vacuum), where the simplest choice is the square of the $\mathcal{U}_\pi$ used so far, i.e.,

$$\mathcal{U} = \mathcal{U}_\pi^2 = (1 - \cos\xi)^2. \tag{4.140}$$

After inserting it in the BPS equation (2.36), we obtain the implicit solution

$$\pi - \xi - \sin\xi - \sqrt{2}z = 0, \tag{4.141}$$

where z is the same variable we have introduced in Chapter 2:

$$z = \frac{\sqrt{2}\mu r^3}{3|B|\lambda}. \tag{4.142}$$

Then, asking for $\xi(Z) = 0$, we can trivially get the compacton radius Z,

$$Z = \frac{\pi}{\sqrt{2}} \tag{4.143}$$

Therefore, since $z \propto r^3/B$, we also conclude that the compacton radius grows like $B^{1/3}$, which is just the well-known nuclear behaviour.

The fact that the solution appears in an implicit form implies some small difficulties; we cannot have analytical expressions for everything so a formula similar to (4.135) will be no possible. However, we will be able to translate all the integrals over the z coordinate into much simpler integrals over the ξ field. This can be done by using the square root of the Bogomolny equation

$$\sin^2\xi\,\xi_z = -\sqrt{2\mathcal{U}}, \tag{4.144}$$

so we can just write

$$dz = -\frac{\sin^2\xi}{\sqrt{2\mathcal{U}}}\,d\xi = \frac{1}{\sqrt{2}}\frac{\sin^2\xi}{1-\cos\xi}\,d\xi. \tag{4.145}$$

Furthermore, from the implicit solution (4.141) we get

$$z = \frac{1}{\sqrt{2}}(\pi - \xi - \sin\xi). \tag{4.146}$$

In this fashion we can calculate the classical static energy, which after using the BPS equation reads, in the z variable,

$$E_0 = 4\sqrt{2}\pi\mu\lambda|B|\int dz\,\mathcal{U}(\xi(z)) = 4\pi\mu\lambda|B|\int_0^\pi d\xi\sin^2\xi(1-\cos\xi) = 2\pi^2\mu\lambda|B|, \tag{4.147}$$

where we have arrived at an integral over ξ as commented above. It is worth noting that here we do have an analytical expression for the energy and there exists again a linear relation between the static energy and the baryon number which is the required behaviour from a phenomenological point of view.

Our purpose in this section will be to calculate again the binding energies within the BPS Skyrme model although with the quartic potential $\mathcal{U}_\pi^2$. We have already obtained the classical energy but we still need the additional

contributions discussed above. To see how they change we can take advantage of the general expressions. Let us see:

i) **Semi-classical quantization**

The $\mathcal{H}_{\rm rot}$ coming from the collective quantization of the spin and isospin degrees of freedom is exactly the same expression as in Eq. (4.67) [or Eq. (4.7) for the $B = 1$ solution], where the only difference is the value of the integral $\int dr\, \xi_r^2 \sin^4\xi$ appearing in the moments of inertia tensors which depends on the potential through the BPS equation. Then, for this quartic potential after a numerical integration we get the value (we assume we just have matter and no antimatter, so $|B| = B$)

$$\begin{aligned}\int dr\, \xi_r^2 \sin^4\xi &= \frac{2\sqrt{2}\mu}{\lambda|B|}\int_0^Z dz \left(\frac{3|B|\lambda}{\sqrt{2}\mu}z\right)^{2/3}(1-\cos\xi)^2 \\ &= \left(\frac{18\mu}{\lambda|B|}\right)^{1/3}\int_0^\pi d\xi \sin^2\xi(1-\cos\xi)(\pi-\xi-\sin\xi)^{2/3} \\ &= 2.15707\left(\frac{\mu}{\lambda B}\right)^{1/3} \end{aligned} \tag{4.148}$$

where we have changed from the r variable to z and finally written the integration over the profile function ξ. Once we have calculated this integral, it is trivial to evaluate the corresponding $E_{\rm rot}$ contribution to the energy.

ii) **Coulomb energy**

In this case, the expansion into spherical harmonics shown before does not change. We still have the same two different contributions, ρ_{00} and ρ_{20}, [just ρ_{00} for the hedgehog skyrmion] which before inserting the corresponding solution read

$$\rho_{00}(r) = -\frac{B}{2\pi^{3/2}r^2}\sin^2\xi\,\xi_r + \frac{2\sqrt{\pi}}{3}\frac{\lambda^2 i_3}{r^2\mathcal{I}_3}\sin^4\xi\,\xi_r^2, \tag{4.149}$$

$$\rho_{20}(r) = \frac{4}{3}\sqrt{\frac{\pi}{5}}\frac{1}{3B^2+1}\frac{\lambda^2 i_3}{r^2\mathcal{I}_3}\sin^4\xi\xi_r^2, \tag{4.150}$$

where $\mathcal{I}_3$ was given by

$$\mathcal{I}_3 = \frac{4\pi}{3}\lambda^2 \int dr\, \xi_r^2 \sin^4\xi, \tag{4.151}$$

which is the integral we have just calculated. Note that inserting here the solution for the standard Skyrme potential we would directly arrive at equations (4.111) and (4.112).

Finally, to obtain the Coulomb energy we just have to use these ρ_{00} and ρ_{20} to calculate the Q_{lm} and U_{lm}, although now we will do it numerically and transforming all integrals into integrals over ξ.

iii) **Isospin-breaking**

Obviously, this does not change and the $E_{\rm I}$ contribution is exactly the same as given by (4.125)

Thus, in order to calculate the binding energies we will proceed as before. The first thing is to get the value of the parameters. We fit again our model expressions to the experimental proton mass, Eq. (4.127), the neutron-proton mass difference, Eq. (4.123), and the mass of the nucleus with magic numbers $^{138}_{56}$Ba, Eq. (4.128). Then, the new parameter values are

$$\lambda\mu = 47.0563 \text{ MeV}, \quad \left(\frac{\mu}{\lambda}\right)^{1/3} = 0.536386 \text{ fm}^{-1}, \quad a_{\rm I} = -1.65821 \text{ MeV}. \tag{4.152}$$

which allow us to calculate the binding energies by means of Eq. (4.133).

The comparison of the results within the BPS Skyrme model to data [111] is shown in Fig. 4.4 for the quartic potential $\mathcal{U}_\pi^2$. Moreover, looking again at Fig. 4.1 where the standard potential was considered, we see both cases do not differ much. In fact, they are quite similar, the only difference might be a less pronounced slope in the binding energy curve for the quartic potential. As well, the values we get from the fit here, Eq. (4.152), are not so different from the ones with the $\mathcal{U}_\pi$ potential, Eq. (4.132), either.

In addition, we have also studied more kinds of potentials which we can call step-like potentials. They are partially flat and their general definition is

$$\mathcal{U} = \begin{cases} U(\xi) & \xi \in [0, \xi_0], \\ 1 & \xi \in [\xi_0, \pi], \end{cases} \tag{4.153}$$

where U is a non trivial part representing the surface of nuclei (please, do not confuse with the Skyrme field U). For instance, we can introduce a family of potentials with a quadratic approach to the vacuum,

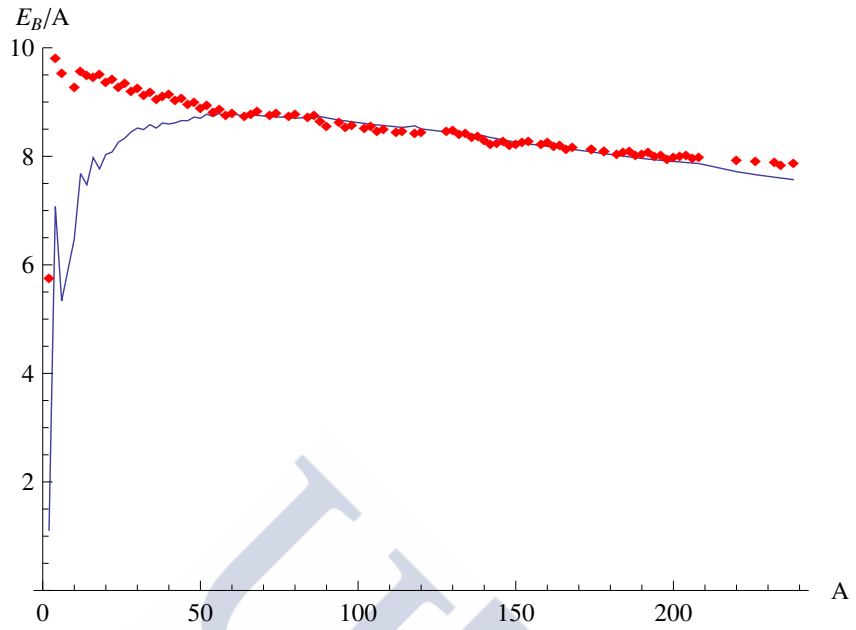

Figure 4.4: Binding energies per nucleon in MeV for the $\mathcal{U}_\pi^2$ potential. The experimental values are described by the (blue) solid line whereas our model results are represented by the (red) diamonds.

$$\mathcal{U} = \begin{cases} \sin^2(k\xi) & \xi \in [0, \frac{\pi}{2k}], \\ 1 & \xi \in [\frac{\pi}{2k}, \pi], \end{cases} \tag{4.154}$$

or as we have done before, a family where the approach is quartic,

$$\mathcal{U} = \begin{cases} \sin^4(k\xi) & \xi \in [0, \frac{\pi}{2k}], \\ 1 & \xi \in [\frac{\pi}{2k}, \pi], \end{cases} \tag{4.155}$$

In both cases, increasing k makes the potential more similar to the step-function potential, although the approach to the vacuum remains unmodified. Then, following the procedure described for the $\mathcal{U}_\pi^2$ potential we can easily arrive at the corresponding binding energies. We have plotted some examples in Fig. 4.5 and it is difficult to see how they differ from each other or even from the $\mathcal{U}_\pi$ and $\mathcal{U}_\pi^2$ potentials.

All in all, we can conclude that the choice of the exact shape of the potential has no dramatic effect, at least when dealing with quadratic or quartic potentials; and small differences which can appear are due to how they approach the vacuum. This fact is of great importance because it allows us to play with the potentials to choose, trying to improve in this way some drawbacks of the standard Skyrme potential, but without altering at the same time the excellent behaviour of binding energies for high baryon number.

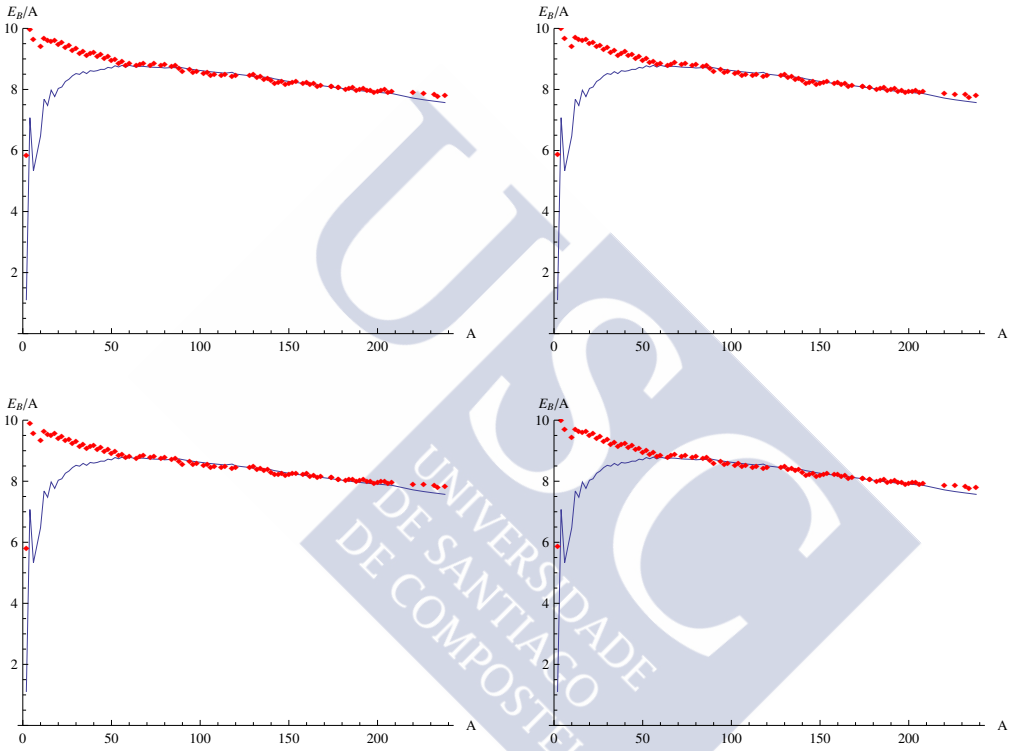

Figure 4.5: Binding energies per nucleon in MeV. Upper plots: Quadratic step-like potentials for $k = 1$ (left) and $k = 3/2$ (right). Lower plots: Quartic step-like potentials for $k = 1$ (left) and $k = 3/2$ (right).

Chapter 5

Skyrmions Coupled to Gravity: Neutron Stars

In this final chapter, we want to couple the Skyrme field to gravity within the BPS Skyrme model and study the neutron stars it gives rise to [113, 114]. For this purpose we will numerically solve the Einstein equations, and exact solutions with back-reaction will be found. Furthermore, we will develop a mean-field theory allowing us to proceed with the usual Tolman-Oppenheimer-Volkoff (TOV) mechanism, so both approaches can be compared.

Several attempts to implement neutron stars using the original Skyrme model have been made. For instance, a hedgehog ansatz for high B was considered in [115], but these hedgehogs remain unstable even when coupled to gravity (it also happens for non-gravitating solutions). Of course, some attempts have been made with approximate rational maps minimization [116, 117], although the most promising approach was with Skyrmion crystals [118, 119, 120], which are the true structures minimizing the original Skyrme action for high B. However, the drawback is that neutron stars' core is most likely in a superfluid phase (see [121] for an accessible review of these crystal Skyrmionic stars).

5.1 Einstein Equations

In order to introduce gravity in the BPS Skyrme model and be able to properly study the corresponding neutron stars, we need to minimally couple the model to gravity. Doing that for a general metric $g_{\mu\nu}$, the resulting action reads ($g = \det g_{\mu\nu}$)

$$\begin{aligned} S &= \int d^4x\sqrt{|g|}\left(\frac{1}{\kappa^2}R + \mathscr{L}_{06}\right) \\ &= \int d^4x\sqrt{|g|}\left(\frac{1}{\kappa^2}R - \lambda^2\pi^4|g|^{-1}g_{\mu\nu}\mathcal{B}^\mu\mathcal{B}^\nu - \mu^2\mathcal{U}\right), \end{aligned} \tag{5.1}$$

where R is the curvature or Ricci scalar given by (note that Einstein summation convention is used throughout the chapter)

$$R = g^{\mu\nu} R_{\mu\nu} = g^{\mu\nu} R^{\lambda}_{\mu\lambda\nu} = g^{\mu\nu} \left(\partial_\lambda \Gamma^{\lambda}_{\nu\mu} - \partial_\nu \Gamma^{\lambda}_{\lambda\mu} + \Gamma^{\lambda}_{\lambda\sigma} \Gamma^{\sigma}_{\nu\mu} - \Gamma^{\lambda}_{\nu\sigma} \Gamma^{\sigma}_{\lambda\mu} \right), \quad (5.2)$$

with $\Gamma^{\lambda}_{\mu\nu}$ the Christoffel connection,

$$\Gamma^{\lambda}_{\mu\nu} = \frac{1}{2} g^{\lambda\rho} \left(\partial_\mu g_{\nu\rho} + \partial_\nu g_{\rho\mu} - \partial_\rho g_{\mu\nu} \right). \quad (5.3)$$

$R^{\lambda}_{\mu\kappa\nu}$ and $R_{\mu\nu} = R^{\lambda}_{\mu\lambda\nu}$ are the Riemann-Christoffel curvature tensor and the Ricci tensor, respectively.

Minimizing this action (5.1) is equivalent to solving the Einstein equations

$$G_{\mu\nu} = \frac{\kappa^2}{2} T_{\mu\nu}, \quad (5.4)$$

where $\kappa^2 = 16\pi G = 6.654 \cdot 10^{-41}$ fm MeV^{-1} (G is the Newton gravitational constant), $T_{\mu\nu}$ is the energy-momentum tensor and $G_{\mu\nu}$ is the Einstein tensor given by

$$G_{\mu\nu} = R_{\mu\nu} - \frac{1}{2} R g_{\mu\nu}. \quad (5.5)$$

Then, we will solve these Einstein equations for the axially symmetric ansatz, Eq. (2.31), with a static spherically symmetric metric which is given, in Schwarzschild coordinates, by

$$ds^2 = \mathbf{A}(r) dt^2 - \mathbf{B}(r) dr^2 - r^2 (d\theta^2 + \sin^2\theta d\phi^2) = g_{\mu\nu} dx^\mu dx^\nu, \quad (5.6)$$

with the corresponding determinant being

$$|g| = \mathbf{A}(r) \mathbf{B}(r) r^4 \sin^2\theta. \quad (5.7)$$

Note that in this case the axially symmetric ansatz leading to a spherical symmetric metric, energy density and pressure (see Chapter 3 and below) is the right one since gravity disfavours all deviations from spherical symmetry.

The first step in solving the Einstein equations is to calculate both the Einstein tensor $G_{\mu\nu}$ given by Eq. (5.5) and the energy-momentum tensor $T_{\mu\nu}$. Therefore, focusing on the former, we need to calculate the non-zero Christoffel symbols, $\Gamma^{\lambda}_{\mu\nu}$, and from them obtain the expressions for the Ricci tensor and curvature scalar. To get these Christoffel connections we need not only the metric $g_{\mu\nu}$ given by Eq. (5.6), but also the inverse of this metric tensor, $g^{\mu\nu}$, defined by

$$g^{\mu\alpha} g_{\alpha\nu} = \delta^{\mu}_{\nu}, \quad (5.8)$$

as well as the corresponding derivatives:

$$\partial_t g_{\mu\nu} = \partial_\phi g_{\mu\nu} = 0 \tag{5.9}$$

because the metric does not depend on the variables t and ϕ while

$$\partial_r g_{\mu\nu} = \begin{pmatrix} \mathbf{A}'(r) & 0 & 0 & 0 \\ 0 & -\mathbf{B}'(r) & 0 & 0 \\ 0 & 0 & -2r & 0 \\ 0 & 0 & 0 & -2r\sin^2\theta \end{pmatrix}, \tag{5.10}$$

$$\partial_\theta g_{\mu\nu} = \begin{pmatrix} 0 & 0 & 0 & 0 \\ 0 & 0 & 0 & 0 \\ 0 & 0 & 0 & 0 \\ 0 & 0 & 0 & -2r^2\sin\theta\cos\theta \end{pmatrix}. \tag{5.11}$$

Then, using Eq. (5.3), we can easily get the non-zero Christoffel symbols for different values of λ (the $'$ refers to the derivative with respect to the argument, i.e., $' \equiv \partial_r$):

i) $\boldsymbol{\lambda = t} \;\Rightarrow\; \Gamma^t_{\mu\nu} = \frac{1}{2}g^{tt}(\partial_\mu g_{\nu t} + \partial_\nu g_{t\mu})$,
with the non-zero components

$$\Gamma^t_{rt} = \Gamma^t_{tr} = \frac{1}{2}\frac{\mathbf{A}'}{\mathbf{A}}. \tag{5.12}$$

ii) $\boldsymbol{\lambda = r} \;\Rightarrow\; \Gamma^r_{\mu\nu} = \frac{1}{2}g^{rr}(\partial_\mu g_{\nu r} + \partial_\nu g_{r\mu} - \partial_r g_{\mu\nu})$,
so we have

$$\Gamma^r_{tt} = \frac{1}{2}\frac{\mathbf{A}'}{\mathbf{B}}, \qquad \Gamma^r_{rr} = \frac{1}{2}\frac{\mathbf{B}'}{\mathbf{B}}, \qquad \Gamma^r_{\theta\theta} = -\frac{r}{\mathbf{B}}, \qquad \Gamma^r_{\phi\phi} = -\frac{r}{\mathbf{B}}\sin^2\theta. \tag{5.13}$$

iii) $\boldsymbol{\lambda = \theta} \;\Rightarrow\; \Gamma^\theta_{\mu\nu} = \frac{1}{2}g^{\theta\theta}(\partial_\mu g_{\nu\theta} + \partial_\nu g_{\theta\mu} - \partial_\theta g_{\mu\nu})$,
where the non-vanishing quantities are

$$\Gamma^\theta_{r\theta} = \Gamma^\theta_{\theta r} = \frac{1}{r}, \qquad \Gamma^\theta_{\phi\phi} = -\sin\theta\cos\theta. \tag{5.14}$$

iv) $\boldsymbol{\lambda = \phi} \;\Rightarrow\; \Gamma^\phi_{\mu\nu} = \frac{1}{2}g^{\phi\phi}(\partial_\mu g_{\nu\phi} + \partial_\nu g_{\phi\mu})$,
so we arrive at

$$\Gamma^\phi_{r\phi} = \Gamma^\phi_{\phi r} = \frac{1}{r}, \qquad \Gamma^\phi_{\theta\phi} = \Gamma^\phi_{\phi\theta} = \frac{\cos\theta}{\sin\theta}. \tag{5.15}$$

These expressions allow us to calculate the diagonal components of the Ricci tensor we need, namely,

$$\begin{aligned} R_{tt} &= \partial_\lambda \Gamma^\lambda_{tt} + \Gamma^\lambda_{\lambda\sigma}\Gamma^\sigma_{tt} - \Gamma^\lambda_{t\sigma}\Gamma^\sigma_{\lambda t} \\ &= \partial_r \Gamma^r_{tt} + (\Gamma^\phi_{tr} + \Gamma^r_{rr} + \Gamma^\theta_{\theta r} + \Gamma^\phi_{\phi r})\Gamma^r_{tt} - \Gamma^t_{tr}\Gamma^r_{tt} - \Gamma^r_{tt}\Gamma^t_{rt} \\ &= \frac{1}{2}\left(\frac{\mathbf{A}'}{\mathbf{B}}\right)' - \frac{1}{4}\frac{(\mathbf{A}')^2}{\mathbf{AB}} + \frac{1}{4}\frac{\mathbf{A}'\mathbf{B}'}{\mathbf{B}^2} + \frac{1}{r}\frac{\mathbf{A}'}{\mathbf{B}} \end{aligned} \tag{5.16}$$

$$\begin{aligned} R_{rr} &= \partial_\lambda \Gamma^\lambda_{rr} - \partial_r \Gamma^\lambda_{\lambda r} + \Gamma^\lambda_{\lambda\sigma}\Gamma^\sigma_{rr} - \Gamma^\lambda_{r\sigma}\Gamma^\sigma_{\lambda r} \\ &= -\partial_r \Gamma^t_{tr} - \partial_r \Gamma^\theta_{\theta r} - \partial_r \Gamma^\phi_{\phi r} + (\Gamma^t_{tr} + \Gamma^\theta_{\theta t} + \Gamma^\phi_{\phi r})\Gamma^r_{rr} \\ &\quad -\Gamma^t_{rt}\Gamma^t_{tr} - \Gamma^\theta_{r\theta}\Gamma^\theta_{\theta r} - \Gamma^\phi_{r\phi}\Gamma^\phi_{\phi r} \\ &= -\frac{1}{2}\left(\frac{\mathbf{A}'}{\mathbf{A}}\right)' - \frac{1}{4}\left(\frac{\mathbf{A}'}{\mathbf{A}}\right)^2 + \frac{1}{4}\frac{\mathbf{A}'}{\mathbf{A}}\frac{\mathbf{B}'}{\mathbf{B}} + \frac{1}{r}\frac{\mathbf{B}'}{\mathbf{B}} \end{aligned} \tag{5.17}$$

$$\begin{aligned} R_{\theta\theta} &= \partial_\lambda \Gamma^\lambda_{\theta\theta} - \partial_\theta \Gamma^\lambda_{\lambda\theta} + \Gamma^\lambda_{\lambda\sigma}\Gamma^\sigma_{\theta\theta} - \Gamma^\lambda_{\theta\sigma}\Gamma^\sigma_{\lambda\theta} \\ &= \partial_r \Gamma^r_{\theta\theta} - \partial_\theta \Gamma^\phi_{\phi\theta} + (\Gamma^t_{tr} + \Gamma^r_{rr} + \Gamma\theta_{\theta r} + \Gamma^\phi_{\phi r})\Gamma^r_{\theta\theta} \\ &\quad -\Gamma^r_{\theta\theta}\Gamma^\theta_{r\theta} - \Gamma^\theta_{\theta r}\Gamma^r_{\theta\theta} - \Gamma^\phi_{\theta\phi}\Gamma^\phi_{\phi\theta} \\ &= 1 - \left(\frac{r}{\mathbf{B}}\right)' \frac{1}{2}\frac{\mathbf{A}'}{\mathbf{A}}\frac{r}{\mathbf{B}} - \frac{1}{2}\frac{\mathbf{B}'}{\mathbf{B}^2}\, r \end{aligned} \tag{5.18}$$

$$\begin{aligned} R_{\phi\phi} &= \partial_\lambda \Gamma^\lambda_{\phi\phi} - \partial_\phi \Gamma^\lambda_{\lambda\phi} + \Gamma^\lambda_{\lambda\sigma}\Gamma^\sigma_{\phi\phi} - \Gamma^\lambda_{\phi\sigma}\Gamma^\sigma_{\lambda\phi} \\ &= \partial_r \Gamma^r_{\phi\phi} + \partial_\theta \Gamma^\theta_{\phi\phi} + (\Gamma^t_{tr} + \Gamma^r_{rr} + \Gamma^\theta_{\theta r} + \Gamma^\phi_{\phi r})\Gamma^r_{\phi\phi} \\ &\quad +\Gamma^\phi_{\phi\theta}\Gamma^\theta_{\phi\phi} - \Gamma^r_{\phi\phi}\Gamma^\phi_{r\phi} - \Gamma^\theta_{\phi\phi}\Gamma^\phi_{\theta\phi} - \Gamma^\phi_{\phi r}\Gamma^r_{\phi\phi} - \Gamma^\phi_{\phi\theta}\Gamma^\theta_{\phi\phi} \\ &= \sin^2\theta - \left(\frac{r}{\mathbf{B}}\right)' \sin^2\theta - \frac{1}{2}\frac{\mathbf{A}'}{\mathbf{A}}\frac{r}{\mathbf{B}}\sin^\theta - \frac{1}{2}\frac{\mathbf{B}'}{\mathbf{B}^2}\, r\sin^2\theta. \end{aligned} \tag{5.19}$$

Thus, the Ricci scalar given by Eq. (5.2) reads

$$\begin{aligned} R &= g^{\mu\nu}R_{\mu\nu} = g^{tt}R_{tt} + g^{rr}R_{rr} + g^{\theta\theta}R_{\theta\theta} + g^{\phi\phi}R_{\phi\phi} \\ &= \frac{\mathbf{A}''}{\mathbf{AB}} - \frac{1}{2}\frac{\mathbf{A}'\mathbf{B}'}{\mathbf{AB}^2} - \frac{1}{2}\frac{(\mathbf{A}')^2}{\mathbf{A}^2\mathbf{B}} + \frac{2}{r}\frac{\mathbf{A}'}{\mathbf{AB}} - \frac{2}{r^2}\left(1 - \left(\frac{r}{\mathbf{B}}\right)'\right), \end{aligned} \tag{5.20}$$

and finally, the Einstein tensor is trivially calculated with (5.5), being the diagonal components

$$G_{tt} = R_{tt} - \frac{1}{2}Rg_{tt} = \frac{\mathbf{A}}{r^2}\left(1 - \frac{1}{\mathbf{B}}\right) + \frac{\mathbf{A}}{r}\frac{\mathbf{B}'}{\mathbf{B}^2}, \tag{5.21}$$

$$G_{rr} = R_{rr} - \frac{1}{2}Rg_{rr} = \frac{1}{r}\frac{\mathbf{A}'}{\mathbf{A}} - \frac{\mathbf{B}}{r^2}\left(1 - \frac{1}{\mathbf{B}}\right), \tag{5.22}$$

$$\begin{aligned} G_{\theta\theta} = \; & R_{\theta\theta} - \frac{1}{2}Rg_{\theta\theta} = \frac{1}{2}r\frac{\mathbf{A}'}{\mathbf{AB}} - \frac{1}{2}r\frac{\mathbf{B}'}{\mathbf{B}^2} \\ & + \frac{1}{2}r^2\frac{\mathbf{A}''}{\mathbf{AB}} - \frac{1}{4}r^2\frac{\mathbf{A}'\mathbf{B}'}{\mathbf{AB}^2} - \frac{1}{4}r^2\frac{(\mathbf{A}')^2}{\mathbf{A}^2\mathbf{B}}, \end{aligned} \tag{5.23}$$

$$G_{\phi\phi} = R_{\phi\phi} - \frac{1}{2}Rg_{\phi\phi} = \sin^2\theta G_{\theta\theta}. \tag{5.24}$$

Once we have obtained the Einstein tensor, we only need the energy-momentum tensor, which was already studied in Chapter 3 with the general expression given by Eq. (3.28). It can be easily seen that it corresponds to the tensor of a perfect fluid

$$T^{\mu\nu} = (p + \rho)u^\mu u^\nu - pg^{\mu\nu} \tag{5.25}$$

with u^μ the four-velocity, ρ the energy density and p the pressure (we have slightly changed the notation of Chapter 3 to embrace the usual notation used in the study of neutron stars), namely,

$$u^\mu = \mathcal{B}^\mu / \sqrt{g_{\alpha\beta}\mathcal{B}^\alpha\mathcal{B}^\beta}, \tag{5.26}$$

$$\rho = \lambda^2\pi^4|g|^{-1}g_{\mu\nu}\mathcal{B}^\mu\mathcal{B}^\nu + \mu^2\mathcal{U}, \tag{5.27}$$

$$p = \lambda^2\pi^4|g|^{-1}g_{\mu\nu}\mathcal{B}^\mu\mathcal{B}^\nu - \mu^2\mathcal{U}. \tag{5.28}$$

This is an important property since a liquid phase seems adequate for the description of the neutron star core. Moreover, in the static case and if a diagonal metric is considered (which will be the case here), the four-velocity reads $u^\mu = (\sqrt{g^{00}}, 0, 0, 0)$, with the energy-momentum tensor components

$$T^{00} = \rho g^{00}, \qquad T^{ij} = -pg^{ij}, \tag{5.29}$$

so in a flat space we exactly recover the T^{00} and T^{ij} given by equations (3.29) and (3.30) when studying the thermodynamics of the BPS Skyrme model with

the equivalence in notation $\rho \equiv \mathcal{E}$ and $p \equiv \mathcal{P}$. It is also worth noting that both ρ and p are functions of the space-time coordinates, so a universal equation of state valid for all solutions is not achieved in general, although, as we will see, it is possible by means of an approximation.

Finally, in order to arrive at the Einstein equations, we need to write the components of the energy-momentum tensor by means of the axially symmetric ansatz (2.31) we are interested in. Then, defining a new target space variable h,

$$h = \frac{1}{2}(1 - \cos\xi) = \sin^2\frac{\xi}{2}, \tag{5.30}$$

with $h \in [0, 1]$, the energy density ρ and the pressure p read

$$\rho = \frac{4B^2\lambda^2}{\mathbf{B}r^4}h(1-h)h_r^2 + \mu^2\mathcal{U}(h), \tag{5.31}$$

$$p = \frac{4B^2\lambda^2}{\mathbf{B}r^4}h(1-h)h_r^2 - \mu^2\mathcal{U}(h) = \rho - 2\mu^2\mathcal{U}(h), \tag{5.32}$$

where $h_r \equiv \partial_r h$. Please note here the difference between the metric function $\mathbf{B} = \mathbf{B}(r)$ and the baryon number B.

All together, with the Einstein tensor given by equations (5.21) to (5.23) and the energy momentum tensor (5.29), we get from (5.4) the three independent Einstein equations

$$\frac{1}{r^2}\left(1 - \frac{1}{\mathbf{B}}\right) + \frac{1}{r}\frac{\mathbf{B}'}{\mathbf{B}^2} = \frac{\kappa^2}{2}\rho, \tag{5.33}$$

$$\frac{1}{r}\frac{\mathbf{A}'}{\mathbf{A}} - \frac{\mathbf{B}}{r^2}\left(1 - \frac{1}{\mathbf{B}}\right) = \frac{\kappa^2}{2}\mathbf{B}p, \tag{5.34}$$

$$\frac{\mathbf{A}''}{\mathbf{A}\mathbf{B}} - \frac{1}{2}\frac{(\mathbf{A}')^2}{\mathbf{A}^2\mathbf{B}} - \frac{1}{2}\frac{\mathbf{A}'\mathbf{B}}{\mathbf{A}\mathbf{B}^2} + \frac{1}{r}\frac{\mathbf{A}'}{\mathbf{A}\mathbf{B}} - \frac{1}{r}\frac{\mathbf{B}'}{\mathbf{B}^2} = \kappa^2 p \tag{5.35}$$

We see there is no dependence on the $\mathbf{A}$ field in the first equation. As well, we can write an expression for $\frac{\mathbf{A}'}{\mathbf{A}}$ from the second equation [see Eq. (5.38) below] and use it in the third one, so the three equations we are going to work with are

$$\frac{1}{r}\frac{\mathbf{B}'}{\mathbf{B}} = -\frac{1}{r^2}(\mathbf{B} - 1) + \frac{\kappa^2}{2}\mathbf{B}\rho, \tag{5.36}$$

$$r(\mathbf{B}p)' = \frac{1}{2}(1 - \mathbf{B})\mathbf{B}(\rho + 3p) + \frac{\kappa^2}{4}r^2\mathbf{B}^2(\rho - p)p. \tag{5.37}$$

$$\frac{\mathbf{A}'}{\mathbf{A}} = \frac{1}{r}(\mathbf{B}-1) + \frac{\kappa^2}{2} r \mathbf{B} p, \tag{5.38}$$

which is a system of ODEs (ordinary differential equations) made by two equations for h [encoded in the definitions of ρ and p, Eqs. (5.31) and (5.32) respectively] and $\mathbf{B}$ plus another equation determining $\mathbf{A}$ as a function of the other fields h and $\mathbf{B}$.

5.2 Self-gravitating Skyrmions: Neutron Stars

In this section, we will solve numerically the system given by the Einstein equations (5.36) and (5.37) [note that $\mathbf{A}$ follows trivially from (5.38) once h and $\mathbf{B}$ are known] using a shooting from the centre with a Runge Kutta method. Then, the first step will be to fix the parameters μ and λ for the potentials used. For these neutron stars we will study not only the standard Skyrme potential given by (2.38), $\mathcal{U}_\pi = 2h$, but also the quartic one defined by Eq. (4.140), $\mathcal{U}_\pi^2 = 4h^2$ [we have already expressed them in the new variable h, Eq. (5.30)].

We think that infinite nuclear matter is a more suitable choice for neutron stars instead of using the parameters we have got from nuclei. Thus, we will consider the binding energy per nucleon of infinite nuclear matter, $E_\mathrm{b} = 16.3$ MeV, and the nuclear saturation density (baryon density of nuclear matter at equilibrium at zero pressure), $n_0 = 0.153$ fm^{-3} [122], for fitting the model parameters. Then, for the nucleon mass $E_\mathrm{n} = 939.6$ MeV, the soliton energy per nucleon is $E_{B=1} = E_\mathrm{n} - E_\mathrm{b} = 923.3$ MeV, whilst the volume reads $V_{B=1} = (1/0.153)$ fm^3. Comparing these values with our expressions for the classical energy and volume (see Chapter 4) we can easily fit the parameters getting

$$\begin{aligned} \mathcal{U}_\pi: \qquad & E = \frac{64\sqrt{2}\pi}{15} B\lambda\mu, \quad V = \frac{8}{3}\sqrt{2}\pi B \frac{\lambda}{\mu} \\ & \Rightarrow \lambda^2 = 26.88 \text{ MeV fm}^3, \quad \mu^2 = 88.26 \text{ MeV fm}^{-3}, \end{aligned} \tag{5.39}$$

$$\begin{aligned} \mathcal{U}_\pi^2: \qquad & E = 2\pi^2 B\lambda\mu, \quad V = 2\pi^2 B \frac{\lambda}{\mu} \\ & \Rightarrow \lambda^2 = 15.493 \text{ MeV fm}^3, \quad \mu^2 = 141.22 \text{ MeV fm}^{-3}, \end{aligned} \tag{5.40}$$

where we used that $V = (4\pi/3)R^3$ with R the corresponding compacton radius.

Then, the procedure to perform the shooting requires to impose the following boundary conditions at the centre: $h(r=0)=1$ (the anti-vacuum value) and $\mathbf{B}(r=0)=1$ (the value corresponding to a flat space metric since no matter is enclosed at $r=0$). Therefore, one free parameter is left, the h_2 coming from an expansion around the centre, i.e., $h \sim 1-\frac{1}{2}h_2 r^2+\ldots$, which is also equivalent to the value of the energy density at $r=0$ because $\rho_0 \equiv \rho(r=0) = B^2\lambda^2 h_2^3 + \mu^2\mathcal{U}(h=1)$. Once we have set this value we integrate from $r=0$ up to a point $r=R$, the compacton radius, where the field h takes the vacuum value, $h(R)=0$, that means $p=0$. However, this is not enough because for a non-singular metric $\mathbf{B}$ to exist, the derivative of the pressure at the surface must vanish, $p'(R)=0$, which gives as a result a condition on the derivative $h_r(R)$:

$$\frac{4B^2\lambda^2}{\mathbf{B}(R)R^4}h_r^2(R) - \mu^2\mathcal{U}_h(0) = 0. \tag{5.41}$$

Thus, it is necessary to sweep different values of ρ_0 until this condition is fulfilled, otherwise $\mathbf{B}$ cannot be joined smoothly to the Schwarzschild solution for $r \geq R$ (empty space), which is the only physically possible situation.

Solving numerically the system we find three different behaviours depending on the value of the baryon number B. For small B, we arrive at a unique solution, i.e., there is only one value of ρ_0 fulfilling (5.41) and giving rise to a neutron star. The next possibility corresponds to larger values of the baryon number falling in an interval $B \in [B^*, B_{\text{max}}]$. In this case, the condition holds for two different values of ρ_0 leading to a pair of solutions. This situation is similar to the TOV mechanism (see [123], Chapter 11.4, p. 321), and in an analogous fashion we will take the solution with the lower value of ρ_0. For $B > B_{\text{max}}$ Eq. (5.41) is not satisfied, so no physical solutions exist. This means that Skyrmions are unstable and collapse to a black hole.

Finally, we have to join the solution found in this way with the vacuum solution for $r \geq R$, which corresponds to

$$h(r)=0, \qquad B = \left(1-\frac{2GM}{r}\right)^{-1}, \qquad r \geq R. \tag{5.42}$$

From the expression for B we can easily get M, the value of the physical mass with the gravitational loss taken into account.

The main result we get is the maximum baryon number B_{max}, with the corresponding maximal mass, M_{max}, and radius, R_{max}. Both M and B will be given in solar units so for the latter we define a new variable $n = \frac{B}{B_\odot}$, with $B_\odot$ the solar baryon mass defined as

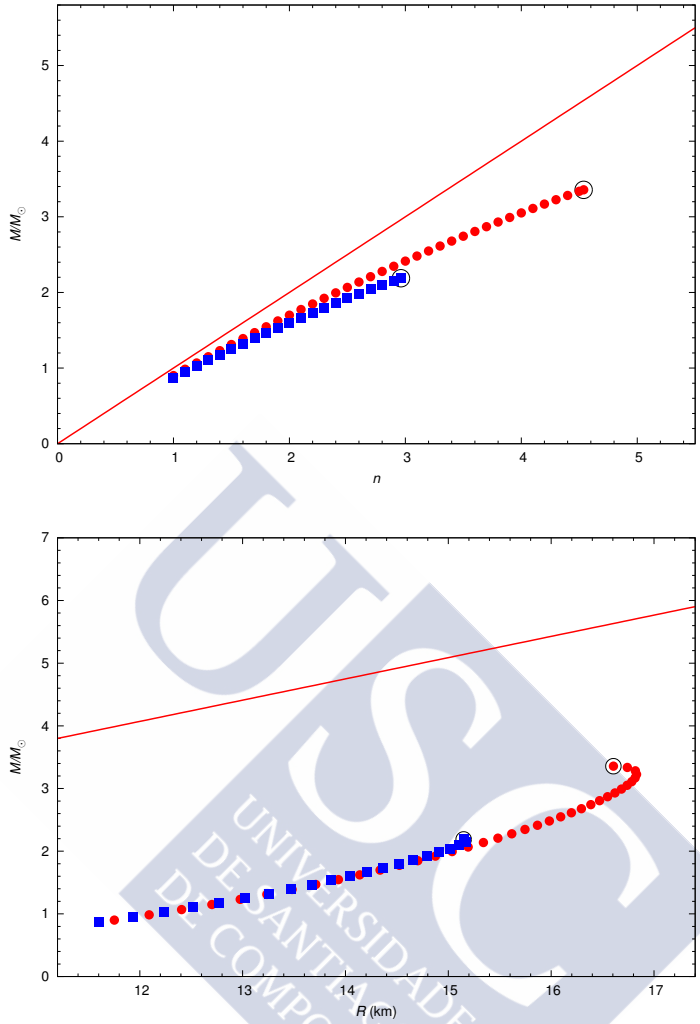

Figure 5.1: Neutron star masses, red dots and blue squares correspond to $\mathcal{U}_\pi$ and $\mathcal{U}_\pi^2$ potentials, respectively; maximum values are enclosed by circles. Upper plot: Neutron star mass as a function of baryon number, both in solar units; the straight line represents no mass loss. Lower plot: Neutron star mass as a function of the star radius; the straight line is the Schwarzschild mass.

$$B_\odot = \frac{M_\odot}{m_\mathrm{p}} = \frac{1.988 \cdot 10^{30}\ \mathrm{kg}}{1.673 \cdot 10^{-27}\ \mathrm{kg}} = 1.188 \cdot 10^{57}, \tag{5.43}$$

which, strictly speaking, is not the baryon number of the sun, but the number of baryons in a neutron star with the same non-gravitational mass as the sun. Then, the results we found for the two considered potentials are

$$\mathcal{U}_\pi: \quad n_\mathrm{max} = 4.538, \qquad M_\mathrm{max} = 3.3573 M_\odot, \qquad R_\mathrm{max} = 16.606\ \mathrm{km}, \tag{5.44}$$

$$\mathcal{U}_\pi^2: \quad n_\mathrm{max} = 2.963, \qquad M_\mathrm{max} = 2.1882 M_\odot, \qquad R_\mathrm{max} = 15.149\ \mathrm{km}, \tag{5.45}$$

We see we have excellent results for the masses since neutron stars of $M \sim 2M_\odot$ are well known and experimental evidences of masses up to about $2.5M_\odot$ also exist (for instance, recent measurements can be found at [124, 125, 126, 127, 128, 129, 130]). This seems to indicate that the BPS Skyrme model provides a proper description of bulk properties of nuclear matter even when gravitation is included.

On the other hand, the experimental measurements of the radius are not so accurate. Moreover, our radius corresponds to the geometrical definition but other options are possible. For instance, the proper distance from the centre of the star to the surface, $\bar{R} = \int_0^R dr\sqrt{\mathbf{B}(r)}$, or the radiation radius, $R^* = R\sqrt{\mathbf{B}(R)}$. Both are bigger than our radius R since $\mathbf{B}(r) > 1$; even so, the radii we found are in the expected range $R \sim 10 - 20$ km which follows from observational data.

At this point, it is also interesting to come back to the parameter values from the fit and study how a small change can affect our results. For this purpose we can define the product $\boldsymbol{m} \equiv \mu\lambda$ which has units of mass as well as $\boldsymbol{l} \equiv (\lambda/\mu)^{1/3}$ with length units. The value of $\boldsymbol{m}$ follows directly from the fit to the soliton energy per nucleon, $E_{B=1}$, so it is quite precise. However, this does not happen for $\boldsymbol{l}$ which comes from fitting to the volume and here we again have at our disposition other choices for the radius besides the geometrical definition, e.g., charge radii. Furthermore, the inclusion of additional terms to the Lagrangian as the Dirichlet contribution from the near-BPS model, $\mathscr{L}_2$, will tend to increase the radius due to the resulting pion cloud (nevertheless, the obtained $\boldsymbol{l}$ value is quite reasonable and the difference with the true one could reach, at most, $20 - 30\%$ in either direction). Therefore, it is sufficient to analyse the sensitivity of $M_{\max}$ and $R_{\max}$ to the scale transformation $\boldsymbol{l} \to \boldsymbol{l'} = \alpha\boldsymbol{l}$, where the numerical output is that both values change by a factor of $\alpha^{3/2}$.

All the numerical results are summarized in Figures 5.1 to 5.4. Concretely, in the upper Fig. 5.1, we have the neutron star mass for both potentials as a function of the non-gravitational Skyrmionic mass (equivalently, baryon number in solar units), with the limit of no gravitational mass loss represented by a straight line. We can easily infer that the maximal mass loss corresponding to $M_{\max}$ is about 25%. We can also see in the lower Fig. 5.1 the mass as a function of the neutron star radius with the Schwarzschild mass included. Here, the maximal case $R_{\max}$ is still about two times the Schwarzschild radius. It is also important to comment that, except very near to the maximum mass value, the neutron star masses increase with the radius, i.e., $\frac{dM}{dR} > 0$, which is a consequence of the stiffness of the EoS (see Fig. 5.2 and discussion below). This is in contrast with the usual results of TOV calculations with universal algebraic EoS, $p = p(\rho)$, coming from the thermodynamical limit

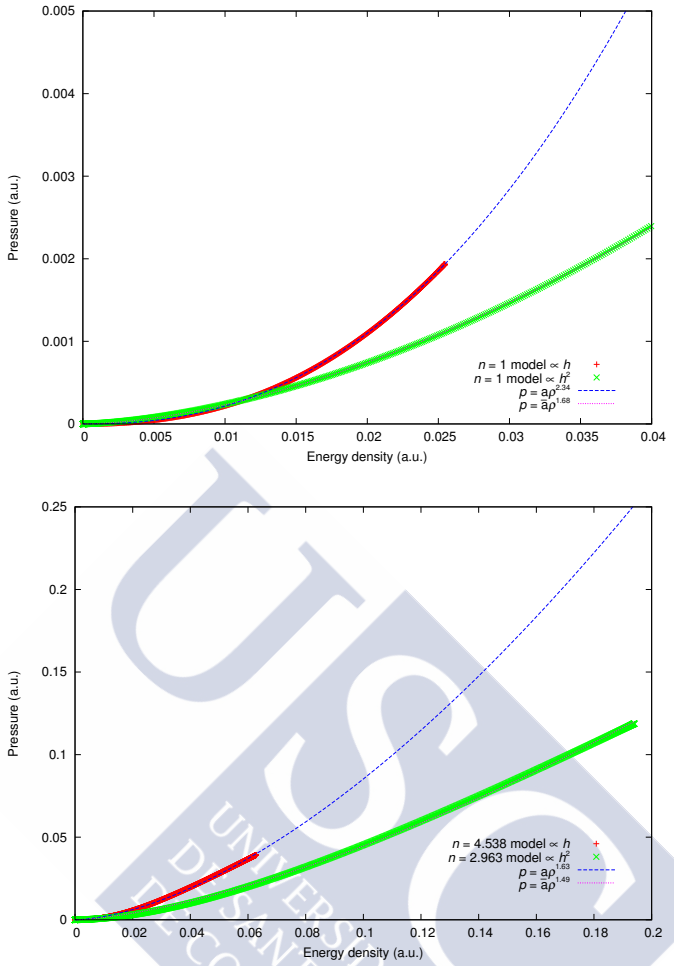

Figure 5.2: Equation of state for $n = 1$ (up) and $n_{\max}$ (down). Red plus, $+$, potential $\mathcal{U}_\pi$, and green cross, $\times$, potential $\mathcal{U}_\pi^2$. Dotted lines correspond to fit functions.

of an effective field theory like Quantum Hadron Dynamics (QHD) [91, 92], where the neutron star radius is almost constant for a range of neutron star masses and then it can even shrink when increasing the mass (see for instance [124, 125, 126, 127]). This behaviour is due to a squeezing effect produced by self-gravitating contributions which cannot be balanced by a soft EoS. However, it can be balanced by stiffer EoS as ours or other examples as the corresponding to a Skyrme crystal [120], which also leads to $\frac{dM}{dR} > 0$ (in fact, the $M(R)$ curve found there is quite similar to our lower Fig. 5.1 for the $\mathcal{U}_\pi$ potential). It is worth emphasizing that, up to now, $\frac{dM}{dR} > 0$ is not ruled out by experimental data which currently are not too accurate, either. In fact, if finally this is the right behaviour, either a large variety of EoS has to be

excluded because they are not stiff enough; or the mean-field approximation is no longer appropriate and gravitational back-reaction has to be taken into account for the derivation of the EoS.

On the other hand, EoSs for two different values of $n = B/B_{\odot}$ ($n = 1$ and $n_{\max}$) are presented in Fig. 5.2. As has been commented before, there are no universal EoSs in the BPS Skyrme model but they depend on geometry. Notwithstanding, this is not the first example of such EoSs, which have already appeared related to anisotropic stars as well as neutron stars [131, 132, 133, 134]. However, since both p and ρ depend on r because of the spherical symmetry, an on-shell EoS is possible once a concrete solution is given. Then, for the axially symmetric ansatz the EoS is of the form

$$p = a(B)\rho^{b(B)}, \tag{5.46}$$

where both a and b depend on the baryon number instead of being universal constants.

In Fig. 5.3 we show the metric function $\mathbf{B}(r)$ for $n_{\max}$ and values nearby for both potentials $\mathcal{U}_\pi$ and $\mathcal{U}_\pi^2$. In the case of the quadratic potential the maximum value of $\mathbf{B}$ is reached near the surface, whereas for $\mathcal{U}_\pi^2$ it happens to be shifted to the centre, which seems to be due to an energy density more concentrated around the centre for the quartic potential (see Fig. 5.4). We easily see that in both cases the value of $\mathbf{B}$ for $n = n_{\max}$ is about $\mathbf{B}_{\max} \sim 2.7$, which can be compared with the result obtained for the Skyrme crystal [120]. In their work, they define a quantity S, which is just our $\mathbf{B}^{-1}$, and find after studying different solutions that the minimal value of this S is always $S_{\min} > 0.4$. This minimal value translated into our B field is equivalent to $\mathbf{B}_{\max} < 2.5$. Thus, although slightly bigger (which means that the self-gravitating effects are slightly stronger), the $\mathbf{B}_{\max}$ value we find for the $n_{\max}$ baryon number is still quite similar to the result of [120].

Finally, in Fig. 5.4 we can see the energy density ρ inside the star as a function of the radial coordinate r. Similarly to the metric function $\mathbf{B}$, we have plotted the energy density for both potentials considering values of n close and equal to $n_{\max}$. It is clear that both potentials present an energy density which is mainly concentrated around the centre. This is specially noticeable for the $\mathcal{U}_\pi^2$ case but it should not be strange because this potential is peaked around the centre. Then, by means of the BPS equation (remember it relates the square of the topological density to the potential) it is basically equivalent to a sharply concentrated baryon density around the centre even without gravity, which is also translated into the energy density behavior. Therefore, it is interesting to compare the central values of the energy density in the neutron star with the values without gravity, i.e. $\rho_{\mathrm{PBS}}(r = 0) = 2\mu^2\mathcal{U}(h = 1)$.

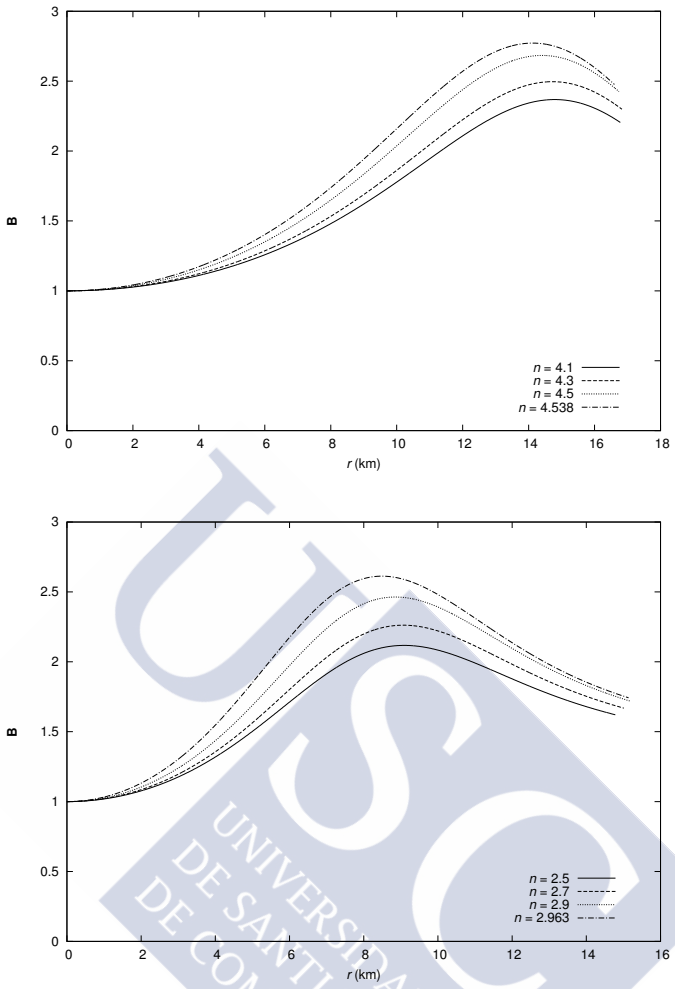

Figure 5.3: Metric function $\mathbf{B}(r)$ for solutions close to $n_{\max}$ for both potentials $\mathcal{U}_\pi$ (up) and $\mathcal{U}_\pi^2$ (down).

Thus, using the values (5.39), for the potential $\mathcal{U}_\pi$ we find $\rho_{\rm BPS}(r=0) = 353$ MeV fm^{-3}, so the central energy density for $n_{\max}$ is about 2.7 times the non gravitational one (see upper Fig. 5.4). On the other hand, from (5.40) we see that for $\mathcal{U}_\pi^2$ the non-gravitational value is $\rho_{\rm BPS}(r=0) = 1130$ MeV fm^{-3}, and in this case the corresponding energy density at the centre for the neutron star with $n_{\max}$ is about 2.6 times $\rho_{\rm BPS}(r=0)$ (see lower Fig. 5.4). In both cases, the results indicate a high stiffness of the effective EoS for self-gravitating Skyrmions and present a good comparison with [120] where no more than a factor of three appears.

All in all, the BPS model seems to provide a good description of bulk properties also for neutron stars. For instance, it implements the liquid phase

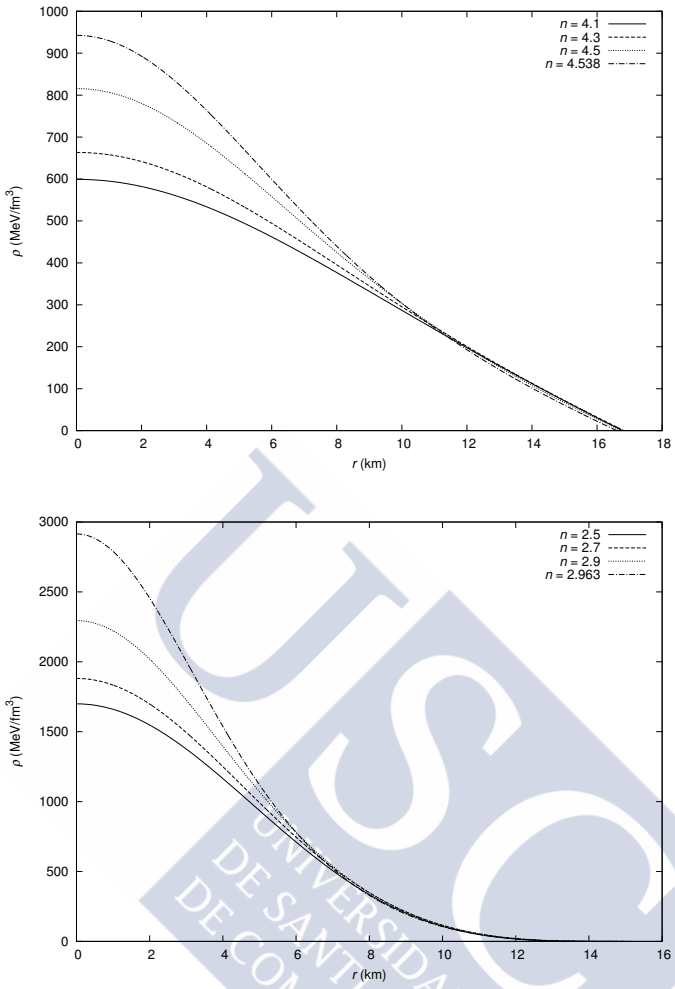

Figure 5.4: Energy density $\rho(r)$ for solutions close to $n_{\max}$ for both potentials $\mathcal{U}_\pi$ (up) and $\mathcal{U}_\pi^2$ (down).

and a $M_{\max}$ which is compatible with the observed $M \sim 2.5 M_\odot$ constraint. However, it must be emphasized that, strictly speaking, this is not yet a prediction since we know that a complete description of nuclear matter would required the addition of small contribution from more derivative terms in the Lagrangian, i.e., the near-BPS Skyrme model. Indeed, these contributions become important near the surface where the $\mathscr{L}_6$ term approaches the vacuum faster. In addition, they prefer a crystal structure so this near-BPS model would implement a neutron star crust at the surface with liquid phase describing the bulk, which is exactly what current models predict [135, 136, 137].

Finally, it is worth commenting that it is due to the symmetry of this BPS Skyrme model that a full theoretic description of neutron stars with

gravitational back-reaction is possible. Nevertheless, this is not the usual approach to the study of neutron stars where a mean-field approximation is used to solve the TOV equations [138, 139]. Fortunately, as we have already seen in Chapter 3, our BPS theory allows for an easy derivation of a mean-field equation of state (MF-EoS), so this limit can also be studied and compared.

5.3 The Mean-field Limit

In this section, we will follow the usual approach to neutron stars and study the mean-field equation of state (MF-EoS) and use it to solve the TOV equations. Here, we will take advantage of the possibility the BPS model offers to easily write down an algebraic (not depending on coordinates) EoS. Recalling what we have seen in Chapter 3, we make use of the thermodynamical properties of the BPS Skyrme model to introduce the external pressure. Then, we can implement the mean-field limit by an averaging procedure, so the average (mean-field) equation of state, $\bar{\rho} = \bar{\rho}(P)$ is simply defined by

$$\bar{\rho}(P) = \frac{E(P)}{V(P),} \tag{5.47}$$

where

$$E(P) = 2\pi\lambda\mu|B|\tilde{E}, \qquad V = 2\pi|B|\frac{\lambda}{\mu}\tilde{V}, \tag{5.48}$$

with $\tilde{E}$ and $\tilde{V}$ being defined by the same expressions as in equations (3.57) and (3.51), i.e.,

$$\tilde{E} = \int_0^\pi d\xi \sin^2\xi \frac{2\mathcal{U} + P/\mu^2}{\sqrt{\mathcal{U} + P/\mu^2}}, \tag{5.49}$$

$$\tilde{V} = \int_0^\pi d\xi \sin^2\xi \frac{1}{\sqrt{\mathcal{U} + P/\mu^2}}. \tag{5.50}$$

Therefore, the MF-EoS reads

$$\bar{\rho}(P) = \mu^2 \frac{\left\langle \frac{2\mathcal{U}}{\sqrt{\mathcal{U}+P/\mu^2}} \right\rangle}{\left\langle \frac{1}{\sqrt{\mathcal{U}+P/\mu^2}} \right\rangle} + P, \tag{5.51}$$

which is just a function of target space averages because

$$\langle F(\mathcal{U})\rangle \equiv \frac{1}{\mathrm{Vol}_{\mathbb{S}^3}} \int \mathrm{vol}_{\mathbb{S}^3} F(\mathcal{U}) = \frac{2}{\pi}\int_0^\pi d\xi \sin^2\xi F(\mathcal{U}), \tag{5.52}$$

where we have used the identification between the SU(2) target space manifold and the unit three-sphere $\mathbb{S}^3$. Further, $\mathrm{Vol}_{\mathbb{S}^3} = 2\pi^2$ is the volume of the target space whilst $\mathrm{vol}_{\mathbb{S}^3}$ corresponds to the volume form.

In a similar fashion, we can define an average baryon density, $\bar{\rho}_B$, as the baryon number divided by the volume:

$$\bar{\rho}_B = \frac{B}{V} = \frac{\mu}{\pi^2 \lambda \left\langle \frac{1}{\sqrt{\mathcal{U}+P/\mu^2}} \right\rangle}. \tag{5.53}$$

It is worth noting that no explicit solution is needed to calculate both quantities since they just depend on the geometry (topology) of the target space. Then, before taking any specific potential in consideration, some general remarks can be made. For instance, we can study the high pressure limit, which allows for a series expansion in P,

$$\bar{\rho}(P) = \mu^2 \frac{\langle 2\mathcal{U} \rangle}{\langle 1 \rangle} + P = P + 2\mu^2 \langle \mathcal{U} \rangle \tag{5.54}$$

(obviously, $\langle 1 \rangle = 1$). This is equivalent to an EoS for bag type matter which is given by

$$\bar{\rho}(P) = P + B_\infty, \tag{5.55}$$

with the asymptotical bag constant B_∞

$$B_\infty = 2\mu^2 \langle \mathcal{U} \rangle. \tag{5.56}$$

Therefore, we conclude that at high pressure and from the mean-field point of view of the EoS, the BPS Skyrme model presents the same behaviour as matter in a bag type model. Concretely, we compare it to the MIT bag model equation of state [140]

$$P = \frac{1}{3}(\bar{\rho} - 4B_{\mathrm{MIT}}). \tag{5.57}$$

Thus, the BPS Skyrme model can be thought of as a hadronic bag model describing nuclear matter instead of quark matter (remember in our BPS theory quark contributions are integrated out and mesonic fields correspond to fundamental degrees of freedom) although with different proportionality constants between pressure and energy density: 1/3 in the MIT bag model and 1 in our theory.

Furthermore, at high pressure (high energy density), the exact non-average equation of state tends to be constant with $\rho \sim \bar{\rho}$ and $\mathcal{B}_0 \sim \bar{\rho}_B \equiv B/V$ so the approximate equation of state coincides with the MF-EoS reading

$$\bar{\rho} = P = \pi^4 \lambda^2 \bar{\rho}_{\mathcal{B}}^2. \tag{5.58}$$

In addition, this is also the high energy density limit of EoSs from other models of nuclear matter as the Walecka mode [91, 92] (see [122] for an overview), where instead of $\pi^4\lambda^2$ we have $\frac{1}{2}(g_\omega^2/m_\omega^2)$ (g_ω and m_ω are the coupling constant and mass of the vector meson ω of the Walecka model respectively). As well, $\bar{\rho} \sim P$ corresponds to the high energy density limit for an EoS from a modification of the MIT bag model where interactions with higher mesons are also included so asymptotically the equation of state $P \sim \bar{\rho}$ is found [141].

On the other hand, we can also study the small pressure limit although it is slightly more complicated since no expansion in P can be made. The problem arises, because arbitrary negative powers of the target space average potential would appear, i.e., $\langle \mathcal{U}^{-\alpha} \rangle$ with $\alpha > 0$. Then, since $\mathcal{U}$ has at least one zero (it corresponds to the vacuum), for sufficiently large α, $\langle \mathcal{U}^{-\alpha} \rangle$ becomes singular. However, we can write the general behaviour of the MF-EoS (5.51) at small pressure like

$$\bar{\rho}(P) = 2\mu^2 \frac{\langle \mathcal{U}^{1/2} \rangle}{\langle \mathcal{U}^{-1/2} \rangle} + f(P), \tag{5.59}$$

where $f(P)$ is a non-polynomial function such that $f(P) = 0$ when $P \to 0$. Similar to the high pressure limit with the bag type EoS, here an equilibrium bag constant, B_0, can be defined

$$B_0 = 2\mu^2 \frac{\langle \mathcal{U}^{1/2} \rangle}{\langle \mathcal{U}^{-1/2} \rangle}. \tag{5.60}$$

It will be non-zero if $\langle \mathcal{U}^{-1/2} \rangle$ is not singular, which, by means of the definition of the geometrical volume above, is equivalent to having a finite volume at $P = 0$. As already stated in Chapter 3, this happens when the solution at zero-pressure is a compacton, which means a vacuum approach weaker than sextic, i.e., $\lim_{\xi \to 0} \mathcal{U} \sim \xi^\alpha$ with $\alpha < 6$. All the potentials we will use behave like this.

At this point, it is interesting to comment that, as a consequence of the Chebyshev integral inequality, the asymptotic bag constant B_∞ is always larger than or equal to the equilibrium bag constant B_0:

$$B_\infty \geq B_0. \tag{5.61}$$

Finally, from the physical point of view it is important to require that our MF-EoS satisfies causality, that is to say, the speed of sound has to be smaller than or equal to the speed of light,

$$v \leq 1, \tag{5.62}$$

where v is the speed of sound defined by

$$\frac{1}{v^2} = \frac{\partial \bar{\rho}}{\partial P}. \tag{5.63}$$

Therefore, causality means

$$\frac{\partial \bar{\rho}}{\partial P} \geq 1, \tag{5.64}$$

which translated into our target space averages reads

$$\left\langle \mathcal{U}\left(\mathcal{U}+\frac{P}{\mu^2}\right)^{-1/2}\right\rangle\left\langle \left(\mathcal{U}+\frac{P}{\mu^2}\right)^{-3/2}\right\rangle - \left\langle \mathcal{U}\left(\mathcal{U}+\frac{P}{\mu^2}\right)^{-3/2}\right\rangle\left\langle \left(\mathcal{U}+\frac{P}{\mu^2}\right)^{-1/2}\right\rangle \geq 0. \tag{5.65}$$

This inequality imposes a constraint on the possible potentials. Nevertheless, it is not a problem for the potentials studied here, namely the step-function potential, the standard Skyrme potential $\mathcal{U}_\pi$ and the standard Skyrme potential squared $\mathcal{U}_\pi^2$.

5.3.1 Choosing the potential: Examples

We will analyse the mean-field equation of state arising for the three potentials we will use to study neutron stars in the mean-field approach: the step-function potential, the standard Skyrme potential and the standard Skyrme potential squared.

i) **The step-function potential.**

The first potential we will consider corresponds to the simplest case, the step-function potential

$$\mathcal{U} = \Theta(\mathrm{Tr}(1-U)). \tag{5.66}$$

We have already seen in Chapter 3, section 3.1, that it is not a good potential from the phenomenological point of view since the corresponding compression modulus is too large. However, it is of great interest because for this potential the EoS from the exact full field theory and

the mean-field approach agree. Indeed, the equation of state for both descriptions is

$$\rho = P + 2\mu^2, \tag{5.67}$$

so the values of the bag constants trivially follow:

$$B_\infty = B_0 = 2\mu^2. \tag{5.68}$$

Obviously, for this potential $\rho = \bar{\rho}$, where this equivalence between both approaches comes from the fact that the energy density is a constant in the full field theory. But even more, in the high pressure limit, every MF-EoS for a reasonable potential looks like the step-function EoS. This can be easily seen from the BPS equation for non-zero pressure (3.42), i.e.,

$$\frac{|B|\lambda}{2r^2}\sin^2\xi\,\xi_r = -\mu\sqrt{\mathcal{U} + \frac{P}{\mu^2}}. \tag{5.69}$$

Then, for $P/\mu^2 >> 1$ the field-dependent right hand side behaves like $-\mu\sqrt{\mathcal{U} + P/\mu^2} \sim -\sqrt{P}$ and since $\mathcal{U}$ is negligible, the left hand side, which corresponds to the baryon density, is also constant. Thus, so is the energy density.

ii) **The standard Skyrme potential**.

The next potential to analyse is the standard Skyrme potential, which is usually used to introduce the pionic masses:

$$\mathcal{U} = \mathcal{U}_\pi = 1 - \cos\xi \equiv 2h, \tag{5.70}$$

where we have already written it as a function of the h variable defined above, Eq. (5.30). Now, we do not have a constant energy density as in the previous case, so the MF-EoS reads

$$\bar{\rho} = \frac{\mu^2}{5}\left(2 - 3\frac{P}{\mu^2} + \frac{6}{1 + \frac{P}{\mu^2}\left(1 - \frac{K\left[\frac{2}{2+P/\mu^2}\right]}{E\left[\frac{2}{2+P/\mu^2}\right]}\right)}\right), \tag{5.71}$$

with K and E the elliptic integrals of the first and second kind, respectively. Then, the asymptotical and at equilibrium bag constants are

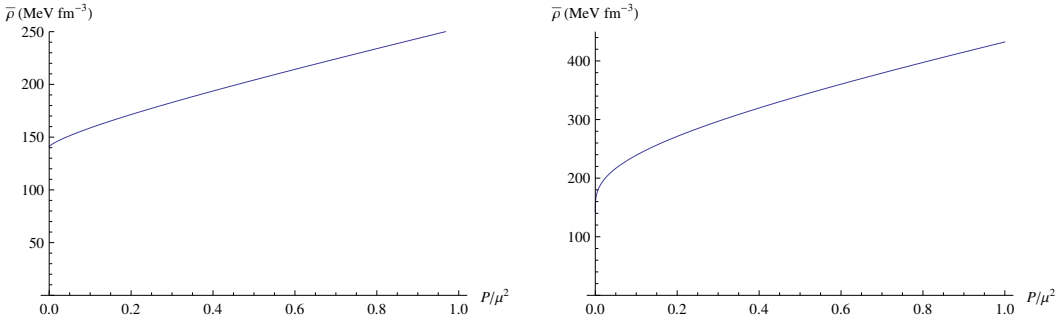

Figure 5.5: MF-EoS for potentials $\mathcal{U}_\pi$ (left) and $\mathcal{U}_\pi^2$ (right) with $\mu^2 = 88.26$ MeV fm^{-3} and $\mu^2 = 141.22$ MeV fm^{-3}, respectively.

$$B_\infty = 2\mu^2, \qquad B_0 = \frac{8}{5}\mu^2. \tag{5.72}$$

Whilst the expansion at small P with the leading terms is

$$\bar{\rho} = \frac{\mu^2}{5}\left(8 - \frac{P}{\mu^2}\ln\frac{P}{2\mu^2}\right) \tag{5.73}$$

It is easy to see that at $P = 0$, the derivative $\frac{\partial\bar{\rho}}{\partial P} = \infty$. Moreover, as shown before, at large P the EoS tends to $\bar{\rho} = P + B_\infty$, so the speed of sound is always smaller than 1 and causality holds. In Fig. 5.5 left, the mean-field equation of state has been plotted for the value of μ^2 presented in section 5.2, i.e., $\mu^2 = 88.26$ MeV fm^{-3}. The linear dependence with the pressure is clear for large values of P.

iii) **The standard Skyrme potential squared**.

The last potential we will take in consideration is just the square of the standard one:

$$\mathcal{U} = \mathcal{U}_\pi^2 = (1 - \cos\xi)^2 = 4h^2. \tag{5.74}$$

Here, the MF-EoS we get presents a more involved dependence with the pressure,

$$\bar{\rho} = \mu^2\left(\frac{P}{\mu^2} + \frac{5\,{}_3F_2[\frac{1}{2},\frac{7}{4},\frac{9}{4};\frac{5}{2},3;-\frac{4\mu^2}{P}]}{2\,{}_3F_2[\frac{1}{2},\frac{3}{4},\frac{5}{4};\frac{3}{2},2;-\frac{4\mu^2}{P}]}\right), \tag{5.75}$$

where ${}_pF_q[a_1,\ldots,a_p;b_1,\ldots,b_q;z]$ is a generalization of the hypergeometric function ${}_pF_q[a;b;z]$. As well, the bag constants are given by

$$B_\infty = \frac{5}{2}\mu^2, \qquad B_0 = \mu^2, \tag{5.76}$$

and causality can also be shown. In Fig. 5.5 right, we show the mean-field equation of state for the corresponding value $\mu^2 = 141.22$ MeV fm^{-3} (see section 5.2). As expected, it quickly reproduces the linear average energy density-pressure relation (it approaches the step function EoS).

5.4 Mean-field Theory vs. Full Field Theory

In section 5.2 we have already solved the Einstein equations and studied the neutron stars arising from the full field theory. It is the main purpose of the present section to solve the corresponding mean-field theory in order to establish a comparison between both approaches and draw some conclusions. Therefore, to find a solution in this mean-field approximation the first step is to define the TOV system we have to compute. It is given by the Einstein equations (5.36) and (5.37) but with the average energy density $\bar{\rho}$ and pressure p instead (i.e., their mean-field values), plus the MF-EoS relating both quantities: $\bar{\rho} = \bar{\rho}(p)$. Then, the procedure to follow consists in treating $\bar{\rho}$ and p as independent variables and imposing the initial condition on the metric field, $\mathbf{B}(r = 0) = 1$. It is important to note that for the step-function potential, since the EoS and the MF-EoS are exactly the same, both approaches are equivalent.

The other thing to take into account is the numerical value of the coupling constants μ and λ. The corresponding values for the potentials $\mathcal{U}_\pi$ and $\mathcal{U}_\pi^2$ have been presented above in (5.39) and (5.40) respectively. Then, in a similar fashion we get for the step-function potential

$$\begin{aligned} \mathcal{U} = \Theta(h): \qquad & E = 2\pi^2 B\lambda\mu, \quad V = \pi^2 B\frac{\lambda}{\mu} \\ & \Rightarrow \lambda^2 = 30.99 \text{ MeV fm}^3, \quad \mu^2 = 70.61 \text{ MeV fm}^{-3}. \end{aligned} \tag{5.77}$$

There exists an important difference in solving the system in the mean-field theory with respect to the full field theory since no extra condition on the derivative of the pressure at the neutron star radius, $p'(R)$, must be imposed. Thus, different values of the average energy density at the centre, $\bar{\rho}(0)$, give solutions with different neutron star masses. These solutions cease to be stable when an increase in $\bar{\rho}(0)$ has a reduction of the mass as a result. However, for practical reasons of the numerical calculation both branches are plotted in some figures (the numerical integration cannot distinguish them).

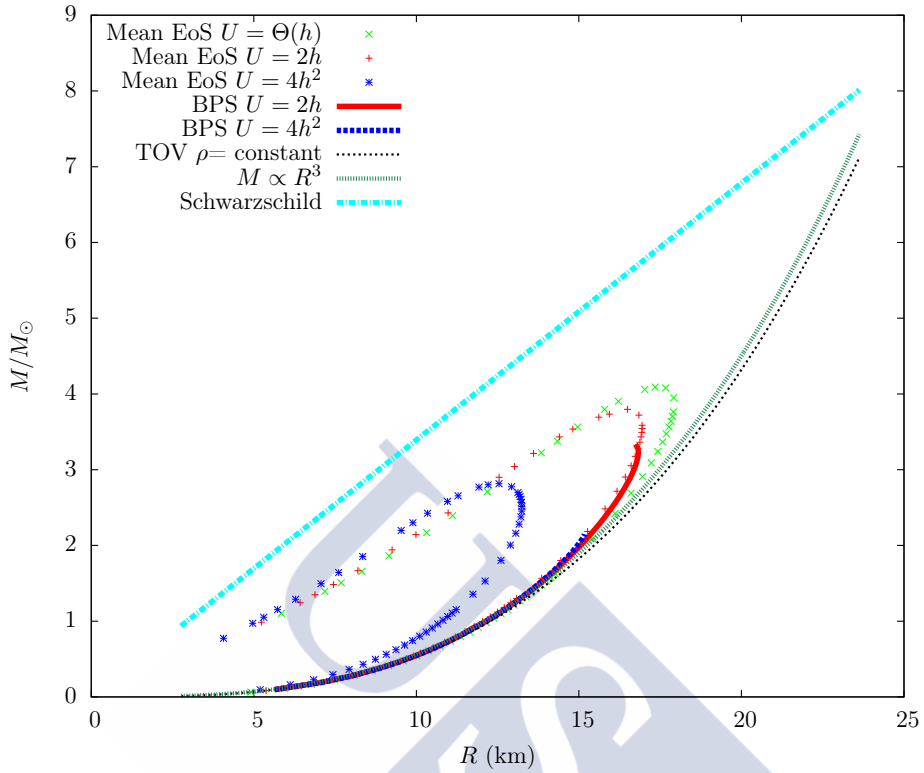

Figure 5.6: Neutron star masses in solar units as a function of the radius (in km) for both exact theory and MF approach (with unstable branches included).

On the other hand, in this mean-field approach the baryon number B is found *a posteriori* in terms of the mean-field (average) baryon density $\bar{\rho}_B$,

$$B = 4\pi \int_0^R dr r^2 \sqrt{\mathbf{B}} \bar{\rho}_B, \tag{5.78}$$

with $\bar{\rho}_B$ defined by Eq. (5.53), where P has to be replaced by the TOV solution $p(r)$.

The procedure we have followed to solve the system corresponds again to a shooting from the centre with a Runge Kutta method. As commented before, the initial condition is $\mathbf{B}(0) = 1$ and $\bar{\rho}(0) = \bar{\rho}_0$ is chosen as the parameter to play with ($p(0) = p_0$ immediately follows from the MF-EoS). Then, we integrate until the condition $p(R) = 0$ holds with R the neutron star radius whereas the neutron star mass comes from the integral

$$M = 4\pi \int_0^R dr r^2 \bar{\rho}(r) \tag{5.79}$$

(remember that in the full field theory the mass M was read off from the asymptotical value of the metric field $\mathbf{B}$).

Hence, Fig. 5.6 shows the curves $M(R)$, i.e., the neutron star masses as functions of the neutron star radii. Again, we find that the mass increases with the radius even for the MF case (except very close to the maximum masses). As commented before, this effect seems to be due to the stiffness of the equation of state within the BPS Skyrme model framework. Moreover, for small masses we find they behave like $M \propto R^3$, which means that the EoS approaches $\bar{\rho} =$ constant, whilst for the unstable branches of the MF theory (they are also shown in this figure), which corresponds to a very large value of the average energy density at the centre, $\bar{\rho}_0$, we can easily see they approach the behaviour $M \propto R$, which implies the EoS $\bar{\rho} = p$ for large $\bar{\rho}$. On the other hand, there exist some differences in the behaviour between the exact theory and the MF approximation for a given potential. In the case of the step-function potential it is exactly the same. Both approaches agree so we arrive at identical results. For the standard Skyrme potential $\mathcal{U}_\pi = 2h$ we have rather similar results and curves with slightly larger neutron star masses in the MF theory (about $3.7M_\odot$) than in the full theory (about $3.3M_\odot$). Finally, regarding the quartic potential $\mathcal{U}_\pi^2 = 4h^2$, quite notable differences appear. The curve corresponding to the exact theory is similar to the $2h$ case but with a smaller mass. However, in the MF approximation not only the curve is different but also the compactness parameter $\frac{2GM}{R}$ (here $c = 1$) is bigger, meaning that for the same mass the radius is smaller. See Fig. 5.7.

To understand why the case of the potential $\mathcal{U} = 4h^2$ differs so much from the MF results of the other two potentials we recall the MF-EoS quickly approaches the hadronic bag type equation of state

$$\bar{\rho} = P + B_\infty. \tag{5.80}$$

Then, from the definitions (5.68), (5.72) and (5.76), and from the corresponding values of μ^2 we get different expressions for B_∞ depending on the potential:

$$\begin{aligned} \Theta(h): &\quad B_\infty = 2\mu^2 \sim 141 \text{ MeV fm}^{-3}, \\ 2h: &\quad B_\infty = 2\mu^2 \sim 176 \text{ MeV fm}^{-3}, \\ 4h^2: &\quad B_\infty = \frac{5}{2}\mu^2 \sim 353 \text{ MeV fm}^{-3}. \end{aligned} \tag{5.81}$$

It is clear from these values that the asymptotical bag constant B_∞ is much bigger for the quartic potential $\mathcal{U}_\pi^2 = 4h^2$, so for a fixed value of the pressure the average energy density $\bar{\rho}$ is much bigger, which results in a more compact neutron star. It is still true in the full theory that the neutron star is quite

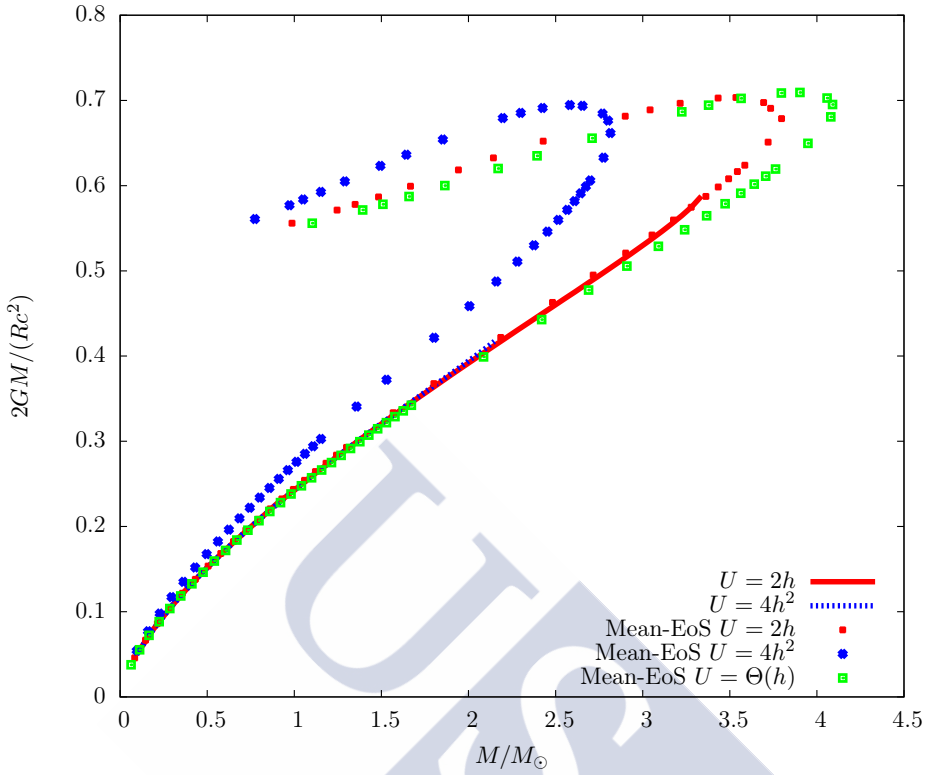

Figure 5.7: Compactness of neutron stars as a function of the neutron star mass in solar units for different solutions. Unstable branches from the MF approach are also included.

compressed at the centre since we have a peaked potential. However, it approaches the vacuum value $h = 0$ faster than the other potentials considered here with a large tail of low energy density which tends to increase the neutron star radius. Therefore, the $4h^2$ potential has two opposite effects. On the one hand, it is quite peaked about the centre leading to high energy densities and thus, to quite compressed neutron stars near the centre. On the other hand, due to the quick approach to the vacuum, a large tail with low values of ρ appears. Then, it would be interesting to find potentials where these two effects could be under control and varied independently.

Up to now we have focused on global properties where no dramatic difference between MF or full theory exists. Essentially, we observed that the exact theory gives smaller neutron star masses. On the other hand, considering local quantities like the energy density, the pressure or the metric function, differences start to be important. For instance, in Fig. 5.8 we show the energy density as function of the radial coordinate for both approaches and different

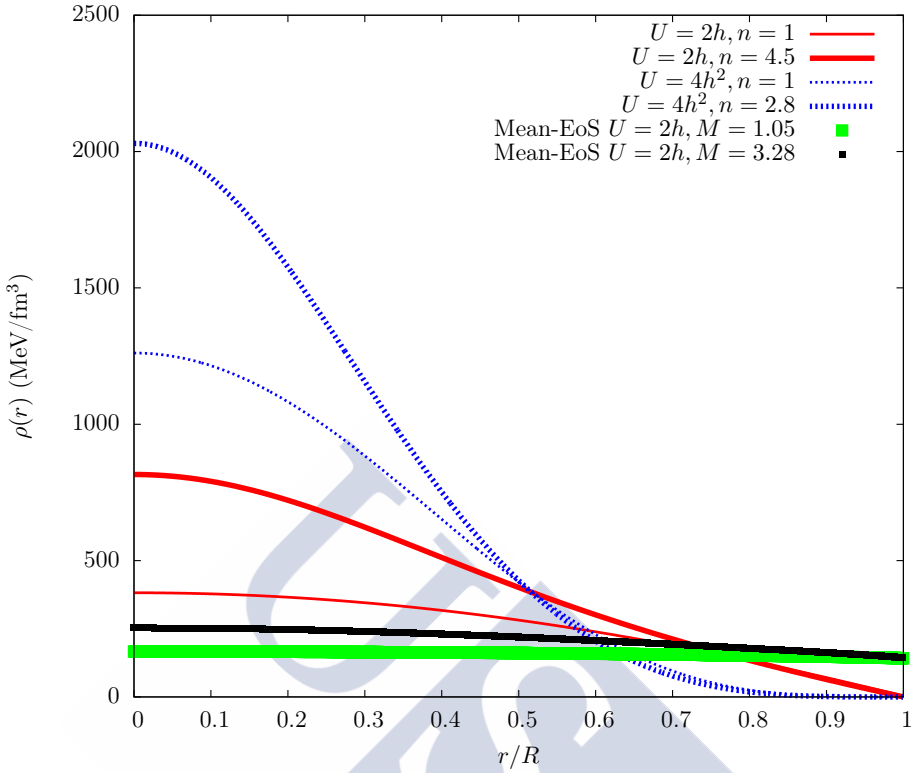

Figure 5.8: Energy density as a function of the radial coordinate r normalized to the neutron star radius R.

potentials (remember $n = B/B_\odot$). In the full theory the energy density ρ takes high values at $r = 0$ while it is zero at the neutron star radius R. However, we see that the MF results do not vary too much with r (just a factor two or three) and they present non-zero values at $r = R$. It is important to note that this does not imply they are under different compression, in fact the compression is similar. The shape of ρ without gravity is quite similar and, as stated in section 5.2, the compression induced by gravity at the centre is always less than a factor three. Therefore, although the absolute values of the energy density at $r = 0$ are much bigger in the exact calculations, the real effect in both approaches is rather similar.

Similarly, in Fig. 5.9 the pressure as a function of the radius is plotted in the exact and the average approach. We find again peaked values about the centre for the full theory whilst the pressure varies very slowly for the MF-EoS. Furthermore, in Fig. 5.10 the metric function $\mathbf{B}(r)$ is shown with an interesting difference. In the full theory the maximum value of the function is inside the star (in fact, for the $4h^2$ potential it is not even close to the

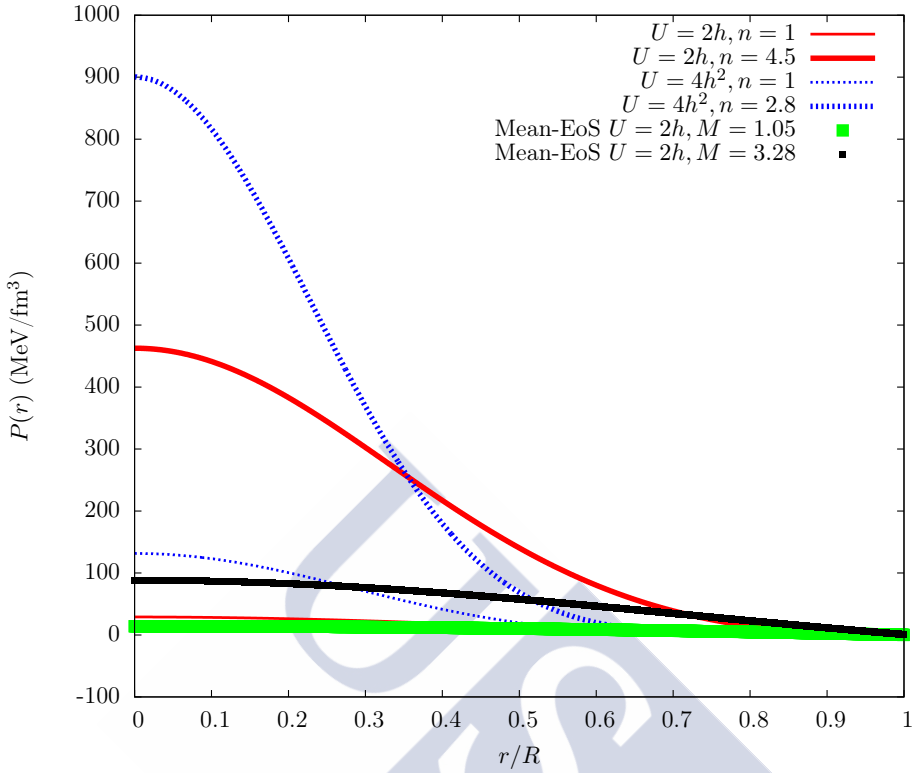

Figure 5.9: Pressure as a function of the radial coordinate r normalized to the neutron star radius R.

surface), but, however, in the MF approach the metric function $\mathbf{B}$ reaches its maximum exactly at the surface $r = R$.

Then, taking into account these three local quantities, it is clear that quite important differences between exact and MF theory appear. Thus, we can expect global physical observables depending on local quantities to strongly differ in both approaches. One of the most important observables we can have in mind is the moment of inertia which is relevant for the description of neutron stars' (slow) rotations. Indeed, in the Newtonian case it is just given by the volume integral of tensorial expressions such as $x^i x^j \rho(\vec{x})$, where the dependence both on the total energy and on the corresponding shape of the density ρ is evident. Although in the relativistic case the calculation of the moment of inertia tensor is not so easy (it is necessary to solve the Einstein equations with a more general metric depending on three independent metric functions [142, 143]), the Newtonian arguments are expected to be valid from a qualitative point of view so this difference between MF and exact calculations would have important consequences on the calculation of the moments of

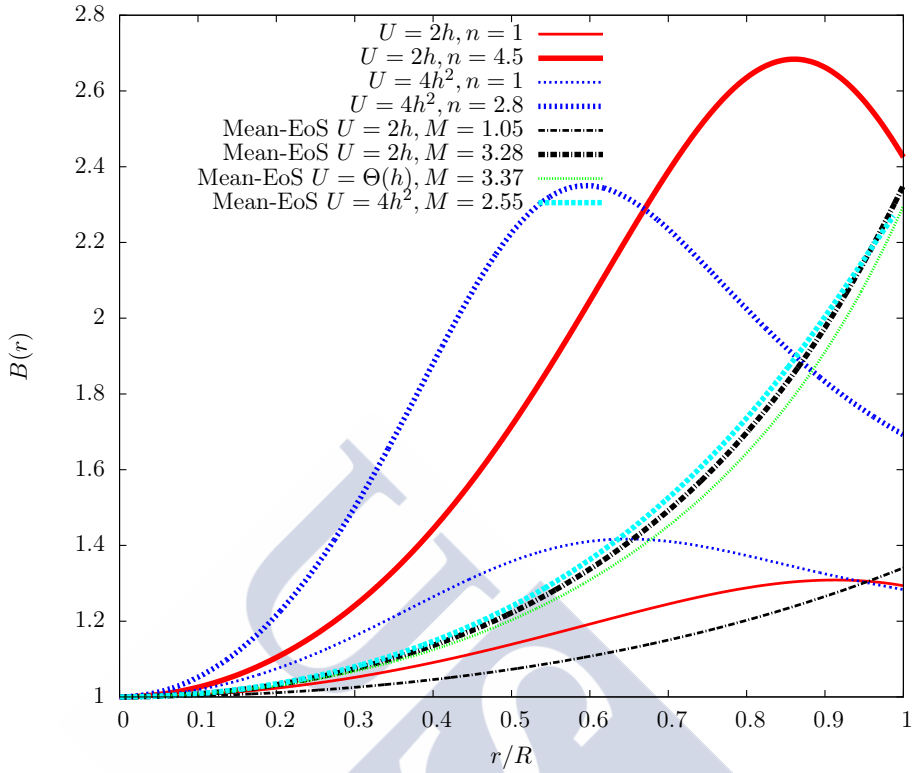

Figure 5.10: Metric function $\mathbf{B}(r)$ as a function of the radial coordinate r normalized to the neutron star radius R.

inertia.

Moreover, in Fig. 5.11 and Fig. 5.12 we plot the central values of the energy density and pressure as functions of the neutron star masses in solar units, and p as function of the neutron star radii R respectively, for the exact theory and the MF limit. We appreciate a huge difference between both approaches with larger values for the potential $\mathcal{U} = 4h^2$ than for $\mathcal{U} = 2h$. Also the value of the pressure at the centre as a function of $\rho(r = 0)$ is shown in Fig. 5.13. Here we see that for a given value of the pressure at the centre we have much higher values of the energy density at $r = 0$ for the full theory than for the MF limit. Furthermore, since in the MF approach different solutions for the same potential correspond to the same mean-field equation of state, these curves are at the same time the MF-EoS graphs for the corresponding potential. This situation does not happen in the exact theory where different solutions have different on-shell equations of state even when the potential is the same.

These equations of state $p(\rho)$ for both approaches are shown in Fig. 5.14.

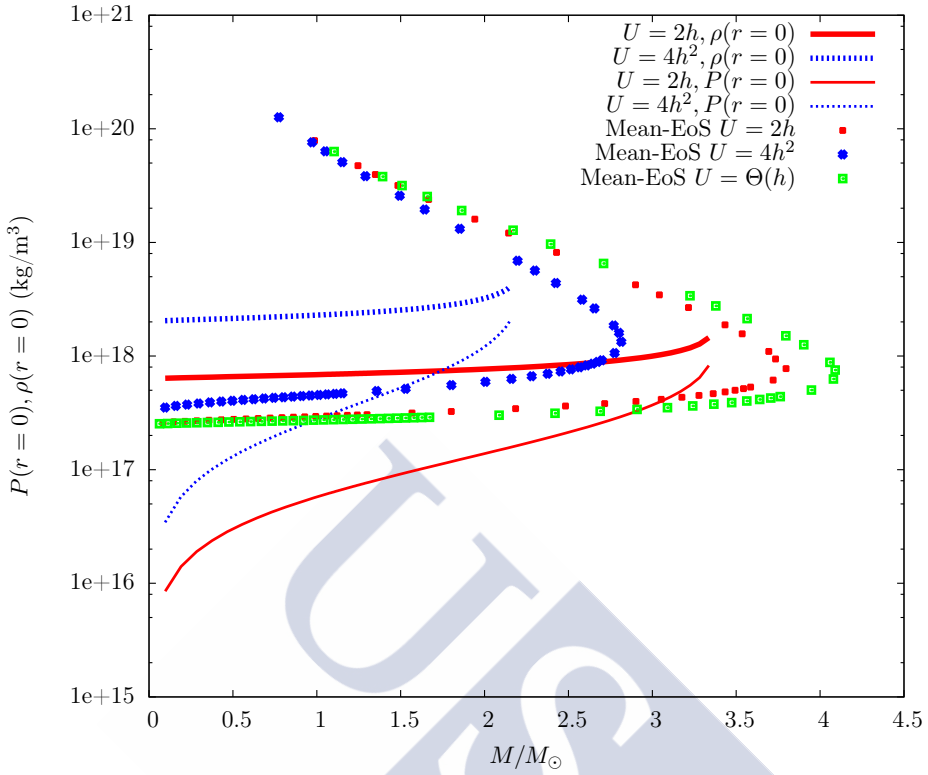

Figure 5.11: Central values of pressure and energy density as functions of the neutron star masses for different solutions. Unstable branches are also shown.

They are on-shell EoS in the sense that they are obtained from the numerical solutions $p(r)$ and $\rho(r)$ by eliminating the dependence on the coordinate r. Of course, this on-shell EoS in the TOV approach coincides with the original MF-EoS, which is equal for all solutions with the same potential and is explicitly seen in the MF-EoS for $\mathcal{U} = 2h$ where the equations of state for $M = 1.05M_\odot$ and $M = 3.28M_\odot$ exactly overlap. As well, it is quite clear how the MF-EoS for $\mathcal{U} = 4h^2$ is substantially different from the step-function and $2h$ potentials. On the other hand, it is also rather evident how the on-shell equations of state differ for different solutions even with the same potential in the case of the full theory. Indeed, remember these on-shell equations of state are of a polytropic type (see section 5.2), i.e., $p \sim a\rho^b$, with $a = a(B)$ and $b = b(B)$ being parameters depending on the baryon number B.

Summarizing, we have found that in the BPS Skyrme model the difference between the MF limit and the full field theory is the bigger the more the chosen potential differs from the step-function one which gives flat energy and particle densities. Thus, taking into account other theories beyond the

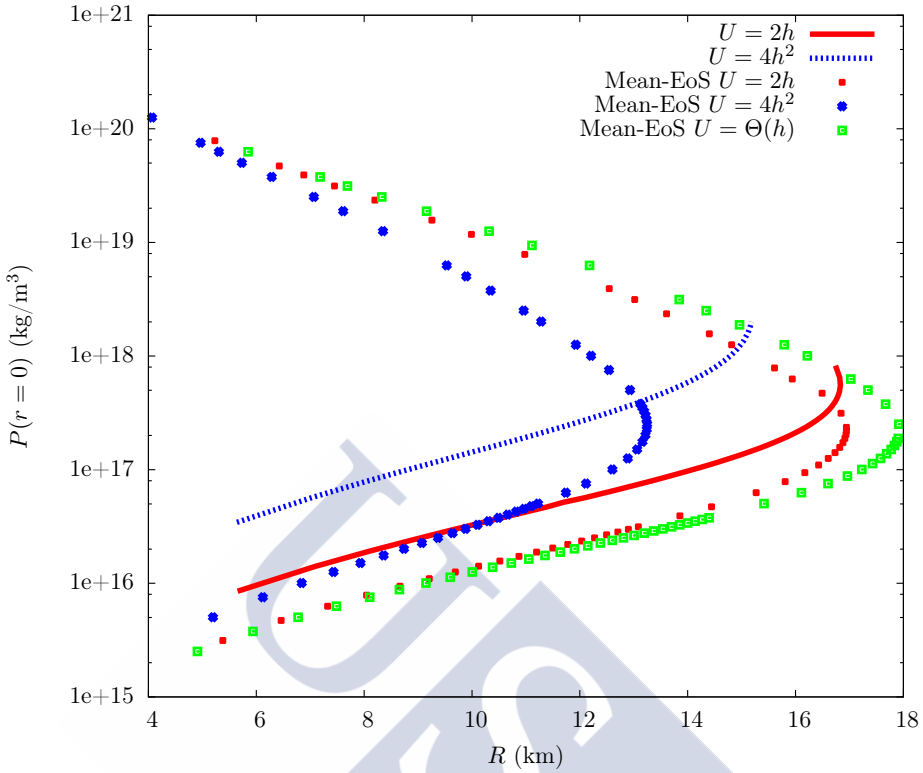

Figure 5.12: Pressure at the centre as a function of the neutron star radius R. Unstable branches are also shown.

BPS Skyrme model, the differences are more relevant for those with more important inhomogeneities in the energy and particle densities. For instance, in the standard Skyrme model, where the minimal solution is the Skyrmionic crystal which presents appreciable energy inhomogeneities [120, 144, 145].

On the other hand, we have also seen that in the MF limit the equations of state approach at large $\bar{\rho}$ and p what we have called bag type EoS and which in the neutron star literature is known as maximally compact equation of state. In fact, this maximally compact EoS results in a $M(R)$ curve quite similar to ours but slightly more compact [124, 125, 126, 127], whereas at small pressure our average equations of state are much softer. Therefore, the general picture following from our BPS theory is that of a maximal compactness in the core of the neutron star, i.e., for densities rather above the nuclear saturation density, whilst near the neutron star surface, i.e., about the nuclear saturation density, matter becomes much softer. The transition between the core and mantle of the neutron star depends on the potential we have chosen.

At this point, we should remember what we have mentioned before. We do

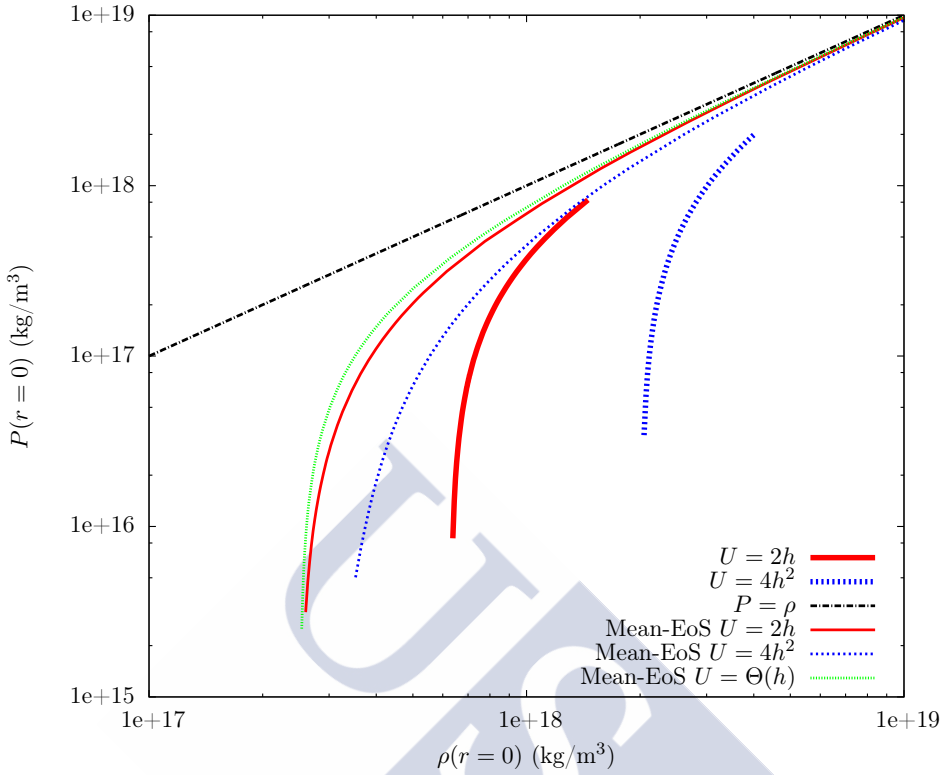

Figure 5.13: Central value of the pressure as a function of the central value of the energy density. The EoS $p = \rho$ is also shown.

not have precise quantitative predictions because we know that near the surface of the neutron star other terms from the near-BPS Skyrme become important. However, bulk properties are not expected to change. For instance, we think the maximum masses and the $M(R)$ curves are bound to remain rather the same, which implies the robust prediction $\frac{dM}{dR} > 0$ for almost all neutron stars, maybe except those close to the maximum mass. This behaviour is opposite to that coming from a large class of equations of state which are used in nuclear physics (see e.g. [124, 125, 126, 127, 128, 129, 130, 135, 136, 137]), but perfectly compatible with the (still not very precise and not very abundant) observational data.

In this spirit and following [146], we have compared in Fig. 5.15 our $M(R)$ curve in the full theory for the $\mathcal{U} = 2h$ potential with the model DBHF (Bonn A) [147, 148] which is a representative of the typical equations of state in nuclear physics (the acronym DBHF stands for the *ab initio* relativistic Dirac-Brueckner-Hartree-Fock approach [149]). Moreover, we have also included some constraints in the mass-radius relation coming from observational data,

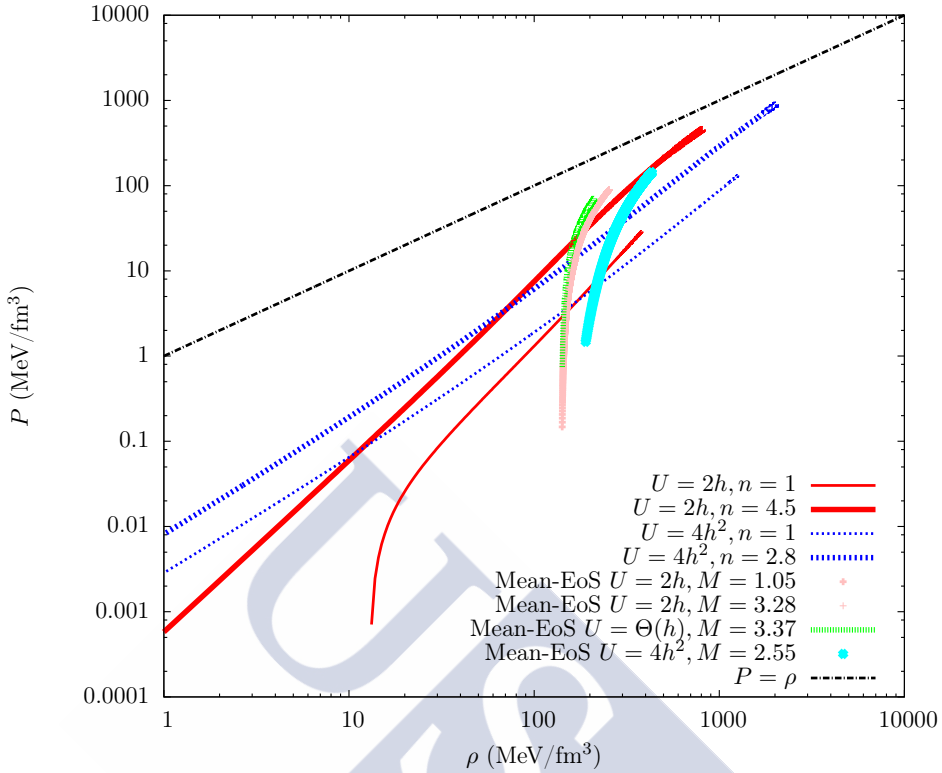

Figure 5.14: Equations of state $p(\rho)$ for different solutions in both approaches: exact field theory and mean-field limit. The EoS $p = \rho$ is also shown.

namely, from the estimated mass $2.0 \pm 0.1\, M_\odot$ for the low-mass X-ray binary (LMXB) 4U 1636-536 [150], from quasi-periodic oscillations at high frequencies of the LMXB 4U 0614+09 [151] and from the thermal radiation of the isolated pulsar RX J1856.5-3754 [152]. Hence, we see that our EoS fulfils all the constraints in a very natural way.

There is one more important check for the predictions of our BPS model based on the double pulsar J0737-3039 [153]. This object offers some precisely known properties of neutron stars. In fact, the mass of the lighter pulsar, P_2, makes it the lightest firmly established neutron star with a value $M_{P_2} = 1.249 \pm 0.001\, M_\odot$. In addition, assuming this pulsar comes from an ONeMg white dwarf via an electron-capture supernova, it is possible to determine the baryon number quite accurately. Then, the baryonic mass $\bar{M}_{P_2}$ lies in the interval $1.366 \leq (\bar{M}_{P_2}/M_\odot) \leq 1.375$ [153], where this $\bar{M}_{P_2}$ was determined by assuming a mass per baryon number equal to the atomic mass unit $u = 931.5$ MeV (this value was chosen due to the abundant elements in an ONeMg white dwarf). In our model, we have the baryon number as a more natural

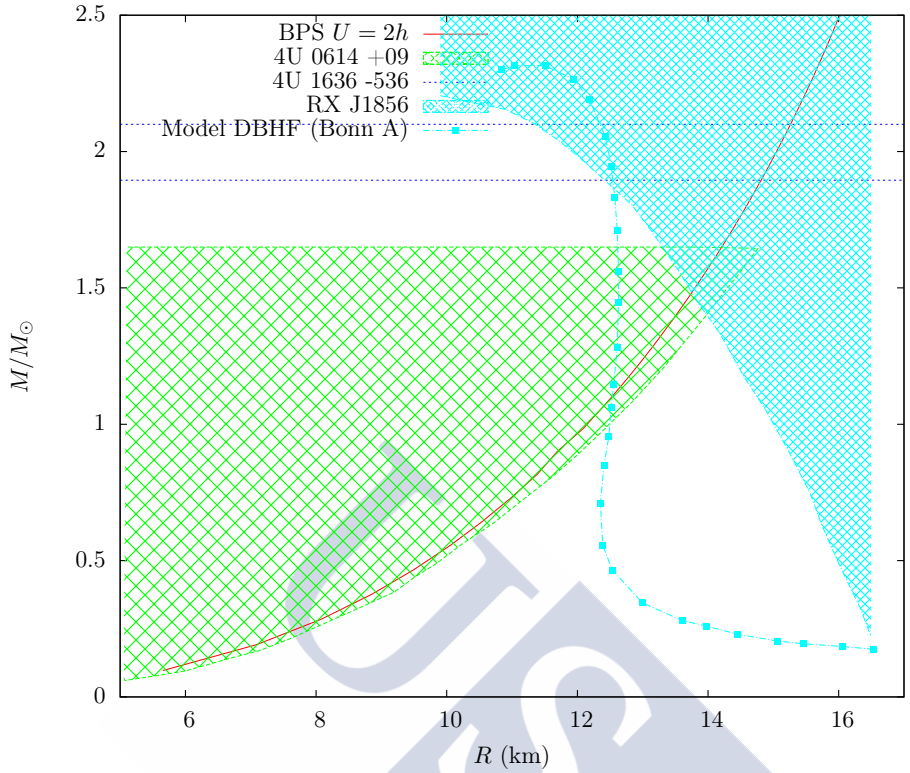

Figure 5.15: Neutron star mass-radius relation for the potential $\mathcal{U}_\pi = 2h$ in the exact theory compared to the nuclear physics model DBHF (Bonn A). Constraints coming from observational data are also included, concretely from the low-mass X-ray binaries 4U 1626-536 and 4U 0614+09, and the isolated pulsar RX J1856.5-3754 (just RX J1856 in the figure).

observable, where the solar baryon number is defined as the solar mass divided by the proton mass, see Eq. (5.43). Therefore, to go from $\bar{M}_{\mathrm{P}_2}/M_\odot$ to $B_{\mathrm{P}_2}/B_\odot$ we just have to multiply by a factor of $m_p/u = (938.3\ \mathrm{MeV})/(931.5\ \mathrm{MeV}) = 1.0073$ which gives the interval

$$1.376 \leq B_{\mathrm{P}_2}/B_\odot \leq 1.385. \tag{5.82}$$

Thus, as it is also done in [146] for equations of state coming from different models of nuclear matter, we compare in Fig. 5.16 the $M(B)$ curve of the BPS Skyrme model with the interval from the double pulsar J0737-3039 (yellow rectangle in the figure). We see that our model gives a reasonable agreement especially for the step-function potential, $\mathcal{U} = \Theta(h)$, which seems to indicate that rather flat potentials are the preferred ones.

Finally, we would like to remind that these are preliminary and not very

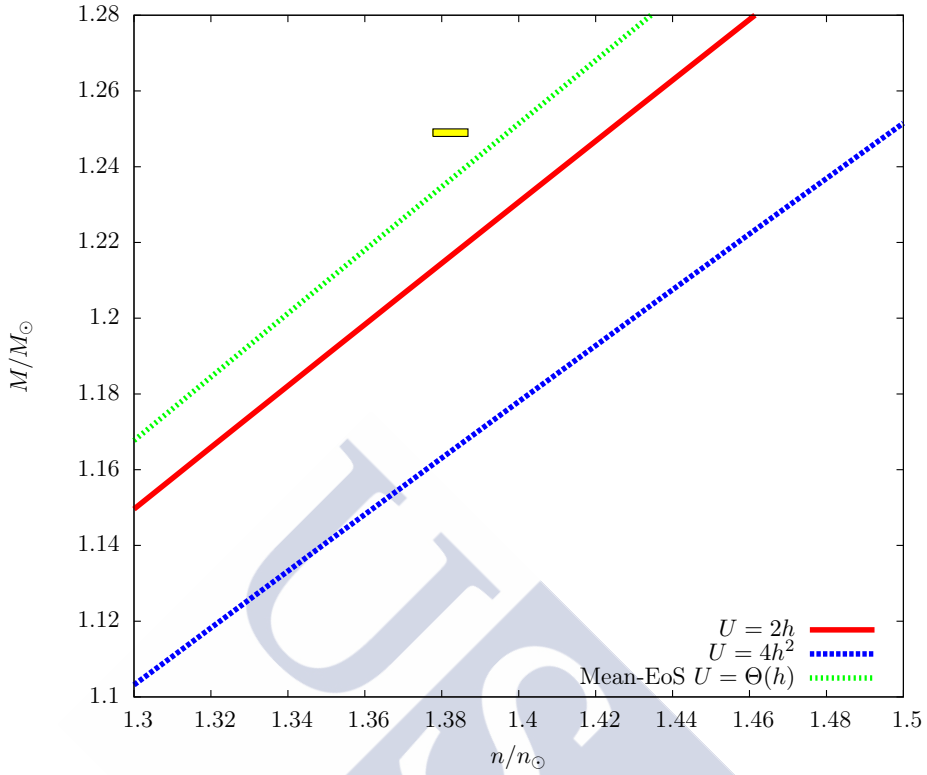

Figure 5.16: Relation between mass and baryon number in solar units for the three different potentials ($\Theta(h)$, $2h$ and $4h^2$) studied in the BPS Skyrme model with the exact calculation compared to the value derived from the lighter neutron star of the double pulsar J0737-3039 (yellow rectangle). Here n corresponds to the baryon number usually referred to as B throughout the text.

precise predictions. Not only because small contributions from the other near-BPS terms are (again) required for a complete and precise description, but also two more reasons exist. Firstly, remember that the parameter values we used come from a fit. On the one hand, we have used the value of the infinite nuclear matter mass per baryon number, $E_{B=1} = 923.3$ MeV, which is an accurate quantity with almost all nuclear models giving values in the interval $923 \leq E_{B=1}/\text{MeV} \leq 926$ (see Table 1 in [154]). However, on the other hand, the second quantity was the saturation density $n_0 = 0.153$ fm^{-3}, which seems to be quite model dependent with an interval $0.145 \leq n_0 \cdot \text{fm}^3 \leq 0.175$ (see Table 1 in [154] again). And secondly, we do not know which potential is the right one yet, so at this point we have freedom of choice.

USC
UNIVERSIDADE
DE SANTIAGO
DE COMPOSTELA

Chapter 6

Conclusions and Outlook

6.1 Conclusions

In this PhD thesis we have explored the nuclear world, from nuclei to neutron stars and even gone through the thermodynamics of nuclear matter. Trying to achieve a better understanding of this low-energy limit of QCD, we have found a promising candidate within the family of effective field theories known as Skyrme models, namely, the near-BPS Skyrme model. One reasonable proposal for this near-BPS model is as follows

$$\mathscr{L} = \mathscr{L}_{BPS} + \varepsilon(\mathscr{L}_0 + \mathscr{L}_2 + \mathscr{L}_4), \tag{6.1}$$

with $\mathscr{L}_{BPS} = \tilde{\mathscr{L}}_0 + \mathscr{L}_6$ and ε a small parameter, so we add the standard Skyrme contributions to the BPS model in a perturbative way. Here we should choose $\mathscr{L}_0$ to be the standard Skyrme potential because with this choice we have the advantage that the relative strengths of the sigma model term and standard Skyrme potential may be fixed to their physical values so the correct pion mass is trivially reproduced. Hence, the main conclusion we can draw from this thesis is the fact that the near-BPS model constitutes a very promising effective theory of strong interactions together with the idea that the main contribution comes from the BPS part. In fact, we have found strong evidence for this statement throughout this work which not only sustains the assumption that this BPS Skyrme model provides the leading contribution to the theory but also that it describes some very important properties of nuclear matter. For instance, it immediately follows from the BPS property that mass and baryon number are linearly related, i.e., $E \sim |B|$, as well as the phenomenological relation for the nuclear radii $R_0 \sim |B|^{1/3}$ (both behaviours are basic experimental facts). This is one of the main reasons why we have focused on the BPS Skyrme model in this work. We know that, although the complete theory requires the addition of the perturbative contributions, this BPS theory can provide a first and important insight into the nuclear world at least qualitatively. Indeed, this model can be seen as the limit of the near-BPS theory when $\varepsilon \to 0$. From what was said above, it is, in fact, more natural to consider potentials for $\tilde{\mathscr{L}}_0$ with a faster than quadratic approach to the vaccum. We, nevertheless, considered $\tilde{\mathscr{L}}_0$ equal to the standard Skyrme

potential frequently, essentially for simplicity and assuming that many properties of BPS Skyrmions do not depend too much on this choice.

There are also other important results from this work like the study of Roper resonances or the thermodynamics of the BPS Skyrme model at zero temperature and the calculation of Skyrmionic solutions for non-zero external pressure reviewed in Chapter 3. Here we found that all static solutions of the BPS Skyrme model are constant pressure solutions. Concretely, the BPS Skyrmions have zero pressure whilst non-zero pressure solutions need to be stabilized by external pressure. Furthermore, we could conclude that for compact solutions with a definite radius the geometrical volume corresponds to the physical volume since the thermodynamical relation $P = -\frac{dE}{dV}$ holds. This is quite an important fact because this relation is not obvious at all for Skyrme models.

In this thermodynamical framework, we have also studied two important quantities, the compressibility and the baryon chemical potential. In the case of the compressibility we have used the simple potentials $\mathcal{U}(\eta) = \eta^\beta$ with $\eta = \frac{1}{2}(\xi - \sin\xi\cos\xi)$ and ξ the usual profile function. The relevant point here is that the result does not depend on the the specific form of the potential but on the approach to the vacuum $\mathcal{U}(\eta) = \eta^\beta \sim \xi^\alpha$ with $\alpha = 3\beta$. Then, in the framework of the BPS Skyrme model we obtain an infinite compressibility for $\alpha \geq 2$ whereas for $\alpha < 2$ we get finite values. However, these potentials are problematic since the second variation around the vacuum is infinite. Therefore, the physically acceptable potentials are those with an approach $\alpha \geq 2$ implying that the infinite compressibility at equilibrium (at $P = 0$) is a generic property. In addition, this calculation also deals with the high compression modulus (low compressibility) obtained within the Skyrme models. One source of this problem can be due to the assumption of a uniform (Derrick) rescaling of baryon density under external pressure which leads to Skyrmions much more incompressible than nuclear matter. However, we have seen that this hypothesis only applies when the baryon density is constant. This is clearly not the case for the BPS Skyrme model, so this rescaling cannot be considered and the correct value of the compression modulus found is, in fact, zero (or equivalently, infinite compressibility).

We have also analised another important thermodynamical quantity at $T = 0$, the baryon chemical potential, which was shown to be just the baryon density multiplied by an overall constant. At this point we also introduced a mean-field (MF) description based on average integrals over the target space so a specific solution of the model is not needed. Then, this approach produces space independent quantities although both chemical potentials obey all required thermodynamical relations. Moreover, since the step-function potential is constant the two approaches agree in this case. However, for other

potentials we have found that the exact baryon chemical potential is more suitable than the MF version because local quantities change substantially in the mean-field limit.

Going to the realm of nuclei, we have used the BPS Skyrme model for the study of their binding energies. This is a key calculation since it shows the importance of the contribution from the BPS part of the Lagrangian, but at the same time shows the necessity of perturbative contributions from the other terms for a better description of small nuclei. Here, the BPS property is crucial in order to get the physically small binding energies of nuclei because it gives exactly zero binding energies. Then, the non-zero values are obtained by additional contributions, namely, the semiclassical quantization of spin and isospin, the Coulomb energy and the breaking of the isospin symmetry. Following this procedure, and with only three free parameters, we have achieved very successful binding energies for nuclei with large baryon numbers. The fact that it does not work so well for lighter nuclei was also expected because the BPS Skyrme model is based on a collective description of the fundamental degrees of freedom. This approach is quite realistic for high nuclei, but, when studying small ones, single-particle properties and the pionic degrees of freedom become more relevant, so the extension to the near-BPS theory is required.

It is also worth commenting that in our study of binding energies, the fact that real nuclei are not exactly axially symmetric will not influence too much our results, because their deviation from a spherically symmetric baryon density is not too pronounced. Nevertheless, for other issues like nuclear spectroscopy and the corresponding Finkelstein-Rubinstein constraints, the right symmetries are actually important. Furthermore, concerning the choice of the potential, it seems again it is more important how it approaches the vacuum than its specific shape, at least for the BPS model.

Finally, we have successfully coupled the BPS Skyrme model to gravity so the description of neutron stars was also possible. Thus, we achieved a unified description of nuclear matter, where from a fit of the parameters to nucleon mass and radius we obtained very promising values of neutron star masses and radii. Indeed, they agree quite well with the observational constraint $M_{\max} \sim 2.5 M_{\odot}$ (observational neutron star radii are not so well established). Furthermore, using the nuclear matter fitted parameters for neutron stars also supposes an extrapolation from a non-relativistic to a relativistic regime.

It is also important to note that the exact calculation with the back-reaction included is different from the usual TOV approach, which we can also implement by means of the mean-field approximation. The TOV calculation is based on a universal equation of state (EoS) $p = p(\rho)$, but in the full field theory this does not hold in general, and it can only be an approximation.

Nevertheless, it is possible to numerically arrive at an on-shell EoS from the solutions $p(r)$ and $\rho(r)$, although this EoS is not universal and depends on the baryon number B. Concretely, we found $p = a(B)\rho^{b(B)}$. Moreover, we have seen that the stiffness of this EoS highly differentiates the $M(R)$ curves of the exact calculations from the usual TOV results. In general, we have masses growing with the radius of neutron stars in contrast with the usual behaviour of an essentially constant radius which can even decrease with the mass. However, we should emphasize that observational data do not rule out any behaviour, and in fact, our full theory approach fulfils the imposed observational constraints in a rather natural fashion.

Considering the mean-field approach, it provides similar results when global properties are studied but local quantities differ a lot. In addition, we can conclude that for flatter potentials the agreement between both approaches is higher (and equal for the step-function potential).

Thus, taking into account all that was exposed here, it is not an overstatement to say we are at an exciting revival of Skyrme's ideas pointing into the correct direction for an effective-theory description of the low-energy limit of QCD.

6.2 Outlook

Before focusing on the outlook and future research, it is worth briefly commenting about the importance of studying the *little brother* of the Skyrme model in 2+1 dimensions known as the baby Skyrme model [155, 156, 157, 158, 159] (see also [160, 161, 162] or [163, 164, 165, 167, 168, 169, 170, 171, 172, 173, 174, 175, 176, 177, 178, 179, 180, 181] for more recent investigations). It was also used in the development of the present PhD thesis, although no direct results are included. Nevertheless, this baby version helped a lot in a better understanding of this BPS Skyrme model, besides providing some hints for an extension of some properties to its 3-dimensional version. One example of how the baby model can be useful to the study of the corresponding model in three dimensions can be found in the framework of the Skyrme model coupled to a vector omega meson, where after analysing the vector BPS baby Skyrme model [182] we were able to extend it to three dimensions [183].

On the other hand, when thinking about an interesting direction for a further development of the BPS Skyrme model, one idea coming quickly to our mind is that of coupling these Skyrmions to a electromagnetic field. However, it turns out that this is a really complicated task with important problems to overcome (for instance, the magnetic field is a pseudovector instead of its pseudoscalar character in the baby version). Therefore, it is helpful here to

previously gauge the BPS baby Skyrme model [184] and study its properties [185, 186] so we can take advantage of it in a future extension to the 3-dimensional system (interestingly, this BPS baby Skyrme model also allows for a supersymmetric extension, see, e.g. [189, 190, 191, 192]).

The other obvious direction in which this research should continue corresponds to an implementation of the near-BPS Skyrme model. In order to achieve it, we need to find the minimizers of the perturbative part of the Lagrangian among all the possible solutions of the BPS model in each topological sector. Remember we have the VPDs as symmetries so finding the right minimizers seems a quite complicated task. Once these solutions are found, we should proceed like in the present thesis with the semiclassical quantization of the spin and isospin degrees of freedom and the inclusion of the Coulomb energy and the isospin breaking potential. Then, these new solutions should not be too different from classical solutions calculated here since they would just imply a small change in the value of the fitted parameters. However, their symmetries would be different, which is relevant for the moments of inertia and consequently, also for the isospin contributions to the binding energies. They could even help to correctly reproduce the asymmetry term of the semi-empirical mass formula. Furthermore, they would determine the correct Finkelstein-Rubinstein constraints for nuclear wave functions which are responsible for the forbidden and allowed spin and isospin excitations, i.e., responsible for the nuclear spectroscopy.

At this point, trying to improve the description of small nuclei, the study of the deuteron will be really important. In this case, its concrete symmetry is known, and the standard Skyrme model already offers exciting new results for dinucleon states.

Considering neutron stars, the near-BPS Skyrme model is required to make some predictions. This is because even though the BPS contribution is responsible for the bulk properties of neutron stars, the perturbative part becomes dominant near the vacuum, that is to say, near the neutron star surface. Thus, this improvement would imply not only more complicated calculations (gravity couples non-linearly) but also the need for a detailed knowledge of the application of the near-BPS theory to nuclei and nuclear matter. Other steps forward in the issue of neutron stars in the BPS Skyrme model could be the study of rotating neutron stars and neutron stars in magnetic fields. Both subjects are possible *a priori* since it is known how to rotate Skyrmions [27] as well as the right gauge coupling of Skyrmions to magnetic interactions [105]. However, they appear as rather complicated numerical tasks.

Further investigations can be carried out in the other important topic treated in this thesis, the thermodynamics of Skyrme models. Here we have seen that at least the BPS Skyrme model does not react with a uniform

(Derrick) rescaling to external pressure. Thus, the Derrick rescaling parameter Λ is not the softest monopole mode, i.e. it is not the softest excitation which preserves the rotational symmetry. It turns out that this softest mode is given by the pressure, so probably the pressure should be quantized. To achieve this quantization we can think of the pressure as a collective coordinate describing a spherically symmetric deformation of the original Skyrmion at equilibrium. This corresponds to the softest possible monopole vibrational mode because the deformed Skyrmion still obeys the static field equations. Then, from the resulting excitation energies after quantization we could extract the true compression modulus of (BPS) Skyrmionic matter.

In addition, we can take advantage of another important thermodynamical quantity, the baryon chemical potential, in the study of neutron stars. We know that the core of the neutron star is well described by the BPS Skyrme mode. However, for a more complete and realistic description of neutron stars we might consider a skin with more usual matter an known equation of state. Then, the transition between the hadronic and the skin phase would be ruled by the equivalence of the chemical potential. This should modify the mass-radius relation for low massive stars and maybe even with the appearance of a minimal neutron star mass [187]. Obviously, we could always study new potentials not only related to neutron stars but to the BPS model in general, and here we could try to use observational data to constrain the possible allowed potentials.

Finally, it is worth emphasizing that the Skyrme model is not only restricted to studying particle physics. Indeed, it is used in other realms of theoretical physics (see [188] for instance) and in condensed matter physics where Skyrmions are successfully considered especially in 2-dimensional systems [193, 194, 195, 196, 197].

Chapter 7
Conclusións

Nesta tese de doutoramento exploramos o mundo nuclear, dende os núcleos até as estrelas de neutróns, incluso pasando pola termodinámica da materia nuclear. Tratando de acadar unha mellor comprensión deste límite de QCD a baixas enerxías, atopamos un candidato prometedor no marco da familia das teorías de campos efectivas coñecidas como modelos Skyrme, concretamente, o modelo Skyrme *near-BPS*. Unha proposta razoable para este modelo near-BPS é a seguinte

$$\mathscr{L} = \mathscr{L}_{BPS} + \varepsilon(\mathscr{L}_0 + \mathscr{L}_2 + \mathscr{L}_4), \tag{7.1}$$

con $\mathscr{L}_{BPS} = \tilde{\mathscr{L}_0} + \mathscr{L}_6$ e ε sendo un parámetro pequeno, polo que engadiríamos as contribucións Skyrme estándares ao modelo BPS dun xeito perturbativo. Aquí deberiamos escoller $\mathscr{L}_0$ como o potencial Skyrme estándar xa que con esta elección temos a vantaxe de que as intensidades relativas entre o termo do modelo sigma e o potencial Skyrme estándar poden ser fixadas aos seus valores físicos para reproduciren trivialmente a masa correcta do pión. Polo tanto, a conclusión principal que se pode sacar desta tese é o feito de que o modelo near-BPS consitúe unha teoría efectiva das interaccións fortes moi prometedora, xunto coa idea de que a contribución principal vén da parte BPS. En realidade, ao longo desta tese temos atopado fortes evidencias que non só sosteñen a hipótese de que este modelo Skyrme BPS proporciona a contribución principal á teoría, senón que tamén describe propiedades moi importantes da materia nuclear. Por exemplo, séguese inmediatamente da propiedade BPS que a masa e o número bariónico están relacionados linealmente, i.e., $E \sim |B|$, ademais da relación fenomenolóxica para os radios nucleares $R_0 \sim |B|^{1/3}$ (ambos comportamentos son feitos experimentais básicos). Esta é unha das principais razóns polas que nos centramos no modelo Skyrme BPS neste traballo. Sabemos que, aínda que a teoría completa precisa a inclusión de contribucións adicionais, esta teoría BPS pode proporcionar unha primeira e importante ollada ao mundo nuclear, polo menos cualitativamente. En realidade, este modelo pódese ver coma o límite da teoría near-BPS cando $\varepsilon \to 0$. De feito, polo comentado anteriormente, é máis natural considerar potenciais $\tilde{\mathscr{L}_0}$ cunha approximación ao baleiro máis rápida que cuártica. Non obstante, consideramos $\tilde{\mathscr{L}_0}$ igual ao potencial Skyrme estándar con frecuen-

cia, esencialmente por simplicidade e asumindo que moitas propiedades dos Skyrmións BPS non dependen demasiado desta escolla.

Hai tamén outros resultados importantes deste traballo coma o estudo das resonancias Roper ou a termodinámica do modelo Skyrme BPS a cero temperatura, e o cálculo de solucións Skyrmiónicas para presión externa non nula que presentamos no Capítulo 3. Aquí atopamos que todas as solucións estáticas do modelo Skyrme BPS son solucións de presión constante. Concretamente, os Skyrmións BPS teñen presión cero mentres que solucións con presión non nula precisan ser estabilizados pola presión externa. Ademais, concluímos que no caso de solucións compactas cun radio definido, o volume xeométrico correspóndese co volume físico dado que cumpre a relación termodinámica $P = -\frac{dE}{dV}$. Trátase dun feito moi importante porque esta relación non é nada obvia dentro dos modelos Skyrme.

Neste marco termodinámico, tamén estudamos dúas cantidades importantes, a compresibilidade e o potencial químico bariónico. No caso da compresibilidade usamos potenciais simples da forma $\mathcal{U}(\eta) = \eta^\beta$ con $\eta = \frac{1}{2}(\xi - \sin\xi\cos\xi)$ e ξ a función perfil habitual. Aquí, o punto destacado é que o resultado non depende da forma específica do pontecial senón da súa aproximación ao baleiro $\mathcal{U}(\eta) = \eta^\beta \sim \xi^\alpha$ con $\alpha = 3\beta$. Deste xeito, considerando o modelo Skyrme BPS, obtemos una compresibilidade infinita para $\alpha \geq 2$, mentres que para $\alpha < 2$ obtemos valores finitos. Non obstante, estes ponteciais son problemáticos debido a que a segunda variación ao redor do baleiro é infinita. Polo tanto, os potenciais físicamente aceptables son aqueles cunha aproximación $\alpha \geq 2$, o que implica que a compresibilidade infinita no equilibrio (a $P = 0$) é unha propiedade xeral. Ademais, tamén tratamos co alto módulo de compresión (baixa compresibilidade) obtido para os modelos Skyrme. Unha fonte deste problema pódese deber á suposición dun rescalado uniforme (Derrick) da densidade bariónica baixo presión externa que leva á Skyrmións moito máis incompresibles que a materia nuclear. Sen embargo, vimos que esta hipótese só é aplicable cando a densidade bariónica é constante. Claramente, non é o caso do modelo Skyrme BPS, polo que este rescalado non pode ser considerado e o valor correcto do módulo de compresión é, en realidade, cero (ou equivalentemente, unha compresibilidade infinita).

Tamén analizamos outra cantidade termodinámica importante a $T = 0$, o potencial químico bariónico que resultou ser simplemente a densidade bariónica multiplicada por unha constante global. Neste punto tamén introducimos unha descrición de campo medio baseada en integrais promedio sobre o espazo de chegada, polo que non precisamos coñecer ningunha solución específica do modelo. Ademais, dado que o potencial escalón é constante, neste caso, os dous tratamentos coinciden. Non obstante, para outros potenciais atopamos que o potencial químico bariónico exacto é máis axeitado que a versión de

campo medio, xa que as cantidades locais cambian substancialmente no límite de campo medio.

Respecto aos núcleos, empregamos o modelo Skyrme BPS para o estudo das súas enerxías de enlace. Trátase dun cálculo clave xa que amosa a importancia da contribución da parte BPS do Lagranxiano, pero ao mesmo tempo, tamén amosa a necesidade das contribucións perturbativas dos outros termos para unha mellor descrición dos núcleos pequenos. Aquí, a propiedade BPS é crucial para obter as pequenas enerxías de enlace físicas porque dá, exactamente, enerxías de enlace nulas. Así, os valores distintos de cero obtéñense grazas a contribucións adicionais que veñen dadas por: a cuantización semiclásica de espín e isospín, a enerxía de Coulomb e a rotura da simetría de isospín. Seguindo este procedemento, e con só tres parámetros libres, acadamos moi bos resultados para as enerxías de enlace dos núcleos con número bariónico alto. O feito de que non funcione tan ben para núcleos máis lixeiros é tamén de esperar, dado que o modelo Skyrme BPS baséase nunha descrición colectiva dos graos de liberdade fundamentais. Este tratamento é bastante realista para núcleos grandes, pero ao estudar os pequenos, as propiedades dunha partícula e os graos de liberdade piónicos tórnanse relevantes, polo que a extensión á teoría near-BPS é precisa.

Tamén paga a pena comentar que no estudo das enerxías de enlace, o feito de que os núcleos reais non son axialmente simétricos non inflúe moito nos nosos resultados, debido a que a súa desviación dunha densidade bariónica esféricamente simétrica non é moi marcada. Non obstante, noutros eidos como a espectroscopía nuclear e as correspondentes restricción s de Finkelstein-Rubinstein, as verdadeiras simetrías son realmente importantes. Ademais, no que atinxe á elección do potencial, parece que outra vez é máis importante como se achega ao baleiro que a súa forma concreta, polo menos para o modelo Skyrme BPS.

Finalmente, acoplamos con éxito o modelo Skyrme BPS á gravidade facendo posible unha descrición das estrelas de neutróns. Deste xeito, acadamos unha descrición unificada da materia nuclear, onde dende un axuste dos parámetros á masa e o radio do nucleón, obtivemos resultados moi prometedores das masas e radios das estrelas de neutróns. De feito, coinciden bastante ben coa restricción observacional $M_{\max} \sim 2.5 M_{\odot}$ (os radios observacionais das estrelas de neutróns non están tan ben establecidos). Ademais, a utilización destes parámetros axustados á materia nuclear para o estudo das estrelas de neutróns, supón unha extrapolación dende un réxime non relativista a un relativista.

É importante decatarse de que o cálculo exacto, co efecto da gravidade incuído, é diferente do tratamento TOV habitual, o cal tamén se pode levar a cabo por medio dunha aproximación de campo medio. O cálculo TOV baséase

nunha equación de estado universal $p = p(\rho)$, pero na teoría de campos completa isto non se cumpre en xeral e só se pode acadar cunha aproximación. A pesar disto, é posible chegar numericamente a unha ecuación de estado *on-shell* grazas ás solucións $p(r)$ e $\rho(r)$, aínda que esta ecuación non é universal e depende do número bariónico B. En contreto, atopamos $p = a(B)\rho^{b(B)}$. Ademais, observamos que a rixidez desta ecuación de estado diferencia en gran medida as curvas $M(R)$ dos cálculos exactos dos resultados habituais do tratamento TOV. En xeral, temos masas que crecen co radio das estrelas de neutróns en contraste co comportamento común dun radio que se mantén basicamente constante e que pode incluso diminuír coa masa. Non obstante, debemos salientar que os datos observacionais non desbotan ningún comportamento, e de feito, o noso tratamento exacto da teoría cumpre coas restricción observacionais impostas dun xeito moi natural.

Se consideramos o límite de campo medio, obtemos resultados similares ao estudar propiedades globais, mentres que as cantidades locais difiren notablemente. Asemade, podemos concluír que canto máis plano é un potencial, maior é a concordancia entre ambos os dous tratamentos (e igual para o potencial escalón).

Polo tanto, tendo en conta todo o que foi aquí exposto, non é unha esaxeración dicir que estamos ante un excitante rexurdimento das ideas de Skyrme apuntando cara a correcta dirección para acadar unha teoría efectiva que describa o límite de baixas enerxías de QCD.

Appendix A

Eigenstates of Spin and Isospin

The key objects for the calculation of matrix elements are the eigenstates of spin and isospin. Thus, following [198], we have a possible candidate:

$$\mathscr{D}^{j}_{m,m'}(A) = [(j+m)!(j-m)!(j+m')!(j-m')!]^{1/2} \sum_{n_i>0} \frac{a^{n_1} b^{n_2} c^{n_3} d^{n_4}}{n_1! n_2! n_3! n_4!} \quad \text{(A.1)}$$

with $A \in \mathrm{SU}(2)$. Now, we want these states to be eigenstates of the spin and isospin operators given in [10]:

$$\begin{aligned} I_k &= \frac{1}{2} i \left(a_0 \frac{\partial}{\partial a_k} - a_k \frac{\partial}{\partial a_0} - \varepsilon_{klm} a_l \frac{\partial}{\partial a_m} \right) \\ &\Rightarrow I_3 = \frac{1}{2} i \left(a_0 \frac{\partial}{\partial a_3} - a_3 \frac{\partial}{\partial a_0} - a_1 \frac{\partial}{\partial a_2} + a_2 \frac{\partial}{\partial a_1} \right), \end{aligned} \quad \text{(A.2)}$$

$$\begin{aligned} J_k &= \frac{1}{2} i \left(a_k \frac{\partial}{\partial a_0} - a_0 \frac{\partial}{\partial a_k} - \varepsilon_{klm} a_l \frac{\partial}{\partial a_m} \right) \\ &\Rightarrow J_3 = \frac{1}{2} i \left(a_3 \frac{\partial}{\partial a_0} - a_0 \frac{\partial}{\partial a_3} - a_1 \frac{\partial}{\partial a_2} + a_2 \frac{\partial}{\partial a_1} \right). \end{aligned} \quad \text{(A.3)}$$

After some modifications of the expression (A.1) in order to have the same states appearing in [10], we can conclude that the eigenstates are given by the hyperspherical harmonics on $\mathbb{S}^3$:

$$Y_{2j,m_I,m_S} = [(2j+1)/2\pi^2]^{1/2} \mathscr{D}^{j}_{m_I,m_S}(A), \quad \text{(A.4)}$$

$$2j = 0, 1, \ldots \qquad -j \leq m_i \leq j, \qquad A \in \mathrm{SU}(2),$$

where

$$\mathscr{D}^{j}_{m_I,m_S}(A) = [(j+m_I)!(j-m_I)!(j+m_S)!(j-m_S)!]^{1/2} \sum_{n_i>0} \frac{a^{n_1} b^{n_2} c^{n_3} d^{n_4}}{n_1! n_2! n_3! n_4!}, \quad \text{(A.5)}$$

with

$$\begin{aligned} a &= ia_0 - a_3, & c &= ia_2 + a_1, \\ b &= ia_2 - a_1, & d &= -ia_0 - a_3, \\ n_1 + n_2 &= j - m_I, & n_3 + n_4 &= j + m_I, \\ n_1 + n_3 &= j + m_S, & n_2 + n_4 &= j - m_S. \end{aligned} \tag{A.6}$$

And which reproduce the expressions of the states given in [10].

All this discussion is useful for the case $n = 1$, where iso-rotations and rotations are equivalents. However, for $n \neq 1$, we have to consider the basis for nuclear states as the direct product:

$$|X\rangle = |i\, i_3\, k_3\rangle\ |j\, j_3\, l_3\rangle, \tag{A.7}$$

where each ket has the expression of the states on $\mathbb{S}^3$ seen in (A.4) as function of the SU(2) matrices A and B for the isospin and spin states respectively.

Looking at those expressions, for the isospin ket we are going to consider the third component of the isospin as the same we had before in Eq. (A.2), whereas the third component of the spin becomes the third component of the body-fixed isospin operator, K_3:

$$I_3 = \frac{1}{2} i \left(a_0 \frac{\partial}{\partial a_3} - a_3 \frac{\partial}{\partial a_0} - a_1 \frac{\partial}{\partial a_2} + a_2 \frac{\partial}{\partial a_1} \right), \tag{A.8}$$

$$K_3 = \frac{1}{2} i \left(a_3 \frac{\partial}{\partial a_0} - a_0 \frac{\partial}{\partial a_3} - a_1 \frac{\partial}{\partial a_2} + a_2 \frac{\partial}{\partial a_1} \right). \tag{A.9}$$

This assumption is confirmed by calculating the corresponding commutators (see [13])

$$[I_i, A] = -\frac{1}{2} \tau_i A, \qquad [K_i, A] = \frac{1}{2} A \tau_i. \tag{A.10}$$

On the other hand, for the spin part of the basis we can identify now the old third component of isospin with L_3, so the corresponding commutators are also satisfied:

$$[J_i, B] = \frac{1}{2} B \tau_i \qquad [L_i, B] = -\frac{1}{2} \tau_i B. \tag{A.11}$$

Thus, the operators we have, are:

$$J_3 = \frac{1}{2} i \left(b_3 \frac{\partial}{\partial b_0} - b_0 \frac{\partial}{\partial b_3} - b_1 \frac{\partial}{\partial b_2} + b_2 \frac{\partial}{\partial b_1} \right), \tag{A.12}$$

$$L_3 = \frac{1}{2} i \left(b_0 \frac{\partial}{\partial b_3} - b_3 \frac{\partial}{\partial b_0} - b_1 \frac{\partial}{\partial b_2} + b_2 \frac{\partial}{\partial b_1} \right). \tag{A.13}$$

Finally, we need a parametrization as function of angular variables to calculate the integrals corresponding to the matrix elements, i.e.,

$$\begin{aligned} a_0 &= \cos\chi_a, \\ a_1 &= \sin\chi_a\ \sin\theta_a\ \cos\phi_a, \\ a_2 &= \sin\chi_a\ \sin\theta_a\ \sin\phi_a, \\ a_3 &= \sin\chi_a\ \cos\theta_a, \end{aligned} \tag{A.14}$$

where the angles take the values

$$\chi_a, \theta_a \in [0, \pi], \qquad\qquad \phi_a \in [0, 2\pi],$$

and the solid angle element is

$$d\Omega_a = \sin^2\chi_a\ \sin\theta_a\, d\chi_a d\theta_a d\phi_a. \tag{A.15}$$

Of course we will have similar expressions for the B matrix coordinates.

It is also useful to notice that there exist an alternative but similar definition for the partial states of spin and isospin using the Euler angles α, β and γ. For instance, the quantum state corresponding to isospin will be given, up to a $(-1)^{m'}$ factor, by the complex conjugate of Wigner's D matrix, $D^{(j)}_{mm'}(\alpha, \beta, \gamma)$, where j, m and m' are the total isospin and the third component of the isospin in the space-fixed and body-fixed frames respectively. Equivalently,

$$|j\, m\, m'\rangle = (-1)^{m'} D^{(j)*}_{m-m'}(\alpha, \beta, \gamma). \tag{A.16}$$

And Wigner's matrix reads [199]

$$D^{(j)}_{mm'}(\alpha, \beta, \gamma) = e^{-im\alpha} d^{(j)}_{mm'}(\beta) e^{-im'\gamma}, \tag{A.17}$$

where

$$\begin{aligned} d^{(j)}_{mm'}(\beta) = \quad & (-1)^{m-m'} \left[\frac{(j+m)!(j-m)!}{(j+m')!(j-m')!}\right]^{1/2} \left(\cos\frac{\beta}{2}\right)^{m+m'} \left(\sin\frac{\beta}{2}\right)^{m-m'} \\ & \cdot P^{(m-m', m+m')}_{j-m}(\cos\beta), \end{aligned} \tag{A.18}$$

with

$$P^{(\mu,\nu)}_n(\cos\beta) = \begin{pmatrix} n+\mu \\ n \end{pmatrix} F(-n, n+\mu+\nu; \mu+1; \sin^2(\beta/2)), \tag{A.19}$$

and F being the hypergeometric function.

USC
UNIVERSIDADE
DE SANTIAGO
DE COMPOSTELA

Appendix B

Vanishing Non-diagonal Matrix Elements

We will show that the non-diagonal matrix elements $\langle X|R_iK_j + K_jR_i|X\rangle$ which appear when calculating the expectation value of the electric charge density vanish. Here, we will use the Euler angles, so the body-fixed isospin angular momentum reads

$$\begin{aligned} K_1 &= -i\left(\frac{\cos\gamma}{\sin\beta}\frac{\partial}{\partial\alpha} - \sin\gamma\frac{\partial}{\partial\beta} - \cot\beta\cos\gamma\frac{\partial}{\partial\gamma}\right), \\ K_2 &= -i\left(-\frac{\sin\gamma}{\sin\beta}\frac{\partial}{\partial\alpha} - \cos\gamma\frac{\partial}{\partial\beta} + \cot\beta\sin\gamma\frac{\partial}{\partial\gamma}\right), \\ K_3 &= i\frac{\partial}{\partial\gamma}, \end{aligned} \tag{B.1}$$

While the $\vec{R}$ coming from the isospin collective coordinates is

$$R_1 = -\cos\gamma\sin\beta, \qquad R_2 = \sin\gamma\sin\beta, \qquad R_3 = \cos\beta, \tag{B.2}$$

where the relation used between the a_0, a_i SU(2) coordinates and the Euler angles is

$$a_0 = -\cos\frac{\beta}{2}\cos\left[\frac{1}{2}(\alpha+\gamma)\right], \tag{B.3}$$

$$a_1 = -\sin\frac{\beta}{2}\sin\left[\frac{1}{2}(\alpha-\gamma)\right], \tag{B.4}$$

$$a_2 = \sin\frac{\beta}{2}\cos\left[\frac{1}{2}(\alpha-\gamma)\right], \tag{B.5}$$

$$a_3 = \cos\frac{\beta}{2}\sin\left[\frac{1}{2}(\alpha+\gamma)\right]. \tag{B.6}$$

Therefore, it can be easily checked that the following commutator holds

$$[K_i, R_j] = i\varepsilon_{ijk} R_k. \tag{B.7}$$

As we have commented at the end of Appendix A, the nuclear wave function can be defined in terms of Wigner's D matrices, Eq. (A.16). Since for the present purpose we are only interested in the isospin part, it will be enough to consider just

$$|j\, m\, m'\rangle = (-1)^{m'} D^{(j)*}_{m,-m'}. \tag{B.8}$$

where we will use j for the isospin quantum number to avoid the confusion with the imaginary unit. Furthermore, m and m' will be the space-fixed and body-fixed third components of isospin respectively.

This D matrix is given by

$$\begin{aligned} D^{(j)}_{mm'} &= \langle jm|R(\alpha,\beta,\gamma)|jm'\rangle = \langle jm|e^{-i\alpha J_z} e^{-i\beta J_y} e^{-i\gamma J_z}|jm'\rangle \\ &= e^{-im\alpha}\langle jm|e^{-i\beta J_y}|jm'\rangle e^{-im'\gamma} = e^{-im\alpha} d^{(j)}_{mm'}(\beta) e^{-im'\gamma}, \end{aligned} \tag{B.9}$$

Then, it is trivial to see that when applying K_3 to the nuclear state,

$$K_3|jmm'\rangle = m'|jmm'\rangle. \tag{B.10}$$

so we expect the action of $\vec{K}$ on nuclear states to be equivalent to the action of the standard representation of angular momentum [in our case $\vec{K}$ fulfils the standard angular momentum algebra, see Eq. (4.63)]. Indeed, we can define

$$\left.\begin{aligned} K_+ &= K_1 - iK_2 \\ K_- &= K_1 + iK_2 \end{aligned}\right\} \Longrightarrow K_1 = \frac{1}{2}(K_+ + K_-), \qquad K_2 = \frac{1}{2} i (K_+ - K_-), \tag{B.11}$$

with these K_+ and K_- acting as follows,

$$K_+|j,m,m'\rangle = \sqrt{j(j+1) - m'(m'+1)}\,|j,m,m'+1\rangle, \tag{B.12}$$

$$K_-|j,m,m'\rangle = \sqrt{j(j+1) - m'(m'-1)}\,|j,m,m'-1\rangle. \tag{B.13}$$

Now, we can focus on our nuclear states (remember we always have $m' = 0$) where the situation is even simpler because the D matrix can be written as a spherical harmonic [199],

$$D^{(j)}_{m0}(\alpha,\beta,\gamma) = \sqrt{\frac{4\pi}{2j+1}} Y^*_{jm}(\beta,\alpha), \tag{B.14}$$

so the isospin state reads

$$|j\,m\,0\rangle = D^{(j)*}_{m0}(\alpha,\beta,\gamma) = \sqrt{\frac{4\pi}{2j+1}}Y_{jm}(\beta,\alpha), \tag{B.15}$$

Now, we can study the non-diagonal matrix elements. Because of the symmetry of our ansatz, it is just enough to see if the three following ones vanish (we avoid to repeatedly write the $k_3 = 0$ in the nuclear state): $\langle j\,m|K_1R_2 + R_2K_1|j\,m\rangle$, $\langle j\,m|K_1R_3 + R_3K_1|j\,m\rangle$ and $\langle j\,m|K_3R_1 + R_1K_3|j\,m\rangle$. As well, we will find useful this property of spherical harmonics,

$$Y^*_{jm}(\alpha,\beta) = (-1)^m Y_{j,-m}(\alpha,\beta). \tag{B.16}$$

i) $\langle \boldsymbol{j\,m|K_1R_2 + R_2K_1|j\,m}\rangle$

This is the most complicated case. The corresponding matrix element is given by

$$\langle j\,m|K_1R_2 + R_2K_1|j\,m\rangle = \langle j\,m|2R_2K_1 + [K_1,R_2]|j\,m\rangle. \tag{B.17}$$

For the first integral we need to analyse how the operator K_1 acts on the nuclear state $|j\,m\rangle \sim Y_{jm}(\beta,\alpha)$. Looking its definition we see it contains three derivatives with respect to the three Euler angles α, β and γ. Since the nuclear state does not depend on the angle γ, the corresponding derivative vanishes. As well, the derivative ∂_α is multiplied by $\sin\gamma\cos\gamma$ (remember that $R_2 = \sin\gamma\sin\beta$) which integrates to zero, i.e.,

$$\int_0^{2\pi} d\gamma \sin\gamma\cos\gamma = 0. \tag{B.18}$$

Thus, the β derivative term leads to

$$\langle j\,m|2R_2K_1|j\,m\rangle = \frac{-8i}{2i+1}\int_0^{2\pi} d\alpha \int_0^{2\pi} d\gamma \int_0^{2\pi} \sin\beta d\beta \sin^2\gamma Y^*_{jm} \sin\beta\partial_\beta Y_{jm} = 0. \tag{B.19}$$

To see this integral vanishes we can write the spherical harmonic as function of the associated Legendre functions, $Y_{jm}(\beta,\alpha) = c_{jm}e^{im\alpha}P_{jm}(t)$, where $t = \cos\beta$ and $\sin\beta\partial_\beta = -(1-t^2)\partial_t$. Then, using the recurrence formula

$$(1-t^2)\partial_t P_{jm}(t) = \frac{1}{2j+1}[(j+1)(j+m)P_{j-1,m}(t) + j(j-m+1)P_{j+1,m}(t)], \tag{B.20}$$

we see that the derivative of the spherical harmonic Y_{jm} will give rise to two different terms: one term proportional to $Y_{j-1,m}$, and another one with $Y_{j+1,m}$. Therefore, the integral is zero because of the orthogonality of the spherical harmonics.
We still have to calculate the second term of the matrix element. Taking into account the commutator relations we can write

$$[K_1, R_2] = iR_3 = i\cos\beta = i\sqrt{\frac{4\pi}{3}}Y_{10}, \tag{B.21}$$

so we find

$$\langle j\, m|[K_1, R_2]|j\, m\rangle = \frac{(4\pi)^{3/2}i}{\sqrt{3}(2j+1)}\int_0^{2\pi} d\alpha \int_0^{2\pi} d\gamma \int_0^{\pi} \sin\beta d\beta Y^*_{jm} Y_{10} Y_{jm}. \tag{B.22}$$

Now, we will use the expression for the integral of three spherical harmonics [remember property (B.16)]:

$$\int_0^{2\pi} d\phi \int_0^{\pi} \sin\theta d\theta Y_{l_1 m_1}(\theta,\phi)\theta Y_{l_2 m_2}(\theta,\phi)\theta Y_{l_3 m_3}(\theta,\phi)$$

$$= \sqrt{\frac{(2l_1+1)(2l_2+1)(2l_3+1)}{4\pi}} \begin{pmatrix} l_1 & l_2 & l_3 \\ m_1 & m_2 & m_3 \end{pmatrix} \begin{pmatrix} l_1 & l_2 & l_3 \\ 0 & 0 & 0 \end{pmatrix}, \tag{B.23}$$

where these last two elements are known as Wigner 3-j symbols [199]. One of their properties is

$$\begin{pmatrix} l_1 & l_2 & l_3 \\ 0 & 0 & 0 \end{pmatrix} = 0 \qquad \text{if} \quad l_1 + l_2 + l_3 \quad \text{is odd.} \tag{B.24}$$

Since in our case we have $l_1 = j$, $l_2 = 1$, $l_3 = j$, then $l_1 + l_2 + l_3 = 2j + 1$, so this integral is also zero and the matrix element vanishes.

ii) $\langle j\, m|K_1R_3 + R_3K_1|j\, m\rangle$

This case is much easier. The matrix element is given by

$$\langle j\, m|K_1R_3 + R_3K_1|j\, m\rangle = \langle j\, m|2R_3K_1 + [K_1, R_3]|j\, m\rangle. \tag{B.25}$$

Now, in the first term we have R_3K_1, where $R_3 = \cos\beta$, so the γ dependence will be a factor of $\sin\gamma$ or $\cos\gamma$ in the K_1 operator. Therefore, when integrating

this term will vanish. On the other hand, the commutator of the second term is $[K_1, R_3] = -iR_2 = -i \sin\gamma \sin\beta$. Since the isospin states do not depend on γ because $m' = 0$, the integral over γ, which is just the integral of $\sin\gamma$, is zero. The matrix element also vanishes.

iii) $\langle j\, m|K_3R_1 + R_1K_3|j\, m\rangle$

In this case we have

$$\langle j\, m|K_3R_1 + R_1K_3|j\, m\rangle = \langle j\, m|2R_1K_3 + [K_3, R_1]|j\, m\rangle. \tag{B.26}$$

The K_3 operator only has a derivative with respect to the angle γ, as a consequence, the first term is trivially zero, whereas the term with the commutator is just the same as before but with an extra minus sign, i.e., $[K_3, R_1] = iR_2 = i \sin\gamma \sin\beta$, so it also vanishes and the corresponding matrix element is zero again.

USC
UNIVERSIDADE
DE SANTIAGO
DE COMPOSTELA

Bibliography

[1] D. J. Gross and F. Wilczek, Phys. Rev. Lett. **30**, 1343 (1973). (Cited on page 1.)

[2] H. D. Politzer, Phys. Rev. Lett. **30**, 1346 (1973). (Cited on page 1.)

[3] T. H. R. Skyrme, Proc. Roy. Soc. Lon. **260**, 127 (1961). (Cited on pages 1 and 5.)

[4] T. H. R. Skyrme, Nucl. Phys. **31**, 556 (1962). (Cited on pages 1 and 5.)

[5] T. H. R. Skyrme, J. Math. Phys. **12**, 1735 (1971). (Cited on pages 1 and 5.)

[6] A. T. Filippov, *The Versatile Soliton* (Birkhäuser, Boston, 2000). (Cited on page 1.)

[7] G. t'Hooft, Nucl. Phys. B **72**, 461 (1974). (Cited on page 2.)

[8] E. Witten, Nucl. Phys. B **160**, 57, (1979). (Cited on page 2.)

[9] E. Witten, Nucl. Phys. B **223**, 433 (1983). (Cited on page 2.)

[10] G. S. Adkins, C. R. Nappi, and E. Witten, Nucl. Phys. B **228**, 552 (1983). (Cited on pages 2, 60, 137 and 138.)

[11] G. S. Adkins and C. R. Nappi, Nucl. Phys. B **233**, 109 (1984). (Cited on pages 2, 6, 17 and 60.)

[12] E. Braaten and L. Carson, Phys, Rev. Lett., **56**, 1897 (1986). (Cited on pages 2 and 60.)

[13] E. Braaten and L. Carson, Phys. Rev. D **38**, 3525 (1988). (Cited on pages 2, 60, 69 and 138.)

[14] L. Carson, Phys. Rev. Lett. **66**, 1406 (1991). (Cited on page 2.)

[15] L. Carson, Nucl. Phys. A **535**, 479 (1991). (Cited on page 2.)

[16] T. S. Walhout, Nucl. Phys. A **531**, 596 (1991). (Cited on page 2.)

[17] P. O. Mazur, M. A. Nowak, and M. Praszalowicz, Phys. Lett. B **147**, 137 (1984). (Cited on page 2.)

[18] C. G. Callan and I. Klebanov, Nucl. Phys. B **262**, 365 (1985). (Cited on page 2.)

[19] N. N. Scoccola, H. Nadeau, M. A. Nowak, and M. Rho, Phys Lett. B **201**, 425 (1988). (Cited on page 2.)

[20] O. V. Manko, N. S. Manton, and S. W. Wood, Phys. Rev. C **76**, 055203 (2007). (Cited on page 2.)

[21] R. A. Battye, N. S. Manton, P. M. Sutcliffe, and S. W. Wood, Phys. Rev. C **80**, 034323 (2009). (Cited on pages 2 and 7.)

[22] P. M. Sutcliffe, JHEP **08**, 019 (2010). (Cited on page 2.)

[23] C. Adam, J. Sanchez-Guillen, and A. Wereszczynski, Phys. Lett. B **691**, 105 (2010). (Cited on pages 2, 5, 9, 15 and 77.)

[24] C. Adam, J. Sanchez-Guillen, and A. Wereszczynski, Phys. Rev. D **82**, 085015 (2010). (Cited on pages 2, 5, 9, 11, 15, 17 and 77.)

[25] E. B. Bogomolny, Sov.J.Nucl.Phys. **24**, 449 (1976). (Cited on page 2.)

[26] M. K. Prasad and C. M. Sommerfield, Phys.Rev.Lett. **35**, 760 (1975). (Cited on page 2.)

[27] R. A. Battye, M. Haberichter, and S. Krusch, Phys. Rev. D **90**, 125035 (2015). (Cited on pages 3 and 131.)

[28] D. Foster and S Krusch, arXiv: 1412.8719 [hep-th]. (Cited on page 3.)

[29] P. H. C. Lau and N. S. Manton, Phys. Rev. Lett. **113**, 232503 (2014). (Cited on page 3.)

[30] M. Gillard, D. Harland, and J. M. Speight, Nucl. Phys. B **895**, 272 (2015). (Cited on page 3.)

[31] D. Harland, Phys. Lett. B **728**, 518 (2014). (Cited on page 3.)

[32] C. Adam and A. Wereszczynski, Phys. Rev. D **89**, 065010 (2014). (Cited on page 3.)

[33] C. Adam, C. Naya, J. Sanchez-Guillen, and A. Wereszczynski, Phys. Lett. B **726**, 892 (2013). (Cited on pages 5 and 16.)

[34] G. H. Derrick, J. Math. Phys. **5**, 1252 (1964). (Cited on page 6.)

[35] V. G. Makhankov, Y. P. Rybakov, and V. I. Sanyuk, *The Skyrme Model* (Springer-Verlag, Berlin, 1993). (Cited on page 7.)

[36] N. Manton and P. Sutcliffe, *Topological Solitons* (Cambridge University Press, Cambridge, England, 2007). (Cited on page 7.)

[37] R. A. Battye and P. M. Sutcliffe, Phys. Rev. Lett. **79**, 363 (1997). (Cited on page 7.)

[38] R. A. Battye and P. M. Sutcliffe, Phys. Rev. Lett. **86**, 3989 (2001). (Cited on page 7.)

[39] R. A. Battye and P. M. Sutcliffe, Rev. Math. Phys. **14**, 29 (2002). (Cited on page 7.)

[40] R. A. Battye and P. M. Sutcliffe, Nuc. Phys. B **705**, 384 (2005). (Cited on pages 7 and 17.)

[41] R. A. Battye and P. M. Sutcliffe, Phys. Rev. C **73**, 055205 (2006). (Cited on pages 7 and 17.)

[42] A. Jackson, A. D. Jackson, A. S. Goldhaber, G. E. Brown, and L. C. Castillejo, Phys. Lett. B **154**, 101 (1985). (Cited on page 8.)

[43] K. Arthur, G. Roche, D. H. Tchrakian, and Y. Tang, J. Math. Phys. **37**, 2569 (1996). (Cited on page 8.)

[44] I. Floratos and B. Piette, Phys. Rev. D **64**, 045009 (2001). (Cited on page 8.)

[45] V. B. Kopeliovich, A. M. Shunderuk, and G. K. Matushko, Phys. Atom. Nucl. **69**, 120 (2006). (Cited on pages 8 and 86.)

[46] C. Adam, T. Klähn, C. Naya, J. Sanchez-Guillen, R. Vazquez, and A. Wereszczynski, arXiv: 1504.05185 [hep-th]. (Cited on pages 9 and 23.)

[47] C. Adam, J. Sanchez-Guillen, and A. Wereszczynski, J. Math. Phys. **47**, 022303 (2006). (Cited on page 11.)

[48] C. Adam, J. Sanchez-Guillen, and A. Wereszczynski, J. Math. Phys. **48**, 032302 (2007). (Cited on page 11.)

[49] R. Slobodeanu, Int. J. Geom. Methods Mod. Phys. **08**, 1763 (2011). (Cited on page 11.)

[50] O. Alvarez, L. A. Ferreira, and J. Sanchez-Guillen, Nucl. Phys. B **529**, 689 (1998). (Cited on page 11.)

[51] J. M. Speight, J. Geom. Phys. **92**, 30 (2015). (Cited on page 13.)

[52] P. Sutcliffe, Phys. Rev. D **79**, 085014 (2009). (Cited on page 17.)

[53] C. Hajduk and B. Schwesinger, Phys. Lett. B **140**, 172 (1984). (Cited on page 17.)

[54] L. C. Biedenharn, Y. Dothan, and M. Tarlini, Phys. Rev. D **31**, 649 (1985). (Cited on pages 17, 21 and 22.)

[55] U.-G. Meissner and I. Zahed, Adv. Nucl. Phys. **17**, 143 (1986). (Cited on pages 17, 21 and 22.)

[56] J. Schechter and H. Weigel, Phys. Rev. D **44**, 2916 (1991). (Cited on page 17.)

[57] J. Schechter and H. Weigel, Phys. Lett. B **261**, 235 (1991). (Cited on page 17.)

[58] K. Nakamura, et al., Particle Data Group, J. Phys. G, Nucl. Part. Phys. **37**, 075021 (2010). (Cited on page 21.)

[59] C. Adam, C. Naya, J. Sanchez-Guillen, J. M. Speight, and A. Wereszczynski, Phys. Rev. D **90**, 045003 (2014). (Cited on pages 23 and 29.)

[60] N. Manton (private communication). (Cited on page 23.)

[61] I. Klebanov, Nucl. Phys. B **262**, 133 (1985). (Cited on page 23.)

[62] L. Castillejo, P. S. J. Jones, A. D. Jackson, J. J. M. Verbaarschot, and A. Jackson, Nucl. Phys. A **501**, 801 (1989). (Cited on page 23.)

[63] M. Kugler and S. Shtrikman, Phys. Lett B **208**, 491 (1988). (Cited on page 23.)

[64] M. Kugler and S. Shtrikman, Phys. Rev. D **40**, 3421 (1989). (Cited on page 23.)

[65] J. M. Speight, Commun. Math. Phys. **332**, 355 (2014). (Cited on page 23.)

[66] L. D. Landau and E. M. Lifshitz, *Statistical Physics* (Pergamon Press, London, 1958). (Cited on page 23.)

[67] B. K. Jennings and A. D. Jackson, Phys. Rep. **66**, 141 (1980). (Cited on pages 23 and 25.)

[68] J. P. Blaizot, Phys. Rep. **64**, 171 (1980). (Cited on pages 23 and 25.)

[69] M. Nowak and I. Zahed, Phys. Lett. B **230**, 108 (1989). (Cited on page 24.)

[70] K. J. Eskola and K. Kajantie, Z. Phys. C **44**, 347 (1989). (Cited on page 24.)

[71] R. K. Bhaduri, J. Dey, and M. A. Preston, Phys. Lett. B **136**, 289 (1984). (Cited on page 25.)

[72] M. Dutra, O. Lourenco, J. S. Sa Martins, A. Delfino, J. R. Stone, and P. D. Stevenson, Phys. Rev. C **85**, 035201 (2012). (Cited on page 27.)

[73] D. Bazeia, L. Losano, R. Menezes, and J. C. R. E. Oliveira, Eur. Phys. J. C **51**, 953 (2007). (Cited on page 27.)

[74] D. Bazeia, L. Losano, and R. Menezes, Phys. Lett. B **668**, 246 (2008). (Cited on page 27.)

[75] C. Adam, L. A. Ferreira, E. da Hora, A. Wereszczynski, and W. J. Zakrzewski, J. High Energy Phys. **08**, 062 (2013). (Cited on page 29.)

[76] C. Wellenhofer, J. W. Holt, N. Kaiser, and W. Weise, Phys. Rev. C **89**, 064009 (2014). (Cited on page 40.)

[77] H.-J. Lee, B.-Y. Park, D.-P. Min, M. Rho, and V. Vento, Nucl. Phys. A **723**, 427 (2003). (Cited on page 41.)

[78] H.-J. Lee, B.-Y. Park, M. Rho, and V. Vento, Nucl. Phys. A **726**, 69 (2003). (Cited on page 41.)

[79] B.-Y. Park, M. Rho, and V. Vento, Nucl. Phys. A **736**, 129 (2004). (Cited on page 41.)

[80] H.-J. Lee, B.-Y. Park, M. Rho, and V. Vento, Nucl. Phys. A **741**, 161 (2004). (Cited on page 41.)

[81] B.-Y. Park, M. Rho, and V. Vento, Nucl. Phys. A **807**, 28 (2008). (Cited on page 41.)

[82] B.-Y. Park, H.-J. Lee, and V. Vento, Phys. Rev. D **80**, 036001 (2009). (Cited on page 41.)

[83] T. Sakai and S. Sugimoto, Prog. Theor. Phys. **113**, 843 (2005). (Cited on page 54.)

[84] M. Rozali, H.-H. Shieh, M. Van Raamsdonk, and J. Wu, JHEP **01**, 053 (2008). (Cited on page 54.)

[85] F. Nogueira and J. B. Stang, Phys. Rev. D **86**, 026001 (2012). (Cited on page 54.)

[86] M. Loewe, S. Mendizabal, and J. C. Rojas, Phys. Lett. B **632**, 512 (2006). (Cited on page 54.)

[87] M. Loewe, S. Mendizabal, and J. C. Rojas, Phys. Lett. B **638**, 464 (2006). (Cited on page 54.)

[88] J. A. Ponciano and N. N. Scoccola, Phys. Lett. B **659**, 551 (2008). (Cited on page 54.)

[89] T. D. Cohen , J. A. Ponciano, and N. N. Scoccola, Phys. Rev. D **78**, 034040 (2008). (Cited on page 54.)

[90] B.-H. Lee and C. Park, arXiv: 1503.03615 [hep-th]. (Cited on page 57.)

[91] J. D. Walecka, Ann. Phys. **83**, 491 (1974). (Cited on pages 57, 103 and 109.)

[92] B. D. Serot and J. D. Walecka, Int. J. Mod. Phys. E **6**, 515 (1997). (Cited on pages 57, 103 and 109.)

[93] Y.-L. Ma, M. Harada, H. K. Lee, Y. Oh, B.-Y. Park, and M. Rho, Phys. Rev. D **88**, 014016 (2013). (Cited on page 57.)

[94] U.-G. Meissner, A. M. Rakhimov, A. Wirzba, and U. T. Yakhshiev, Eur. Phys. J. A **32**, 299 (2007). (Cited on page 57.)

[95] U. Yakhshiev and H.-C. Kim, Phys. Rev. C **83**, 038203 (2011). (Cited on page 57.)

[96] C. Adam, C. Naya, J. Sanchez-Guillen, and A. Wereszczynski, Phys. Rev. C **88**, 054313 (2013). (Cited on page 59.)

[97] C. Adam, C. Naya, J. Sanchez-Guillen, and A. Wereszczynski, Phys. Rev. Lett. **111**, 232501 (2013). (Cited on page 59.)

[98] E. Bonenfant, L. Harbour, and L. Marleau, Phys. Rev D **85**, 114045 (2012). (Cited on pages 59, 70, 71, 72, 78 and 83.)

[99] M.-O. Beaudoin and L. Marleau, Nucl. Phys. B **883**, 328 (2014). (Cited on pages 59, 70, 71, 72, 78 and 83.)

[100] D. Finkelstein and J. Rubinstein, J. Math. Phys, **9**, 1762 (1968). (Cited on page 60.)

[101] S. Krusch, Ann. Phys. (NY) **304**, 103 (2003). (Cited on page 60.)

[102] Proc. R. Soc. London A **462**, 2001 (2006). (Cited on page 60.)

[103] V. B. Kopeliovich, Yad. Fiz. **47**, 1495 (1988) [Sov. J. Nucl. Phys. **47**, 949 (1988)]. (Cited on page 60.)

[104] C. Houghton and S. Magee, Phys. Lett. B **632**, 593 (2006). (Cited on pages 60 and 69.)

[105] C. G. Callan and E. Witten, Nucl. Phys. B **239**, 161 (1984). (Cited on pages 71 and 131.)

[106] G.-J. Ding and M.-L. Yan, Phys. Rev. C **75**, 034004 (2007). (Cited on pages 71 and 72.)

[107] B. C. Carlson and G. L. Morley, Am. J. Phys. **31**, 209 (1963). (Cited on page 78.)

[108] E. Rathske, Z. Phys. A **331**, 499 (1988). (Cited on page 81.)

[109] P. Jain, R. Johnson, N. W. Park, J. Schechter, and H. Weigel, Phys. Rev. D **40**, 855 (1989). (Cited on page 81.)

[110] U.-G. Meissner, A. M. Rakhimov, A. Wirzba, and U. T. Yakhshiev, EPJ Web Conf. **3**, 06008 (2010). (Cited on page 81.)

[111] G. Audi, A. H. Wapstra, and C. Thibault, Nucl. Phys. A **729**, 337 (2003). (Cited on pages 84 and 90.)

[112] K. S. Krane, *Introductory Nuclear Physics* (John Wiley & Sons, New York, 1988). (Cited on page 85.)

[113] C. Adam, C. Naya, J. Sanchez-Guillen, R. Vazquez, and A. Wereszczynski, Phys. Lett. B **742**, 136 (2015). (Cited on page 93.)

[114] C. Adam, C. Naya, J. Sanchez-Guillen, R. Vazquez, and A. Wereszczynski, arXiv: 1503.03095 [nucl-th]. (Cited on page 93.)

[115] P. Bizon and T. Chmaj, Phys. Lett. B **297**, 55 (1992). (Cited on page 93.)

[116] B. M. A. G. Piette and G. I. Probert, Phys. Rev. D **75** 125023 (2007). (Cited on page 93.)

[117] S. G. Nelmes and B. M. A. G. Piette, Phys. Rev. D **84**, 085017 (2011). (Cited on page 93.)

[118] T. S. Walhout, Nucl. Phys. A **484**, 397 (1988). (Cited on page 93.)

[119] T. S. Walhout, Nucl. Phys. A **519**, 816 (1990). (Cited on page 93.)

[120] S. G. Nelmes and B. M. A. G. Piette, Phys. Rev. D **85**, 123004 (2012). (Cited on pages 93, 103, 104, 105 and 121.)

[121] S. G. Nelmes, *Skyrmion Stars*, Durham theses (Durham University, 2012), available online at : http://etheses.dur.ac.uk/5258/. (Cited on page 93.)

[122] A. Schmitt, *Dense Matter in Compact Stars*, Lecture Notes in Physics 811 (Springer Verlag, Heidelberg, 2010). (Cited on pages 99 and 109.)

[123] S. Weinberg, *Gravitation and Cosmology* (Wiley, New York, 1972). (Cited on page 100.)

[124] J. M. Lattimer, Annu. Rev. Nucl. Part. Sci. **62**, 485 (2012). (Cited on pages 102, 103, 121 and 122.)

[125] A. W. Steiner, K. M. Lattimer, and E. F. Brown, Astrohphys. J. **765**, L5 (2013). (Cited on pages 102, 103, 121 and 122.)

[126] K. Hebeler, J. M. Lattimer, C. J. Pethick, and A. Schwenk, Astrophys J. **773**, 11 (2013). (Cited on pages 102, 103, 121 and 122.)

[127] J. M. Lattimer and A. W. Steiner, Astrophys. J. **784**, 123 (2014). (Cited on pages 102, 103, 121 and 122.)

[128] F. Özel, G. Baym, and T. Güver, Phys. Rev. D **82**, 101301 (2010). (Cited on pages 102 and 122.)

[129] F. Özel, D. Psaltis, R. Narayan, and A. Santos Villarreal, Astrophys. J. **757**, 55 (2012). (Cited on pages 102 and 122.)

[130] T. Güver and F. Özel, Astrophys. J. **765**, L1 (2013). (Cited on pages 102 and 122.)

[131] C. Cattoen, T. Faber, and M. Visser, Class. Quantum Grav. **22**, 4189 (2005). (Cited on page 104.)

[132] M. Visser, PoS BHGRS 001 (2008). (Cited on page 104.)

[133] D. Horvat, S. Ilijic, and A. Marunovic, Class. Quantum Grav. **28**, 025009 (2011). (Cited on page 104.)

[134] H. Silva, C. Macedo, E. Berti, and L. Crispino, arXiv: 1411.6286 [gr-qc]. (Cited on page 104.)

[135] H. Horowitz and J. Piekarewicz, Phys. Rev. Lett. **86**, 5647 (2001). (Cited on pages 106 and 122.)

[136] H. Horowitz, M. A. Perez-Garcia, D. K. Berry, and J. Piekarewicz, Phys. Rev. C **72**, 035801 (2005). (Cited on pages 106 and 122.)

[137] J. Piekarewicz, J. Phys. Conf. Ser. **492**, 012008 (2014). (Cited on pages 106 and 122.)

[138] R. C. Tolman, Phys. Rev. **55**, 364 (1939). (Cited on page 107.)

[139] J. R. Oppenheimer and G. M. Volkoff, Phys. Rev. **55**, 374 (1939). (Cited on page 107.)

[140] G. Baym and S. A. Chin, Phys. Lett. B **62**, 241 (1976). (Cited on page 108.)

[141] T. Klähn and T Fischer, arXiv: 1503.07442 [nucl-th]. (Cited on page 109.)

[142] J. B. Hartle, Astrophys. J. **150**, 1005 (1967). (Cited on page 118.)

[143] J. B. Hartle and K. S. Thorne, Astrophys. J. **153**, 807 (1968). (Cited on page 118.)

[144] Y-L. Ma, Y. Oh, G-S. Yang, M. Harada, H. K. Kee, B-Y. Park, and M. Rho, Phys. Rev. D **86**, 074025 (2012). (Cited on page 121.)

[145] Y-L. Ma, G-S. Yang, Y. Oh, and M. Harada, Phys. Rev. D **87**, 034023 (2013). (Cited on page 121.)

[146] T. Klähn et al, Phys. Rev. C **74**, 035802 (2005). (Cited on pages 122 and 124.)

[147] E. N. E. van Dalen, C. Fuchs, and A. Faessler, Nucl. Phys. A **744**, 227 (2004). (Cited on page 122.)

[148] E. N. E. van Dalen, C. Fuchs, and A. Faessler, Phys. Rev. C **72**, 065803 (2005). (Cited on page 122.)

[149] C. Fuchs, Lec. Notes Phys. **641**, 119 (2004). (Cited on page 122.)

[150] D. Barret, J. F. Olive, and M. C. Miller, Mon. Not. Roy. Astron. Soc. **361**, 855 (2005). (Cited on page 123.)

[151] M. C. Miller, AIP Conf. Proc. **714**, 365 (2004). (Cited on page 123.)

[152] J. E. Trümper, V. Burwitz, F. Haberl, and V. E. Zavlin, Nucl. Phys. Proc. Suppl. **132**, 560 (2004). (Cited on page 123.)

[153] P. Podsiadlowski, J. D. M. Dewi, P. Lesaffre, J. C. Miller, W. G. Newton, and J. R. Stone, Mon. Not. R. Astron. Soc. **361**, 1243 (2005). (Cited on page 123.)

[154] F. Weber, Prog. Part. Nucl. Phys. **54**, 193 (2005). (Cited on page 125.)

[155] R. A. Leese, M. Peyrard, and W. J. Zakrzewski, Nonlinearity **3**, 773 (1990). (Cited on page 130.)

[156] P. M. Sutcliffe, Nonlinearity **4**, 1109 (1991). (Cited on page 130.)

[157] B. M. A. G. Piette, B. J. Schoers, and W. J. Zakrzewski, Z. Phys. C **65**, 165 (1995). (Cited on page 130.)

[158] B. M. A. G. Piette, B. J. Schoers, and W. J. Zakrzewski, Nucl. Phys. B **439**, 205 (1995). (Cited on page 130.)

[159] B. M. A. G. Piette and W. J. Zakrzewski, Chaos Solitons Fractals **5**, 2495 (1995). (Cited on page 130.)

[160] A. E. Kudryavtsev, B. Piette, and W. J. Zakrzewski, Eur. Phys. J. C **1**, 333 (1998). (Cited on page 130.)

[161] T. Weidig, Nonlinearity **12**, 1489 (1999). (Cited on page 130.)

[162] P. Eslami, M. Sarbishaei, and W. J. Zakrzewski, Nonlinearity **13**, 1867 (2000). (Cited on page 130.)

[163] M. Karliner and I. Hen, Nonlinearity **21**, 399 (2008). (Cited on page 130.)

[164] M. Karliner and I. Hen, arXiv: 0901.1489 [hep-th]. (Cited on page 130.)

[165] C. Adam, P. Klimas, J. Sanchez-Guillen, and A. Wereszczynski, Phys. Rev. D **80**, 105013 (2009). (Cited on page 130.)

[166] C. Adam, T. Romanczukiewiz, J. Sanchez-Guillen, and A. Wereszczynski, Phys. Rev. D **81**, 085007 (2010). (Not cited.)

[167] D. Foster and P. Sutcliffe, Phys. Rev. D **79**, 125026 (2010). (Cited on page 130.)

[168] D. Foster, Nonlinearity **23**, 465 (2010). (Cited on page 130.)

[169] J. M. Speight, J. Phys. A **43**, 405201 (2010). (Cited on page 130.)

[170] J. Jaykka and M. Speight, Phys. Rev. D **82**, 125030 (2010). (Cited on page 130.)

[171] J. Jaykka, M. Speight, and P. Sutcliffe, Proc. R. Soc. A **468**, 1085 (2012). (Cited on page 130.)

[172] Y. Brihaye, T. Delsate, N. Sawado, and Y. Kodama, Phys. Rev. D **82**, 106002 (2010). (Cited on page 130.)

[173] T. Delsate, M. Hayasaka, and N. Sawado, Phys. Rev. D **86**, 125009 (2012). (Cited on page 130.)

[174] R. A. Battye and M. Haberichter, Phys. Rev. D **88**, 125016 (2013). (Cited on page 130.)

[175] A. Halavanau and Y. Shnir, Phys. Rev. D **88**, 085028 (2013). (Cited on page 130.)

[176] M. Kobayashi and M. Nitta, Phys Rev D **87**, 125013 (2013). (Cited on page 130.)

[177] M. Nitta, Phys. Rev. D 87, 025013 (2013). (Cited on page 130.)

[178] S. Bolognesi and P. Sutcliffe, J. Phys. A **47**, 135401 (2014). (Cited on page 130.)

[179] P. Jennings and P. Sutcliffe, J. Phys. A **46**, 465401 (2013). (Cited on page 130.)

[180] B. A. Malomed, Y. Shnir, and G. Zhilin, Phys. Rev. D **89**, 085021 (2014). (Cited on page 130.)

[181] P. Salmi and P. Sutcliffe, J. Phys. A **48**, 035401 (2015). (Cited on page 130.)

[182] C. Adam, C. Naya, J. Sanchez-Guillen, and A. Wereszczynski, Phys. Rev. D **86**, 045015 (2012). (Cited on page 130.)

[183] C. Adam, C. Naya, J. Sanchez-Guillen, and A. Wereszczynski, Phys. Rev. D **86**, 085001 (2012). (Cited on page 130.)

[184] C. Adam, C. Naya, J. Sanchez-Guillen, and A. Wereszczynski, Phys. Rev. D **86**, 045010 (2012). (Cited on page 131.)

[185] C. Adam, T. Romanczukiewiz, J. Sanchez-Guillen, and A. Wereszczynski, JHEP **1411**, 095 (2014). (Cited on page 131.)

[186] C. Adam, C. Naya, T. Romanczukiewiz, J. Sanchez-Guillen, and A. Wereszczynski, arXiv: 1501.0387 [hep-th]. (Cited on page 131.)

[187] L. Bratek and J. Jalocha, in progress. (Cited on page 132.)

[188] C. Adam, C. Naya, J. Sanchez-Guillen, and A. Wereszczynski, JHEP 1303, 012 (2013). (Cited on page 132.)

[189] C. Adam, J. M. Queiruga, J. Sanchez-Guillen, and A. Wereszczynski, Phys. Rev. D **84**, 025008 (2011). (Cited on page 131.)

[190] C. Adam, J. M. Queiruga, J. Sanchez-Guillen, and A. Wereszczynski, JHEP **1305**, 108 (2013). (Cited on page 131.)

[191] M. Nitta and S. Sasaki, Phys. Rev. D **90**, 105001 (2014). (Cited on page 131.)

[192] S. Bolognesi and W. Zakrzewski, Phys. Rev. D **91**, 045034 (2015). (Cited on page 131.)

[193] S. L. Sondhi, A. Karlhede, S. A. Kivelson, and E. H. Rezayi, Phys. Rev. B **47** 16419 (1993). (Cited on page 132.)

[194] O. Schwindt and N. R. Walet, Europhys. Lett. **55** 633 (2001). (Cited on page 132.)

[195] X. Z. Yo et al., Nature **465**, 901 (2010). (Cited on page 132.)

[196] M. Ezawa, Phys. Rev. Lett. **105**, 197202 (2010). (Cited on page 132.)

[197] M. Ezawa, Phys. Rev. B **83**, 100408 (2011). (Cited on page 132.)

[198] M. Bander and C. Itzykson, Rev. Mod. Phys. **38**, 330 (1966). (Cited on page 137.)

[199] A. deShalit and H. Feshbach, *Theoretical Nuclear Physics Volume I: Nuclear Structure* (John Wiley & Sons, New York, 1974). (Cited on pages 139, 142 and 144.)